The behavioural and molecular characterisation of a novel LRRK2 BAC transgenic rat model of Parkinson's disease

A thesis submitted towards the degree of Doctor of Philosophy

by

Maximilian Sloan

Christ Church College

Department of Physiology, Anatomy and Genetics

University of Oxford

Michaelmas Term 2014

Abstract

Mutations in the leucine-rich repeat kinase II (*LRRK2*) gene cause autosomal-dominant Parkinson's disease (PD) which is indistinguishable from sporadic forms of the disease. However, the mechanism by which *LRRK2* mutation promotes PD pathology and the functions of the LRRK2 protein itself are currently unknown. Transgenic animal models, expressing PD-linked genes, have been crucial in developing a clearer picture of the mechanisms behind PD progression. Bacterial artificial chromosome (BAC) transgenics, in particular, allow for physiologically relevant disease models to be generated, encompassing entire gene sequences and using endogenous promoters, which result in an accurate recapitulation of spatiotemporal gene expression. We have, therefore, developed BAC transgenic rats expressing human *LRRK2*. These lines express either human wild-type, G2019S mutant (the most common *LRRK2* mutation) or R1441C mutant (the *LRRK2* mutation leading to a more aggressive pathology) *LRRK2*. These rats display *LRRK2* transgene expression patterns in the brain which highly resemble human *LRRK2* expression. We subsequently aged these lines for the purposes of behavioural and molecular analysis. Additionally, we have performed a number of *in vitro* studies in neurons cultured from these rats to further investigate the effects of pathological forms of LRRK2. Mutant *LRRK2* transgenic rats displayed progressively impaired striatal dopaminergic release along with corresponding behavioural deficits, both motor and cognitive. These motor deficits could be rescued by treatment with levodopa, implying a similar underlying pathological process to PD. These phenotypes occurred in the absence of any overt degeneration of the dopaminergic neurons of the substantia nigra pars compacta or other PD-associated neuropathological markers. We also detected a number of molecular alterations associated with mutant LRRK2 expression including altered LRRK2 phosphorylation and *in vitro* evidence of altered autophagic processes. In conclusion, these rats recapitulate a number of the key features of Parkinson's disease and provide clues as to the progression of pathology in PD.

This thesis is dedicated to my departed friend and colleague, Paul Robertson, a brilliant scientist and a charming man.

Acknowledgements

There are a great many people who, without whom, this thesis would not have been possible. My supervisor, Dr Richard Wade-Martins has been immensely supportive over the course of the highs and lows of my project. How he has dealt with my strops and my idiosyncrasies I do not know, but I imagine that I would not have been nearly so patient. I would also like to thank Dr Javier Alegre-Abarrategui for being the driving force behind the genesis and many of the subsequent areas of the project. Richard's lab, too, is a group of wonderfully special people who helped me greatly at various points in my PhD. In particular, I'm not sure if I can say anything about Milena Cioroch's irreplaceable contribution to the lab which hasn't already been said by other colleagues of mine, sufficed to say that this thesis and the work that it contains simply would not have been completed without her immense help.

Of all the individuals who have helped me, Dr Brent Ryan has been the one who has given the most with the least personal gain. I have pestered him endlessly and he has always made time for me. Similarly, Dr Thierry Deltheil, Dr Marika Doucet, Dr Liz Hartfield, Rozzy Roberts and Dr Nathalie Connor-Robson have all coached me through fundamental parts of the project and are all brilliant people who are generous with their time. Furthermore, my friends Dr Hugo Fernandes, Dr Michele Lufino and Dr Matthew Thomas have given me endless hours of engaging and hilarious conversation, the kind which makes Richard's lab such a special place to be.

Outside of the lab, I would like to make special mention of Dr Dawid Potgieter who worked with me on the transgenic rats and who remains the most effortlessly cheerful and kind person I think I have ever met. I would also like to thank the rest of Dr Stephanie-Cragg's lab, especially Dr Sarah Threlfell and Dr Richard Exley, who directly advanced the work on our collaborative project. Furthermore, I would like to thank Dr Pete Magill for giving me time to talk to him when I worked over in his lab.

I am also thoroughly and unreservedly grateful to Nicholas and Ruth Pitts-Tucker for supporting me financially over the course of my PhD. They have given me the chance to do something which I love and I will never be able to express my gratitude for their help.

Lastly, I want to thank, and apologise to, my friends and family, especially my parents, Fiona and Howard, and my siblings, Astrid and Ollie. I know how distant I have been over these years but you are never far from my thoughts and my heart. Furthermore, my friends, Paul, Tom, Robin, Nils, Anna E. and Anna C.S. have stuck with me despite my long periods of non-communication and are all wonderful and weird in my favourite ways. I also know that I would not have been able to make it through these years in Oxford without Soha, who is, in so many ways, the most amazing person I have ever met. Each day is better because of her. Most of all, I would like to acknowledge the rats, who had the ultimate sacrifice made for them so that I could hopefully contribute to the development of our understanding of Parkinson's disease.

Thesis Figures

Chapter 1

Chapter 2

Chapter 3

Chapter 4

Chapter 5

Chapter 6

Thesis Tables

Chapter 1

Chapter 2

Abbreviations

$[DA]_o$	Extracellular dopamine
5-HTergic	Serotonergic
6-OHDA	6-hydroxydopamine
ABC	Avidin-biotin complex
AD	Autosomal dominant
ANOVA	Analysis of variance
AR	Autosomal recessive
ATP	Adenosine triphosphate
AV	Autophagic vacuoles
BAC	Bacterial artificial chromosome
BBB	Blood brain barrier
BCA	Bicinchoninic acid
BG	Basal Ganglia
BSA	Bovine serum albumin
COR	Carboxy-terminal of ROC
DA	Dopamine
DAB	3,3'-Diaminobenzidine
DAergic	Dopaminergic
DAPI	4',6-diamidino-2-phenylindole
DAT	Dopamine transporter
DLB	Dementia with Lewy Bodies
DMEM	Dulbecco's modified eagle medium
DNA	Deoxyribonucleic acid
dNTP	Deoxynucleotide triphosphate
E[--]	Embryonic day [--]
EDTA	Ethylenediaminetetraacetic acid
EPSC	Excitatory post-synaptic current
FBS	Fetal bovine serum
FCV	Fast cyclic voltammetry
FISH	Fluorescent in situ hybridisation
GBA	Glucocerebrosidase
GFP	Green fluorescent protein
GP	Globus Pallidus
GPe	Globus Pallidus external
GPi	Globus Pallidus internal
GTP	Guanosine triphosphate
GWAS	Genome-wide association study
HBSS	Hank's balanced salt solution
hLRRK2	YPet tagged human LRRK2
HPLC	High-performance liquid chromatography
HRP	Horseradish peroxidase
hWT	Human wild-type
IP	Intraperitoneal
KO	Knockout

LB	Lewy Body
LC	Locus Coeruleus
L-DOPA	L-3,4-dihydroxyphenylalanine (levodopa)
LF	Left forepaw
LH	Left hind paw
LN	Lewy Neurites
LPS	Lipopolysaccharide
LRRK1	Leucine rich repeat kinase-I
LRRK2	Leucine rich repeat kinase-II
MAP2	Microtubule-associated protein 2
MAPT	Microtubule-associated protein tau
MPP+	1-methyl-4-phenylpyridinium
MPTP	1-methyl-4-phenyl-4-propionpiperidine
mRNA	Messenger RNA
MVB	Multivesicular bodies
NDS	Normal donkey serum
NGS	Normal goat serum
Oligo	Oligonucleotide
P[--]	Postnatal day [--]
PAC	Bacterial-P1-artificial chromosome technology
PB	Phosphate buffer
PBMC	Peripherally derived mononuclear cell
PBS	Phosphate buffered saline
PCR	Polymerase chain reaction
PD	Parkinson’s disease
PFA	Paraformaldehyde
PVDF	Polyvinylidene fluoride
QPCR	Quantitative PCR
RBD	Rapid eye movement behavioural disorder
RF	Right forepaw
RH	Right hind paw
RIPA	Radio-immunoprecipitation
ROC	Ras-of complex
ROS	Reactive oxygen species
SD	Sprague Dawley
SDS	Sodium dodecyl sulphate
SEM	Standard error of the mean
SNAP25	Synaptosomal-associated protein 25
SNARE	Soluble N-ethylmaleimide-sensitive factor attachment protein receptor
SNCA	Synuclein, alpha (non A4 component of amyloid precursor)
SNpc	Substantia nigra pars compacta
SNpr	Substantia nigra pars reticulata
STN	Subthalamic Nucleus
TBE	Tris/Borate/EDTA
TBS	Tris-buffered saline
TBS-T	Tris-buffered saline with 0.1 % Triton X-100
TBS-Tw	Tris-buffered saline with 0.1 % Tween-20
TH	Tyrosine hydroxylase

VAMP2	Vesicle-asociated membrane protein 2
VMAT2	Vesicular monoamine transporter 2
VTA	Ventral Tegmentral Area
YAC	Yeast-artificial chromosome
YPet	Yellow fluorescent protein

This thesis contains 44,940 words.

Contents

CHAPTER 1 – THESIS INTRODUCTION

1.1 Parkinson's disease: a general introduction

Parkinson's disease (PD) is the second most common neurodegenerative disease, affecting around 1.5% of individuals over the age of 60 and increasing in incidence with the progression of age (von Campenhausen *et al.,* 2005). The disease was first described almost two centuries ago, and is characterised clinically by a suite of motor symptoms, often accompanied by a wide range of non-motor symptoms (Parkinson, 1817; Chaudhuri *et al.,* 2006). Post-mortem patients reveal preferential degeneration of pigmented dopaminergic (DAergic) neurons within the substantia nigra pars compacta (SNpc), an area within the basal ganglia (BG), which is thought to lead to the motor symptoms (Fearnley & Lees, 1991). Surviving SNpc neurons often develop proteinaceous cytoplasmic inclusions, known as Lewy bodies (LBs), positive for the protein α-synuclein (Forno, 1987; Spillantini, *et al.,* 1997). The processes which lead to the loss of these neurons and the development of LBs are currently unclear although great efforts have been made to explore the underlying molecular pathways. PD is currently irreversible and incurable and its costs upon society are immense ($14.4 billion in the U.S. in 2010) with the disease being estimated to double in prevalence by 2040 due, primarily, to an ageing population (Kowal *et al.,* 2013). While PD is largely sporadic in nature, genetic screening of patients has revealed that mutations or multiplications of certain genes can lead to an increased propensity for disease development (Klein & Westenberger, 2012). It is hoped that an understanding of the molecular pathways underlying these cases may inform upon the disease as a whole and, eventually, lead to the development of curative treatments.

1.2 The clinical and pathological features of Parkinson's disease

1.2.1 The motor tetrad of Parkinson's disease

PD is characterised in the clinic by a motor tetrad of resting tremor, rigidity, bradykinesia and postural instability, although not all symptoms need to be present for a diagnosis and disease symptoms can be heterogeneous (Samii *et al.,* 2004; Jankovic, 2008).

Resting tremor - Usually seen in the arms, resting tremor refers to a mid-frequency (3-6 Hz) rotation of a body part about a fixed axis. This tremor, seen in roughly 75% of patients, tends

to develop in an asymmetrical fashion and is often the presenting symptom noted in the clinic (Hughes *et al.,* 1993).

Rigidity - Often observed in the limbs but also seen in the neck and trunk, patients regularly develop increased resistance to passive joint movement which is often more pronounced in the tremor-affected limbs (Samii *et al.,* 2004). Patients also often report pain along with this rigidity (Jankovic, 2008).

Bradykinesia - Often seen as the most disabling feature of early PD, bradykinesia refers to slowed movement, affecting both fine and gross motor tasks. Furthermore, patients often display impaired reaction times and suffer difficulties when planning and executing motor tasks (Jankovic, 2008).

Postural instability - A variety of postural abnormalities develop later in the progression of PD. These include, in particular, a loss of balance which contributes to the development of a shuffling gait. This impaired balance greatly increases the risk of falls (Samii *et al.,* 2004). In combination with bradykinesia, patients with postural instability often have great difficulty commencing movements or navigating obstacles.

Responsiveness of these symptoms to L-3,4-dihydroxyphenylalanine (L-DOPA), an anti-Parkinsonian dopamine (DA) precursor which is able to cross the blood-brain barrier (BBB), is also frequently used for a clinically definitive diagnosis (Samii *et al.,* 2004). This can allow clinicians to distinguish between PD and disorders which have a similar clinical presentation such as progressive supranuclear palsy (Morris *et al.,* 1999). As PD progresses, symptoms tend to worsen and, while many patients respond well to L-DOPA treatment, the development of L-DOPA induced dyskinesia and other complications is common (Cotzias *et al.,* 1969).

1.2.2 Non-motor symptoms of Parkinson's disease

While PD has historically been viewed as a motor disorder first and foremost, this perspective has likely been heavily influenced by the salience of the motor symptoms compared to other, more

subtle, non-motor symptoms. These symptoms include cognitive and neuropsychiatric disorders such as depression, dementia and anxiety, olfactory dysfunction, gastrointestinal dysfunction, sleep disturbances and many others and are likely underreported by patients who may not draw the connection between their non-motor symptoms and PD (Chaudhuri *et al.,* 2006). In fact, patients often report the non-motor symptoms of PD to be more detrimental to their quality of life than the motor symptoms (Müller *et al.,* 2013). The existence of these non-motor symptoms is unsurprising given the widespread pathology reported in PD patient brains (Braak *et al.,* 2003). Furthermore, LB pathology has been reported in the peripheral autonomic nervous system, throughout the body (Dickson *et al.,* 2009). No treatment exists for non-motor symptoms as a whole and they often are unresponsive to L-DOPA therapy. Rather, symptomatic treatment is usually prescribed (e.g. serotonin reuptake inhibitors for depression, DA agonists for sleep disorders). Importantly, it is often unclear as to whether some of the non-motor symptoms reflect side-effects caused by treatments administered to deal with patients' motor symptoms. Nonetheless, some appear to manifest prior to the onset of the motor symptoms and so, likely, reflect genuine pathological PD processes. Below is a non-exhaustive list of some of the key non-motor symptoms reported by PD patients.

Cognitive deficits - Cognitive deficits are highly common amongst sufferers of PD, with incidences of dementia being six times higher than in non-PD patients (Aarsland *et al.,* 2001). Reported cognitive deficits include impaired executive function, working and long-term memory deficits, particularly concerning visuospatial memory, and attentional problems (Park & Stacy, 2009). These symptoms often occur in early PD and become progressively more severe over time.

Mood disorders - Rates of depression and anxiety are also higher in PD patients than in the general population, at around 40% for both disorders (Cummings *et al.,* 1992; Park & Stacy, 2009). The source of these symptoms is often disputed, with some suggesting them to be a result of the life-changing effects of Parkinsonism or the administration of high levels of L-DOPA, which has been reported to have anxiogenic effects. However, others have reported a

two-fold increase in lifetime depression diagnosis at the time of PD diagnosis (Schurmann *et al.,* 2002) and it has been suggested that dysfunction of the serotonergic (5-HTergic) system may underlie the development of PD-related mood disorders (Cummings *et al.,* 1992).

Olfactory dysfunction - Olfactory dysfunction is developed by the vast majority of PD patients and is seen by many as a preclinical marker of the disease (Braak *et al.,* 2003). Around 10% of asymptomatic PD patient relatives with hyposmia were found to develop PD within 2 years of the diagnosis, while none showing normal olfaction did (Montgomery *et al.,* 1999). Similarly, in a study of twins discordant for PD, those with PD were more likely to have olfactory problems (Marras *et al.,* 2005).

Sleep disturbances - Over 60% of PD patients report sleep disturbances of some kind, often early in the course of PD progression (Tandberg *et al.,* 1998). Excessive daytime sleepiness and narcolepsy-like symptoms are also frequently reported by patients. Additionally, rapid eye movement behavioural disorder (RBD) occurs in around a third of PD patients and over 50% of patients suffering from RBD go on to develop PD (Boeve *et al.,* 2003; Scaglione *et al.,* 2005).

Autonomic dysfunction - PD patients also manifest autonomic dysfunction including dizziness, gastrointestinal, erectile and bladder dysfunction (Park & Stacy, 2009). In particular, constipation affects around 40% of PD patients (Magerkurth *et al.,* 2005). Individuals who suffer from constipation have a threefold risk of developing PD in later life (Abbott *et al.,* 2001).

In summary, there is a wide variety of non-motor symptoms experienced by PD patients, at least some of which appear to pre-date the onset of motor symptoms and can act as predictors of disease. These symptoms are currently under-investigated and their study could lead to a better understanding of overall PD mechanisms.

1.2.3 Neuropathological features of Parkinson's disease

Neuropathological post-mortem studies of PD patients reveal a preferential loss of neuromelanin-positive DAergic neurons in the SNpc, in particular, the ventrolateral areas (Fearnley & Lees, 1991). Motor symptoms only tend to emerge after more than 70% of the DAergic neurons in the ventrolateral SNpc are lost, indicating a degree of compensatory function of the surviving neurons (Fearnley & Lees, 1991). The death of the DAergic SNpc neurons is thought to result in decreased innervation of the caudate putamen (dorsal striatum) and a dramatic reduction in striatal DA content (Ehringer & Hornykiewicz, 1960). The SNpc and striatum form part of a larger circuit of subcortical nuclei, the BG, which are, among other processes, involved in voluntary motor function (Albin *et al.,* 1989). The BG are comprised of both inhibitory and excitatory connections between the major nuclei which include the internal and external segments of the globus pallidus, the subthalamic nucleus, striatum, substantia nigra and thalamus (Albin *et al.,* 1989). The BG both receive inputs from, and output to, cortical regions. The consequences of neuronal loss within the SNpc upon activity within the BG are illustrated, in a simplified form, below (Fig. 1.1).

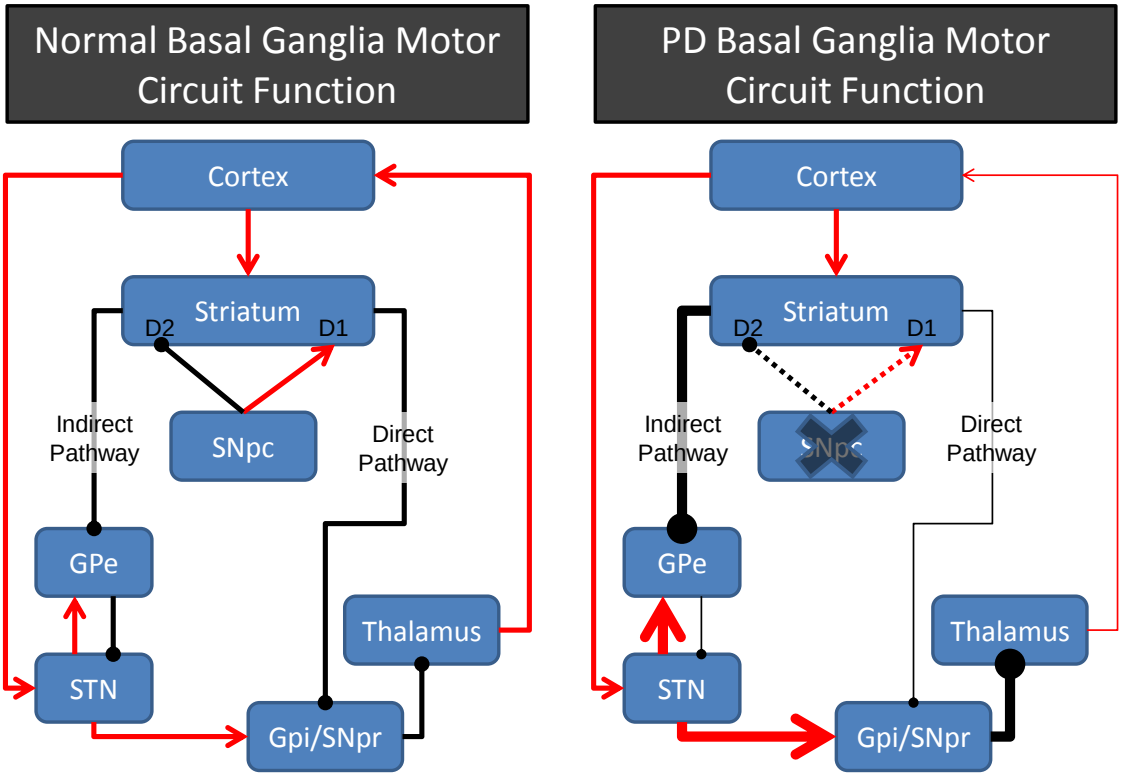

Figure 1.1. An illustration of the effect of SNpc neuronal loss upon BG circuitry. The loss of neurons within the SNpc causes altered DAergic modulation of striatal activity. This leads to an eventual reduction in excitatory input from the thalamus to the cortex. SNpc = substantia nigra pars compacta, SNpr = substantia nigra pars reticulata, STN = subthalamic nucleus, GPe = globus pallidus external, GPi = globus pallidus internal. Black arrows represent inhibitory connections. Red arrows represent excitatory connections. Dotted lines represent connections diminished due to the loss of SNpc neurons in PD. Line thickness represents connection strength. DA receptor subtypes (D1 and D2) in the striatum are illustrated. (Figure adapted from Wichmann *et al.,* 2002).

The DAergic neurons of the midbrain can largely be broken down into the ventral tegmental area (VTA) and two sub-regions of the substantia nigra: the pars compacta and the pars reticulata (SNpr). Neurons in the VTA and SNpr are largely spared in PD compared to those in the SNpc (German *et al.,* 1992; Halliday *et al.,* 2005). The reason for the particular vulnerability of the SNpc DA neurons in PD is still not entirely clear, though it is likely that a cocktail of protective and susceptibility factors contribute to this specificity, rather than any single characteristic. It is additionally unclear what role the presence of neuromelanin plays in the reported neuronal loss as dorsal regions of the SNpc,

which are similarly neuromelanin positive, are comparatively more spared than ventral regions (Halliday *et al.,* 2005). It is likely, therefore, that, at most, neuromelanin plays only a partial role in SNpc neuronal vulnerability. Similarly, while DA has been shown to be toxic (Filloux & Townsend, 1993) the relative sparing of other DAergic areas suggests that the presence of DA may play only a contributory role to neurodegeneration, perhaps promoting toxicity downstream of initial pathological processes.

SNpc DAergic neurons have extremely long, frequently unmyelinated, axons which are highly branched, with estimations of hundreds of thousands of striatal synaptic release sites in rats and around 10-fold more in humans (Bolam & Pissadaki, 2009). Additionally, SNpc neurons are unusual in that they use L-type calcium channels for pacemaking activity (Surmeier *et al.,* 2010). It has been proposed that maintenance of proper calcium gradients can place an extremely high energy burden on these cells, exacerbated by the energy demand of such elaborate processes. These energy burdens, in addition to the fact that high levels of cytosolic calcium can be toxic to cells (Szabadkai & Rizzuto, 2004), may lead to mitochondrial dysfunction and cell death. This theory may explain the comparative resistance of VTA neurons to degeneration as they express protein calbindin-D28k, a calcium-binding protein, which may act as a neuroprotective factor (Yuan *et al.,* 2013). It is important to note, however, that SNpc neurons are not the only cell group to degenerate in PD. For example, noradrenergic neurons of the locus coeruleus (LC), which are also neuromelanin-pigmented and possess similarly elaborate arborisation, are, too, often lost in PD and can demonstrate Lewy pathology (Gesi *et al.* 2000; Braak *et al.,* 2003).

While LBs were described almost a century ago by Frederic Lewy, it was only relatively recently that α-synuclein was found to be a key LB constituent (Spillantini *et al.,* 1997). Post-mortem studies show that, in addition to LBs, susceptible neurons frequently exhibit ‘pale bodies’, which are considered precursors to LBs, along with accumulations of α-synuclein within neuronal processes, called Lewy neurites (LN) (Forno, 1987; Dickson *et al.,* 2009). α-Synuclein within LBs is densely aggregated and frequently post-translationally modified (Spillantini *et al.,* 1997). Lewy pathology is found in other

neurodegenerative diseases including dementia with LBs (DLB) and incidental LB disease (Sulzer & Surmeier, 2013). The pathological similarity between these diseases and PD is debated, with DLB, for example, demonstrating considerable pathological overlap with PD (Burke *et al.,* 2008; Sulzer & Surmeier, 2013). It is still not clear whether LBs are toxic or whether they represent a cellular attempt to sequester toxic proteins away from vital organelles. However, it has been proposed that earlier forms of α-synuclein aggregates are the most toxic to cells (Kalia *et al.,* 2013). Furthermore, while not common, microtubule-associated protein tau (MAPT) pathology or inclusions of TAR DNA-binding protein 43 within the same neuron or neuronal population have also been reported in PD patients, including those with early onset autosomal recessive Parkinsonism (Dickson *et al.,* 2009). What role MAPT, traditionally more associated with Alzheimer's disease, has in PD pathology is unclear, although genome-wide association studies (GWAS) implicate *MAPT*, the gene for protein tau, as having a central role in PD (Simon-Sanchez *et al.,* 2009; Do *et al.,* 2011; Nalls *et al.,* 2014).

In what is becoming a more accepted hypothesis, Braak and colleagues (2003) have suggested that, in fact, PD pathology does not begin in the SNpc. Rather this pathology reflects later stages of a disease which begins in non-DAergic structures of the lower brainstem, olfactory bulb, LC and potentially, autonomic regions. Over time, this pathology is thought to spread to the midbrain and, eventually, to cortical regions, with accompanying clinical symptoms which reflect the brain regions affected by Lewy pathology (Braak *et al.,* 2003). Although it has received a great deal of support, a certain amount of criticism has been directed at the so-called Braak hypothesis. These criticisms include the question of whether early stage pathology is guaranteed to evolve into later-stage pathology and the observation of high degrees of inter-patient heterogeneity (Burke *et al.,* 2008). It is also important to note that, the link between Lewy pathology and cell loss can be overestimated given that it is not uncommon for PD patients with extensive neuronal loss to present with little or no Lewy pathology. Little is known about how Lewy pathology might spread throughout the brain, although it has been theorised that α-synuclein may act as a prion protein whereby aberrantly folded α-synuclein is secreted by affected cells , potentially through vesicular structures such as

exosomes, and acts as a seed in healthy cells to promote further aggregation (Emmanouilidou et al, 2010; Olanow & Brundin, 2013).

1.3 The aetiology of Parkinson's disease

1.3.1 Environmental risk and protective factors for Parkinson's disease

While it is thought that genetics plays a significant role in the aetiology of PD, a number of environmental risk factors have also been proposed which are likely to play, at least, an interactive or additive role in disease development. A study of 542 twins showed an idiopathic PD concordance rate of 11% for monozygotic and 4% for same-sexed dizygotic twins, suggesting a considerable environmental role in the development of PD (Wirdefeldt *et al.,* 2011).

The most recognised risk factor for the development of PD is age. While a number of monogenic forms of the disease have an earlier onset, sporadic PD typically tends to be a disease of old age and increases with incidence over a person's lifetime (Bower *et al.,* 1999). The pre-symptomatic disease course and the inevitability, given enough time, of disease development in all individuals are contentious issues. While likely to reflect genetic differences, gender is also a significant risk factor in PD with men showing a roughly 50% increased incidence of PD development compared to women (Taylor *et al.,* 2007). A number of explanations for this link have been posited including a potential protective effect of oestrogen, a recessive X chromosome-linked susceptibility or gender-specific lifestyle choices (Kieburtz & Wunderle, 2012). A number of studies have also suggested that exposure to particular pesticides results in a roughly 3-fold increase in risk for the development of PD (Tanner *et al.,* 2011). These pesticides, which include rotenone and paraquat, tend to act by causing oxidative stress and impairing mitochondrial function (Bové & Perier, 2011). Administration of these pesticides has subsequently been used to generate animal models of PD. Finally, traumatic brain injuries, especially those of high frequency and severity, have been associated with increased PD risk (Goldman *et al.,* 2006). It is possible that serious head injury may lead to an immune response or impaired BBB function which, in turn, may contribute to the onset of PD.

A number of environmental factors also have been suggested to have a protective effect against PD. Frequent users of tobacco and caffeine reportedly show decreased risk of PD development by around 40% in both cases (Hernan *et al.,* 2002). Similarly, long-term use of non-steroidal anti-inflammatory drugs such as ibuprofen has been linked with reduced risk of PD development (Chen *et al.,* 2005). It is important to note that without the use of long-term randomised control trials, despite efforts to control factors, co-occurring behaviours can make conclusions difficult to draw, especially with a disease that may take decades to develop.

1.3.2 The genetics of Parkinson's disease

While the majority of PD cases are sporadic, around 5-10% are familial (Klein & Westenberger, 2012). This strongly suggests a genetic component to the aetiology of PD. Furthermore, while initial twin studies suggested a rather low concordance for sporadic PD, GWAS studies have suggested a more central role of genetics in PD susceptibility than was initially thought (Wirdefeldt *et al.,* 2011; Simon-Sanchez *et al.,* 2009; Do *et al.,* 2011; Nalls *et al.,* 2014). A number of genes have been linked to the development of PD, determined chiefly by pedigree linkage analysis, candidate gene approaches and GWAS. These genes tend to be designated with a '*PARK*' locus and are summarised in Table 1.1. A sub-group of these genes is considered to cause rare 'monogenic' PD, i.e. a mutation (or multiplication in the case of α-synuclein) in one of these genes is considered to be sufficient to cause PD. These genes cause what can be broken down into either autosomal dominant (AD) or autosomal recessive (AR) PD. Crucially, while far more common in familial than sporadic PD, mutations in these genes explain only between 3-5% of occurrences of PD (Klein & Westenberger, 2012). It is hoped, however, that an understanding of the functions of these genes and the effect of these mutations upon their function might contribute towards an understanding of the pathogenesis of sporadic PD.

Table 1.1. An overview of the *PARK* genes. (Table adapted from Klein & Westenberger, 2012).

Symbol	Locus	Gene	Disorder	Inheritance	Method of identification
PARK 1/4	4q21-22	*SNCA*	EOPD	AD	Linkage analysis
PARK 2	6q25.2-q27	*PRKN*	EOPD	AR	Linkage analysis
PARK 3	2p13	Unknown	Classical PD	AD	Linkage analysis
PARK 5	4p13	*UCHL1*	Classical PD	AD	Candidate gene approach
PARK 6	1p35-p36	*PINK1*	EOPD	AR	Linkage analysis
PARK 7	1p36	*DJ-1*	EOPD	AR	Linkage analysis
PARK 8	12q12	*LRRK2*	Classical PD	AD	Linkage analysis
PARK 9	1p36	*ATP13A2*	Atypical PD	AR	Linkage analysis
PARK 10	1p32	Unknown	Classical PD	Risk factor	Linkage analysis
PARK 11	2q36-27	Unknown	Late-onset PD	AD	Linkage analysis
PARK 12	Xq21–q25	Unknown	Classical PD	Risk factor	Linkage analysis
PARK 13	2p12	*HTRA2*	Classical PD	AD/risk factor	Candidate gene approach
PARK 14	22q13.1	*PLA2G6*	EO atypical PD	AR	Linkage analysis
PARK 15	22q12–q13	*FBX07*	EO atypical PD	AR	Linkage analysis
PARK 16	1q32	Unknown	Classical PD	Risk factor	GWAS
PARK 17	16q11.2	*VPS35*	Classical PD	AD	Exome sequencing
PARK 18	3q27.1	*EIF4G1*	Classical PD	AD	Linkage analysis

Autosomal dominant monogenic Parkinson's genes

α-Synuclein (*PARK1/4*)

In 1997, Polymeropoulos and colleagues discovered a PD-causing point mutation (A53T) in a European family in the gene encoding the α-synuclein protein - synuclein, α (non A4 component of amyloid precursor) (*SNCA*). The *SNCA* gene is situated on chromosome 4q21 and was attributed the *PARK1* locus. Subsequently, it was found that, along with other mutations, A30P and E46K, *SNCA* duplications and triplications can similarly cause PD (Krüger *et al.,* 1998; Singleton *et al.,* 2003; Zarranz *et al.,* 2004; Fuchs *et al.,* 2007). The finding that α-synuclein was a major constituent of LBs lent further credence to the centrality of α-synuclein to PD development (Spillantini *et al.,* 1997). More recently, variants in the *SNCA* gene have been identified as PD risk factors in GWAS studies (Simon-Sanchez *et al.,* 2009; Do *et al.,* 2011; Nalls *et al.,* 2014). The onset of PD in the cases of mutant *SNCA* carriers is around 40-50 years, showing a high degree of penetrance and, while reports have suggested some clinical differences when compared to sporadic PD, pathologies appear largely similar (Klein & Westenberger, 2012). While the function of the α-synuclein protein is currently

unclear, it is likely that it plays a role in synaptic machinery (Bendor *et al.,* 2013). The fact that wild-type α-synuclein overexpression can promote the development of PD in a dose-dependent fashion and the pathological *SNCA* mutations promote the formation of toxic α-synuclein oligomers, leading to fibrillization, led to the concept that improper clearance and subsequent build-up of toxic α-synuclein aggregates may lead to the formation of LBs and eventual cell death seen in sporadic PD.

Leucine-rich repeat kinase II (*PARK8)*

In 2002, the *PARK8* locus, lying on chromosome 12q12, was mapped in a Japanese family presenting AD PD (Funayama *et al.,* 2002). This locus contains the gene which encodes for leucine rich repeat kinase II (*LRRK2*). Subsequently, six missense mutations have been identified which are thought to be pathogenic in nature – R1441C/G/H, Y1699C, G2019S, I2020T (Zimprich *et al.,* 2004; Nichols *et al.,* 2005; Gilks *et al.,* 2005). These mutations are clustered in the enzymatic domains of the LRRK2 protein and have been proposed to alter the activity of these domains. An analysis of over 750 cases of familial PD found roughly 5% to have a G2019S mutation, the most common *LRRK2* mutation, which is located in the kinase domain of the protein (Nichols *et al.,* 2005). In addition to familial PD, around 1-2% of purportedly sporadic PD patients were also found to have a *LRRK2* G0291S mutation (Gilks *et al.,* 2005). Higher proportions of *LRRK2* mutations in PD patients have also been described in specific populations such as Ashkenazi Jews where *LRRK2* mutations account for 13% of sporadic and 30% of familial PD (Ozelius *et al.,* 2006). Mutations at the R1441 amino acid, located in the guanosine triphosphate (GTP)ase region of the protein, are the second most common mutation and appear to cause a somewhat earlier onset form of PD with a higher degree of penetrance (Haugarvoll *et al.,* 2008; Klein & Westenberger, 2012). Caution is needed when interpreting the data, however, due to the relatively low sample size for R1441C/G/H patients. Unlike α-synuclein, no occurrences of *LRRK2* multiplications have been found in patients, so it is not clear whether overexpression of the wild-type protein is sufficient to cause PD development in patients. Like α-synuclein, the function of LRRK2 protein is currently unclear; the many roles that have been ascribed to it will be discussed in later sections of this introduction.

In addition to missense mutations, several *LRRK2* polymorphic risk variants exist. In 2007, the G2385R variant was identified within a Chinese population (Tan *et al.,* 2007) and, later, the R1628P variant (Ross *et al.,* 2008). The estimated population attributable risk for PD is 4% and 6% for the G2385R and R1628P variants, and they lie in the WD40 and COR domain regions of the LRRK2 protein respectively (Tan *et al.,* 2007; Ross *et al.,* 2008). The location of the G2385R variant is interesting given that it lies outside the catalytic core of the LRRK2 protein, although it has been suggested that the WD40 domain is necessary for LRRK2 toxicity (Jorgensen *et al.,* 2009). In addition to the G2385R and R1628P variants, subsequent GWAS studies have identified numerous common variants in the *LRRK2* gene which appear to be linked to PD (Simon-Sanchez *et al.,* 2009; Nalls *et al.,* 2014).

Autosomal recessive monogenic Parkinson's genes

AR monogenic forms of PD share a number of characteristics in that they tend to cause PD that is early onset (<45 years), responds well to L-DOPA and has, somewhat paradoxically, a generally more slow rate of progression than late onset forms of the disease (Klein & Westenberger, 2012). Due to the rarity of some of these disorders, substantial data does not exist on the neuropathology in the case of many of these mutations.

PRKN (*PARK2*) mutations were discovered in a Japanese family with a high incidence of early-onset PD (Kitada *et al.,* 1998). The *PRKN* protein, parkin, is an E3 ubiquitin ligase which acts to ubiquitinate proteins for degradation (Trinh & Farrer, 2013). *PRKN* mutations are the most common cause of autosomal recessive PD cases (Klein & Westenberger, 2012). Interestingly, an AD PD-causing missense mutation in *UCHL-1* (*PARK5*), a protein also involved in the ubiquitin system, was reported in a German family (Leroy *et al.,* 1998) but such findings have not been replicated since. Mutations in *PINK-1* (*PARK6*) were discovered in a European family and were found to cause PD very similar to that caused by parkin mutations (Valente *et al.,* 2004). PINK-1 is a mitochondria-associated protein which appears to function in the same molecular pathway as parkin, namely, mitochondrial quality control (McLelland *et al.,* 2014). *DJ-1* (*PARK7*) mutations were identified in a Dutch cohort (Bonifati

et al., 2003). DJ-1 protein seems to act protectively against oxidative stress (Canet-Avilés *et al.,* 2004). ATP13A2 (*PARK9*) was discovered in a Jordanian family with early-onset PD with dementia (Ramirez *et al.,* 2006). *ATP13A2* encodes an adenosine triphosphate (ATP)-ase which localises to the lysosomal membrane (Ramirez *et al.,* 2006). PD-causing mutations of *ATP13A2* have been found to cause impaired lysosomal function in patient-derived cell-lines (Dehay *et al.,* 2012). More recently, mutations in *PLA2G6 (PARK14)*, a gene associated with infantile neuroaxonal dystrophy, were found to cause atypical PD with dystonia (Paisan-Ruiz *et al.,* 2009). Finally, mutations in the *FBXO7* (*PARK15*), a gene encoding an E3 ubiquitin ligase, were first reported to cause AR PD in a Persian family and FBXO7 has more recently been implicated to interact with parkin to mediate mitophagy (Shojaee *et al.,* 2008; Burchell *et al.,* 2013).

Other genes associated with Parkinson's disease

MAPT and GBA

While not designated with *PARK* loci, it is highly likely that the *MAPT* and glucocerebrosidase (*GBA*) genes have significant roles to play in PD. Recent GWAS studies have identified variations in the *MAPT* gene as being a highly significant contributor to the development of PD (Simon-Sanchez *et al.,* 2009; Do *et al.,* 2011; Nalls *et al.,* 2014). *MAPT* is linked to a number of neurodegenerative disorders which are often accompanied by the hyperphosphorylation of tau in the form of neurofibrillary tangles (Trinh & Farrer, 2013). Interestingly, hyperphosphorylated tau is an occasionally reported feature of *LRRK2* PD, although the processes by which this occurs are currently unknown (Haugarvoll & Wszolek, 2009).

Heterozygous mutations in *GBA*, which encodes a lysosomal enzyme, can lead to development of Gaucher disease, a lysosomal storage disorder. Gaucher sufferers can develop midbrain LB pathology similar to that seen in PD (Neumann *et al.,* 2009). It was observed that parents and second-degree relatives of Gaucher patients frequently suffered from PD and subsequently found that mutations in *GBA* were a common characteristic amongst them (Goker-Alpan *et al.,* 2004). Recent GWAS studies have also found variations in *GBA* to significantly predispose individuals to the development of PD

(Do *et al.,* 2011; Nalls *et al.,* 2014). Neumann and colleagues (2009) found that PD sufferers carrying heterozygous *GBA* mutations tend to have an earlier onset than sporadic PD (~50 years of age) and similar neuropathological features.

In addition to those genes already described, variants and mutations in a relatively large number of other genes have been linked with PD thanks, primarily, to a number of recent GWAS studies, next generation sequencing techniques and candidate gene approaches. A recent meta-analysis of previously performed GWAS studies identified 28 independent risk loci for PD (Nalls *et al.,* 2014). Some of these genes have been attributed with '*PARK*' loci while others require confirmation of their role in PD. As of yet, many of these genes have been under-investigated and their link to the pathogenesis of PD remains unknown.

1.4 Leucine-rich repeat kinase II: structure, function and disease role

1.4.1 The features of *LRRK2* Parkinson's disease

Mutations in *LRRK2* lead to the development of AD PD with incomplete penetrance (Healy *et al.,* 2008). An individual with a heterozygous G2019S mutation has an estimated 28% chance of PD development by the age of 59, increasing to 74% at 79 years (Healy *et al.,* 2008). However, disagreement exists as to the penetrance of *LRRK2* mutations with estimates varying substantially.

Clinically, mutant *LRRK2* PD patients are often considered indistinguishable from sporadic patients. Mutant *LRRK2* PD patients show cell loss within the SNpc, often the presence of LB and occasionally, neurofibrillary tangles (Haugarvoll & Wszolek, 2009). Healy and colleagues, in a large case-controlled study of over 350 patients found that, compared to sporadic PD patients, *LRRK2* mutant carriers show similar age of onset, motor and non-motor symptom development and responsiveness to L-DOPA treatment (Healy *et al.,* 2008). Healy and colleagues did report reduced incidences of cognitive impairment and sleep disturbances in addition to a somewhat more benign disease progression. However, these findings may reflect biases in methodological approaches to data collection (see Elbaz, 2008). Importantly, while all known mutations were studied, due to the infrequence of some

mutations (R1441C/G/H, I2020T, Y1699C), it was not clear if their effects differed significantly from the more common G2019S mutation. Overall, the high levels of similarity between *LRRK2* PD and sporadic forms suggest similar pathological mechanisms.

1.4.2 LRRK2 protein

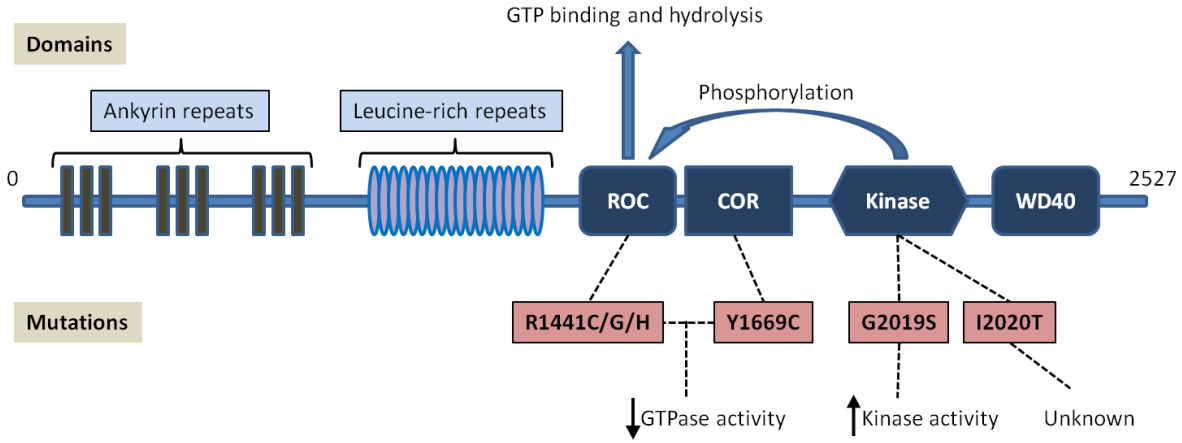

Figure 1.2. The domains and PD mutations in the LRRK2 protein. A schematic representation of the LRRK2 protein. The *LRRK2* gene encodes a 2527 amino acid, 286 kDa protein. Repeat regions precede the 'catalytic core', comprised of the ROC-COR domain, which functions as a GTPase, and the kinase domain which appears to highly phosphorylate the ROC domain. Closest to the C-terminus is the WD40 domain which is thought to serve a scaffolding function. Mutations (R1441C/G/H and Y1669C) in the ROC-COR domain have the effect of reducing GTPase activity while G2019S mutations cause a ~3–fold increase in kinase activity (adapted from Cookson, 2010).

Structure and the effects of pathogenic mutations

The *LRRK2* (*PARK8*) gene encodes a 286 kDa, 2527 amino acid, multidomain protein consisting of several repeat-containing regions, followed by a ROC-COR GTPase, kinase and WD40 domain (Cookson *et al.,* 2010) (Fig. 1.2). The 'catalytic core', consisting of the Ras of complex (ROC), the carboxy-terminal of ROC (COR) and the kinase domain, mediates the catalytic function of the protein, along with protein dimerisation (Taymans, 2012). The repeat containing regions and the WD40 domain are thought to primarily serve a scaffolding function (Piccoli *et al.,* 2014). The PD-causing mutations lie in either the GTPase (R1441G/C/H and Y1699C) or kinase (G2019S and I2020T) domain of the protein. Risk variants G2385R and R1628P lie in the ROC and WD40 repeat regions, respectively (Tan *et al.,* 2007; Ross *et al.,* 2008). It has been proposed that, compared to cytosolic

LRRK2, which is monomeric, LRRK2 exists as a dimer when membrane bound, with greatly heightened enzymatic activity (Berger *et al.,* 2010).

LRRK2 belongs to a sub-group of the superfamily of Ras-like GTPase proteins called ROC or ROCO proteins due to the sequential existence of a ROC sequence followed by a COR sequence. These proteins share the characteristic of possessing a GTPase embedded in amongst multiple protein domains (Taymans, 2012). LRRK2 has a number of homologues in mammals including the paralogue, leucine-rich repeat kinase I (LRRK1), a GTPase with ~50% amino acid sequence similarity, including the presence of a kinase domain (Gilsbach & Kortholt, 2014). The LRRK2 kinase is a serine/threonine kinase, sharing homology with mixed-lineage kinases which act as mitogen activated protein kinase kinase kinases involved in cell death processes (Esteves *et al.,* 2014). It is thought that phosphorylation of the kinase domain at a number of potential sites within the activation loop may mediate kinase activity, and it has been proposed that this kinase activity is crucial for the toxic effects of LRRK2 when expressed in cells (Greggio *et al.,* 2006). While numerous targets of LRRK2 phosphorylation have been proposed, no protein has been shown to be phosphorylated in a consistent and physiologically relevant manner to date. Numerous autophosphorylation sites have been proposed however (e.g. ser1292), particularly within the ROC domain, although their physiological and functional relevance, in particular with regards to GTPase activity, is still unclear (Sheng *et al.,* 2012).

The G2019S mutation has the effect of increasing the activity of the kinase domain by around three-fold *in vitro* while the other PD-linked mutations appear to have little or no effect upon LRRK2 kinase activity (West *et al.,* 2005; Greggio *et al.,* 2006; Xiong *et al.,* 2012a). Mutations in the kinase domain do not appear to modulate the GTPase activity of LRRK2 (Xiong *et al.,* 2010) although some have recently suggested that G2019S mutations reduce GTPase activity (Xiong *et al.,* 2012a). Pathological mutations in the GTPase domain appear to decrease GTPase activity which has been proposed to be critical for proper kinase function (Xiong *et al.,* 2012b) although others have reported that GTPase mutations may lead to an increase in kinase activity (West *et al.,* 2005). It has been suggested that

the exchanging of a GDP for a GTP molecule causes LRRK2 to switch to its 'active state' where it is able to interact with downstream targets until the GTP molecule is hydrolysed to GDP, returning LRRK2 to its inactive state (Taymans, 2012). However, this model has received criticism for being overly simplistic.

Reduction in LRRK2 phosphorylation has been observed as a consequence of LRRK2 kinase inhibition, in addition to the mutation of certain residues to impair LRRK2 kinase function, suggesting that LRRK2 kinase activity may affect phosphorylation, at least at certain sites, although potentially in an indirect fashion (Longo *et al.,* 2014; Cinaru *et al.,* 2014; Ito *et al.,* 2014). It is also likely that phosphorylation of LRRK2 affects its interaction with certain proteins. While numerous LRRK2 interactors have been proposed, often by co-immunoprecipitation studies, the most promising finding is an interaction with the 14-3-3 proteins which has been replicated by several studies (Nichols *et al.,* 2010; Li *et al.,* 2011; Piccoli *et al.,* 2014). This is interesting due to the fact that 14-3-3 proteins have been attributed the function of determining the correct sub-cellular localisation of the proteins which they interact with, and mutant LRRK2 reportedly shows abnormal sub-cellular localisation (Alegre-Abarrategui *et al.,* 2009; Nichols *et al.,* 2010). It has been shown that inhibiting phosphorylation of LRRK2 at serine 910 and serine 935 disrupts binding of LRRK2 to 14-3-3 proteins (Nichols *et al.,* 2010; Li *et al.,* 2011). Several of the LRRK2 mutations in addition to the G2385R variant have been identified as reducing 14-3-3 protein binding at these sites suggesting a potential pathological mechanism of action. Finally, it has been proposed that 14-3-3 proteins may facilitate the dimerisation of LRRK2 (Rudenko & Cookson, 2010). Determining the downstream effects of LRRK2 and its interactors will likely be crucial for determining the function and dysfunction of LRRK2.

LRRK2 expression patterns

Human LRRK2 has a roughly 90% and 95% amino acid sequence conservation with rodents and non-human primates, respectively, and LRRK2 expression in the brains of humans and rodents appears largely similar (Sharma *et al.,* 2011; West *et al.,* 2014). Interestingly, however, considerable differences have been reported between the rodent and human promoter sequence (West *et al.,*

2014). *LRRK2* messenger RNA (mRNA) and protein is widely expressed throughout the brain, in areas which include the olfactory bulb, striatum, hippocampus, cortex, brainstem and cerebellum and to a lesser extent, in the DA neurons of the SNpc (Biskup *et al.,* 2006; Sharma *et al.,* 2011; Giesert *et al.,* 2014). While LRRK2 levels appear to be very low, it has been suggested that *LRRK2* is alternatively spliced within the SNpc (Trabzuni *et al.,* 2013) which may be functionally relevant to SNpc neurons' enhanced vulnerability to degeneration. LRRK2 is expressed in a number of cell types in the brain including neurons and various immune cells (Miklossy *et al.,* 2006; Maekawa *et al.,* 2010). In addition, LRRK2 is expressed in various other organs including the kidney, lung, liver, spleen and heart (Miklossy *et al.,* 2006; Westerlund *et al.,* 2008; Esteves *et al.,* 2014; Giesert *et al.,* 2014). Intracellularly, LRRK2 exists as a cytoplasmic protein which has been found to associate with numerous organelles such as various vesicular structures (e.g. synaptic vesicles), mitochondria and microtubules (Biskup *et al.,* 2006; Sharma *et al.,* 2011; Kett *et al.,* 2012; Esteves *et al.,* 2014, Piccoli *et al.,* 2014). Post-mortem studies of idiopathic and G2019S PD patients have not reported any changes in LRRK2 expression throughout the brain although LRRK2 protein has been found to be associated with LBs (Sharma *et al.,* 2011). The functional relevance of this is not clear, however.

Studying developing rats, Westerlund and colleagues (2008) found that *LRRK2* mRNA is not highly expressed until 1 week after birth, although more recent studies report the presence of *LRRK2* mRNA at around E10 in mice (Giesert *et al.,* 2014). Neurons, cultured from E13-15 mice have been shown to express LRRK2 protein 7 days after culture (Piccoli *et al.,* 2011). Once adulthood is reached, mRNA expression levels do not appear to vary in rodents throughout the lifetime of the animal (Westerlund *et al.,* 2008).

1.4.3 *In vitro* studies of LRRK2 function and dysfunction

In an attempt to understand the pathological processes underlying the effects of *LRRK2* mutations, wild-type and PD-promoting, mutant forms of the *LRRK2* gene are frequently expressed *in vitro* and *in vivo* (e.g. MacLeod *et al.,* 2006). Alternatively, *LRRK2* can be knocked out, knocked down or inhibited using LRRK2 kinase inhibitors (e.g. Piccoli *et al.,* 2011). It is hoped that these approaches

will lend insight into the function of LRRK2, in addition to elucidating pathological processes underlying PD progression. Since the study of *LRRK2* began, a wide variety of functions have been ascribed to the protein including implicated roles in apoptosis, neurogenesis, the cytoskeleton, autophagy, vesicle trafficking, protein transcription/translation and the immune system. It is perfectly possible that more than one of these proposed functions is indeed true, especially given the relative size, complexity and diverse expression of the LRRK2 protein. The overview below focuses on the areas which appear to be most reliably associated with LRRK2 function.

One of the earliest reported and most reproduced cellular phenotypes in primary neuronal cultures is impaired neurite length and branching in response to overexpression of mutant LRRK2, while knock-out (KO), knock-down of *Lrrk2* or the expression of a kinase-dead, K1906M, mutant LRRK2 has the converse effect (MacLeod *et al.,* 2006; Parasiadou *et al.,* 2009; Dächsel *et al.,* 2010; Lee *et al.,* 2010; Ramonet *et al.,* 2011) (although see Gillardon, 2009; Tsika *et al.,* 2014). Overexpression of wild-type LRRK2 seems to have no effect upon branching in the majority of these cases although some have suggested the effects of wild-type LRRK2 overexpression to mimic those of mutant LRRK2 (Lee *et al.,* 2010). It has been suggested that these effects are a consequence of apoptotic processes (MacLeod *et al.,* 2006) but morphological neuritic changes could have a number of sources potentially occurring as a result of changes to autophagic or cytoskeletal processes (Plowey *et al.,* 2008; Parasiadou *et al.,* 2009). The extent to which the neurite branching phenotype reflects a process central to *LRRK2* PD pathology is currently unclear although it is often used as a read-out of the efficacy of experimental manipulations to reverse the effect of the pathological mutations.

A potential explanation for the modulation of neurite growth is LRRK2's implicated role in cytoskeletal processes. In particular, the function of microtubules - which are comprised of α/β-tubulin heterodimers - have been reportedly altered by *Lrrk2* KO or mutation. LRRK2 has been shown to phosphorylate β-tubulin (Gillardon, 2009) and has been shown to, dependent upon intact kinase function, be recruited to microtubules (Kett *et al.,* 2012). *LRRK2* mutations were found to enhance both of these effects. *In vitro* studies have also shown mutant LRRK2 expression to result in

increased microtubule stability (Gillardon, 2009). This stability may be mediated by LRRK2's interaction with tau, which LRRK2 has been reported to phosphorylate when in the presence of tubulin (Kawakami *et al.,* 2012). Tau phosphorylation typically decreases its affinity for microtubules which may lead to an increased propensity for aggregation.

Actin cytoskeleton-genes have also been found to be disregulated in peripheral blood mononuclear cells (PBMCs) of patients carrying the G2019S mutation (Mutez *et al.,* 2011). Parasiadou and colleagues (2009) found, in neuronal cultures, that mutant LRRK2 caused an accumulation of polymerised actin and phosphorylated ezrin, radixin and moesin proteins, which act to cross-link the actin cytoskeleton, and that reversal of these cytoskeletal effects could rescue impaired neurite outgrowth caused by LRRK2 mutations. While the interaction between the actin and microtubule cytoskeleton is well documented, it is unclear how LRRK2 may affect the interplay between them.

It has additionally been proposed that LRRK2 is involved in vesicle trafficking, in which the cytoskeleton plays a key role (Piccoli *et al.,* 2011). Indeed, neurotransmitter release appears to be disrupted as a result of *LRRK2* mutation with chromaffin cells, derived from *LRRK2* mutant mice, displaying impaired release of catecholamines (Tong *et al.,* 2009). In line with this, Piccoli and colleagues (2011) found that, following LRRK2 knockdown in primary cultures, the probability and amplitude of an excitatory post-synaptic current (EPSC) in response to electrical stimulation was increased, but reduced for subsequent stimulation-induced EPSCs. Subsequent electron microscopy of LRRK2 knockdown neurons revealed a reduced number of docked vesicles at the presynaptic membrane but a greater number in the 'reserve pool'. More recent investigations have also shown LRRK2 to associate with various pre-synaptic proteins, further suggesting a role for LRRK2 in vesicle dynamics (Piccoli *et al.,* 2014).

LRRK2 has also been found to be associated with Rab5b, a regulator of endocytic vesicular transport, and has itself been implicated in vesicle endocytosis (Shin *et al.,* 2008). Overexpression or knockdown of LRRK2 was found to cause reduced endocytosis speeds which could be rescued by the overexpression of Rab5b (Shin *et al.,* 2008). Rab5b is involved in early stages of the endosomal

pathway which is responsible for the formation of autophagosomes and lysosomes. This is interesting due to the numerous lines of evidence which point to autophagy as playing a central role in LRRK2 dysfunction. LRRK2 has been found to colocalise with multivesicular bodies (MVB) and autophagic vacuoles (AV) in human cells, and increased autophagic activity has been reported in cell lines expressing mutant LRRK2 (MacLeod *et al.,* 2006; Alegre-Abarrategui *et al.,* 2009; Plowey *et al.,* 2008; Gomez-Suaga *et al.,* 2012). LRRK2 has also been found to promote toxicity by autophagic processes in patient derived cell lines and has been proposed to regulate autophagic gene expression (Ferree *et al.,* 2012; Yakhine-Diop *et al.,* 2014). Recently, Orenstein and colleagues (2013) suggested that mutant and wild-type LRRK2 have an inhibitory effect upon chaperone mediated autophagy which, in turn, may lead to the impaired degradation of proteins, including α-synuclein. Additionally, LRRK2 overexpression was also found to cause alterations to lysosomal acidity which may impair autophagic function, potentially linking LRRK2 to other PD-associated genes such as GBA (Gomez-Suaga *et al.,* 2012).

Finally, links have been drawn between LRRK2 and the immune system. This has been fuelled partially by the discovery that LRRK2 plays a significant role in inflammatory bowel disease and is highly expressed in immune cells, particularly, B-lymphocytes and microglia (Miklossy *et al.,* 2006; Barrett *et al.,* 2008; Maekawa *et al.,* 2010). When treated with interferon ɣ, a pro-inflammatory cytokine, human PBMCs show an upregulation of LRRK2, suggesting it to be involved in the immune response (Gardet *et al.,* 2011). Similarly, inhibition of LRRK2 has been found to restrict microglial activity in response to pro-inflammatory stimulation (Moehle *et al.,* 2012). The prospective role of LRRK2 in the immune system is particularly interesting given that the immune system has long been suspected as playing a role in the development of PD and the GWAS implication of human leukocyte antigen genes in PD appears to be solidifying this connection (Trinh & Farrer, 2013).

In conclusion, *in vitro* studies of LRRK2 function have helped elucidate a number of potential pathways through which LRRK2 may contribute to the development of PD. However, it is highly likely that there are elements of disease that are dependent upon network and long-term ageing effects

which cannot be recapitulated in a dish. When modelling a disease which is defined largely by motor symptoms and impaired regional connectivity*, in vitro* studies are sorely lacking. To study disease processes in the context of a functioning brain, therefore, animals such as *C. elegans, Drosophila* and various mammals are frequently used. In particular, rodents are considered highly useful because they possess a number of valuable characteristics including a relatively short life span, rapid breeding, high genetic similarity to humans, relatively well-developed DAergic systems and an expression of key PD-linked genes.

1.5 Rodent models of Parkinson's disease

1.5.1 Toxic lesion studies

Models which attempt to recapitulate PD through the administration of toxic compounds have been useful in modelling aspects of the disease, particularly the pathogenesis of PD motor dysfunction. These toxins tend to share the characteristic of causing degeneration of neurons in the SNpc and include 6-hydroxydopamine (6-OHDA), 1-methyl-4-phenyl-1,2,3,6-tetrahydropyridine (MPTP), rotenone and paraquat. These approaches possess a number of key strengths within the context of modelling PD, including the ability to rapidly cause Parkinsonian symptoms and DAergic cell death without relying upon the ageing process and, thus, allowing for the rapid study of the consequences and mechanisms of DAergic dysfunction. None of these models has been able to cause the formation of *bona fide* LBs however, even in monkeys receiving intermittent injections of MPTP for over 10 years (Halliday *et al.,* 2009). Furthermore, while toxic models can rapidly produce Parkinsonian phenotypes, it is unclear how similar the underlying pathological processes are to those seen in sporadic PD patients.

6-OHDA, often administered directly to the brain, unilaterally in rat models, causes damage to cathecolaminergic neurons, including DAergic neurons (Jeon *et al.,* 1995; Lee *et al.,* 1996). After being taken up by the DA transporter (DAT), 6-OHDA causes cell toxicity by the production of reactive oxygen species (ROS) which leads to oxidative stress and, eventually, cell death (Bové & Perier, 2011). When injected into the SNpc or medial forebrain bundle, neurons undergo near-total

degeneration within around 3-4 days with clear neuronal loss occurring as early as 12 hours post-treatment (Jeon *et al.,* 1995). If injected into the striatum, 6-OHDA causes retrograde SNpc neuronal degeneration over the course of several weeks (Lee *et al.,* 1996). Both techniques have the effect of dramatically reducing levels of DA within the striatum. The unilateral approach allows for a 'within animal' control and reduces animal morbidity. Unilateral 6-OHDA treatment leads to a rotational behaviour in the animal following the administration of DA agonists and defective use of limbs contralateral to the lesion – often assessed by the cylinder test (Bové & Perier, 2011). A principal problem with the 6-OHDA model, however, is that it fails to take into account pathological processes elsewhere in the brain and may reinforce the perception of PD being a disease of the DAergic system alone.

MPTP is a synthetic opioid which, in humans, produces irreversible, L-DOPA-sensitive Parkinsonism (Langston *et al.,* 1983). Humans who have received MPTP show profound loss of midbrain DAergic neurons several days post-administration (Langston *et al.,* 1999). After intraperitoneal (IP) or subcutaneous injection and crossing the BBB, MPTP is converted into its toxic metabolite, 1-methyl-4-phenylpyridinium (MPP+). MPP+ is taken up by DAT and impairs mitochondrial respiration by the inhibition of complex 1 activity which, in turn, leads to ROS production (Nicklas *et al.,* 1985). MPTP tends to be used in primates and mice as opposed to rats due to rats' resistance to the drug, which is thought to be an issue of BBB permeability (Boyce *et al.,* 1984). MPTP-treated mice and primates develop numerous motor dysfunctions; and primates additionally have been reported to show non-motor symptoms such as sleep disorders, psychotic-like behaviour and attention deficits. Similarly to 6-OHDA models, MPTP-treated animals display extensive SNpc DA neuronal loss and greatly decreased striatal DA levels (Bové & Perier, 2011).

Finally, rotenone, an insecticide, and paraquat, a herbicide, have both been linked to increased incidences of PD in humans (Tanner *et al.,* 2011). Rotenone acts to impair mitochondrial function by inhibiting complex-1 function and leading to oxidative stress. In addition, rotenone has been implicated in altered microtubule and proteasomal activity (Chou *et al.,* 2010). Sustained

intravenous administration of rotenone can cause selective DA SNpc neurodegeneration in rats along with rigidity and hypokinesia (Betarbet *et al.,* 2000). These rats also develop ubiquitin and α-synuclein positive cytoplasmic inclusions, reminiscent of LBs. Further investigation has found that the effects of rotenone are wide-spread, affecting 5-HTergic, noradrenergic and cholinergic systems (Hoglinger *et al.,* 2003). Paraquat, unlike rotenone, is not able to cross the BBB and administration to mice results in a milder phenotype with conflicting reports of the occurrence of DA neuronal loss and a general absence of behavioural abnormalities. While paraquat causes oxidative stress, it has been shown that recruitment of microglia is required for the degeneration of DA neurons suggesting an inflammatory response to be crucial in the degenerative process (Bové & Perier, 2011).

1.5.2 Genetic rodent models of Parkinson's disease

Numerous transgenic rodent models have been created which overexpress, modify or suppress particular PD-linked genes in an attempt to recapitulate features of PD. The expression of foreign genes in animals can be achieved by a number of methods all of which possess certain advantages and disadvantages. Dawson and colleagues (2010) highlight a number of key features which an ideal animal model of PD should possess. These include an age dependent, progressive degeneration of DA neurons of the SNpc along with motor dysfunction resembling the PD tetrad that is responsive to DA replacement therapy. Furthermore, one would expect to see the development of LBs and Lewy neurites positive for the protein α-synuclein and other ubiquitin-proteasome related proteins (Dawson *et al.,* 2010). One might add that the degeneration of the DA neurons should be, to at least some degree, more severe than neurodegeneration elsewhere in the brain and that the model accurately recapitulates non-motor PD symptoms. As of yet, no 'perfect' model of PD exists with each model possessing certain advantages and disadvantages.

Viral models of transgene expression are useful in that they are able to induce relatively dramatic cellular phenotypes in a short period of time, compared to that required when ageing a cohort of animals to late life time points. These models usually administer viral particles, such as adenoviral vectors, which induce the rapid expression of a transgene in the infected cells. In the case of PD

models, this administration tends to be delivered to either the striatum or the SNpc by stereotaxic injection (Lee *et al.,* 2010; Dusonchet *et al.,* 2011; Daher *et al.,* 2014). Many of the limitations of viral models are similar to those of acute toxic models. Specifically, the injection site has the effect of biasing the investigation towards a pre-defined brain region. Given the widespread pathology seen in PD, it is important to keep this selectivity in mind, an issue which has become evermore clear during the development of the Braak hypothesis (Braak *et al.,* 2003). Also, the rapid occurrence of events may make the causal progression of pathology difficult to determine. Finally, the observed pathology may not resemble the slow disease progression seen in human patients and is evidenced by the lack of *bone fide* LBs seen in transgenic models. It is important to note, however, that this criticism could also be levelled at all models attempting to recreate an end-of-life disease in rodents which have lifespans of only a few years.

An alternative approach to transgene expression is the expression of genetic constructs integrated permanently into the genome of the model animal. This can be achieved by pronuclear injection of the desired genetic material into fertilized cells at an early stage of embryonic development and the subsequent introduction of the developing embryo into a recipient female. Largely because of vector capacity restrictions, generated models have tended to utilise cDNA, driven, often, by foreign promoters (Chen *et al.,* 2012; Maekawa *et al.,* 2012; Herzig *et al.,* 2012; Chou *et al.,* 2014). More recently, however, tools such as yeast-, bacterial-P1- and bacterial-artificial chromosome technology (YACs, PACs and BACs), which possess a high cloning capacity, have allowed for the introduction of entire genes with endogenous regulatory sequences, including promoters, for accurate spatiotemporal expression (Li *et al.,* 2009; Janezic *et al.,* 2013; Cannon *et al.,* 2013). This approach allows for the expression of a transgene in the cell types and at the stage of development in which they would typically be expressed, causing a more unbiased, 'physiologically relevant' expression pattern and proper gene splicing.

The potential effectiveness of this approach to modelling PD is well illustrated by the numerous studies which have attempted to use wild-type or mutant α-synuclein expression to model AD PD

(see Chesselet & Richter, 2011 for a full review of α-synuclein rodent models). In particular, α-synuclein BAC transgenic mouse and rat models have been generated which develop many of the cardinal symptoms of PD, including motor and non-motor dysfunction, progressive loss of SNpc DA neurons, impaired DA function within the striatum and α-synuclein aggregation, though no LB pathology has been reported (Janezic *et al.,* 2013; Cannon *et al.,* 2013). The success of these models lends credence to the notion that elements of PD can be modelled using transgenic rodents, despite their relatively short life-spans compared to humans.

An issue with α-synuclein transgenic models of PD, which frequently utilise either α-synuclein mutation or truncation, is that occurrences of these genetic modifications in patients are extremely rare, potentially limiting the amount the data gained from them can be generalised to sporadic patients. Conversely, *LRRK2* mutations are comparatively common in sporadic PD patients and produce a highly similar pathological phenotype to patients (Gilks *et al.,* 2005; Healy *et al.,* 2008). These facts have made the generation of *LRRK2* rodents for modelling PD a top priority for research in recent years.

1.5.3 Rodent models of LRRK2 dysfunction

A multitude of *LRRK2* transgenic rodent models have been generated in recent years in an attempt to model PD (Table. 1.2). These models vary widely in numerous aspects, including the species and strain of animal, their use of foreign or endogenous promoters to drive transgene expression, their choice of *LRRK2* mutations, their use of the human or rodent *LRRK2* genes, their use of cDNA or the complete *LRRK2* genetic sequence and the nature of their subsequent characterisation of the model. Unsurprisingly, the models' reported phenotypes differ greatly, though they generally tend to be milder than those seen in α-synuclein overexpressing animals (Chesselet & Richter, 2011). This is likely exacerbated by the fact that, given the incomplete penetrance of *LRRK2* PD, it is probable that variation in genetic background may play a significant role in pathological development and the reduced aggressiveness of *LRRK2* pathology may make the task of driving disease development over a short period of time (~ 2-3 years) challenging. In addition to *LRRK2* transgenic models, a number of

rodent *Lrrk2* KO models have been generated which show little in the way of brain pathology but have granted some insight into LRRK2 function.

Table 1.2 An overview of previously generated *LRRK2* transgenic rodent models. ▲ = increased, ▼ = decreased, Δ = change. For the purposes of clarity, double-transgenics (LRRK2 and α-synuclein) and kinase dead-mutants have been excluded from this table. Abbreviations: end. = endogenous

Author/s	Species	Gene	Estimated expression level	Promoter	Max. age	Behaviour	Dopamine function	Neuropathology
Tsika *et al.*, 2014	Mouse	Human *LRRK2* cDNA (R1441C)	R1441C (1-2x end. LRRK2)	PDGFβ	< 22 months	No Δ in behaviour detected	No Δ in DA function detected	No SNpc neurodegeneration (neuronal changes reported), no pTau/ α-synuclein pathology
Longo *et al.*, 2014	Mouse	Whole mouse *Lrrk2* (G2019S) (same as Herzig *et al.,* 2011)	G2019S (1x end. LRRK2)	Mouse *Lrrk2*	< 19 months	**G2019S** ▼ Weight, ▲ locomotor activity (LRRK2 inhibitor rescue)	-	-
Sanchez *et al.*, 2014	Mouse (same as Li *et al.,* 2009)	Whole human *LRRK2* (R1441G)	R1441G (5-10x end. LRRK2)	Human *LRRK2*	< 6-8 Weeks	-	No Δ in DA function detected	-
Chou *et al.*, 2014	Mouse (same as Chen 2012)	Human *LRRK2* cDNA (G2019S, WT)	G2019S, WT (10x end. LRRK2)	CMVePDGFβ	< 9 months	**G2019S** ▼ Locomotor activity (L-DOPA rescue)	**G2019S** ▼ SNpc neuronal firing ▼ Striatal DA release	No SNpc neurodegeneration
Walker *et al.*, 2014	Rat	Whole human *LRRK2* (G2019S) (same BAC as Melrose *et al.,* 2010)	G2019S (2x end. LRRK2)	Human *LRRK2*	< 12 months	**G2019S** ▼ Motor co-ordination	No Δ in DA function detected	No SNpc neurodegeneration
Lee *et al.*, 2014	Rat	Whole human *LRRK2* (G2019S)	G2019S (5-8 x end. LRRK2)	Human *LRRK2*	< 12 months	**G2019S** ▼ Motor co-ordination ▲ locomotor activity	No Δ in DA function detected	No SNpc neurodegeneration (Δ neuronal morphology)
Bichler *et al.*, 2013	Mouse (same as Li *et al.,* 2009)	Whole human *LRRK2* (R1441G)	R1441G (5-10x end. LRRK2)	Human *LRRK2*	< 21 months	**R1441G** ▼ Locomotor activity ▼ gastrointestinal Function	-	-
Dranka *et al.*, 2013	Mouse (same as Li *et al.,* 2009)	Whole human *LRRK2* (R1441G)	R1441G (5-10x end. LRRK2)	Human *LRRK2*	< 16 months	**R1441G** ▼ Motor co-ordination (diapocynin rescue)	-	No SNpc neurodegeneration
Maekawa *et al.*, 2012	Mouse	Human *LRRK2* cDNA (I2020T)	I2020T (1.5x end. LRRK2)	CMV	< 18 months	**I2020T** ▼ Motor co-ordination ▲ locomotor activity	**I2020T** ▼ Striatal DA and metabolite content	No SNpc neurodegeneration (Δ neuronal morphology), No pTau/ α-synuclein pathology

Author/s	Species	Gene	Estimated expression level	Promoter	Max. age	Behaviour	Dopamine function	Neuropathology
Daher *et al.*, 2012	Mouse	Human *LRRK2* cDNA (G2019S)	G2019S (2-4x end. LRRK2)	CMVePDG Fβ	< 14 months	-	-	No SNpc neurodegeneration
Herzig *et al.*, 2012	Mouse	Human *LRRK2* cDNA (G2019S, WT)	G2019S, WT (3-5x end. LRRK2)	Mouse Thy1	< 28 months	**G2019S** ▲ Locomotor activity	-	No pTau/ α-synuclein pathology
Chen *et al.*, 2012	Mouse	Human *LRRK2* cDNA (G2019S, WT)	G2019S, WT (10x end. LRRK2)	CMVePDG Fβ	< 16 months	**G2019S** ▼ Motor co-ordination ▼ locomotor activity (L-DOPA rescue)	**G2019S** ▼ Striatal DA uptake	SNpc neurodegeneration at 12 and 16 months, **pTau pathology (G2019S),** no α-synuclein pathology
Gillardon *et al.*, 2012	Mouse (same as Li *et al.,* 2009)	Whole human LRRK2 (R1441G)	R1441G (5-10x end. LRRK2)	Human *LRRK2*	< 8 months	-	-	-
Herzig *et al.*, 2011	Mouse	Whole mouse *Lrrk2* (G2019S)	G2019S (1x end. LRRK2)	Mouse *Lrrk2*	< 26 months	No Δ in behaviour detected	No Δ in DA function detected	No SNpc neurodegeneration, No α-synuclein pathology
Ramonet *et al.*, 2011	Mouse	Human *LRRK2* cDNA (G2019S, R1441C, WT)	G2019S, R1441C, WT (3-5x end. LRRK2)	CMVePDG Fβ	< 24 months	**R1441C** ▼ Locomotor activity	**R1441C** ▼ Cortical DA and metabolite content	**SNpc neurodegeneration at 21 months (G2019S),** no pTau/ α-synuclein pathology
Zhou *et al.*, 2011	Rat	Human *LRRK2* cDNA (G2019S)	Similar for all genotypes	TRE promoter	< 18 months	**G2019S** ▲ Locomotor activity	**G2019S** (temporal) ▲ Striatal DA release	No SNpc neurodegeneration, no pTau/ α-synuclein pathology
Dusonchet *et al.*, 2011	Rat	Human *LRRK2* cDNA (G2019S, WT)	G2019S, WT (2x end. LRRK2)	Synapsin-1	< 6 weeks	-	-	**SNpc neurodegeneration following transduction, pTau pathology (G2019S, WT),** no α-synuclein pathology
Li *et al.*, 2010	Mouse	Whole mouse *Lrrk2* (G2019S or WT)	G2019S, WT (6x end. LRRK2)	Mouse *Lrrk2*	< 18 months	**WT** ▲ Motor co-ordination ▲ locomotor activity	**G2019S** ▼ Striatal DA release and reuptake, **WT** ▲ Striatal DA release	No SNpc neurodegeneration, no pTau/ α-synuclein pathology
Winner *et al.*, 2010	Mouse	Whole human *LRRK2* (G2019S) (same as Melrose *et al.,* 2010)	G2019S, WT (2-4x end. LRRK2)	Human *LRRK2*	< 4 months	-	-	-
Melrose *et al.*, 2010	Mouse	Whole human *LRRK2* (G2019S, WT)	G2019S, WT (2-4x end. LRRK2)	Human *LRRK2*	< 24 months	**WT** ▲ Exploration	**G2019S, WT** ▼ Striatal DA release **WT** ▲ D1 receptor levels	No SNpc neurodegeneration, **pTau pathology**, no α-synuclein pathology

Author/s	Species	Gene	Estimated expression level	Promoter	Max. age	Behaviour	Dopamine function	Neuropathology
Lee *et al.*, 2010	Mouse	Human *LRRK2* cDNA (WT, G2019S)	Similar for all genotypes	CMV	< 3 months	-	-	**SNpc neurodegeneration following transduction (G2019S)**
Tong *et al.*, 2009	Mouse	Whole mouse *Lrrk2* (R1441C)	R1441C (1x end. LRRK2)	Mouse *Lrrk2*	< 22 months	No Δ in behaviour detected	**R1441C** Impaired D2 receptor function	No SNpc neurodegeneration, no pTau/ α-synuclein pathology
Li *et al.*, 2009	Mouse	Whole human *LRRK2* (R1441G, WT)	R1441G, WT (5-10x end. LRRK2)	Human *LRRK2*	< 10 months	**R1441G** ▼ Locomotor activity (L-DOPA rescue)	**R1441G** ▼ Striatal DA release	No SNpc neurodegeneration (neuronal changes reported), **pTau pathology (R1441G),** no α-synuclein pathology
Lin, *et al.*, 2009	Mouse	Human *LRRK2* cDNA (G2019S, WT)	G2019S,WT (8-16x end. LRRK2)	CaMKII	< 20 months	**G2019S** ▼ Weight, ▲ locomotor activity	-	No SNpc neurodegeneration, No α-synuclein pathology

In the vast majority of mutant *LRRK2* rodent models, no neurodegeneration within the SNpc has been identified, either in R1441C/G (Li *et al.,* 2009; Lin *et al.,* 2009; Tong *et al.,* 2009; Dranka *et al.,* 2013), G2019S (Li *et al.,* 2010; Chou *et al.,* 2014) or I2020T (Maekawa *et al.,* 2012) mutations, despite the ageing of some models up to 24 months. This includes those using temporal expression in an attempt to eliminate compensatory effects during development (Zhou *et al.,* 2011). Several BAC transgenic models have shown a reduction in SNpc neuronal soma size and a reduction in TH-positive dendrites in the SNpr indicating, perhaps, the initial phases of a neurodegenerative phenotype (Li *et al.,* 2009; Lee *et al.,* 2014). More recent transgenic models have reported a small degree of progressive neurodegeneration but either employ heterologous promoters (Ramonet *et al.,* 2011; Chen *et al.,* 2012) or utilise viral transduction (Lee *et al.,* 2010; Dusonchet *et al.,* 2011). This may be a consequence of high levels of expression. Indeed, LRRK2 expression levels appear to correlate with the severity of phenotype, with knock-in animals showing more subtle phenotypes in general than those expressing higher levels of protein (Tong *et al.,* 2009; Li *et al.,* 2009; Longo *et al.,* 2014; Tsika *et al.,* 2014). Interestingly, the administration of LRRK2 kinase inhibitors has also been shown to attenuate the neurodegeneration caused by LRRK2 G2019S viral transduction, suggesting that the over activity of the kinase domain may underlie the pathological processes of PD development (Lee *et al.,* 2010).

Despite the usual absence of neurodegeneration within the SNpc, many of the *LRRK2* transgenic models report dysfunction within the DAergic system. While some studies report this dysfunction to be specific to the expression of mutant LRRK2, others report the overexpression of wild-type LRRK2 to cause DA transmission defects also (Melrose *et al.,* 2010). Several groups have reported, by microdialysis or voltammetry, reduced striatal DA release as a consequence of mutant LRRK2 expression (Li *et al.,* 2009; Li *et al.,* 2010; Chou *et al.,* 2014) while others have reported impaired DA reuptake (Zhou *et al.,* 2011; Chen *et al.,* 2012). These changes typically occur in the absence of any gross alterations to striatal DA and its metabolites or any proteins related to DA recycling such as

DAT or vesicular monoamine uptake transporter 2 (VMAT2) (Tong *et al.,* 2009; Li, *et al.,* 2010; Ramonet *et al.,* 2011; Zhou *et al.,* 2011; Chou, *et al.,* 2014) (although see Li *et al.,* 2010; Maekawa, *et al.,* 2012). Interestingly, changes in monoaminergic function (DA, 5-HT, noradrenalin) have been reported elsewhere in the brain, including cortical regions, suggesting the effects of LRRK2 dysfunction to be widespread (Ramonet *et al.,* 2011).

As further evidence of DAergic dysfunction, several studies have reported *ex vivo* changes to SNpc neuronal firing in mutant *LRRK2* tissue slices. Reduced firing was reported in patch clamp recordings of SNpc neurons of 8 month old G2019S animals (Chou *et al.,* 2014). Subtle changes in SNpc neuronal action potential characteristics upon exposure to DA have been also reported which were attributed to impaired D2 receptor function (Tong *et al.,* 2009). In support of this, changes in striatal D1 and D2 receptor densities and function in both wild-type and mutant LRRK2 overexpressing animals have been reported (Tong *et al.,* 2009; Melrose *et al.,* 2010) although it is unclear whether these changes are a downstream consequence of impaired DA release.

In 2009, Li and colleagues reported severe hypokinesia in BAC transgenic, 12 month old R1441G animals which could be rescued by L-DOPA or apomorphine administration. In support of this finding, other papers have also reported similar, albeit, less severe and later onset hypokinesia (Ramonet *et al.,* 2011; Chen *et al.,* 2012; Bichler *et al.,* 2013; Chou *et al.,* 2014). However, attempts to replicate the original results of near-total immobility from Li and colleagues (2009), even using the same animal line, have been unsuccessful (Bichler *et al.,* 2013; Dranka *et al.,* 2013). Instead, Bichler and colleagues (2013) report a later, more-mild locomotor defect than that found in the original paper. This may reflect the high level of sensitivity of the mutant LRRK2 phenotype to genetic background. Other papers have reported no detectable or a highly subtle locomotor phenotype (Tong *et al.,* 2009; Melrose *et al.,* 2010; Herzig *et al.,* 2011; Tsika *et al.,* 2014). In fact, many of the subsequent mutant models have reported hyperactivity and weight loss starting at early times in the lifespan of the animal and sometimes disappearing at later stages of life (Lin *et al.,* 2009; Li *et al.,*

2010; Zhou *et al.,* 2011; Herzig *et al.,* 2012; Longo *et al.,* 2014). Similarly, *Lrrk2* KO models have shown weight fluctuations and evidence of excessive grooming behaviour (Andre-Mateos *et al.,* 2009; Ness *et al.,* 2013).

Tests of motor co-ordination have indicated subtle or no impairments in mutant animals (Maekawa *et al.,* 2012; Herzig *et al.,* 2012; Dranka *et al.,* 2013, Walker *et al.,* 2014; Tsika *et al.,* 2014) and, while not as consistently assessed as motor dysfunction, these models show little evidence of non-motor phenotypes such as anxiety, depression, sensory and cognitive deficits (Tong *et al.,* 2009; Maekawa *et al.,* 2012; Herzig *et al.,* 2012; Bichler *et al.,* 2013) although Bichler and colleagues have reported a gastrointestinal functional deficit, emerging prior to motor symptoms.

It is not clear how important high LRRK2 levels within the SNpc are for driving motor dysfunction as models tend to report low levels of transgene expression (Lin, *et al.,* 2009; Ramonet, *et al.,* 2011). Nonetheless, in general, an increase or decrease in locomotor activity is paralleled by a directionally similar increase or decrease in reported DA release in the striatum (Li *et al.,* 2009; Li *et al.,* 2010; Chou *et al.,* 2014). The evidence that these motor deficits are caused by DA dysfunction is supported further by a number of studies which have demonstrated the ability to reverse these locomotor phenotypes using L-DOPA or DA agonists (Li *et al.,* 2009; Chen *et al.,* 2012; Chou *et al.,* 2014) (however, see Walker *et al.,* 2014).

Similarly to *LRRK2* transgenic rodent models, very little has been observed phenotypically in the studies of *Lrrk2* KO rodent brains thus far, be it neuronal loss or DA dysfunction (Andres-Mateos *et al.,* 2009; Lin *et al.,* 2009; Tong *et al.,* 2010; Daher *et al.,* 2014). Behavioural abnormalities are also rarely reported, with a single study reporting improved motor co-ordination and abnormal exploratory behaviours (Hinkle *et al.,* 2012). This finding of opposing effects of *Lrrk2* KO to *LRRK2* mutation is in line with findings that *Lrrk2* KO animals demonstrate opposite transcriptional responses to those of G2019S animals, supporting the notion that *LRRK2* mutation is a gain of

function mutation that is likely similar but exaggerated when compared to wild-type LRRK2 (Nikonova *et al.,* 2012).

In line with the frequent lack of neurodegeneration, the brains of *LRRK2* mutants show almost no signs of α-synuclein pathology (Tong *et al.,* 2009; Li *et al.,* 2010; Melrose *et al.,* 2010; Herzig *et al.,* 2011; Zhou *et al.,* 2011; Maekawa *et al.,* 2012; Dusonchet *et al.,* 2011; Ramonet *et al.,* 2011; Li *et al.,* 2009; Herzig *et al.,* 2009; Chen *et al.,* 2012). Interestingly, while KO animals show no accumulation of α-synuclein in the brain, studies have reported dramatic α-synuclein pathology in the kidneys along with substantial alterations in autophagic processes (Tong *et al.,* 2010). However, the specificity with which α-synuclein is affected in this process remains to be seen.

In an attempt to further explore the potential relationship between LRRK2 and α-synuclein, a number of studies have developed animals which overexpress A53T mutant α-synuclein, which promotes α-synuclein pathology, and examined the effect of either co-expression of mutant LRRK2 or *Lrrk2* KO on the progression of this pathology (Lin *et al.,* 2009; Daher *et al.,* 2012; Herzig *et al.,* 2012). Lin and colleagues (2009) found that co-expression of G2019S with A53T α-synuclein significantly enhanced striatal pathology, neurodegeneration and α-synuclein accumulation. Conversely, *Lrrk2* KO attenuated A53T α-synuclein neuronal loss (Lin *et al.,* 2009). While less dramatic, Daher and colleagues (2012) also reported a similar enhancement and amelioration of the A53T phenotype when expressed on a *LRRK2* G2019S or *Lrrk2* KO background, respectively. However, Herzig and colleagues (2012) found G2019S LRRK2 to have no effect upon A53T pathology.

A number of factors may explain the differences reported. In the Lin *et al.* (2009) study, levels of protein expression were high (LRRK2: 8-16x endogenous LRRK2, A53T: 30x endogenous α-synuclein). Secondly, substantial amounts of the effects of co-expression were not specific to mutant LRRK2; rather, wild-type and even kinase-dead LRRK2 produced similar effects to those of the G2019S mutant. This suggests that some of the results may reflect the effects of overexpression rather than

of the mutation. Finally, each study used a different promoter for the expression of the LRRK2 protein.

Although little α-synuclein pathology has been reported in these models, in line with post-mortem reports of abnormally phosphorylated tau in the brains of *LRRK2* PD patients, several *LRRK2* animal models report changes in tau phosphorylation at numerous residues throughout the brain, including the SNpc, often becoming elevated in an age-dependent fashion (Li *et al.,* 2010; Li *et al.,* 2009; Melrose *et al.,* 2010; Dusonchet *et al.,* 2011). Conversely, *Lrrk2* KO animal brains have been reported to show reduced tau phosphorylation (Gillardon, 2009). Potentially linked to altered tau regulation, a number of papers have also reported overexpression of wild-type or mutant LRRK2 to cause an increase in beta-tubulin polymerisation into microtubules (Lin *et al.,* 2009; Maekawa *et al.,* 2012) while *Lrrk2* KO decreases beta-tubulin polymerisation (Gillardon, 2009). Interestingly, these findings are often reported at early stages in the lifetime of the animal, suggesting potentially early signs of dysfunction.

Despite the consistent links drawn between autophagy and LRRK2 by *in vitro* studies, the evidence for autophagic changes within the brains of *LRRK2* mutants has been scant. A single study found, by transmission electron microscopy, enlarged autophagic vacuoles in the brains of over 20 month old G2019S animals (Ramonet *et al.,* 2011). Interestingly, while mutant *LRRK2* animals show almost no evidence of pathology, KO rats and mice show potent dysregulation of autophagic processes in organs such as the kidney and lungs (Tong *et al.,* 2010; Herzig *et al.,* 2011; Tong *et al.,* 2012). These changes appear to occur in a biphasic fashion in the kidneys which show enlargement followed by massive weight reduction in later life (Tong *et al.,* 2012). Similarly, although attempts to uncover elevated immune activity have revealed little, a growing amount of evidence suggests that LRRK2 may be involved with immune processes. This is supported by several studies which show elevated microglial activity and inflammatory responses in the brains of G2019S mice (Melrose *et al.,* 2010; Lee *et al.,* 2010) though the majority of studies report no changes in immune activity. Interestingly,

long term treatment of R1441G mice with the anti-inflammatory drug, diapocynin, has been shown to reverse the late-life motor deficits observed (Dranka *et al.,* 2013). Furthermore, a recent study showed *Lrrk2* KO to attenuate immune responses to lipopolysaccharide (LPS) or α-synuclein transduction which, in turn, prevented cell death within the SNpc, typically developed by this model (Dranka *et al.,* 2014).

In general, transgenic *LRRK2* models have shown a limited ability to model PD effectively. Mutations within the GTPase domain appear to cause a more severe pathology than those in the kinase domain although, as these mutations are rarely examined simultaneously, it is hard to draw firm conclusions. Data for the effects of wild-type LRRK2 expression are less consistent with some studies suggesting a milder but directionally similar effect to mutant LRRK2 and others suggesting an opposing effect. There also appears to be a degree of developmental compensation given that the post-developmental expression of LRRK2 appears to cause a more severe phenotype than that seen from constitutive expression (Zhou *et al.,* 2011). Still, there remain a great number of unanswered questions with regards to how the DAergic deficits are developed, why such little pathology is observed and why so much variation is seen in the resultant behavioural phenotypes.

1.6 Thesis goals and Chapter layout

1) Chapter 2 – An overview of the thesis methods

2) Chapter 3 – An initial molecular characterisation and selection of the human *LRRK2* BAC transgenic lines expressing either human wild-type (hWT) or G2019S or R1441C mutant forms of the gene for ageing

3) Chapter 4 - A behavioural, longitudinal characterisation of the *LRRK2* BAC transgenic lines including motor and non-motor assessments and the administration of L-DOPA

4) Chapter 5 – A neuropathological, longitudinal characterisation of the *LRRK2* BAC transgenic lines in an attempt to determine the loss of DA SNpc neurons and the presence of pathological PD features

5) Chapter 6 – An *in vitro* exploration of LRRK2 function and dysfunction using primary neuronal culture to investigate neuronal branching and the effects of LRRK2 upon autophagic function

6) Chapter 7 – Thesis discussion and future directions

CHAPTER 2 – METHODS

2.1 Animals and husbandry

2.1.1 Rats

Sprague Dawley (SD) rats were maintained in accordance with the UK Home Office regulations, under the Animals (Scientific Procedures) Act of 1986. Animals were group-housed in (55x40 cm) cages with bedding and had constant access to food and water. Animals were fed RM1 diet (Special Diets Services). Room atmosphere was maintained at 22 °C at 60-70% humidity and animals were kept in a 12 hour light/dark cycle. Schedule 1 killing was performed either by cervical dislocation or rising concentrations of CO_2 (confirmed by cervical dislocation). Experimental animals were matched for age and all experiments were conducted in the light cycle.

2.2 Genotyping and line classification

2.2.1 DNA extraction from tissue clips

Ear or tail clips were incubated in 450 µl homemade lysis buffer (50 mM KCl, 1.5 mM MgCl2, 10 mM Tris, 0.45% NP4O, 0.45% Tween-20 and 0.5 mg/ml proteinase K (pH 8.5)) for 3 hours at 56 °C and at 95 °C for 20 mins to deactivate the proteinase K. For experiments requiring purified DNA (e.g. restriction digest), DNA was extracted using an Illustra tissue and cell genomic Prep Mini Spin Kit (GE Healthcare).

2.2.2 Polymerase chain reaction for genotyping

Polymerase chain reaction (PCR) was performed for the purposes of genotyping (see Table 2.1 and Fig. 2.1 for genotyping PCR components and programme). Human specific primers were designed for each exon of the *LRRK2* transgene in addition to the yellow fluorescent protein (YPet) tag, upstream and downstream sequences (Table 2.2). After confirmation of the presence of the complete *LRRK2* gene in a line, genotyping was restricted to primers targeting exons 8, 20 and 38. PCR products were separated using an agarose gel (1% agarose, 0.005% ethidium bromide in Tris/Borate/

ethylenediaminetetraacetic acid (EDTA) (TBE) buffer) in TBE buffer at 100 V. Gels were imaged using the GelDoc XR system (BioRad).

Table 2.1. Components of genotyping PCR solution.

Genotyping PCR	
Reaction Components	**Volume (µl)**
Genomic DNA	5
10x Buffer	1.5
$MgCl_2$	0.9
dNTP	0.75
Forward primer (10 µM)	1.5
Reverse primer (10 µM)	1.5
Q-solution	3
Ampli Taq-Gold DNA-Polymerase	0.2
MilliQ H_20	0.65

PCR conditions

95 °C 10 mins

95 °C 30 seconds
58 °C 30 seconds } x34 cycles
72 °C 2 mins

72 °C 8 mins

Figure 2.1. PCR conditions for genotyping protocol.

Table 2.2. **Primer sequences targeting each exon of the *LRRK2* transgene.**

Target	Sense Oligo Sequence (5' to 3')	Anti-Sense Oligo Sequence (5' to 3')
Rat Prolactin	GCTTCTGAGCAATGACACCA	ATTCCAGGAGTGCACCAAAC
10 kb+ Upstream	CCAAGCTGTGCTCTGACTACC	GGCTCAAGGGAACTAACAAGG
15 kb+ Upstream	GCACAGTTCTGAGATACAAACCAG	GAAGCAGGATAAGCTAGTAAACAGG
20 kb+ Upstream	TGCTACTTCTGCCAACTACCC	CCCCTGTTGATTGCAGATTG
Downstream Junction	TTTGGCCCTGACCAGTATTC	GCTGCTGTTTAGGGATCTGC
LRRK2 Exon 01	GATAGAAACGCTGGTCCAAATC	CTTTACCTGCTGCACACTCG
LRRK2 Exon 02	GCCTCTGTTGATCGTCTTGG	GGACATGCTCTGTATTGGGAAG
LRRK2 Exon 03	GTCCAGGTACAATGCAAAGC	CAAGGGAAGGTTGTCATGTG
LRRK2 Exon 04	CCAGTGTAAACTTGTCAGTGATTG	GGCTGTCCCATCACTAGGTC
LRRK2 Exon 05	CAGAAACTTGGATGCAAAGC	GGCCAGGCTATGAAATGC
LRRK2 Exon 06	AGAGGAGCAACTGACTGAATTTG	GCTAAGAGACACTGCCTCACTTC
LRRK2 Exon 07	GTCCTCATGAGTGGCAATGTC	GGGATTTTACAATATTTTCATTCAAAG
LRRK2 Exon 08	AAAGCTGTGCAGCAGTACCC	CACAGGACAGAAAAGGCATTG
LRRK2 Exon 09	TTTGGCTGGAAGCCTGTTAC	CATGAATTACCAAATGACCCTTG
LRRK2 Exon 10	TGCTGGGCACTAAATAATCTCC	CTGCTGGCTAGTCACCATAGAAG
LRRK2 Exon 11	TCCCAGCTCATAGGGAAGTG	CATGGCCCACTGCTTACC
LRRK2 Exon 12	CTCCTGAAGTGGCTGAAAGTG	ACGAGATTACATTGCAAAATGC
LRRK2 Exon 13	TGGATATAATGGCAGCAGTGG	GGAAGAGAACAGGTATGAAAATTAGC
LRRK2 Exon 14	AGAAGAATCCAGGGAGGATACAG	CCAGCATGACTCACAAGGTC
LRRK2 Exon 15	GAAATCCTGGGATTCAGAAATG	GTCACCAGCTAATGCCCTAC
LRRK2 Exon 16	GTTCATAGGAACTGGACATCTGC	CTGCTCCAAAAGTGAAATTCG
LRRK2 Exon 17	TTAGCAATCCTCAAATTGTCAGC	CACAAACAATTGCAATAAACTGG
LRRK2 Exon 18	CCTCTGTTGCAAGTGTTTTGC	GTGGAGTGTATCTGGAGACTAAGTTG
LRRK2 Exon 19	GCCAGATCATCAGCTTGCTC	GGCTTAAGGTCCCTCAAACTG
LRRK2 Exon 20	GCTGTGGAAGAAGGAACAGC	CAGATGATTTAGGTCAGGTTTTTG
LRRK2 Exon 21	GAAGTGAAGGCTCATTTCTTGTG	GGACCAACCCACACCATTAG
LRRK2 Exon 22	CCCATTTTTGATCATGAAGATTTAC	GCAATCAGGCTTTCTTCAAGG
LRRK2 Exon 23	GATGCCCTAAGCCAGAAATG	GAGGCACGGGGGACTTATC
LRRK2 Exon 24	GAAATGACATTGGACCCTCAG	CACCATGTTGTTAAAACTCATTGC
LRRK2 Exon 25	TATGCTCCCCCTTGAGACTG	GTTTCACTGCCCTAAAAATCCTC
LRRK2 Exon 26	TTGCCTCCTTCTATGACAATCC	CCCCCAAAATTTCACTCAAAC
LRRK2 Exon 27	TGCGGTCTTTAGATATGAGCAG	GTGGCAATAATCGTCTTACCTC
LRRK2 Exon 28	TCCTCCTGAGATTGGCTGTC	CAATATATGTCCATCAAAGTCACAGAG
LRRK2 Exon 29	GCTGTGCCTTATAACCGAATG	CAGCAACCGATCAAAGTACC
LRRK2 Exon 30	GTACTCATCCCCATTTTATGACG	CCAATAACATTCACCAACATGG
LRRK2 Exon 31	GATGAGAAGCAACGCAAAGC	CCCACAATTTTAAGTGAGTTGC
LRRK2 Exon 32	ATCGGAGCGTAAAAATGTGC	GTGGCCTATTAAAGAACCGTATG
LRRK2 Exon 33	TTCATTTTCAAGACCCAGCAC	CTAGATAGAGGTTTCACAGGCTCAG
LRRK2 Exon 34	GGGCATTATTTCGCGTAGAG	GTGTCAGATGCAATGTTTTATTCC
LRRK2 Exon 35	CCAATGGGATTTTGGTCAAG	GCCTACTCCAAGGTTTTATGAGC
LRRK2 Exon 36	ATTGGCGACAAGGCATTTAC	GCTCAACACCTTGTCTAAACCTC
LRRK2 Exon 37	TTCTTTTGGGCCAAGTTGTG	GTGGTTGGTATTCCGGTTTC
LRRK2 Exon 38	CTCAGATTGCCCCTGACTTG	GGCTGCTTCACTTAACTCACC
LRRK2 Exon 39	TGATGGCAGTTTTGGATCAG	CAAAACTTTCTACTCCACAACGAA
LRRK2 Exon 40	CACCCCAGTTTGATATCTTTGC	GGCACAGTGTTACTGGGAAG

LRRK2 Exon 41	AGACCTGAAACCCCACAATG	CTGAATTTGATTTGCCTCACA
LRRK2 Exon 42	GGTTTCGTGCACCTGAAG	CCAAATGTGGAGTTCTAACAGC
LRRK2 Exon 43	CCAGTTAAAGAATATGGTTGTGC	GTGCCTGGGATGGTGAAAAT
LRRK2 Exon 44	CAGCTGAATTAGTCTGTCTGACG	CTGTCCTCTGTCGGTGTGC
LRRK2 Exon 45	TCCTGGTCATCAATACCGAAG	GGTATGTTTAAGCCTGGCACA
LRRK2 Exon 46	AACCGCTGATGGCAAGTTAG	GTTAATGGCAAGCCATATTTAAAAC
LRRK2 Exon 47	GGATGTGGCACAAAGATTTTC	CTTAAAAATACCCTTCTGCTTTCTG
LRRK2 Exon 48	TTATGCAGCTTTCAGTGATTCC	CCTCTGTGACACATGAAGTGC
LRRK2 Exon 49	TCTTATTCTGGGAGAGTGAAAACC	CAAACATTTTCTTTATTTTCTTTGCTC
LRRK2 Exon 50	GGGCTACAACCGGAAAAATAC	GGTTGAGCTAGTGATTGACACC
LRRK2 Exon 51a	TTTGAACAGTGTTTGAAAAAGC	GATGTCCCAAACGGTCAAG
LRRK2 Exon 51b	TGCTGCAGATCCTACATCATTC	GGTATTTGGCCCTGATACTCC

2.2.3 Restriction digests

Regions of genomic DNA were amplified by PCR (using the method detailed in section 2.2.2), using primer pairs corresponding to regions containing the sites of mutations (R1441C/G2019S) (Table 2.3). PCR products were then digested using the enzymes and protocols detailed below (Table 2.4 and 2.5). Digest products were separated and visualised as described for normal genotyping.

Table 2.3. Primer sequences targeting regions containing mutation sites of *LRRK2* transgene.

Target	Sense Oligo Sequence (5' to 3')	Anti-Sense Oligo Sequence (5' to 3')
LRRK2 Exon 31 (mutation site)	AAGGCATGAAGATGGGAAAG	TGATGGTTTTCCGAAGTTTTG
LRRK2 Exon 41 (mutation site)	AAGGGACAAAGTGAGCACAG	TTTTTGCCCTGAAAAATTACATC

Table 2.4. PCR components and conditions for G2019S mutation restriction digest protocol.

G2019S (exon 41)	
Reaction components	**Volume (µl)**
PCR product	10
Buffer 3	1.25
BSA x 100	0.125
BceA1 enzyme	0.75
H_20	0.375
	37 ^oC for 3 hours

Table 2.5. PCR components and conditions for R1441C mutation restriction digest protocol.

R1441C (exon 31)	
Reaction components	**Volume (µl)**
PCR product	10
Buffer 2	1.25
BstU1	0.25
H_20	1
	60 ^oC for 1 hour

2.2.4 Quantitative PCR

Tail clips were taken from rats and genomic DNA was extracted using Illustra tissue and cell genomic Prep Mini Spin Kit (GE Healthcare). Quantitative PCR (QPCR) was then performed using SYBR Green (Invitrogen) (Table 2.6). Copy thresholds for YPet (the transgene tag) for each sample of genomic DNA were established and normalised against β–actin (Table 2.7).

Table 2.6. PCR components for transgene QPCR.

SYBR Green QPCR	
Reaction Components	**Volume (µl)**
Genomic DNA	5
Forward Primer	3.5
Reverse Primer	3.5
H_20	13
SYBR Green Master Mix	25

Table 2.7. Primer sequences for transgene QPCR.

Target	Sense Oligo Sequence (5' to 3')	Anti-Sense Oligo Sequence (5' to 3')
β-Actin	CAGAAGGGACACCGTAGAGG	ACACCCTAGGCGGAAAGTTA
YPet	CATGAAGCAGCACGACTTCT	GTCTTGTAGTTGCCGTCGTC

2.3 Fluorescent in-situ hybridization analysis

2.3.1 Generation of fibroblasts from tissue

Ear clips were taken from founder rat progeny. Tissue was transported in ice cold Dulbecco's modified eagle medium (DMEM)-complete (DMEM, 2 mM L-glutamine, 2 mM penicillin/streptomycin, 5% FBS), briefly washed with 70% ethanol and placed in Hank's balanced salt solution with calcium and magnesium (HBSS +/+). Tissue was shredded using forceps and resuspended in 1 ml HBSS+/+ containing 1 mg/ml collagenase. Tissue was incubated at 37 ^{o}C for 25 mins and centrifuged at 2000 rpm for 5 mins. Tissue was resuspended in 0.05% trypsin-EDTA and incubated at 37 ^{o}C for 20 mins. Finally, tissue was resuspended in DMEM-complete and plated in a 6-well plate for culture. Once confluent, fibroblasts were transferred to T25 and, once again confluent, T75 flasks. Transgene probes were provided by Dr Javier Alegre Abarrategui and fluorescent in-situ hybridization analysis (FISH) was performed by the Wellcome Trust Centre for Human Genetics Microscopy Core; Oxford, UK.

2.4 Immunohistochemistry

2.4.1 Transcardial perfusion

Rats were anaesthetised using 4.16 ml/kg Ketoset (85%)/Xylazine (15%) and perfused with 30 ml 0.2 M phosphate buffer (PB) followed by 50 ml 4% paraformaldehyde (PFA) in 2 M PB. Brains were removed and placed in 4% PFA at 4 °C.

2.4.2 Free floating tissue staining

Tissue preparation and treatment

Fixed brains were transferred to 30% sucrose in phosphate buffered saline (PBS) for 48 hours at 4 °C prior to slicing using a freezing microtome (Leica). Tissue was frozen using dry ice and sectioned at a

thickness of 35 µm (unless specified otherwise) into PBS with 2 mM sodium azide for storage at 4 °C. In the cases when antigen retrieval was necessary, prior to staining, sections were incubated in 70 °C citrate buffer (pH 6.0) for 30 mins and then cooled to 25 °C before washing in tris-buffered saline (TBS) (3x10 mins). All free-floating tissue was incubated using an orbital shaker (Stuart Scientific).

Peroxidase Immunohistochemistry

Free-floating sections were washed in TBS (3x10 mins) and incubated in 3% H_2O_2 in TBS for 10 mins. Tissue was then washed in TBS (3x10 mins) and blocked in 10% normal goat/donkey serum (NGS/NDS) in TBS plus 0.15% triton X-100 (TBS-T) for 60 mins. Next, sections were incubated in primary antibody (Table 2.8) overnight in blocking solution. Next, tissue was washed in TBS (3x10 mins) and incubated in biotin-SP-conjugated secondary antibody (1 in 200) (Vectorlabs) in blocking solution for 60 mins. Sections were then washed in TBS-T (3x10 mins). Tissue was then incubated in avidin-biotin-peroxidase complex (ABC) solution (Vectorlabs) in TBS-T for one hour. Following this, tissue was washed in TBS-T (3x10 mins) and incubated in 3,3'-diaminobenzidine (DAB) solution (Thermo Scientific Pierce), washed in TBS-T (3x10 mins) and left to dry on SuperFrost Plus slides (VWR International) overnight**.**

Hematoxylin counterstaining and tissue dehydration

Dry, peroxidase-stained tissue was incubated in hematoxylin QS solution (Vector) for 30 seconds, followed by 2x15 second washes with RO (reverse osmosis) water. The sections were then immediately dehydrated by immersion in the following: 1 min 50% ethanol, 1 min 70% ethanol, 1 min 95% ethanol, 2x1 min 100% ethanol, 1 min 50/50 ethanol/xylenes, 2x 2 mins xylenes. After the final xylene treatment, slides were coverslipped using DPX mountant (Fluka Biochemika).

Immunofluorescence

Free floating sections were washed in PBS (3x10 mins). Sections were then treated with 50 mM glycine in PBS for 15 mins and then washed in PBS (3x10 mins). Next, sections were blocked in PBS+ (PBS, 1% fish gelatine, 0.1% triton X-100, 10% NGS/NDS) for 60 mins. Sections were then incubated

in primary antibodies in PBS+ overnight at 4 °C. Next, sections were washed in PBS-T (PBS plus 0.1% triton X-100; 3x10 mins) and incubated in Alexa Fluor fluorescent secondary antibodies (Life Technologies) (1 in 200) for one hour in PBS+. Sections were washed in PBS-T (3x10 mins), incubated in 4',6-diamidino-2-phenylindole (DAPI) (1 in 2000) for 10 mins and then washed in PBS-T (3x10 mins). Sections were then mounted on SuperFrost Plus slides and cover-slipped using FluoroMount (Sigma-Aldrich).

2.4.3 Paraffin embedded tissue staining

Tissue embedding

Fixed brains were paraffin-embedded using a Shandon Excelsior (Thermo). The following steps were taken during the embedding process under vacuum conditions: 90 mins 70% ethanol, 90 mins 80% ethanol, 90 mins 90% ethanol, 3x90 mins 100% ethanol, 2x90 mins Histoclear (Fisher), 120 mins Histoclear, 2x60 mins paraffin wax, 120 mins paraffin wax. Paraffin blocks were sectioned at 4 µm using a microtome and mounted on slides. (Paraffin embedding was performed by Richard Stillion of Sir William Dunn School of Pathology, Oxford).

Tissue rehydration, staining, counterstaining and dehydration

Paraffin embedded tissue was rehydrated by immersion in the following: 2 mins xylenes, 2 mins Histoclear, 2 mins 100% ethanol, 2x2 mins 95% ethanol, 2 mins 70% ethanol, 3x2 mins dH_2O. Tissue was then incubated in 3% H_2O_2 in PBS for 1 hour and then rinsed for 5 mins with tap water. Antigen retrieval was then performed using either pH 6.0 citrate buffer at 100 °C (heat mediated antigen retrieval). Tissue was then washed 3x in PBS and blocked in 10% normal goat/donkey serum in TBS-T for 60 mins. Sections were then incubated in primary antibody (Table 2.8) overnight in blocking solution. Next, tissue was washed in TBS (3x10 mins) and incubated in biotin-SP-conjugated secondary antibody (1 in 200) (Vectorlabs) in blocking solution for 60 mins. Tissue was then washed in TBS-T (3x10 mins). Next, tissue was incubated in ABC solution (Thermo Scientific Pierce) in TBS-T for one hour. Tissue was then washed in TBS-T (3x10 mins) and incubated in DAB solution (Thermo

Scientific Pierce) and washed again in TBS-T (3x10 mins). Following this, tissue was incubated for 5 mins in hematoxylin QS solution followed by 5 washes with dH_2O. Tissue was then dehydrated using the following steps: 2 mins 70% ethanol, 2 mins 95% ethanol, 2 mins 100% ethanol, 2 mins xylenes. After the final xylene treatment, slides were coverslipped using DPX mountant.

2.4.4 Microscopy for immunohistochemistry and immunofluorescence staining

DAB-stained tissue was visualised using a Leica DMR light microscope and captured using a Nikon DS-Fi1 camera. Immunofluorescence microscopy was performed using an EVOS FLAuto automated fluorescent microscope.

2.5 Protein biochemistry

2.5.1 Tissue homogenization

Following schedule 1 killing, brains were removed from animals and frozen on dry ice. Tissue was then homogenised on ice using a tissue tearer (Biospec Products) in radio-immunoprecipitation buffer (RIPA) buffer (50 mM Tris, 150 mM NaCl, 0.1% sodium dodecyl sulphate (SDS), 0.5.% Na deoxycholate, 1% Igepal (pH 7.4)) containing protease (cOmplete EDTA-free, Roche) and phosphatase (PhosSTOP, Roche) inhibitors. Tissue homogenates were then centrifuged at 5,000 rpm at 4 °C. Both the supernatant and the pellet were separated and stored at -80 °C.

2.5.2 Cellular lysis

For the *in vitro* cellular lysis, cells were washed 3x in PBS and then scraped on ice in 5 ml PBS. Cells were centrifuged at 900 g for 10 mins at 4 °C. The supernatants were then removed and the pellets frozen on dry ice. Pellets were then resuspended in 200 µl of RIPA buffer. Lysates were centrifuged at 1000 g at 4 °C for 5 mins. Supernatants were retained and stored at -80 °C.

2.5.3 Protein quantification and sample preparation

Protein concentration in tissue homogenate or cell lysate was quantified by the bicinchoninic acid (BCA) assay. Bovine serum albumin samples (BSA) of increasing concentrations ranging from 0-2000 µg/ml were used as protein standards. Samples were diluted in order to fall into this concentration range. 10 µl of samples were added, in triplicate, to 100 µl of a 1:50 solution of copper sulphate: BCA solution (Sigma). Samples were then incubated at 37 °C for 30 mins. Following incubation, absorbance at 562 nm was measured using a Synergy HT microplate reader (Biotek). Once quantified, samples were reduced and denatured using Laemmli sample buffer (60 mM Tris pH 6.8, 2% SDS, 10% glycerol, 5% β-mercaptoethanol, 0.01% bromophenol blue) at 95 °C for 5 mins (unless stated otherwise).

2.5.4 Western blotting

Typically, 20 µg of protein was loaded onto gels and Spectra Multicolor Broad Range Protein Ladder (Thermo Scientific) was used to determine target protein weight. Samples were loaded into 4–15% Criterion Tris-HCl polyacrylamide gels (BioRad), electrophoresis was performed at 150 V for ~1 hour and proteins were then transferred to a polyvinylidene fluoride (PVDF) membrane using a Trans-Blot Turbo Transfer System (BioRad) which utilises Trans-Blot Turbo Midi PVDF transfer packs (BioRad), in accordance with manufacturer instructions. Membranes were blocked in 5% non-fat milk (Sigma) in TBS plus 0.1% tween (TBS-Tw) for 60 mins and subsequently incubated in primary antibody (see Table 2.8) in blocking solution overnight at 4 °C**.** Membranes were washed in TBS-Tw (5x10 mins) and incubated in horseradish peroxidise (HRP)-conjugated secondary antibody (1 in 5000) (BioRad) in blocking solution for 60 mins. Membranes were washed in TBS-Tw (5x10 mins) and developed using ECL solution (Milipore). Western blots were imaged using the GelDoc XR system (BioRad) and were quantified using densitometry performed using ImageJ.

2.6 Behavioural testing

All behavioural testing was performed in a blinded fashion. All tests were conducted in normal lighting conditions unless otherwise specified. The time of day and room temperature for experimental procedures was also controlled. Both sexes were used for experiments unless otherwise indicated. Rats were used at two ages: young (3-6 months) and aged (18-21 months). Females were used exclusively for the balance and grip test given the large size of aged old male rats (~1000 g).

2.6.1 Weighing and general observation

Rats were weighed prior to undergoing a battery of experiments. Animals were also observed for any overt behavioural abnormalities.

2.6.2 Accelerating rotarod

The rotarod is used to assess motor co-ordination, balance and motor learning (Deacon, 2013). Female rats were placed on the accelerating rotarod (Ugo Basile 7700), revolving at 4 rpm, facing away from the experimenter. After 10 seconds, to allow for stabilisation, the rotor speed was incrementally increased from 4-40 rpm over the course of 300 seconds. Latency to fall from the rotarod was recorded. If animals fell before 10 seconds, they would be placed back on the rotarod. Animals underwent 3 consecutive trials per day and were tested on three consecutive days. The mean performance on each day was calculated.

2.6.3 Static rod

The static rod (or balance beam) is used to assess fine motor coordination and balance (Deacon, 2013). Female rats were placed on a 35 mm diameter, wooden static rod attached, at the opposite end, to a target platform. The beam was suspended roughly 100 cm above a cushioned surface. Animals were placed facing away from the target platform and were required to turn and traverse the rod. The ability of rats to balance independently was ensured before beginning a trial. The rats'

ability to both successfully turn and traverse the beam was video-recorded and marked following experimentation.

2.6.4 Locomotor activity

Rats were placed in transparent cages (47x25 cm) with minimal bedding and no access to food or water. Locomotor activity was assessed using the Photobeam Activity System (San Diego Instruments) which uses an automated infrared beam array system to detect ambulations over the course of 4 hours. The proportion of ambulations within the centre versus the periphery of the cage was also recorded.

2.6.5 Inverted grid

Grip strength was assessed using the inverted grid test. Rats were placed on a 45x45 cm wire grid with wires 1.2 cm apart. The grid was held roughly 50 cm above a cushioned surface and was inverted, with the rat's head dropping first. The grid was then held stably until the rats released their grip.

2.6.6 Catwalk

A variety of gait parameters were assessed using the Noldus Catwalk (Noldus Information Technology). The Catwalk allows for the accurate video recording and subsequent evaluation of animals while traversing a glass panel (Fig. 2.2). To ensure consistent data collection, a number of parameters were set and had to be met for a run to be accepted. Acceptable runs had to be complete within 0.5-5 seconds and show a maximum variance in velocity of 35%. Animals were required to perform a minimum of 5 trial runs consistent with the run criteria before data analysis was performed. Analysis was performed using Catwalk XT (v8.1; Noldus). Video scoring was performed in a semi-automated fashion. Fore- and hind-limbs were labelled by the automated tagging of video recordings and gait parameters corresponding to the mean of the trial runs were

consequently calculated. Runs where limbs could not be differentiated by the software from the animal torso were discarded.

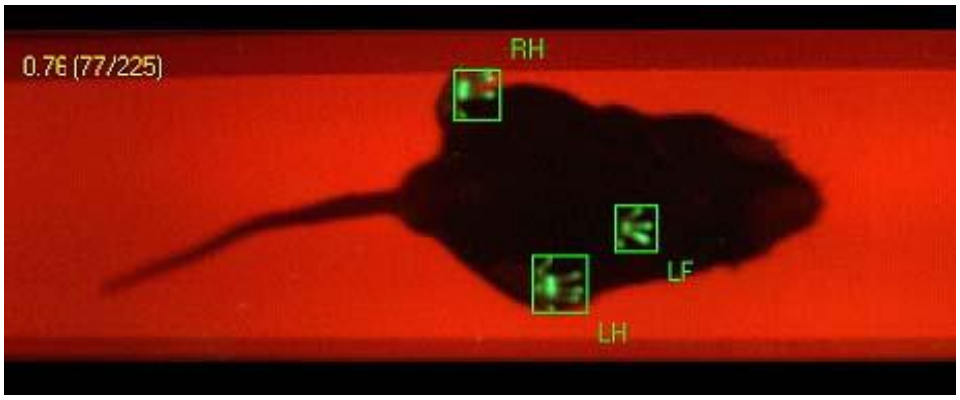

Figure 2.2. An example of Catwalk gait analysis. Animals spontaneously traverse a glass panel lit from below. Animal contact with the glass causes light to be reflected down to a camera where data are recorded. Catwalk XT (v8.1) software allows for the semi-automated labelling of paw-prints and the subsequent extraction of inter- and intra-paw parameters for gait analysis. RH= Right hind paw, LF= Left forepaw, LH= Left hind paw.

The Catwalk allows numerous gait parameters to be assessed. However, we restricted our analysis to parameters which were deemed relevant to the locomotor dysfunction seen in PD (based on Chuang *et al.,* 2010).

● **Stride Length (m) -** The distance between two consecutive placements of the same paw.

● **Intensity -** A measure of paw pressure on the glass panel.

● **Swing speed (m/s) -** The velocity of a moving limb during the swing phase.

● **Phase Dispersion -** The temporal relationship between the placements of two paws over the course of a run. Phase dispersion gives a measure of inter-limb coordination .

● **Base of Support (cm) -** The distance between fore or hind-limbs. This is calculated by determining the mid-points of mass between the two limbs.

● **Max Contact Area (cm^2) -** The maximum size of the paw print area in contact with the glass over the course of a run.

2.6.7 Stool collection

Animals were placed in transparent cages (47x25 cm) without bedding, food or water. Faecal pellets produced over the course of 60 mins were immediately collected in falcon tubes after expulsion. The frequency and mean weight of the pellets were determined. Pellets were then dried at 50 °C for 50 hours and reweighed to determine water content.

2.6.8 Spontaneous alternation

Spontaneous alternation within a T-maze was performed as an assessment of cognitive function as detailed in Deacon and Rawlins, 2006. Briefly, animals were placed, facing away from the goal arms, in the base of a T-maze (72x65 cm), partitioned using a guillotine door. Removal of the door allowed a choice of one of two arms. Once in a goal arm, animals were trapped for 30 seconds and subsequently returned to the start arm. The experiment was then repeated and the choice of the goal arm upon the second attempt (same or different to the first trial) and the time taken for the choice to be made was recorded.

2.6.9 Cylinder test

The cylinder test is typically used to assess locomotor asymmetry in 6-OHDA lesioned rodents but rearing within a cylinder has previously been used to assess motor deficits in *LRRK2* mouse models (Li *et al.,* 2009; Walker *et al.,* 2014). Rats were placed in an empty transparent cylinder (16 cm diameter, 26 cm height) and video-recorded from below. The number of rears within the cylinder over a period of 300 seconds was recorded. A rear was counted as any time both forepaws left the cylinder base, either/both made contact with the cylinder walls and then both returned to the base. The amount of time animals spent grooming was also recorded.

2.7 L-DOPA administration

Animals were administered with 10 mg/kg benzerazide IP followed 30 mins later with 25 mg/kg IP L-DOPA. As a control, a second cohort was given equivalent volumes of saline. Animals were randomly

assigned either L-DOPA or saline treatment. Animals were subjected to behavioural testing 60 mins after L-DOPA administration. Administration and testing were staggered between animals to keep consistent times between treatment and testing. Animals receiving L-DOPA performed the cylinder test, immediately followed by the rotarod test.

2.7.1 L-DOPA administration for cylinder test

Treated animals were subjected to the cylinder test as described in section 2.6.9. Rears in the cylinder following L-DOPA administration were normalised to the animals' previous non-treated performance.

2.7.2 L-DOPA administration for rotarod test

Animals were trained on the rotarod for 5 days, three trials per day, prior to L-DOPA administration, to eliminate the effects of motor learning. Treated animals were subjected to the rotarod test as described in section 2.6.2. Performance on the rotarod following L-DOPA administration was normalised to the previous day's performance.

2.8 Stereology

2.8.1 Tissue preparation

Tissue was sectioned at 50 µm, peroxidase-stained for tyrosine hydroxylase (TH) and counterstained with hematoxylin as described in section 2.4.2.

2.8.2 Stereological cell counting

TH-positive neurons of the SNpc were counted using an unbiased, online counting optional fractionator method using Stereo Investigator software (MicroBrightfield). Cells were counted using a Zeiss Imager M2 light microscope at 40X magnification using a randomly placed counting frame of 50x50 µm on a sample grid of 160 x 160 µm. A 22 µm optical dissector with ±2 µm guard zones was used. Sub-regions of the SNpc (lateral, dorsal, medial) were determined for counting using the

Paxinos & Watson Rat Brain Atlas (6th edition). Neuronal nuclei were differentiated from other cellular nuclei based on morphology. Estimations of TH-positive SNpc cells and neuronal nuclei were performed in every 3rd section from Bregma -4.56 mm to -6.48 mm.

2.9 Neuronal culture

2.9.1 Breeding and genotyping from tail clips

Transgenic male rats were bred with a pair of SD female rats as normal to produce litters. P0-3 rats were tail clipped and marked for genotyping. A minimum of 3 animals were pooled for each experiment. Tail clips were processed and genotyped, as described, with the standard genotyping protocol (Section 2.2).

2.9.2 Generation of neuronal cultures

Genotyped P0-3 rats were chilled on ice and then decapitated. Heads were transported in ice cold HBSS +/+. Cortical areas were removed, shredded and collected in ice cold HBSS +/+. Tissue was then incubated at 37 °C in neurobasal-A medium (Life Technologies) plus 0.5% trypsin for 20 mins. Tissue was then incubated briefly in neurobasal-A medium plus 5% foetal bovine serum (FBS) at 37 °C. Medium was then replaced with 5-10 ml neuronal medium (neurobasal-A medium, 1 mM Na Pyruvate, 2 mM Penicillin/Streptomycin, 2 mM L-Glutamine, B27 with antioxidants (Life Technologies)). Tissue was triturated first (7x) using 10 ml stripettes and then (7x) with fire-polished glass pipettes. Cells were counted using trypan blue and plated (unless stated otherwise) at 200,000/400,00 cells per well respectively in 24/12 well plates on Geltrex (Life Technologies)-coated cover slips. 50% of medium was replaced every 3-4 days with neuronal medium.

2.9.3 Fixation of cells for immunocytochemistry

Cells were washed 3x with PBS and incubated in 4% PFA for 10-15 mins. Cells were then washed 3x with PBS and blocked with PBS-T plus 10% NGS/NDS for 1 hour. Cells were then incubated in primary antibody (Table 2.8) at 4 °C overnight in blocking solution. Cells were then washed 3x with PBS-T and

incubated with Alexa Fluor fluorescent secondary antibodies (Life Technologies) (1 in 200) for 1 hour. Cells were washed 3x with PBS-T, incubated with DAPI (1 in 2000) in PBS-T for 10 mins, washed 3x with PBS-T and mounted using FluoroMount.

2.10 Sholl analysis

Sholl analysis is a technique regularly used for quantifying neurite arborisation in neuronal culture (e.g. Ramonet *et al.,* 2011). Neuronal cultures were generated as described above but were plated at a density of 10,000 cells per well of a 24 well plate in order to accurately differentiate cells from one another.

2.10.1 Cell processing for Sholl analysis

Cortical neuronal cultures were maintained for 3 days following plating. Cells were then washed with PBS and fixed with methanol at -20 °C for 10-15 mins. Cells were subsequently washed 3x with PBS-T and blocked with PBS-T plus 2% BSA for 10 mins. Cells were then incubated in a primary antibody directed against β–III tubulin (see Table 2.8) for 1 hour. Cells were then washed 3x with PBS-T and incubated in an Alexa Fluor fluorescent secondary antibody (Life Technologies) (1 in 200) for 1 hour. Cells were washed 3x with PBS-T, incubated with DAPI (1 in 2000) in PBS-T for 10 mins, washed 3x with PBS-T and mounted using FluoroMount. Immunofluorescence microscopy was performed using an EVOS FLAuto automated fluorescent microscope.

2.10.2 Data acquisition and Sholl analysis

Data acquisition and analysis were performed while blinded to genotype. Neurons were selected randomly from cover slips for Sholl analysis. Only isolated neurons, staining positive for β–III tubulin were considered for analysis. 10 neurons were selected per coverslip and 3 coverslips were sampled per genotype, per experiment. Images of neurons were taken using a 20X objective. Following image acquisition, the contrast of the images was enhanced using ImageJ to properly highlight the neurite network. A semi-automated Sholl analysis software tool, FastSholl, employed using MatLab R2014a,

was used as previously described in Gutierrez and Davies (2007). FastSholl software allowed for the assessment of the following parameters:

● **Number of primary neurites** – defined as those neurites arising from the neuronal soma.

● **Number of branches** – defined as the dividing in two of a neurite for a minimum of 5 µm (estimated).

● **Total neurite length** – defined as the sum of all neurite lengths.

● **Sholl profile** – A Sholl profile is generated by drawing concentric rings at regular intervals around the neuron emerging from the centre of the nucleus. The number of times a neurite crosses each ring is used to generate a Sholl profile and determine the amount of branching seen in a particular neuron, a certain distance away from the nucleus (Fig. 2.3). In experiments, an inter-ring interval of 10 µm was used and 20 concentric rings were used for the analysis.

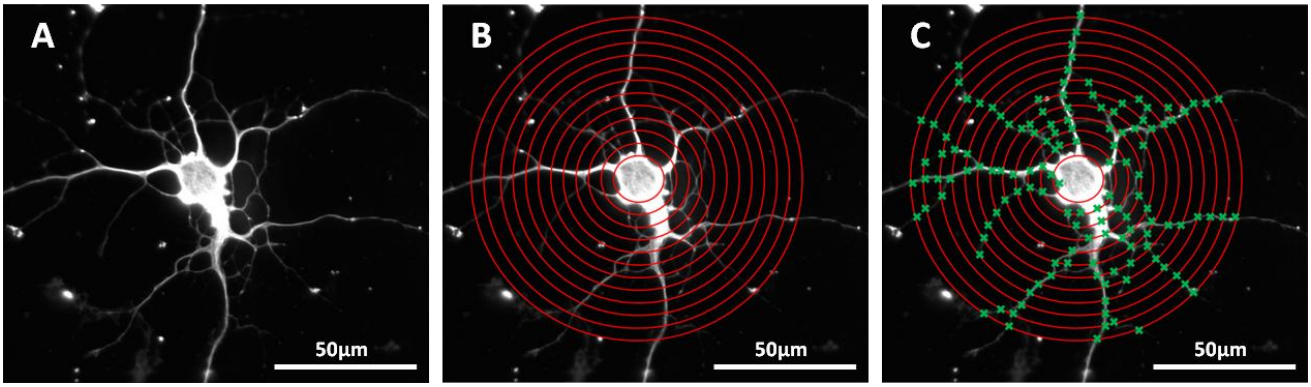

Figure 2.3. An illustration of the process of Sholl analysis. (A) Neurons are stained with β–III tubulin. **(B)** Concentric rings of equal inter-ring distance are drawn from the centre of the nucleus. **(C)** Points at which neurites cross the rings are recorded, as indicated by the green markers, and quantified per ring.

2.11 Autophagy assays

Cortical neuronal cultures were maintained for 2 weeks following plating. Cell media was then replaced with either fresh neuronal medium or HBSS+/+ (to induce autophagy) for 6 hours before cell lysis. Western blots of lysates probing for LC3-II, Lamp-1 and P62 were performed to assess whether any changes to macroautophagic activity were induced.

2.12 Antibodies

Table 2.8 Primary antibodies (product ID, company, concentrations and class) used for experiments. WB= Western blot, IF=immunofluorescence, IHC-FF= DAB immunohistochemistry in free-floating tissue, IHC-P= DAB immunohistochemistry in paraffin embedded tissue, ICC= immunocytochemistry.

Primary Antibody	Product ID	Company	Concentration	Class
Acetylated α-tubulin	[6-11B-1] (ab24610)	Abcam	WB (1:2000)	Mouse Mono.
Complexin	122002	Synaptic systems	WB (1:1000)	Rabbit Poly.
DAT	AB111468	Abcam	WB (1:500)†	Rabbit Poly.
GFP (used to target YPet)	A11122	Life Technologies	WB (1:500)†, IHC-FF (1:250), IF (1:250), ICC (1:200)	Rabbit Poly.
GFP (used to target YPet)	GFP-1020	Aves Labs	IF (1:200)	Chicken Poly.
Iba1	MABN92	Millipore	IHC-P (1:1000)	Mouse Mono.
LRRK2	[MJFF2 (c41-2)] (ab133474)	Abcam	WB (1:500)†, IHC-FF* (1:250), IF (1:250)	Rabbit Mono.
Map2	AB5622	Millipore	ICC (1:500)	Rabbit Poly.
NeuN	MAB377	Millipore	ICC (1:100)	Mouse Mono.
P62	[EPR4844] (ab109012)	Abcam	WB (1:500)	Rabbit Mono.
Phospho-tau (AT8) (Ser202+Thr205)	MN1020B	Thermo	IHC-P (1:200)	Mouse Mono.
Phospho-LRRK2 (ser910)	[UDD1 15(3)] (ab133449)	Abcam	WB (1:500)†	Rabbit Mono.
Phospho-LRRK2 (ser935)	[UDD2 10(12)] (ab133450)	Abcam	WB (1:500)†, IHC-FF* (1:200)	Rabbit Mono.
SNAP-25	610366	BD Biosciences	WB (1:1000)	Mouse Mono.
Synapsin	106004	Synaptic systems	WB (1:1000)	Guinea Pig Poly.
TH	AB152	Millipore	WB (1:1000), IHC-FF (1:2000), IF (1:500)	Rabbit Poly.
Ubiquitin	Z0458	Dako	IHC-P (1:1000)	Rabbit Poly.
VAMP2	v1389	Sigma	WB (1:1000)	Rabbit Poly.
VMAT	AB1767	Millipore	WB (1:500), IHC-FF (1:500)	Rabbit Poly.
α-synuclein	610786	BD Biosciences	WB (1:500), IHC-P (1:2000), IF (1:250)	Mouse Mono.
β-Actin	ab8227	Abcam	WB (1:8000)	Rabbit Poly.
β-III tubulin	MAB1637	Millipore	ICC (1:1000)	Mouse Mono.

* Antigen Retrieval Needed † Samples not boiled

2.13 Statistical analysis

Statistical analyses were performed using Graph Pad Prism (v5.0). Shapiro-Wilk tests for normality were performed on data to determine that they were normally distributed. By default, parametric tests were used to analyse experimental data (Welch's t-test, one/two way analysis of variance (ANOVA)). In the event that data violated the assumptions required for normality, appropriate non-parametric tests (Mann-Whitney U, Kruskal-Wallis one way ANOVA) were used.

For all behavioural tests, two-way ANOVA statistical tests were performed with genders grouped separately. If a significant difference existed between genders, analysis of them was kept separate by two-way ANOVA. If no significant difference was found between genotypes, gender data were collapsed and analysed using a one-way ANOVA. Dunnett (or Dunn's in the case of non-parametric tests) post-hoc tests, were used for behavioural tests due to each genotype being compared to non-transgenic controls. For the analysis of molecular experimental data, Bonferroni post-hoc tests were used due to the need for inter-genotype comparisons.

CHAPTER 3 – LRRK2 BAC TRANSGENIC RAT GENERATION AND LINE SELECTION

3.1 Chapter introduction: motivations and aims

3.1.1 *LRRK2* as a suitable gene for modelling Parkinson's disease

Transgenic animal models of neurodegenerative disease have seen reasonable levels of success in their ability to recapitulate disease symptoms. In particular, α-synuclein models of PD have been reported to recapitulate many of the cardinal symptoms of PD (Chesselet & Richter, 2011). The existence of monogenic forms of PD is incredibly useful for the purposes of animal model generation, in that relatively simple changes to a subject's genome - in many cases, a single amino acid coding sequence - can greatly increase the chance of PD development. However, a general concern is that, while a great deal of effort is made to explore the molecular pathways of dysfunction seen in monogenic forms of PD, their pathogeneses may differ from that seen in sporadic PD. Indeed, these monogenic mutations often cause PD with atypical symptoms such as an early disease onset, slow progression and altered neuropathology (Klein & Westenberger, 2012). If it is indeed the case that underlying pathological processes differ, therapies developed from the investigation of monogenic disease models may prove to be of limited effectiveness when treating sporadic patients. Due to the fact that the vast majority of PD cases are sporadic in nature, this concern has serious implications. *LRRK2* is therefore encouraging as far as monogenic causes of PD are concerned, given that mutations in *LRRK2* explain not only a large proportion of familial PD but 1-2% of sporadic forms of PD (Gilks *et al.,* 2005; Healy *et al.,* 2008). Furthermore, clinically and pathologically, *LRRK2* PD disease progression highly resembles that seen in sporadic PD cases (Healy *et al.,* 2008). In particular, the age of symptomatic onset of *LRRK2* PD patients is greatly similar in nature to that of sporadic PD (Healy *et al.,* 2008). It is hoped that this similarity to sporadic PD in disease presentation is a reflection of similar underlying pathological mechanisms and, thus, the information gained from the study of *LRRK2* PD will have maximal informational and therapeutic value.

3.1.2 The selection of rats as an appropriate transgenic animal model

The selection of any particular animal for disease modelling inevitably involves various tradeoffs. While well-characterised model organisms such as *C. elegans* and *Drosophila* have the advantages of being relatively easy to generate and breed, for the purposes of modelling *LRRK2* PD, they differ from humans in a number of important ways. Firstly, these animals have relatively simplistic DAergic systems, with *C. elegans*, in particular, possessing only a handful of DAergic neurons. Secondly, neither *C. elegans* nor *Drosophila* express α-synuclein or two LRRK proteins as do humans. These issues are pertinent when generating a transgenic *LRRK2* animal in an attempt to model PD, a central feature of which involves the accumulation, over time, of α-synuclein. Thirdly, these animals' behavioural outputs are far enough removed from those of humans to make determination of a Parkinsonian phenotype highly challenging. Finally, both *C. elegans* and *Drosophila* have comparatively limited lifespans. Given that PD typically emerges in humans at a late stage of life, animals with very short lifespans are not ideal for the purposes of modelling PD. At the other end of the spectrum, primates are highly similar to humans. However, due to their long lifetimes and large space requirements, unless using acute models of disease such as viral or toxic models of PD, they are experimentally impractical. While characteristics of end-stage PD phenotypes can be effectively recapitulated by toxic and viral models, in order to better understand and model disease progression as it occurs in patients, transgenic models, although costly and time consuming, are likely to grant greater insight into PD pathogenesis. Rodents, such as mice and rats, represent an effective compromise, given that they have moderately long life spans, express forms of α-synuclein and LRRK2 with high sequence homology to humans and have DAergic systems which more closely resemble those of humans compared to *C. elegans* and *Drosophila*.

Indeed, a large number of *LRRK2* transgenic mice have been developed, although successful symptom recapitulation has been mixed. While many of these models report motor dysfunction and DAergic abnormalities, evidence of neuronal loss and Lewy pathology in these models is minimal to

non-existent. Compared to mouse models, *LRRK2* transgenic rats are rare. Of the dozens of *LRRK2* rodent papers, only two recent studies have been performed in rats (Walker *et al.,* 2014; Lee *et al.,* 2014). These models possess a number of limitations, however, including their characterisation to only a limited age point, their lack of hWT control animals and the restriction of their efforts to the G2019S mutation.

While, at one time, the laboratory rodent of choice, the production of transgenic rats has recently been less common than mice due to their relative difficulty to generate (Zheng *et al.,* 2012). Nonetheless, rats possess a number of advantages over mice when modelling PD. Firstly, because of their size, rats are more suitable for a number of experimental techniques including electrophysiology and neuroimaging. Due to this, rats are also more thoroughly characterised anatomically within these fields. Secondly, rats possess a number of cognitive advantages over mice meaning that they are more capable of performing certain sophisticated behavioural tests. Thirdly, there is a certain amount of evidence that suggests that rats may develop more dramatic neurodegenerative phenotypes than mice. For example, it has been argued that rats show a greater level of susceptibility to viral expression of α-synuclein and PD-promoting toxin exposure than mice (Zheng *et al.,* 2012). Finally, compared to mice, rats are physiologically more similar to humans in a number of ways such as brain size and metabolism.

3.1.3 The use of BAC technology for expression of the *LRRK2* transgene

Early vectors possessed limited cloning capacity and contained genes that were driven, often, by viral promoters due to their relatively small size, ability to promote high levels of transcription and little preference for species or cell type (Ristevski *et al.,* 2005). While extremely effective for driving strong expression, ubiquitously throughout tissue, the physiological localisation and developmental period of the transgene could not be accurately recapitulated. Limited cloning capacity also meant that, for most genes, cDNA, as opposed to complete genetic sequences had to be used, eliminating intronic and promoter sequences. In recent years, accumulating evidence has suggested important

regulatory roles for intronic sequences, which are often absent from cDNA vectors (Brinster *et al.,* 1988). Additionally, while alternative promoters such as the Thy1 promoter have been used in an attempt to drive tissue-specific expression (e.g. Herzig *et al.,* 2012), for the recapitulation of physiological spatiotemporal expression patterns, a gene's native promoter is needed (Heintz *et al.,* 2001).

BAC, along with YAC and PAC technology, offered a solution for many of these issues. Given their dramatically larger cloning capacity, BACs allow for almost any gene to be inserted in its entirety along with native promoter and regulatory regions (Heintz *et al.,* 2001). Furthermore, while cDNA-based transgenes are highly susceptible to positional silencing effects, post-integration, the increased size provided by BACs is thought to eliminate much of these positional effects (Beil *et al.,* 2012). Though, not without their drawbacks (e.g. random integration site and copy number), BACs represent a step forward in the expression of genes in a physiologically relevant manner and, thus, better allow for the study of the appropriate function of these genes.

3.1.4 Chapter aims

1) To screen and select appropriate transgenic founders for the establishment of comparable *LRRK2* BAC transgenic lines expressing YPet-tagged human LRRK2 protein (hLRRK2) with either the G2019S and R1441C mutation or the hWT form for the purposes of ageing and subsequent pathological characterisation

2) To investigate the spatial expression of endogenous rat LRRK2 compared to that of the transgene

3.2 Establishment and selection of *LRRK2* BAC transgenic rat lines

3.2.1 Line selection overview

Previously, vectors containing the full length 144 kb human *LRRK2* gene (R1441C, G2019S or hWT variants) N-terminally tagged with a YPet tag, fused to exon 1, were sub-cloned into BACs (Alegre-

Abarrategui *et al.,* 2009). These BACs were used to generate SD rat founders by pronuclear injection of fertilised pure SD oocytes (Unit for Laboratory Animal Medicine; University of Michigan, US). The use of protein tagging is an effective method with which to localise a protein and distinguish it from endogenous forms (Ristevski *et al.,* 2005). The use of a protein tag was particularly pertinent in the case of LRRK2, where commercially available antibodies, while in existence, were imperfect. The location of the YPet tag at the N-terminus of the *LRRK2* sequence was chosen in order to minimise interference with the functional domains of the protein.

Our objective was to generate rat lines expressing moderate levels of hWT, G2019S or R1441C hLRRK2 for the purposes of ageing and subsequent pathological characterisation. These rats would be hemizygous for the transgene and bred on a wild-type SD background. We therefore eventually selected 3 lines for in-depth characterisation. Because of the eventual selection of these lines, they are used in subsequent sections as examples of the characterisation performed. For clarity, throughout this thesis, the term 'hLRRK2' is used, when discussing the transgenic rats, to distinguish the YPet-tagged human LRRK2 transgene protein from the endogenous rat LRRK2 protein. An overview of our selection process is illustrated in Figure 3.1 below.

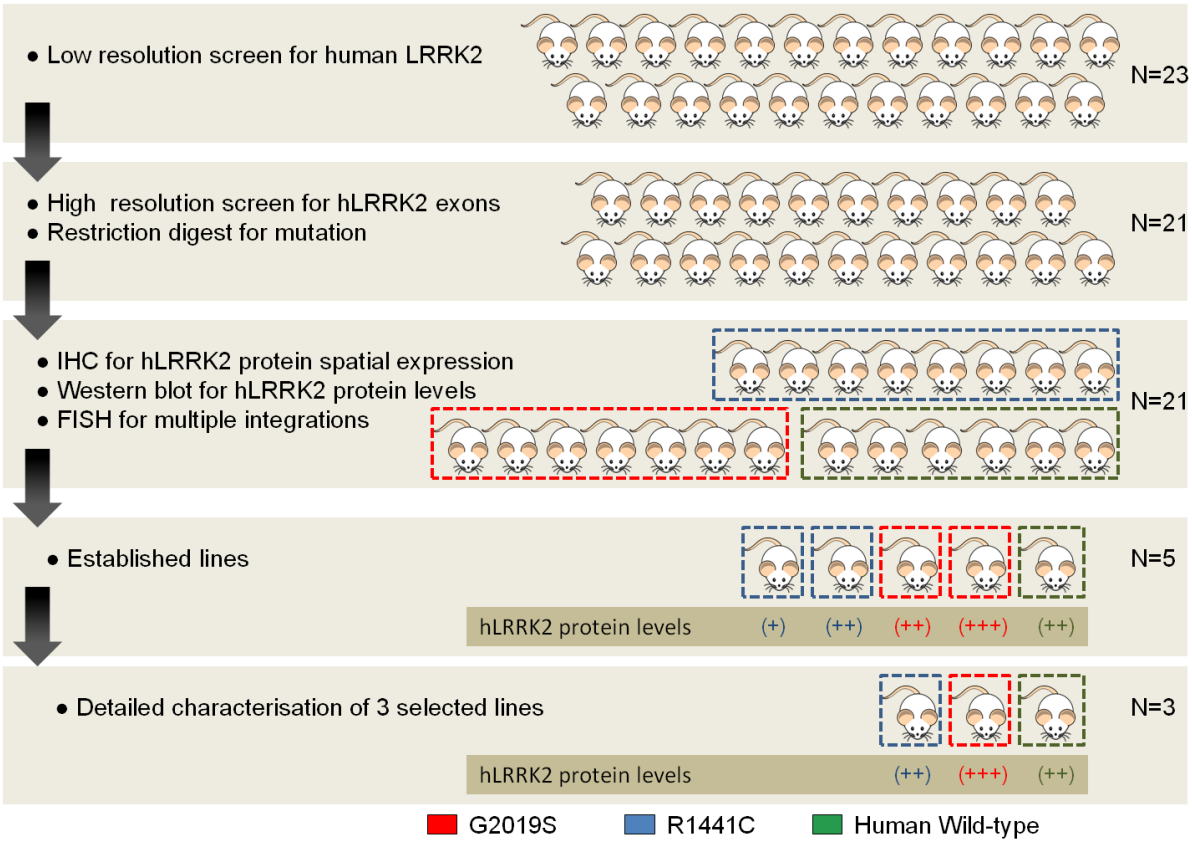

Figure 3.1. An illustration of the selection process for line generation. Founder progeny were initially screened for the *LRRK2* gene by a low-resolution PCR screen. Animals were then screened by PCR for each *LRRK2* exon (plus the *YPet* tag) and restriction digests were performed to determine the presence of the R1441C/G2019S mutations. Immunohistochemistry, Western blotting and FISH analysis were then performed to establish protein expression levels and patterns and determine the number of transgene integration sites. Finally, three lines were selected with two lower expressing lines maintained in reserve. Examples of the molecular profiling performed upon these animals are presented in Figures 3.2-13.

Our choice of the human *LRRK2* gene as opposed to rat *Lrrk2* was made on the basis that reports of phenotypic aggressiveness in other models of neurodegenerative disorders have suggested a more aggressive phenotype in models expressing human genes (Zheng *et al.,* 2012). Similarly, our choice of the G2019S and R1441C mutations were several fold. The G2019S mutation was selected on the basis of it being the most common mutation found in patients, in addition to being the most thoroughly characterised; implications derived from this line would therefore be the most far-reaching. The R1441C mutation was selected due to its relative commonality within patient populations compared to the Y1669C and I2020T mutation (Nichols *et al.,* 2005). In addition to this, a

certain amount of evidence suggests that mutations at the R1441 site cause a more aggressive pathological process, although due to the limited number of reported cases of these mutations, the validity of this claim is not entirely clear (Kumari & Tan, 2009).

3.2.2 Genetic screening to confirm transgene integrity

In a preliminary screen (by Dr Javier Alegre-Abarraregui), 23 potential founder rats were identified to carry the *LRRK2* transgene by PCR targeting the sequence spanning the BAC-transgene junction. To confirm these results and ensure complete integration of the entire *LRRK2* transgene, we generated *LRRK2*-specific primers designed to target each of the 51 exons, up- and down-stream segments, rat prolactin and the *YPet* tag (see methods for primer sequences). Primer pairs were designed to produce products of either ~250 bp or ~500 bp for easier identification. Firstly, a 'low-resolution' PCR screen was performed on DNA extracted from rat ear clips to determine the transgene presence (Fig. 3.2*B*). Following this, a 'high resolution' PCR was performed to verify the presence of all exons and the YPet tag (Fig. 3.2*C*). Founders demonstrating an absence of the transgene were excluded from further work. Following this screen, 21 SD rats, positive for the *LRRK2* transgene remained.

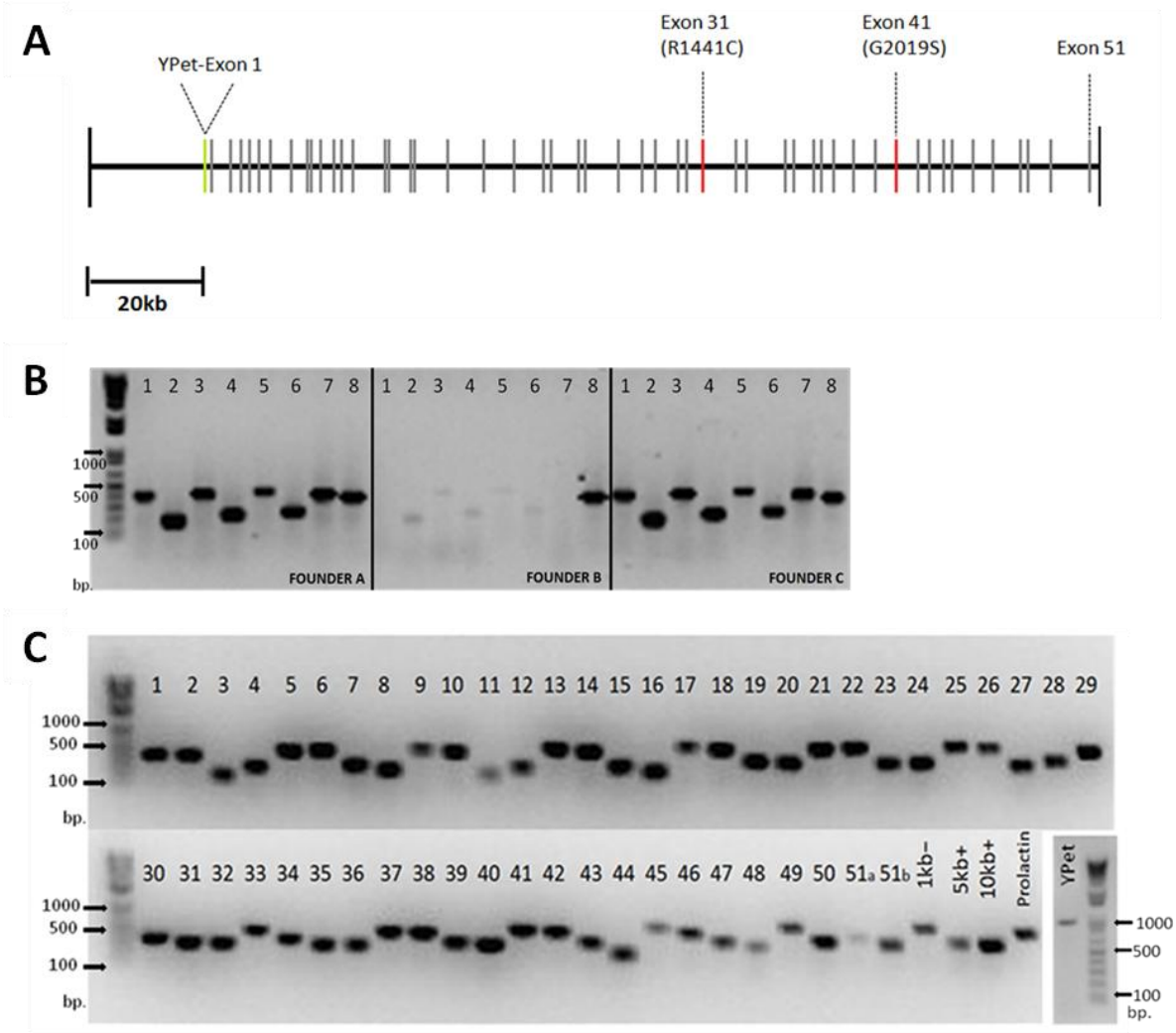

Figure 3.2. Validation of *LRRK2* transgene presence in founders. (A) Linear representation of the *LRRK2* BAC containing the human *LRRK2* genomic locus (144kb) with an N-terminally tagged *YPet.* Upstream sequences are ~20 kb and downstream sequences are ~1kb. **(B)** Example of 'low resolution' PCR screening for *LRRK2* exons in founder animals. Founders A and C show the presence of the transgene while founder B does not.
Lane 1 - Exon 2 **Lane 2** - Exon 8 **Lane 3** - Exon 14 **Lane 4** - Exon 20
Lane 5 - Exon 26 **Lane 6** - Exon 32 **Lane 7** - Exon 38 **Lane 8** - Rat prolactin
(C) Example of 'high resolution' PCR screening of rat founder demonstrating the presence of the complete *LRRK2* transgene. Lane numbers correspond to respective *LRRK2* exons (two primer pairs were designed to target exon 51). Primer pairs targeting regions 5 kb and 10 kb upstream and 1 kb downstream were also used along with primers targeting the *YPet* tag.

3.2.3 Assessment of presence of the R1441C/G2019S mutations

Presence or absence of an R1441C or G2019S mutation was determined by restriction digest. Regions of exon 31 (location of the R1441C mutation) and exon 41 (location of the G2019S mutation) corresponding to mutation sites were amplified by PCR. Digests were designed to cleave hWT sequences (Fig. 3.3). Presence of the R1441C mutation eliminated a BstU1 site while presence

of a G2019S mutation eliminated a BceA1 site. It was confirmed that 6 founders were hWT, 7, G2019S and 8, R1441C genotype variants.

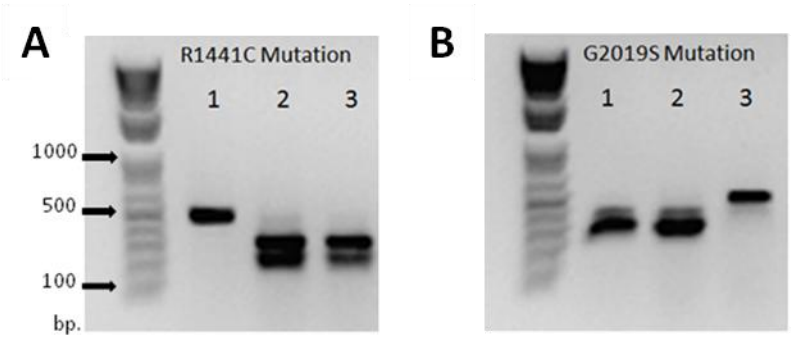

Figure 3.3. Assessing the presence of G0219S/R1441C mutations. (A) Restriction digest assessing the presence of the R1441C mutation (cleavage indicates a hWT genotype). **(B)** Restriction digest assessing the presence of the G2019S mutation (cleavage indicates a hWT genotype).
Lane 1 - R1441C mutant founder **Lane 2** - hWT founder **Lane 3** - G2019S mutant founder

3.2.4 Genotyping

Only rat founders which produced transgene-positive progeny were used to establish lines. To determine the presence of the transgene in rat progeny, a genotyping PCR assay assessing the presence of exons 8, 20 and 38 was performed (Fig. 3.4).

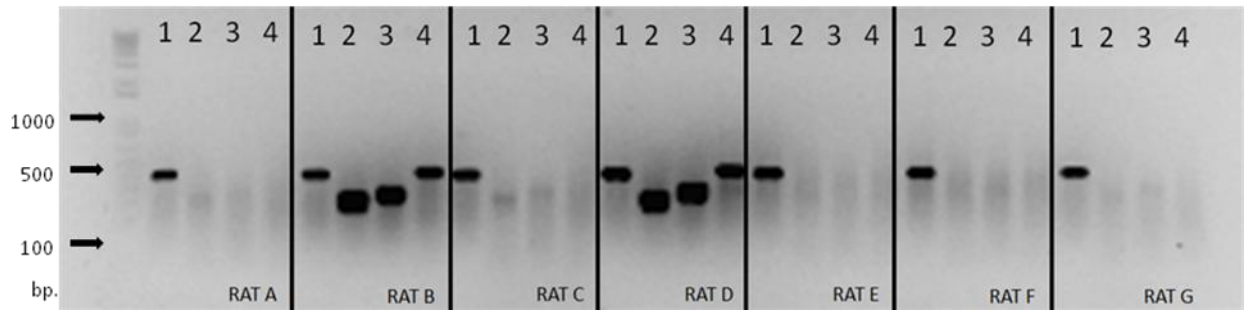

Figure 3.4. Standard genotyping assay. Example of genotyping for the presence of the *LRRK2* transgene in a rat litter. Rats B and D are deemed transgenic while all others are deemed non-transgenic.

Lane 1 – Prolactin **Lane 2**- Exon 8 **Lane 3**- Exon 20 **Lane 4** – Exon 38

3.2.5 Fluorescent in-situ hybridisation analysis

To establish breeding cohorts with consistent transgene expression, we performed FISH analysis to determine the number of transgene insertion sites and estimate copy number integration. Fibroblasts were generated from founder progeny ear clips and a *LRRK2* probe was generated. FISH analysis was then performed to examine chromosomal integration sites (Wellcome Trust Centre for Human Genetics Microscopy Core; Oxford, UK). Insertions on multiple chromosomes were detected in some founders (Fig. 3.5).

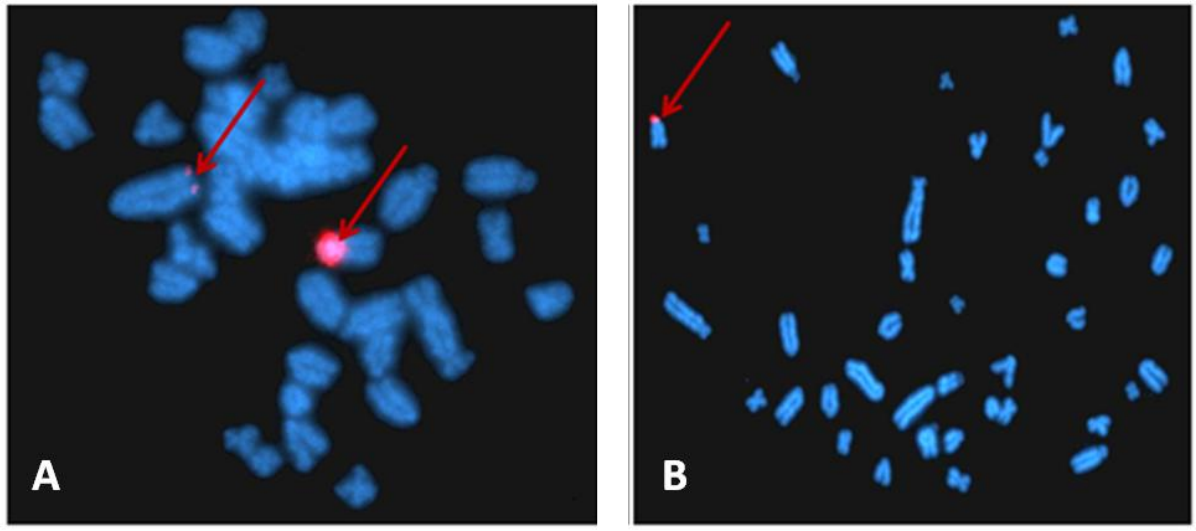

Figure 3.5. FISH analysis for transgene integration. Example of FISH analysis for the presence of *LRRK2* gene insertions in fibroblasts generated from rat founder progeny. The red fluorescent signal indicates the presence of the *LRRK2* transgene. Levels of fluorescence provided a rough approximation of relative transgene copy-number insertions. **(A)** A G2019S founder showing multiple integration sites; one large integration in the centromeric area of an acrocentric chromosome plus a second, smaller integration signal on the subtelomeric region of a larger acrocentric chromosome. **(B)** A hWT founder showing a single centromeric integration on an acrocentric chromosome.

3.2.6 Removal of undesirable integration sites by quantitative PCR

Western blotting for the hLRRK2 protein revealed variable levels in the progeny of a single founder (data not shown). This, in conjunction with the FISH analysis, suggested transgene insertion on multiple chromosomes. To isolate the larger insertion site for the establishment of a G2019S overexpressing line, it was necessary to selectively breed from progeny possessing only the large

integration. To achieve this, we used quantitative PCR (QPCR) to determine relative transgene copy number between littermates. Primers targeting the *YPet* tag were used in QPCR of genomic DNA to establish relative inter-littermate gene copy number (Fig. 3.6). An appropriate first-generation (F1) animal was selected and bred from to produce a second-generation litter (F2). F2 animals were subsequently tail clipped for QPCR and were revealed to possess identical transgene copy numbers indicating the elimination of the multiple integration sites in the line. All subsequent animals in this line were bred from these progeny.

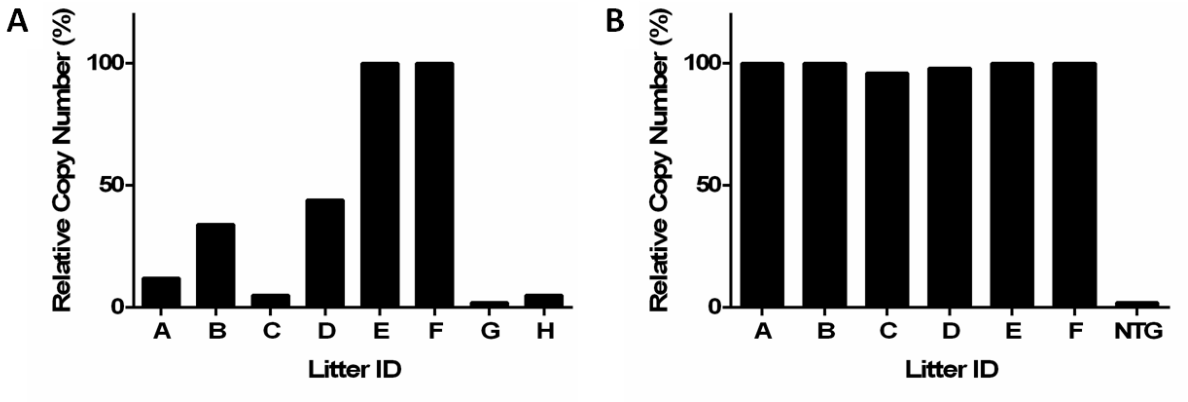

Figure 3.6. Elimination of multiple transgene integration sites. (A) F1 littermates (A-H) bred from a high expressing G2019S founder with evidence of multiple integrations. QPCR revealed different levels of relative *LRRK2* transgene copy number between littermates. These data were used to select the littermate (E) with the high and consistent insertion to breed from. **(B)** F2 littermates (A-F) bred from the selected F1 littermate. Second generation transgene copy number was found to be consistent between all animals. A non-transgenic littermate was used to demonstrate an absence of signal for the *YPet* gene. These results indicate that the uneven gene expression present in F1 animals had been stabilised.

Following the confirmation of the presence of the *LRRK2* transgene along with corresponding mutations and based on initial screens for hLRRK2 expression and correcting for multiple integration sites, three lines, one from each genotype, were selected for more detailed characterisation. Two additional lower expressing mutant lines, one R1441C and one G2019S, were also kept in reserve, although subsequent discussion and characterisation throughout this thesis will focus upon the core three lines. These core lines will hereafter be referred to as G2019S (GS), R1441C (RC) or hWT.

3.2.7 Assessing hLRRK2 protein expression

hLRRK2 protein expression was initially assessed by Western blot of whole-brain homogenates from 2 month old animals (Fig. 3.7). β-actin-normalised hLRRK2 protein levels were estimated, as compared to endogenous rat LRRK2, at 5 times for hWT, 6 times for R1441C and 13 times for G2019S.

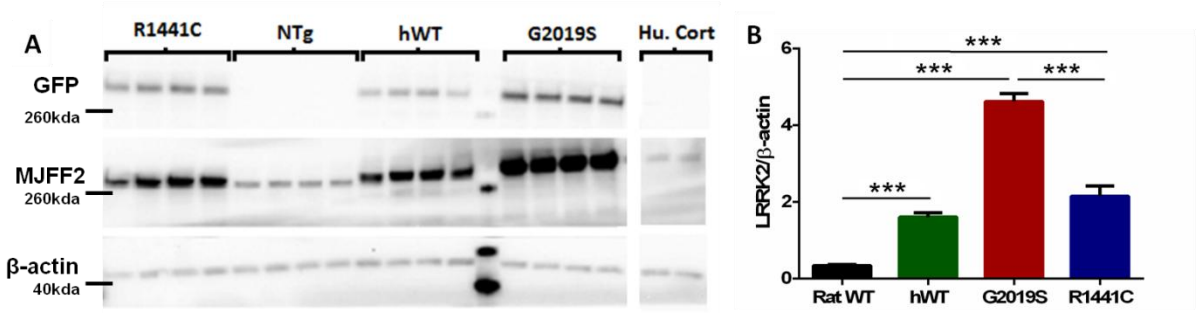

Figure 3.7. Western blotting for hLRRK2 protein in selected lines. (A) Western blot data for overall brain levels of hLRRK2 (~268 kDa) targeting both the YPet tag (anti-GFP antibody) and the hLRRK2 protein (MJFF2 antibody) in selected 3-month old transgenic overexpressing lines (n=4). GFP only detects transgene protein while MJFF2 detects both transgene and endogenous rat LRRK2 (the former having a higher molecular weight due to the YPet tag). Human cortex was used to show that endogenous human LRRK2 has a similar molecular weight to the transgene. As expected, no signal was detected for the YPet tag in the non-transgenic animals or human cortex samples. **(B)** A quantification of LRRK2 levels revealed the selected lines to over express hLRRK2 by roughly 6x for R1441C, 5x for hWT and 14x for G2019S compared to endogenous rat LRRK2 (One-way ANOVA: main effect of genotype: $p<0.0001$; n=4 per genotype). Data are expressed as mean ± standard error of the mean (SEM). Bonferroni post-hoc tests *** $p<0.001$.

3.2.8 hLRRK2 protein localisation

To determine hLRRK2 expression in the selected lines, anatomical transgene protein expression was assessed in 3 month old animals by immunohistochemistry. A polyclonal green fluorescent protein (GFP) antibody was used to detect the hLRRK2 protein tag to allow us to distinguish between endogenous rat LRRK2 and the hLRRK2 protein. While the G2019S overexpressing line showed stronger staining patterns, anatomical distribution of the transgene was similar between lines, as expected, with no detectable signal for the YPet tag seen in the non-transgenic controls. hLRRK2 protein expression was widespread throughout multiple brain regions. Areas showing the highest levels of transgene expression were the cortex (Fig. 3.8) and hippocampus (Fig. 3.9). hLRRK2 was

also expressed at lower levels in the cerebellum (Fig. 3.10), striatum (Fig. 3.11) and SNpc (Fig. 3.12), the latter of which had to be exposed to the DAB reaction for longer for clear detection in the lower expressing lines. hLRRK2 protein was principally detectable in the soma of neurons (absent from the nucleus) although nerve terminals were also labelled, usually in cells expressing high levels of the transgene.

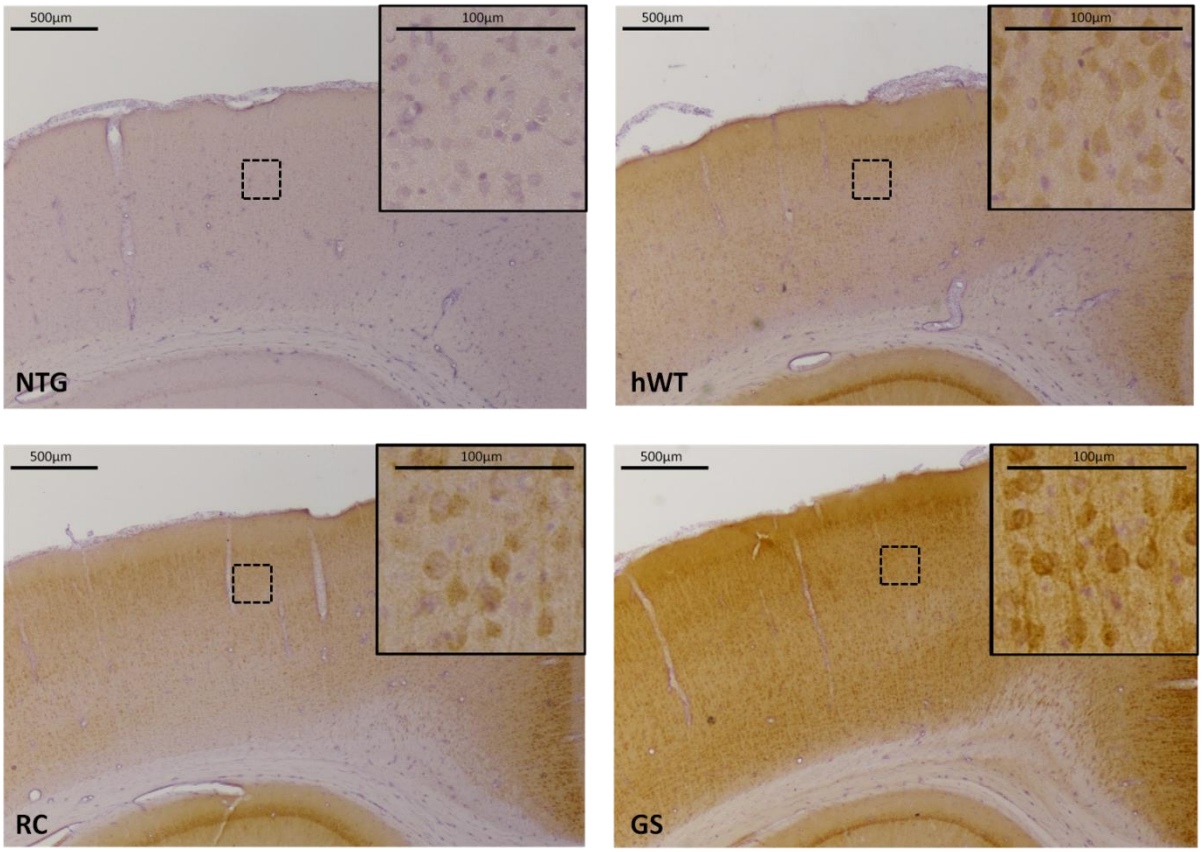

Figure 3.8. Cortical YPet (hLRRK2) immunohistochemistry in selected lines. Representative DAB immunohistochemistry for the YPet tag in 3 month-old cortical sections from the selected lines. Similar expression localisation is apparent throughout various cortical layers although slightly higher levels are seen for the G2019S expresser. No detectable signal for the YPet tag was seen in the non-transgenic controls.

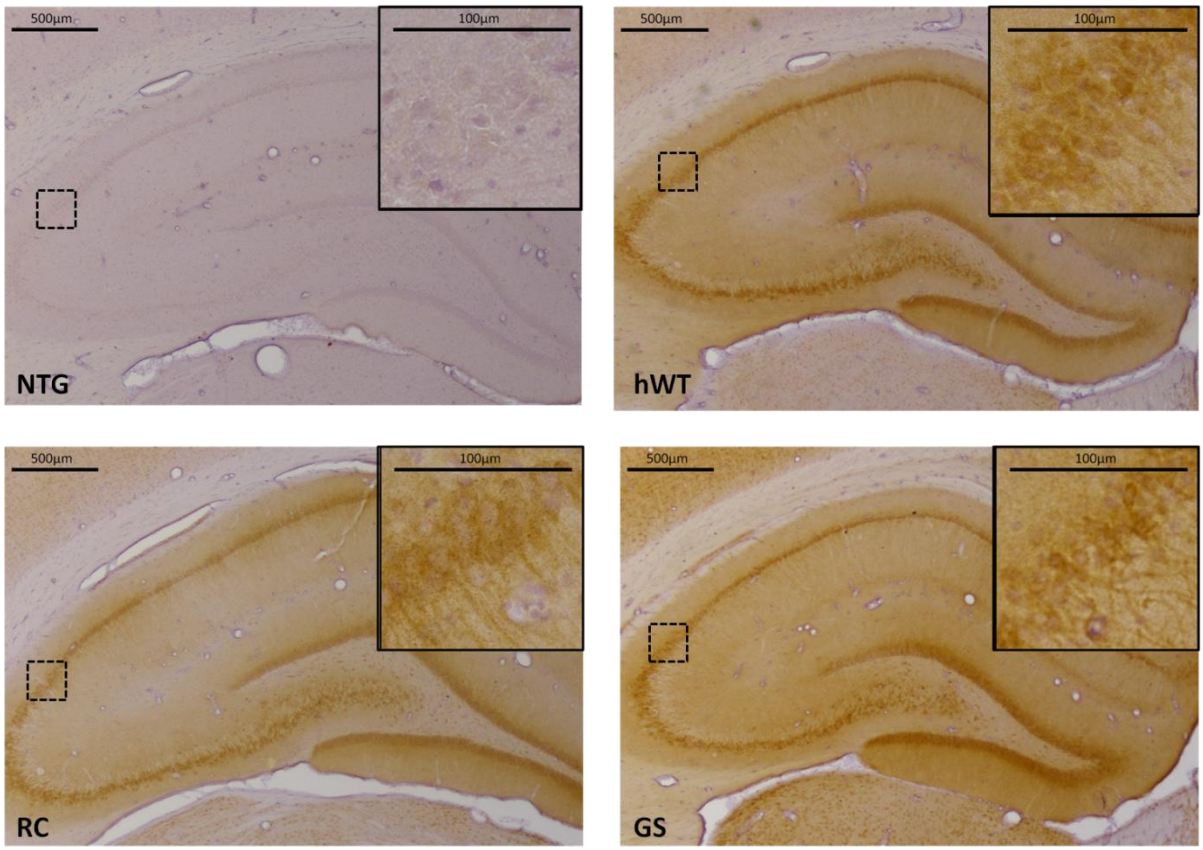

Figure 3.9. Hippocampal YPet (hLRRK2) immunohistochemistry in selected lines. Representative DAB immunohistochemistry for the YPet tag in 3 month-old hippocampal sections from the selected lines. All lines show similar expression localisation with staining apparent in neurons of CA1-3 and the dentate gyrus. No detectable signal for the YPet tag was seen in the non-transgenic controls.

`

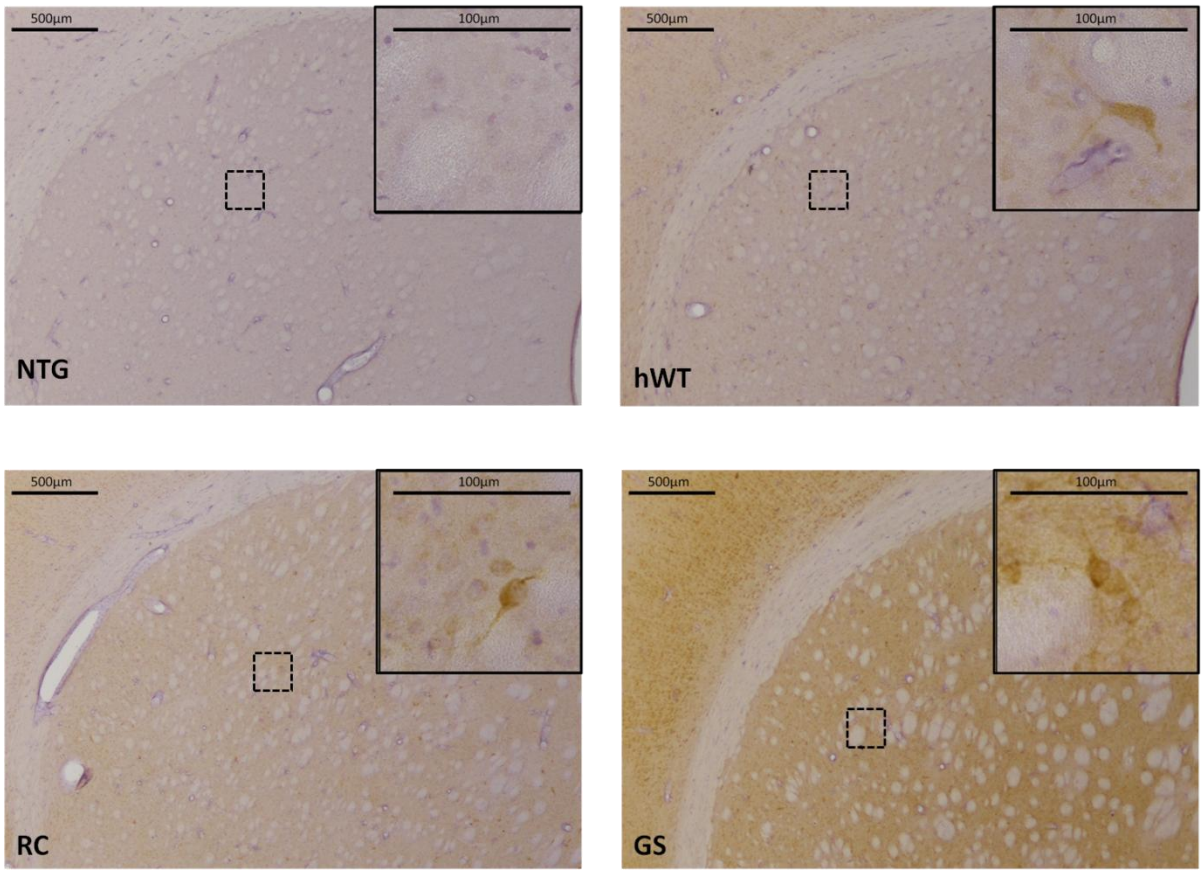

Figure 3.10. Striatal YPet (hLRRK2) immunohistochemistry in selected lines. Representative DAB immunohistochemistry for the YPet tag in 3 month-old striatal sections from the selected lines. Similar expression localisation is apparent with sparsely labelled neurons in all lines. There is potentially more transgene present in terminals in the striatum of the G2019S expresser. No detectable signal for the YPet tag was seen in the non-transgenic controls.

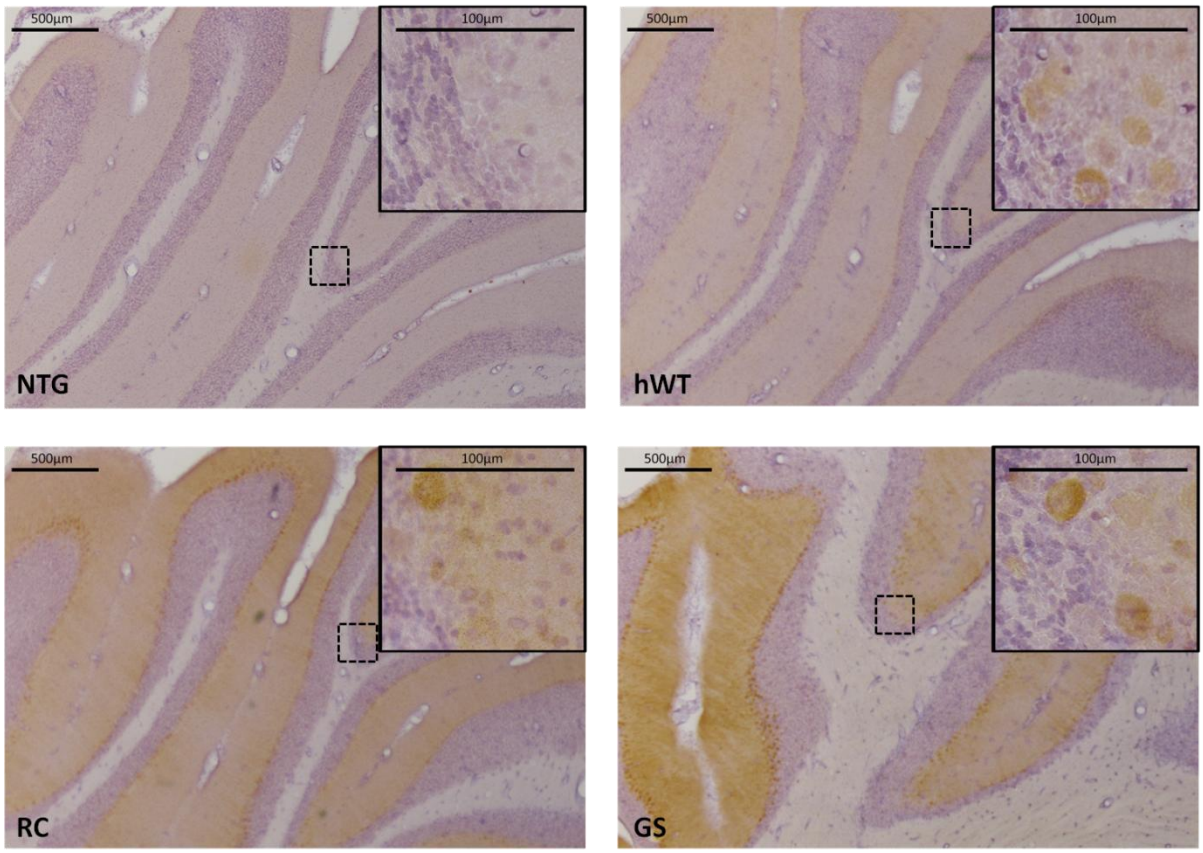

Figure 3.11. Cerebellar YPet (hLRRK2) immunohistochemistry in selected lines. Representative DAB immunohistochemistry for the YPet tag in 3 month-old cerebellar sections from the selected lines. Similar expression localisation is apparent in all lines with transgene expression appearing to be restricted to Purkinje neurons. No detectable signal for the YPet tag was seen in the non-transgenic controls.

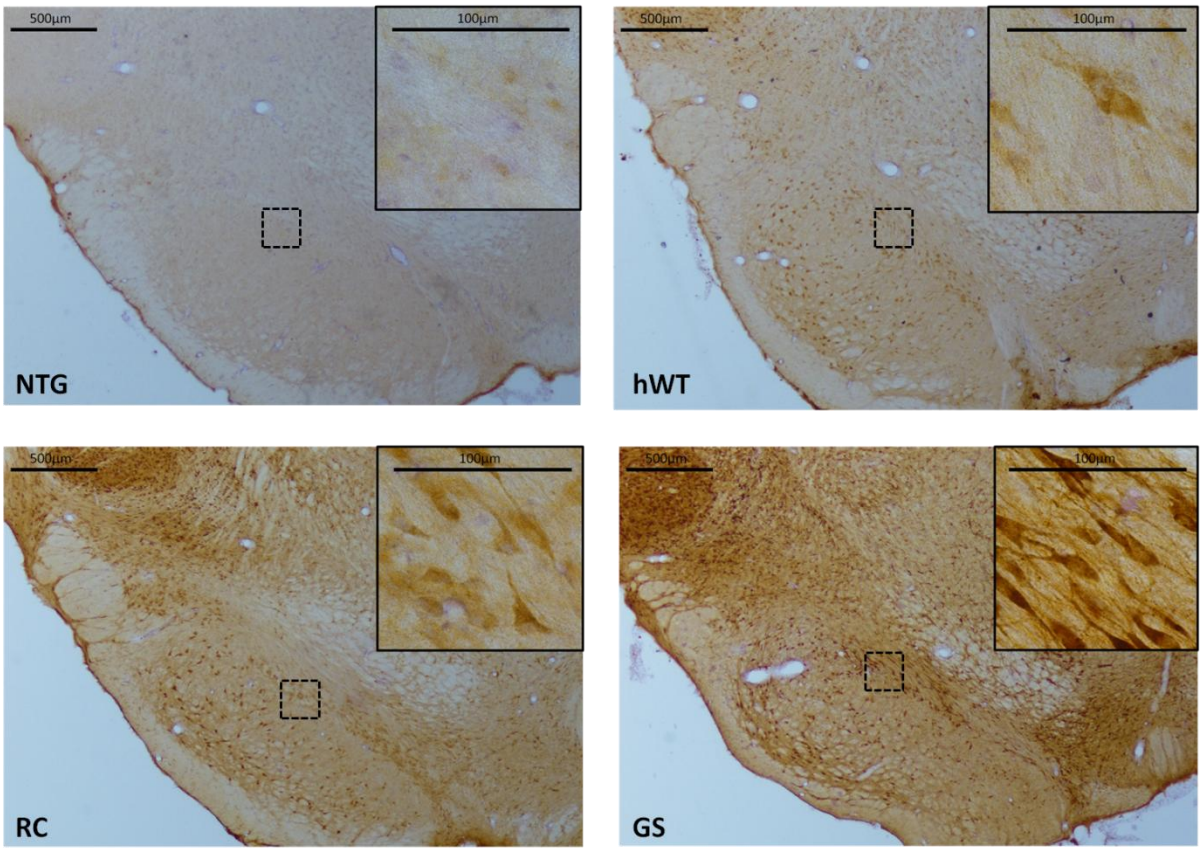

Figure 3.12. SN YPet (hLRRK2) immunohistochemistry in selected lines. Representative DAB immunohistochemistry for the YPet tag in 3 month-old midbrain sections from the selected lines. Similar expression localisation within the SNpc and SNpr is apparent between R1441C and hWT animals while slightly higher levels are seen for the G2019S expresser. No detectable signal for the YPet tag was seen in the non-transgenic controls. N.B. sections were incubated in DAB for a more extended time to reveal transgene protein.

3.2.9 DAergic SNpc neurons express α-synuclein and hLRRK2

While DAB immunohistochemistry revealed hLRRK2 protein expression within the SNpc, it was not clear whether these neurons are positive for DA or express α-synuclein, two characteristics thought to be important in the vulnerability to the development of PD pathology. Consequentially, triple immunofluorescence staining was performed on the SNpc to determine whether the transgene expression co-localised with TH and α-synuclein (Fig. 3.13). TH, commonly used as a marker for DAergic neurons given the lack of effective methods for the detection of DA, is an enzyme which acts to convert the amino acid L-tyrosine into L-DOPA and is generally considered the rate limiting enzyme in the production of catecholamines such as DA. A number of TH-positive SNpc neurons were also positive for α-synuclein and hLRRK2, though levels of the latter were generally low in all transgenic lines.

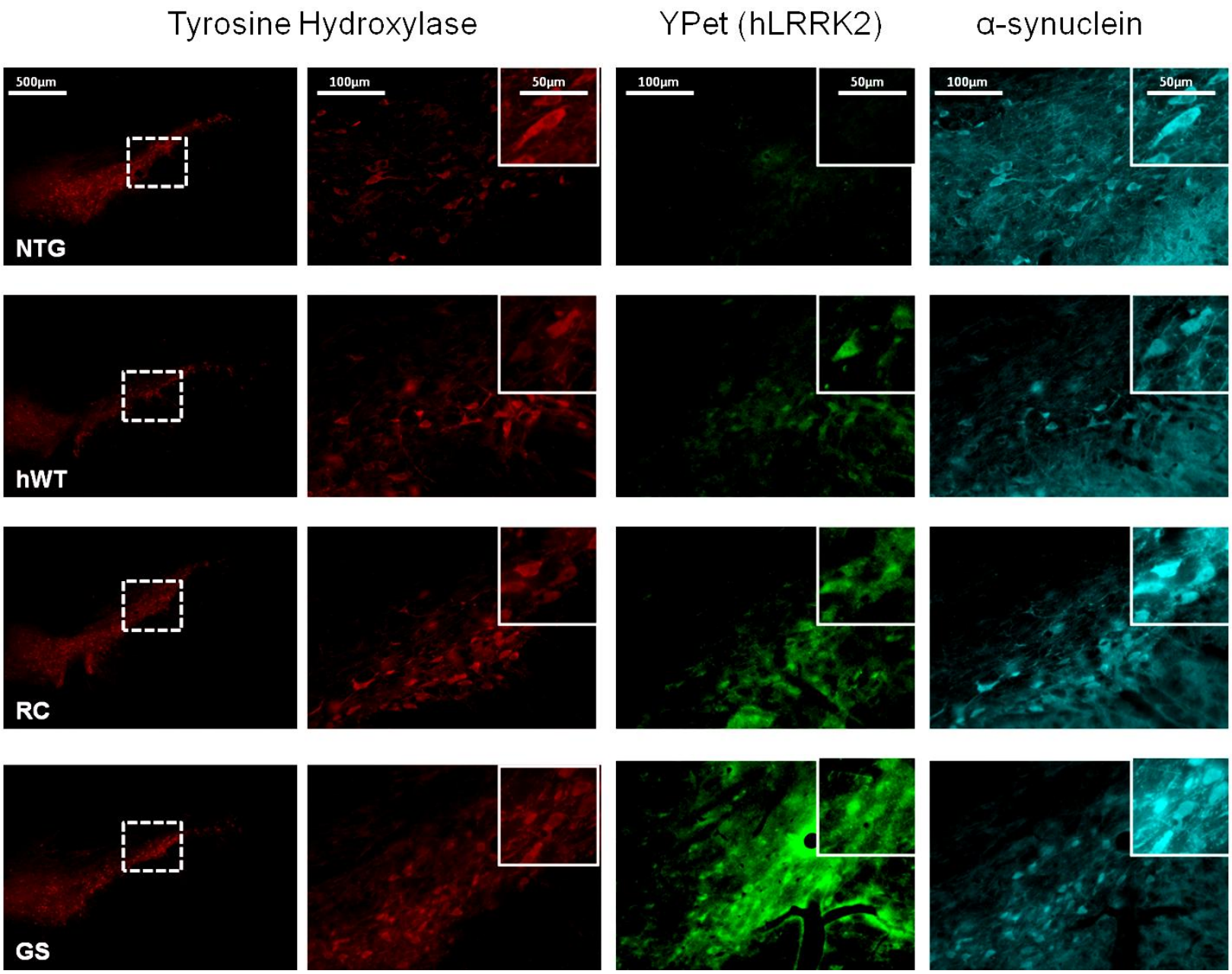

Figure 3.13. Immunofluorescence staining for TH, YPet (hLRRK2) and α-synuclein in the SNpc in selected lines. Representative immunofluorescence staining for TH, YPet (hLRRK2) and α-synuclein in the SNpc of 3 month-old midbrain sections. A number of TH-positive neurons also express both α-synuclein and hLRRK2. Signal for YPet is weak however, particularly in the lower expressing lines. No detectable signal for the YPet tag was seen in the non-transgenic controls.

3.3 Endogenous rat LRRK2 co-localisation

Due to the fact that the *LRRK2* transgene was driven by the human promoter, we were interested to determine the level of anatomical similarity in brain expression patterns between endogenous rat LRRK2 and the hLRRK2 protein. In order to do this, we performed immunohistochemistry on non-transgenic adult rats for LRRK2. As a negative control, Long-Evans *Lrrk2* KO rats (obtained from the Unit for Laboratory Animal Medicine, University of Michigan) were used. The lack of LRRK2 expression in the *Lrrk2* KO rats was first confirmed by Western blot (Fig. 3.14). Subsequent immunohistochemistry demonstrated that, similarly to the hLRRK2 protein, endogenous rat LRRK2 expression appeared widespread throughout the brain. Intracellular localisation of endogenous rat LRRK2 also resembled that of the hLRRK2 protein, being localised mainly to the cytoplasm but also seen in terminals. Endogenous rat LRRK2 was found in cortical, hippocampal and cerebellar sections showing largely similar staining patterns to that of the hLRRK2 protein (Fig. 3.15). Staining in cortical and hippocampal regions appeared somewhat more restricted compared to transgene expression although this may be a result of lower expression levels.

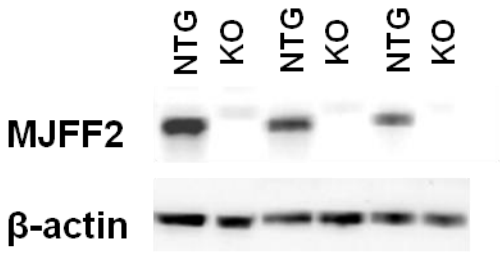

Figure 3.14 Western blotting for LRRK2 protein in *Lrrk2* KO rats. Western blot data for overall brain levels of endogenous rat LRRK2 (MJFF2 antibody) in selected 10-month old *Lrrk2* KO animals compared to non-transgenic (rat wild type) animals (n=3). As expected, no signal was detected for the LRRK2 protein in the *Lrrk2* KO animals.

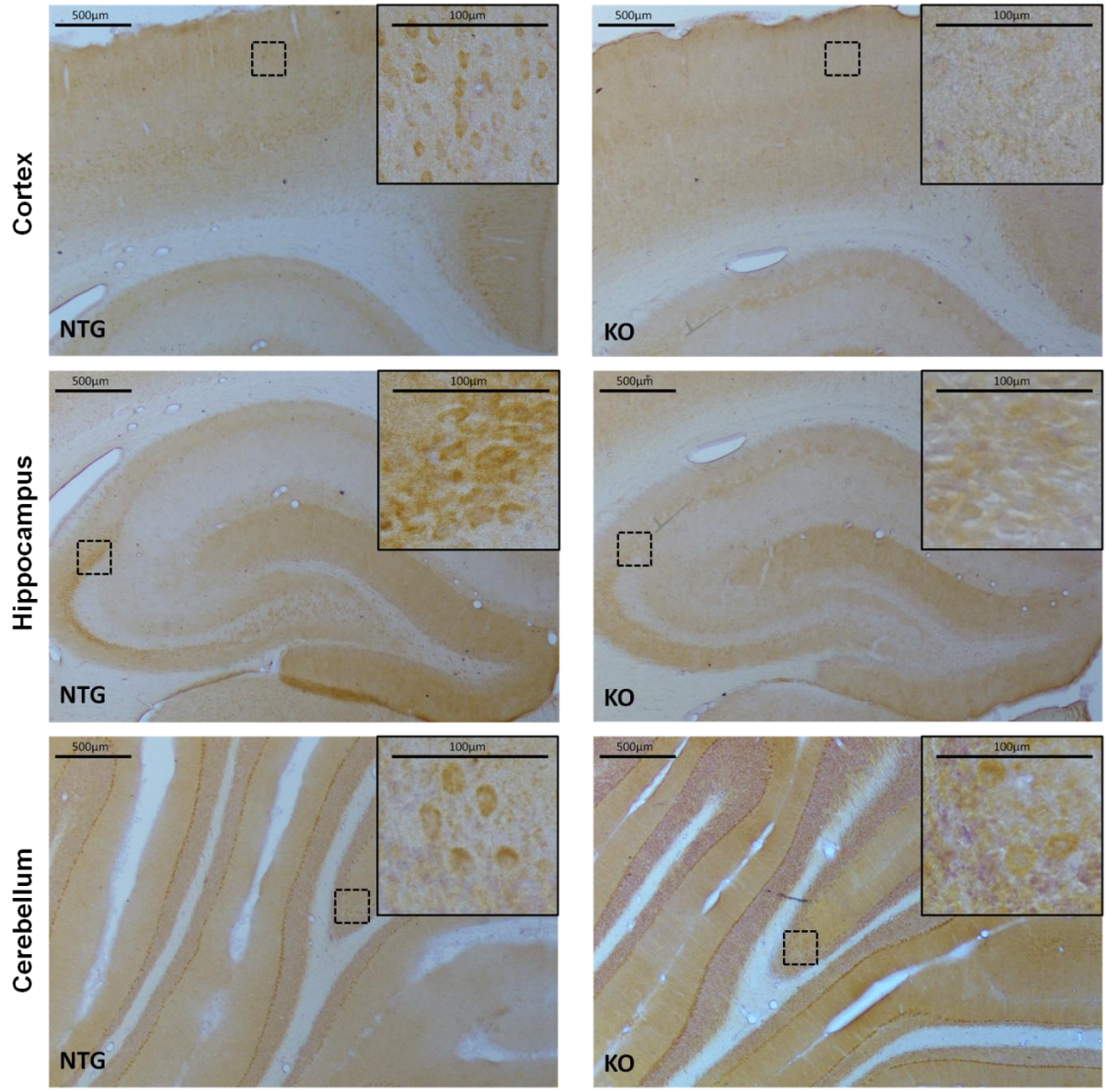

Figure 3.15. Cortical, hippocampal and cerebellar immunohistochemistry for LRRK2 in non-transgenic and *Lrrk2* KO rats. Representative DAB immunohistochemistry for LRRK2 in 10 month-old **(A)** cortical **(B)** hippocampal and **(C)** cerebellar sections from non-transgenic and KO lines. Expression appears to be neuronal and highly resembles that of the hLRRK2 protein. Hippocampal LRRK2 expression appears more restricted to CA2 than the hLRRK2 protein. No detectable signal for the LRRK2 was seen in the KO controls.

Endogenous LRRK2 was also detected in the striatum although the pattern of staining appeared more widespread than that seen of the hLRRK2 protein, with particularly intense staining in the striosomes. Finally, endogenous rat LRRK2 appeared to be expressed within the neurons of the SNpc although our analysis revealed a degree of non-specific staining within the SNpc of the *Lrrk2* KO

rodents (Fig. 3.16). This makes definitive conclusions about the presence of LRRK2 within the SNpc neurons difficult to draw.

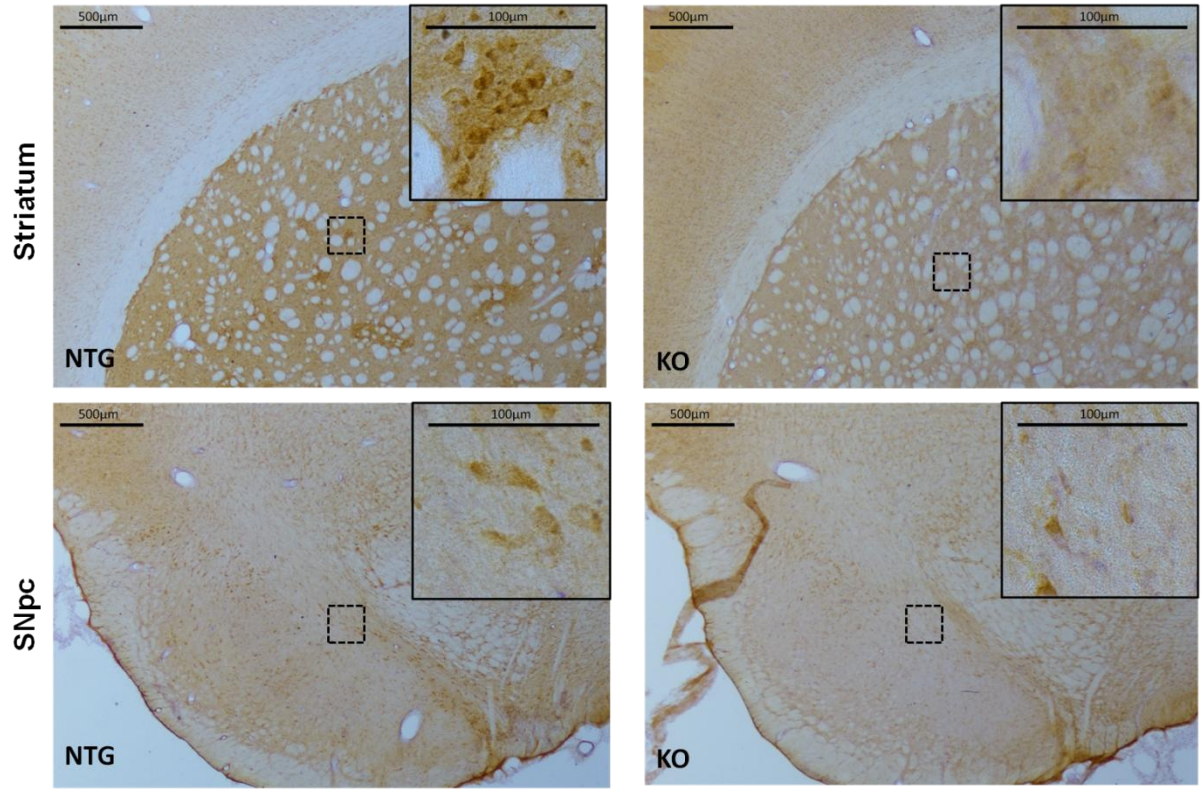

Figure 3.16. Striatal and SNpc immunohistochemistry for LRRK2 in non-transgenic and *Lrrk2* KO rats. Representative DAB immunohistochemistry for LRRK2 in 10 month-old **(A)** striatal **(B)** SNpc sections from non-transgenic and KO lines. Endogenous rat LRRK2 appears more widespread in the striatum when compared to the hLRRK2 protein. Positive staining in the SNpc was apparent although a degree of non-specific staining was seen in the SNpc of the KO.

3.4 The YPet tag is visible by native fluorescence

The YPet tag possesses an excitation peak of 514 nm and an emission peak of 527 nm. It was unclear, however, whether the protein would be functional when fused to the hLRRK2 protein in PFA-fixed conditions. To determine whether the hLRRK2 protein could be visualised by native fluorescence of the YPet tag alone, we performed fluorescent microscopy in unlabelled, fixed tissue sections from transgenic rats. We found that, in areas of high hLRRK2 protein expression, it was possible to locate hLRRK2-YPet positive neurons by direct fluorescence (Figure 3.17). However, in regions or transgenic lines expressing less hLRRK2 protein, we were unable to determine a reliable

signal. Spatially, the intracellular signal detected by native fluorescence highly resembled that seen when labelling neurons with antibodies targeting the YPet tag.

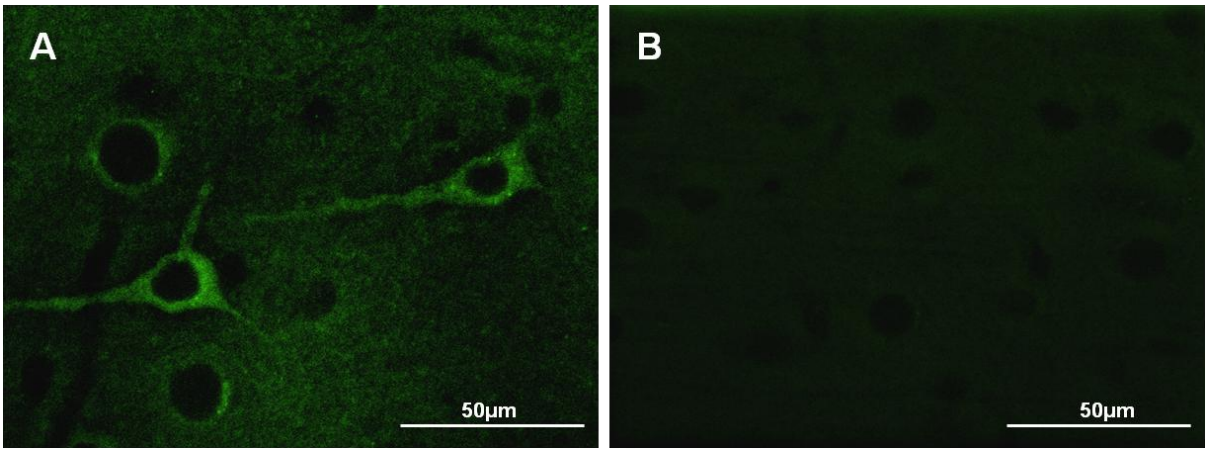

Figure 3.17. YPet-tagged hLRRK2 can be visualised in areas of high expression. Native fluorescence of a cortical section from **(A)** a 3-month old high expressing G2019S line compared to **(B)** a non-transgenic littermate. This shows the YPet tag protein to be functional and detectable in high-expressing regions without the use of immunohistochemistry.

3.5 Breeding and cohort maintenance

Transgenic cohorts were bred and maintained as depicted in Figure 3.18. Transgenic male breeders were bred with SD females (Charles River) who were then separated to give birth alone. Transgenic rats were housed with non-transgenic littermates who served as experimental controls. Following weaning, animals were ear-clipped for identification purposes and the tissue was used for genotyping.

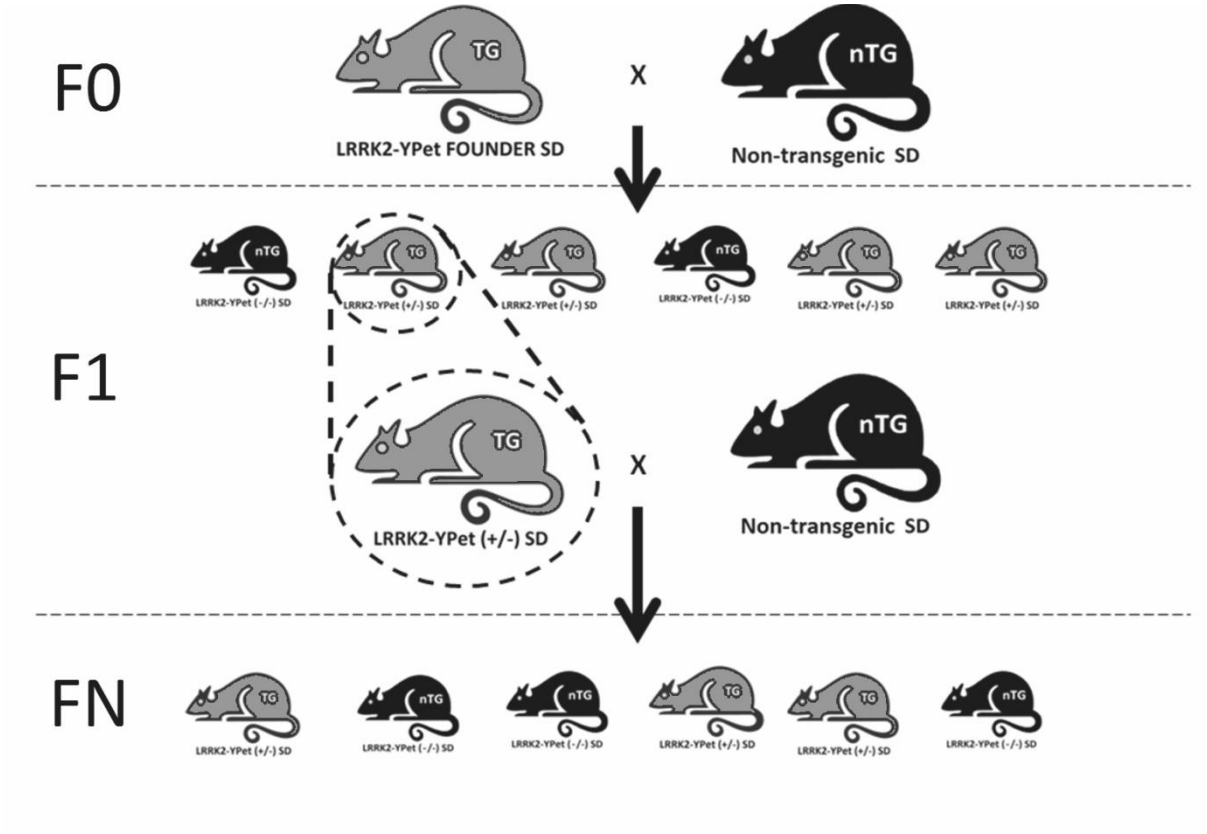

Figure 3.18. Illustration of cohort breeding technique. Chimeric founders (F0) are bred with non-transgenic (positive for endogenous rat LRRK2) SD rats to generate a first-generation litter (F1). For further generations (FN), a transgenic rat is selected and bred with a non-transgenic SD rat to produce further offspring. A 50:50 transgenic to non-transgenic ratio was expected in each litter. Transgenic rats from litters are therefore *LRRK2* hemizygous. Breeding cohorts were maintained with the help of Ms Milena Cioroch.

The choice to breed *LRRK2* lines in a hemizygous rather than homozygous fashion was several-fold. Firstly, this would make the process of genotyping far easier. Secondly, as BACs integrate at random points within the genome, homozygous animals could potentially have both alleles of a gene knocked out, causing a phenotype unintentionally. Regardless, potential loss of function in a single allele is still a concern to be kept in mind but is unfortunately unavoidable. Finally, a hemizygous breeding pattern allows for the generation of roughly equal numbers of littermates which were used as age-matched non-transgenic controls in subsequent experiments.

3.6 Chapter discussion

This Chapter has detailed the generation of three transgenic rat lines which express either hWT, G2019S or R1441C forms of *YPet*-tagged *LRRK2*. These lines consistently express moderate levels of hLRRK2 protein throughout various regions of the brain, including in the SNpc, in a pattern resembling that seen in both humans and rodents. These rat lines therefore represent an excellent opportunity for the modelling of PD developed by mutant *LRRK2* carriers.

3.6.1 *LRRK2* transgenic line generation and selection

Experiments generated 21 initial transgenic rat founders from which we selected three transgenic founder rats, one each of the R1441C, G2019S and hWT genotype, for the purposes of ageing and pathological characterisation. Our selection criteria for these founders were based upon inter-line consistency of expression and moderate levels of transgene expression. Importantly, these lines showed consistent intergenerational transgene expression. Our choice to develop lines of higher, rather than more physiological, expression was based upon previous *LRRK2* transgenic models which indicate that higher levels of LRRK2 expression tend to yield more dramatic phenotypes (e.g. Li *et al.,* 2009; Lin *et al.,* 2009) whereas more physiological levels of expression tend to yield more subtle phenotypes (e.g. Tong *et al.,* 2009; Longo *et al.,* 2014; Tsika *et al.,* 2014). Our selected *LRRK2* lines showed highly similar patterns of hLRRK2 protein throughout the brain and relatively comparable protein expression levels, with a particularly high similarity between our R1441C and hWT lines (around 5-6x endogenous rat LRRK2 levels). It was noted that it is possible that the MJFF2 LRRK2 antibody recognises rat LRRK2 and hLRRK2 with differing efficiency. However, given the high level of sequence homology between human and rat LRRK2 protein and the fact that the MJFF2 antibody was raised against a substantial amount of the LRRK2 sequence (amino acid 970-2527), this was considered unlikely. We also confirmed expression of the hLRRK2 protein within the DAergic neurons of the SNpc. This was deemed highly important given that these neurons are considered central to PD pathogenesis and presence of mutant LRRK2 protein within the neurons of the SNpc

has previously been shown to be necessary for the development of neurodegeneration (Ramonet *et al.,* 2011).

While we were able to localise the hLRRK2 protein using native fluorescence of the YPet tag in areas of high expression, this approach proved far less sensitive than immunofluorescence techniques and was only applicable to the higher-expressing G2019S line. Nonetheless, the YPet tag proved to be an excellent method to specifically detect transgene protein by both Western blot and immunohistochemistry. This advantage was illustrated by the occurrences of non-specific staining in *Lrrk2* KO rats while using the commonly used LRRK2 antibody, c41-2 (West *et al.,* 2014; Lee *et al.,* 2014). It did not appear that the YPet tag interferes with transgene localisation, given the similarity of hLRRK2 expression patterns to recent BAC transgenic rat models expressing human LRRK2 in the absence of a tag (West *et al.,* 2014; Lee *et al.,* 2014). Furthermore, it appeared that the hLRRK2 protein was transcribed and translated in full, given that its molecular weight was, as predicted, slightly higher than endogenous rat and human LRRK2, due to the addition of the YPet protein.

Our immunohistochemical characterisation of hLRRK2 protein in our rats revealed wide-spread expression throughout the brain which resembled that seen in humans (Biskup *et al.,* 2006; Sharma *et al.,* 2011). This included neuronal expression throughout multiple layers of the cortex, CA1-3 and the dentate gyrus, and, to a lesser extent, the cerebellum, striatum and the SNpc and SNpr. This expression also largely resembles that reported in previous BAC transgenic rodent models expressing the human *LRRK2* gene which have, similarly to our observations, also reported more widespread cortical expression compared to endogenous rat LRRK2 (West *et al.,* 2014). Furthermore, intra-cellular expression of the hLRRK2 protein, which appeared to be mainly cytoplasmic, was also in line with previous reports from human post-mortem studies (Biskup *et al.,* 2006).

While the expression patterns between the hLRRK2 protein and endogenous rat LRRK2 appeared to be largely similar, we noted a number of differences. Staining patterns of endogenous rat LRRK2

throughout the striatum appeared widespread, while hLRRK2 protein appeared to be restricted to a more specific set of neuronal cells. A prior study of a human LRRK2 BAC transgenic rat model has indicated that these cells are cholinergic interneurons, though to confirm the nature of these neuronal populations, further characterisation would be needed (West *et al.,* 2014). Similarly, in the hippocampus, endogenous rat LRRK2 appeared more restricted to CA2-3 regions while the hLRRK2 protein showed more consistent expression throughout the hippocampal formation. Contrary to our findings, Biskup and colleagues (2006) found endogenous rat LRRK2 to be expressed consistently throughout the hippocampal formation. It is possible that the use of different antibodies and antigen retrieval methods for the detection of LRRK2 may account for this.

Finally, while we were able to show low levels of hLRRK2 within the SNpc of all our transgenic lines, we were unable to definitively show endogenous rat LRRK2 expression within the SNpc due to a degree of non-specific staining seen in the SNpc of our *Lrrk2* KO rats. It has been previously suggested that this non-specific stain may be attributed to the labelling of astrocytes (Davies *et al.,* 2013). Alternatively, it is possible that the c41-2 antibody recognises LRRK1 protein which shares considerable sequence homology with LRRK2. Though debate exists as to whether LRRK2 is expressed in the rat SNpc, West and colleagues (2014), using the c41-2 LRRK2 antibody, have demonstrated very low levels of LRRK2 in the SNpc DAergic neurons in the rat brain. This is supported by a number of studies which also show rat LRRK2 to be expressed in the SNpc, though at very low levels (Biskup *et al.,* 2006; Taymans *et al.,* 2006).

Our data suggest that while the expression patterns of endogenous rat LRRK2 and the hLRRK2 protein are highly similar, the observed patterns more closely resemble those seen in humans rather than those seen in rats. This is likely a consequence of using the hLRRK2 promoter which has been shown to differ substantially from the rodent *Lrrk2* promoter sequence (West *et al.,* 2014).

In summary, we have developed 3 core BAC transgenic lines expressing mutant (G2019S and R1441C) and hWT hLRRK2. In the following chapters, we describe the subsequent pathological characterisation of these lines, performed in order to further explore the effects of *LRRK2* mutation within the context of PD.

CHAPTER 4 – BEHAVIOURAL CHARACTERISATION

4.1 Chapter introduction: motivations and aims

Clinically, PD is characterised by the motor tetrad of resting tremor, bradykinesia, rigidity and postural instability (Samii *et al.,* 2004; Jankovic, 2008). Often, responsiveness of these symptoms to L-DOPA treatment is also used as a confirmation of *bona fide* PD. In addition to motor symptoms, however, patients suffer from numerous non-motor symptoms including autonomic, mood and cognitive dysfunction (Chaudhuri *et al.,* 2006). Following the generation of *LRRK2* transgenic rats, we set out to determine whether these animals developed a behavioural phenotype which resembled PD. Because of the progressive nature of PD, these animals were assessed at young (3-6 month) and aged (18-21 month) time-points to establish whether any observed phenotypes were age-independent or progressive.

In rodents, motor dysfunction may be assessed in several ways. The accelerating rotarod and static rod are frequently used as measures of motor co-ordination and balance (Deacon, 2013). Furthermore, spontaneous locomotor activity is frequently assessed to determine the development of bradykinesia-like symptoms (Li *et al.,* 2009). While mice and rats vary significantly in size, similar tests can be used for both species, given that appropriate-sized apparatus is used. The presence of impairment on these tests within models of PD is often considered to indicate impaired functionality of the nigro-striatal system. This is supported by acute toxic models which show targeted destruction of the nigro-striatal pathway to result in impaired performance on these tests (Colotla *et al.,* 1990). However, it is also possible that changes elsewhere within the brain (e.g. cerebellum) may cause similar deficits. Hence, treatment with DA agonists or L-DOPA in order to reverse the effects of the motor deficit is often used to confirm that dysfunction lies within the DAergic system.

An advantage of the BAC transgenic approach is its allowance for the use of endogenous promoters which, in turn, grant physiological transgene expression throughout both the brain and peripheral organs. The lack of bias towards the nigro-striatal pathway means that pathology developed outside this system as a result of dysfunction elsewhere can be, in theory, modelled. Due to the fact that PD

is generally considered a motor disorder and that these symptoms in patients tend to be the most overt, we focussed on motor tests when characterising our animals behaviourally. Nonetheless, we also assessed the transgenic rats for select non-motor symptoms, some of which have been previously reported in *LRRK2* rodent models (Bichler *et al.,* 2013).

4.1.1 Chapter aims

1) To determine whether *LRRK2* transgenic animals develop late-stage motor dysfunction, specific to expression of the mutant transgene

2) To determine whether the detected motor symptoms are responsive to treatment with L-DOPA

3) To determine whether transgenic animals develop any Parkinsonian non-motor phenotypes

4.2 The ageing and use of animals for behavioural experiments

4.2.1 General health

Over the course of the ageing process, rats were observed for health defects and overt behavioural phenotypes. Litters consisted, on average, of equal numbers of transgenic versus non-transgenic animals, suggesting the *LRRK2* transgene to have no effect on viability. During the ageing process, a substantial proportion of rats developed pituitary tumours but these were not specific to those animals expressing the transgene or beyond normality for the SD strain (Prejean *et al.,* 1973). Behaviourally, transgenic animals appeared largely identical to non-transgenic animals. However, a proportion of young R1441C animals displayed alopecia on the tops of their heads, potentially reflecting elevated grooming (Andres-Mateos *et al.,* 2009). Additionally, aged male G2019S animals were found to weigh 18% less than non-transgenic controls (Fig. 4.1).

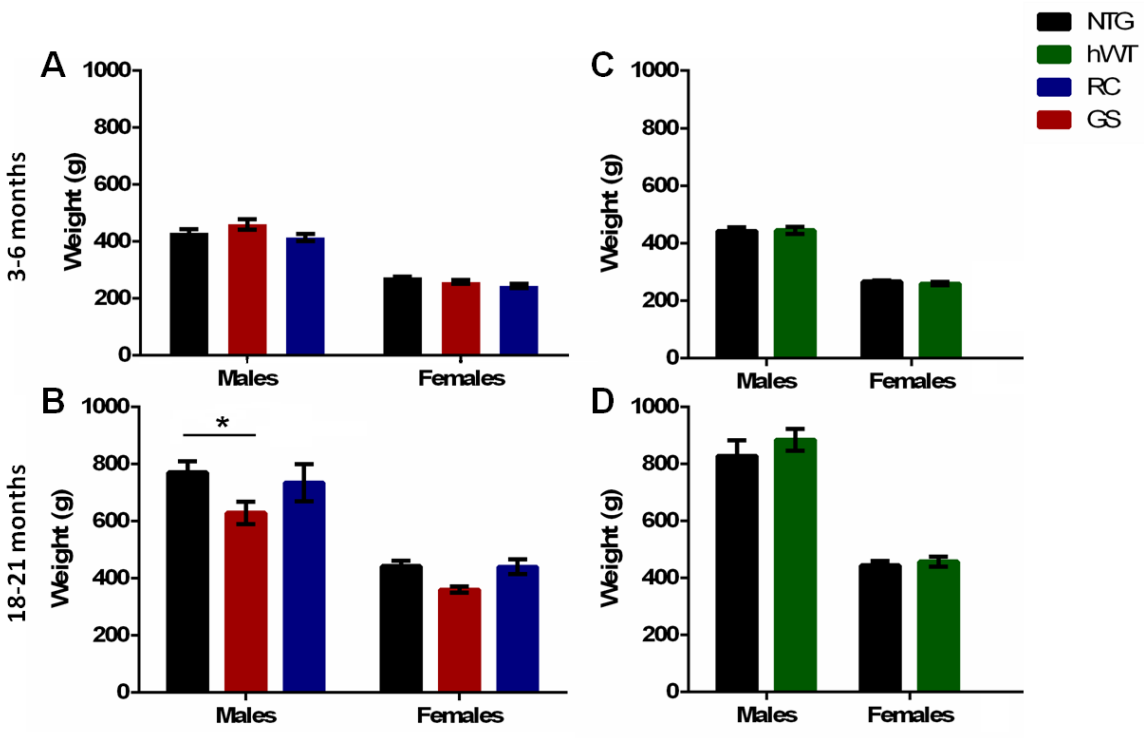

Figure 4.1. Aged G2019S rats show reduced weight. (A) Young G2019S and R1441C animals showed no significant difference in weight compared to age-matched non-transgenic rats (Two-way ANOVA: main effect of gender: $p<0.0001$; no main effect of genotype: $p>0.05$, n=16 per genotype). **(B)** Aged G2019S but not R1441C animals showed decreased weight compared to age-matched non-transgenic rats (Two-way ANOVA: main effect of gender: $p<0.0001$; main effect of genotype: $p<0.001$, n=9-14 per genotype). Neither young hWT **(C)** (Two-way ANOVA: main effect of gender: $p<0.0001$; no main effect of genotype: $p>0.05$; n=16 per genotype) nor aged hWT **(D)** (Two-way ANOVA: main effect of gender: $p<0.0001$; no main effect of genotype: $p>0.05$; n=9-12 per genotype) animals show significant differences in weight compared to age-matched non-transgenic rats. Data are expressed as mean ± SEM. Dunnett post-hoc tests * $p<0.05$.

4.2.2 Experimental approach

In experiments where falling was either an intrinsic part of the test or a potential risk (e.g. rotarod, static rod, inverted grid), only females were used. This was due to the fact a number of males at 18-21 months weighed over 1000g and could not effectively perform a number of these tests. Furthermore, it was considered potentially harmful for animals of such weights to be falling. For other experiments, males and females were subjected to the same experimental conditions. Due to the learning aspect of a number of these tests, animals were not reused for different time points. For the purposes of data analysis, if no significant difference in performance was found between

genders, data from each gender were collapsed. If a main effect of gender was found, data were analysed separately.

4.3 *LRRK2* transgenic rats show late-stage motor dysfunction

4.3.1 Mutant *LRRK2* rats show progressively impaired motor co-ordination

The cardinal clinical features of Parkinson's disease are impairments to motor function (Samii *et al.,* 2004). In rodents, this impairment is typically assessed using assays of motor co-ordination, balance and gait including the rotarod, static rod and tests of stride length.

Motor co-ordination was initially assessed in aged (18-21 month) G2019S, R1441C and non-transgenic rats using the accelerating rotarod (Fig. 4.2). Over three days of testing, aged R1441C and G2019S rats demonstrated an average of 33% and 52% decreased latency to fall on the accelerating rotarod, respectively, compared to non-transgenic controls over three days of testing. To determine whether this effect was seen in young animals, we performed a similar test at 3-6 months. In contrast to that seen in old animals, young G2019S rats demonstrated an average of 45% increased latency to fall from the accelerating rotarod compared to non-transgenic controls while young R1441C transgenic rats showed no significant difference in performance. Finally, to confirm that the effect seen was a result of *LRRK2* mutations rather than hLRRK2 overexpression, both aged and young hWT rats were also subjected to the rotarod test. Neither young, nor aged hWT rats showed significant differences in performance on the rotarod compared to non-transgenic controls.

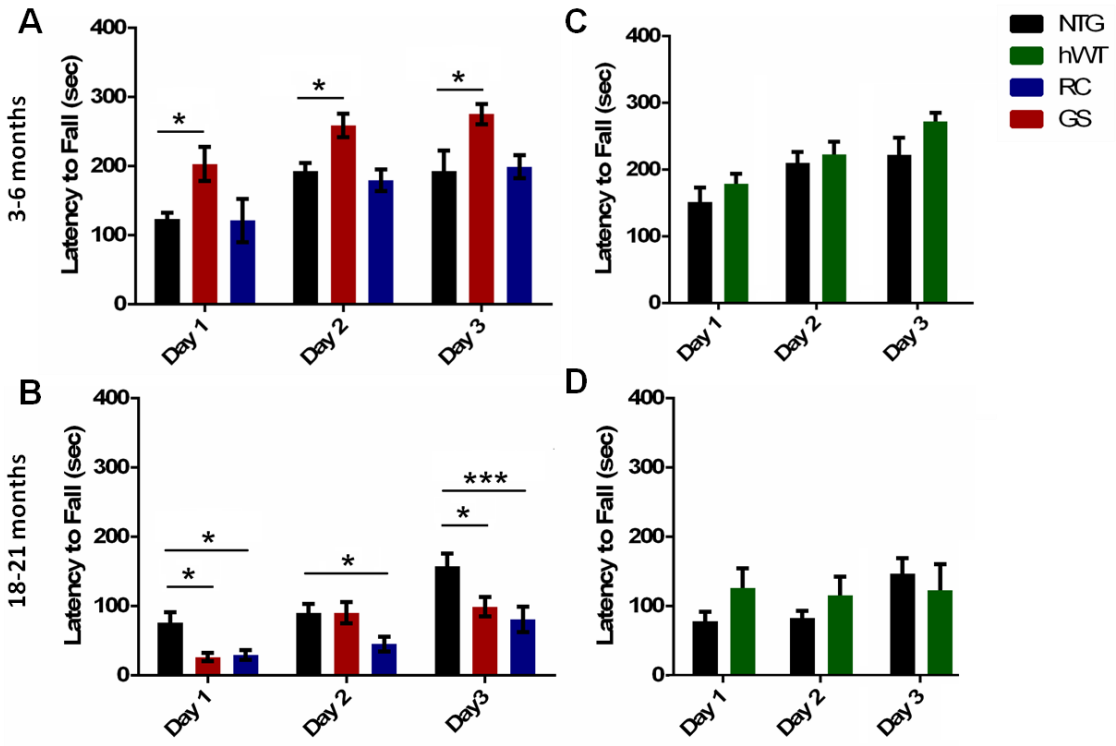

Figure 4.2. Mutant *LRRK2* rats show progressive impairment on the accelerating rotarod. Animals underwent three consecutive days of testing on the accelerating rotarod. **(A)** Young G2019S animals show increased latency to fall on the accelerating rotarod compared to age-matched non-transgenic rats (Two-way ANOVA: main effect of testing day: $p<0.001$; main effect of genotype: $p<0.01$; n=8 per genotype). **(B)** Aged R1441C and G2019S animals showed decreased latency to fall on the accelerating rotarod compared to age-matched non-transgenic rats (Two-way ANOVA: main effect of testing day: $p<0.001$; main effect of genotype: $p<0.01$, n=8-11 per genotype). Neither young hWT **(C)** (Two-way ANOVA: main effect of testing day: $p<0.001$; no main effect of genotype: $p>0.05$; n=8 per genotype) nor aged hWT **(D)** (Two-way ANOVA: no main effect of time: $p>0.05$; no main effect of genotype: $p>0.05$; n=6 per genotype) animals show altered latency to fall compared to age-matched non-transgenic rats. Data are expressed as mean ± SEM. Dunnett post-hoc tests * $p<0.05$, *** $p<0.001$.

To further examine motor coordination in aged R1441C and G2019S rats, we assessed orientation and traversal times on the static rod test (Fig. 4.3). Aged R1441C and G2019S animals were significantly impaired in rod compared to non-transgenic controls on the static rod showing 73% and 89% increased traversal time scores, respectively. This was largely due to an increased tendency to fall from the rod. No effects of genotype were seen in younger animals in either orientation or traversal. Similarly, hWT rats, whether young or aged, showed no significant differences in performance on the static rod compared to non-transgenic controls.

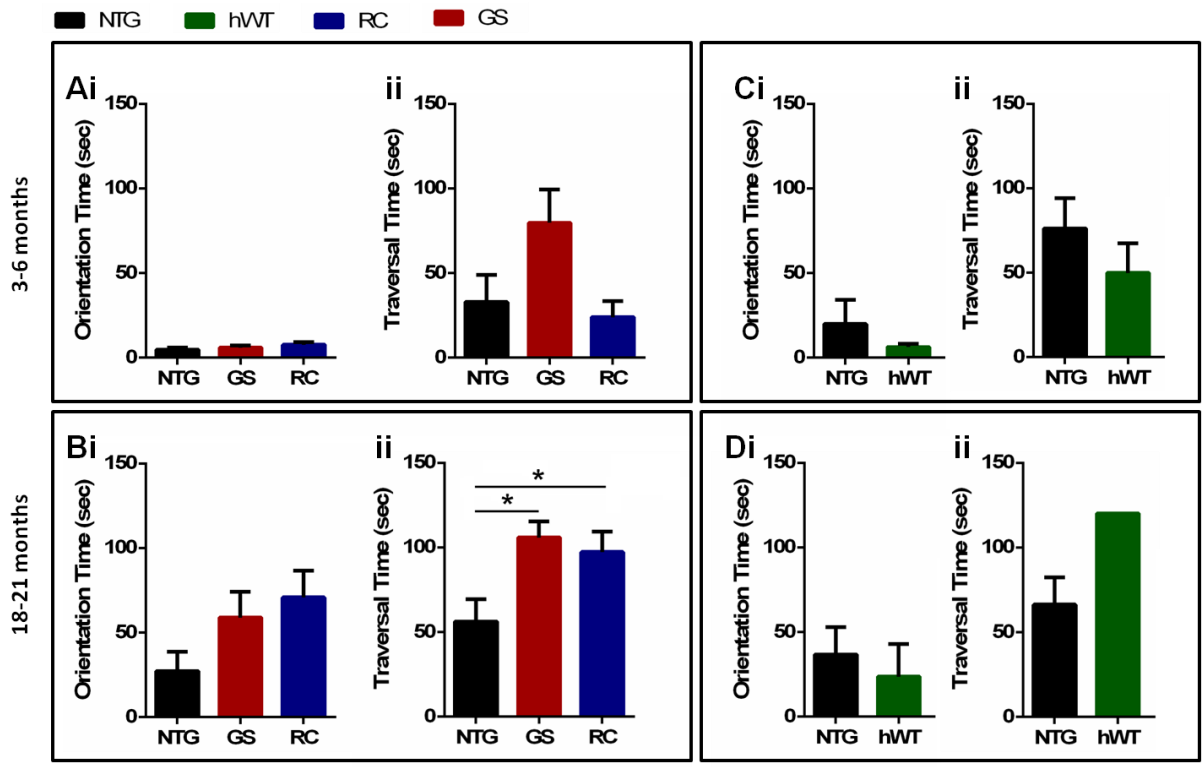

Figure 4.3. Mutant *LRRK2* rats show progressive impairment when traversing but not orienting on the static rod. Animal orientation and traversal times on a 35mm static rod were assessed. **(A)** Young G2019S and R1441C animals showed no significant difference in **(i)** orientation (Kruskal-Wallis One-way ANOVA: no main effect of genotype: $p>0.05$; n=8 per genotype) or **(ii)** traversal (Kruskal-Wallis One-way ANOVA: no main effect of genotype: $p>0.05$; n=8 per genotype) on the static rod compared to non-transgenic rats. **(B)** Aged G2019S and R1441C animals showed **(i)** no significant difference in orientation time (Kruskal-Wallis One-way ANOVA: no main effect of genotype: $p>0.05$; n=14-16 per genotype) but **(ii)** increased traversal time (Kruskal-Wallis One-way ANOVA: main effect of genotype: $p<0.05$; n=14-16 per genotype) on the static rod compared to age-matched non-transgenic rats. **(C)** Young hWT animals showed no significant difference in **(i)** orientation (Mann-Whitney test: $p>0.05$; n=8 per genotype) or **(ii)** traversal (Mann-Whitney test: $p>0.05$; n=8 per genotype) on the static rod compared to non-transgenic rats. **(D)** Aged hWT animals showed no significant difference in **(i)** orientation (Mann-Whitney test: $p>0.05$; n=6-8 per genotype) or **(ii)** traversal (Mann-Whitney test: $p>0.05$; n=6-8 per genotype) on the static rod compared to non-transgenic rats. Data are expressed as mean ± SEM. Dunn's post-hoc tests * $p<0.05$.

Both the rotarod and static rod tests suggest that, at a late age, the mutant hLRRK2 transgenic rats develop dysfunctional balance and motor co-ordination. To further explore the nature of the motor-coordination deficit seen in these animals, the Noldus Catwalk was used to determine whether there were any alterations in gait patterns which may explain the dysfunction seen in earlier tests. The Noldus Catwalk allows for the assessment of a wide variety of gait parameters but we restricted our

analyses to those considered pertinent to a Parkinsonian gait (Chuang *et al.,* 2010; see methods for more details)

A key component of Parkinsonism is the presence of a shuffling gait resulting in a greatly impaired stride length. Forepaw stride length in aged animals was initially assessed using the Catwalk (Fig. 4.4). Somewhat counter-intuitively, G2019S animals showed a 10% increase in stride length while R1441C animals show no significant change compared to controls. Swing speed, a measure of limb movement speed, was also assessed, showing no differences between genotypes.

A number of inter-paw parameters were also assessed. Phase dispersion – a measure of inter limb periodicity – is used to assess motor co-ordination in animal models, with elevated phase dispersion indicating increased levels of impaired motor coordination. Forelimb-hindlimb phase dispersion was found to be increased in R1441C but not G2019S animals, relative to non-transgenic controls, being elevated 34% and 50% for left-fore right-hind and right fore-left hind inter-paw relationships, respectively. Base of support, a measure of the distance between fore or hind limbs, was not found to be different between mutant animals and non-transgenic controls. Finally, maximum paw print area was assessed in order to determine the foot placement of the animals. R1441C but not G2019S animals showed both increased fore- and hind paw maximum print area by 16% and 30%, respectively, when compared to non-transgenic controls, though this effect was only found to be significant in male rats.

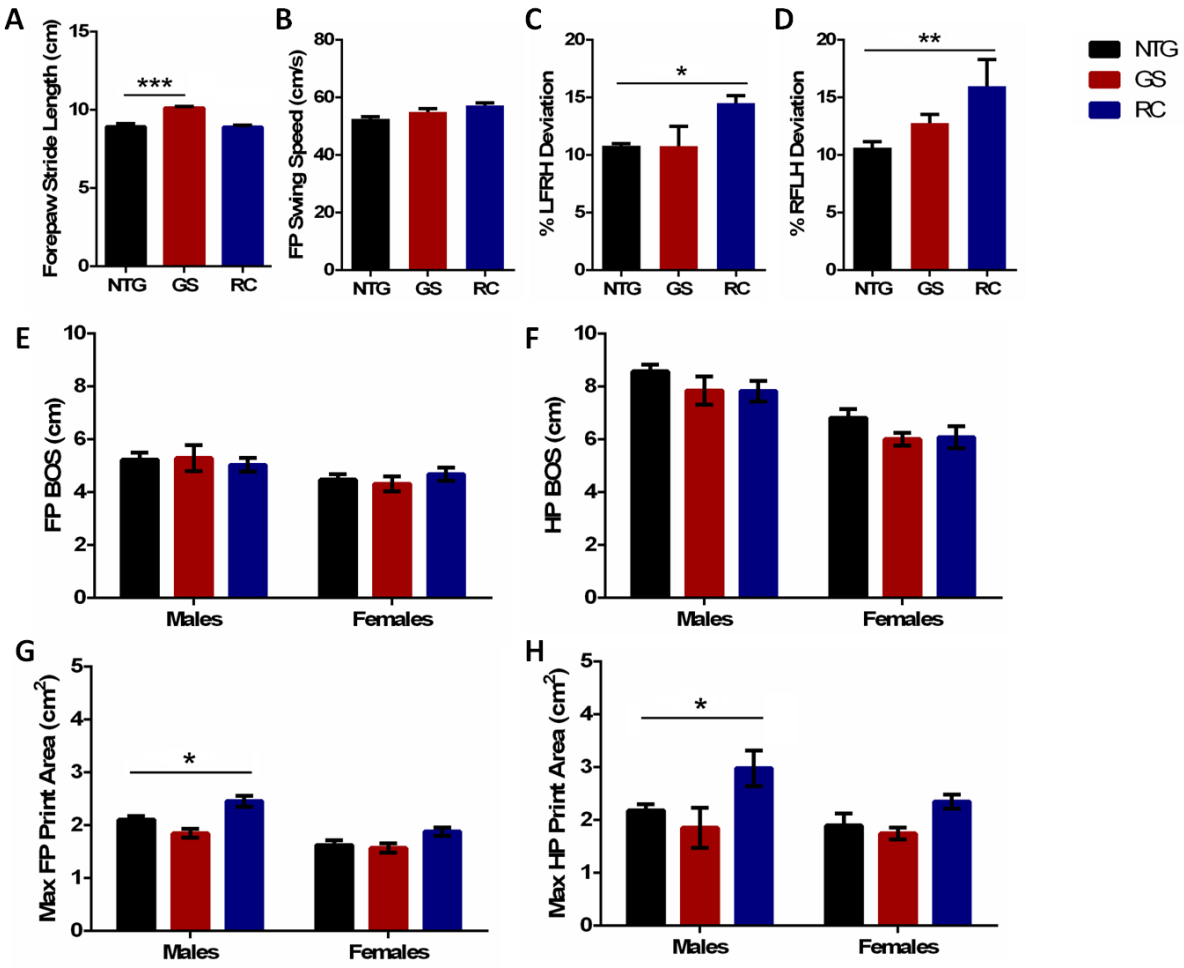

Figure 4.4. Aged *LRRK2* mutant rats show altered gait on the Catwalk. (A) Aged G2019S but not R1441C animals show increased forepaw stride length compared to age-matched non-transgenic rats (One-way ANOVA: main effect of genotype: $p<0.001$; n=9-14 per genotype). **(B)** Aged G2019S and R1441C animals show no difference in forepaw swing speed compared to age-matched non-transgenic rats (One-way ANOVA: no main effect of genotype: $p>0.05$; n=9-14 per genotype). **(C-D)** Aged R1441C but not G2019S animals show increased **(C)** LFRH (One-way ANOVA: main effect of genotype: $p<0.05$; n=9-14 per genotype) and **(D)** RFLH (One-way ANOVA: main effect of genotype: $p<0.01$; n=9-14 per genotype) phase dispersion compared to age-matched non-transgenic rats. **(E-F)** Aged G2019S and R1441C animals show no difference in **(E)** FP BOS (Two-way ANOVA: main effect of gender: $p<0.05$; no main effect of genotype: $p>0.05$, n=9-14 per genotype) or **(F)** HP BOS (Two-way ANOVA: main effect of gender: $p<0.0001$; no main effect of genotype: $p>0.05$, n=9-14 per genotype) compared to age-matched non-transgenic rats. **(G-H)** Aged R1441C but not G2019S animals show increased **(G)** max FP print area (Two-way ANOVA: main effect of gender: $p<0.0001$; main effect of genotype: $p<0.0001$, n=9-14 per genotype) and increased **(G)** max HP print area (Two-way ANOVA: no main effect of gender: $p>0.05$; main effect of genotype: $p<0.01$, n=9-14 per genotype) compared to age-matched non-transgenic rats. Data are expressed as mean ± SEM. Dunnett post-hoc tests * $p<0.05$, ** $p<0.01$.*** $p<0.001$. Abbreviations: FP=forepaw, HP= hind paw, LFRH=left forepaw right hind paw, RFLH=right forepaw left hind paw, BOS= base of support.

4.3.2 Mutant *LRRK2* rats show no changes in muscle strength

In order to determine whether the observed motor dysfunction was a consequence of muscle degeneration, animals were subjected to the inverted screen test (Fig. 4.5). Young and aged G2019S, R1441C and hWT animals performed similarly to non-transgenic controls on the inverted screen test suggesting no effect of transgene expression on muscle strength.

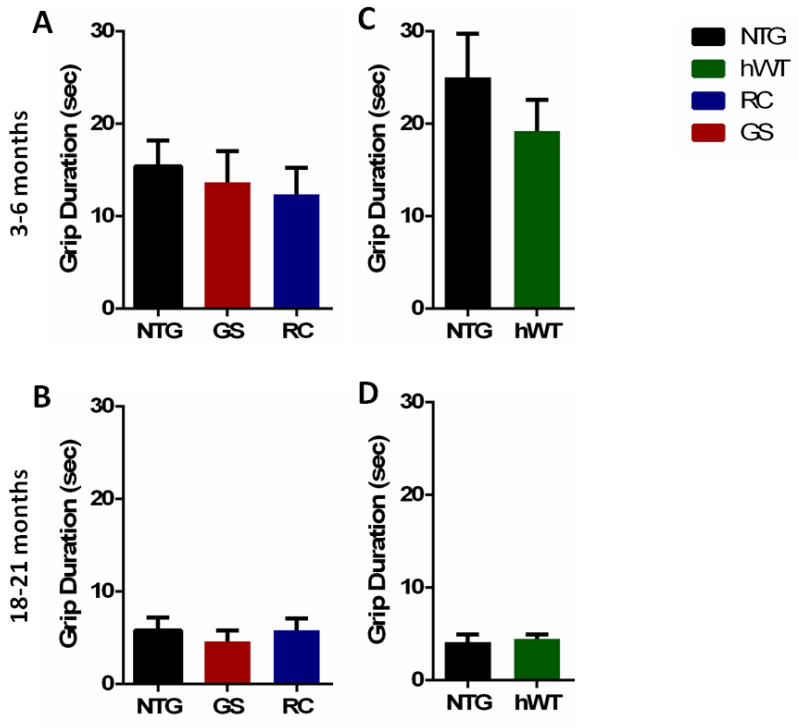

Figure 4.5. Transgenic *LRRK2* rats show no change in muscle strength. (A) Young G2019S and R1441C animals showed no change in latency to fall compared to age-matched non-transgenic rats (One-way ANOVA: no main effect of genotype: $p>0.05$; n=8 per genotype). **(B)** Aged G2019S and R1441C animals also showed no change in latency to fall compared to age-matched non-transgenic rats (One-way ANOVA: no main effect of genotype: $p>0.05$; n=8-11 per genotype). Neither young hWT **(C)** (Welch's t-test: $p>0.05$; n=8 per genotype) nor aged hWT **(D)** (Welch's t-test: $p>0.05$; n=5-6 per genotype) animals showed any change in latency to fall compared to age-matched non-transgenic rats**.** Data are expressed as mean ± SEM.

4.2.3 Mutant *LRRK2* rats display hyperactivity

A defining characteristic of PD is bradykinesia. Earlier *LRRK2* transgenic R1441G mice displayed almost total hypokinesia by 12 months (Li *et al.,* 2009). However, our animals showed no visible signs of slowed movement. To more accurately assess spontaneous locomotor activity in our

animals, we assessed ambulations over a 4 hour period in locomotor activity chambers (Fig. 4.6). At a young age, R1441C but not G2019S animals showed approximately 31% increased total ambulations compared to non-transgenic controls. However, at a late age-point G2019S but not R1441C animals showed approximately 43% increased total ambulations compared to non-transgenic controls. hWT animals showed no differences in ambulations compared to non-transgenic controls at either young or aged time points.

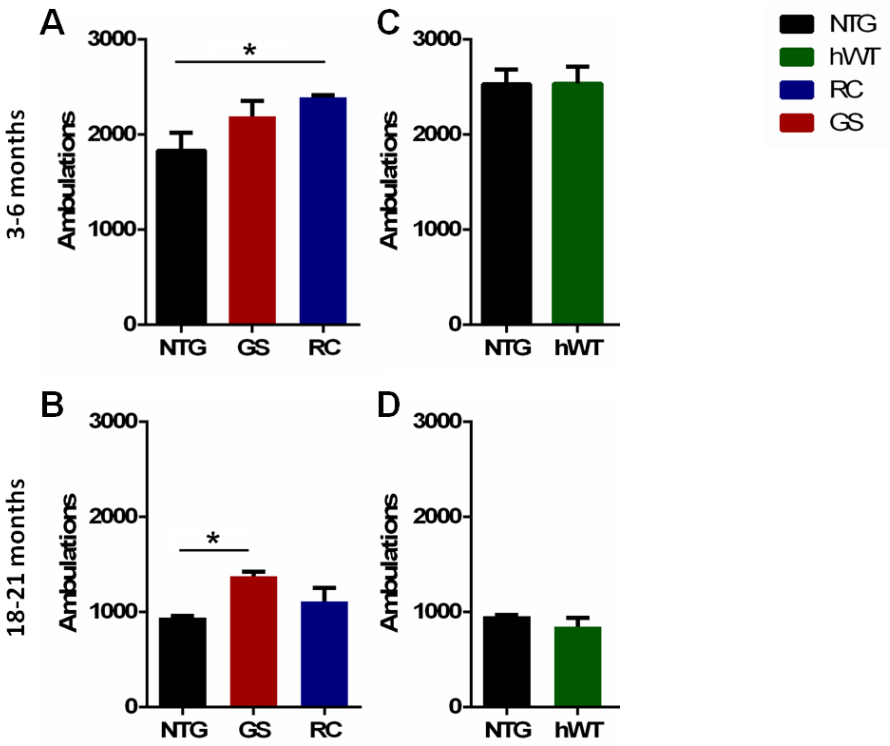

Figure 4.6. G2019S and R1441C rats show increased ambulatory activity. Total locomotor activity over 4 hours was assessed. **(A)** Young R1441C but not G2019S animals show increased ambulatory activity compared to age-matched non-transgenic rats (One-way ANOVA: main effect of genotype: $p<0.05$; n=16 per genotype). **(B)** Aged G2019S but not R1441C animals show increased ambulatory activity compared to age-matched non-transgenic rats (One-way ANOVA: main effect of genotype: $p<0.05$; n=9-14 per genotype). Neither young hWT **(C)** (Welch's t-test: $p>0.05$; n=16 per genotype) nor aged hWT **(D)** (Welch's t-test: $p>0.05$; n=9-12 per genotype) animals show increased ambulatory activity compared to age-matched non-transgenic rats. Data are expressed as mean ± SEM. Dunnett post-hoc tests * $p<0.05$.

Melrose and colleagues (2010) reported increased wall-hugging behaviour in *LRRK2* transgenic mice, potentially indicating anxiety. To assess this, we determined the proportion of ambulations in the centre versus the periphery of the locomotor activity chambers (Fig. 4.7). We found that aged

R1441C but not G2019S female animals showed 13% greater peripheral ambulations than non-transgenic controls, indicating wall hugging behaviour. Young mutant animals and young or aged hWT animals showed no differences in wall hugging behaviour compared to non-transgenic controls at either time points.

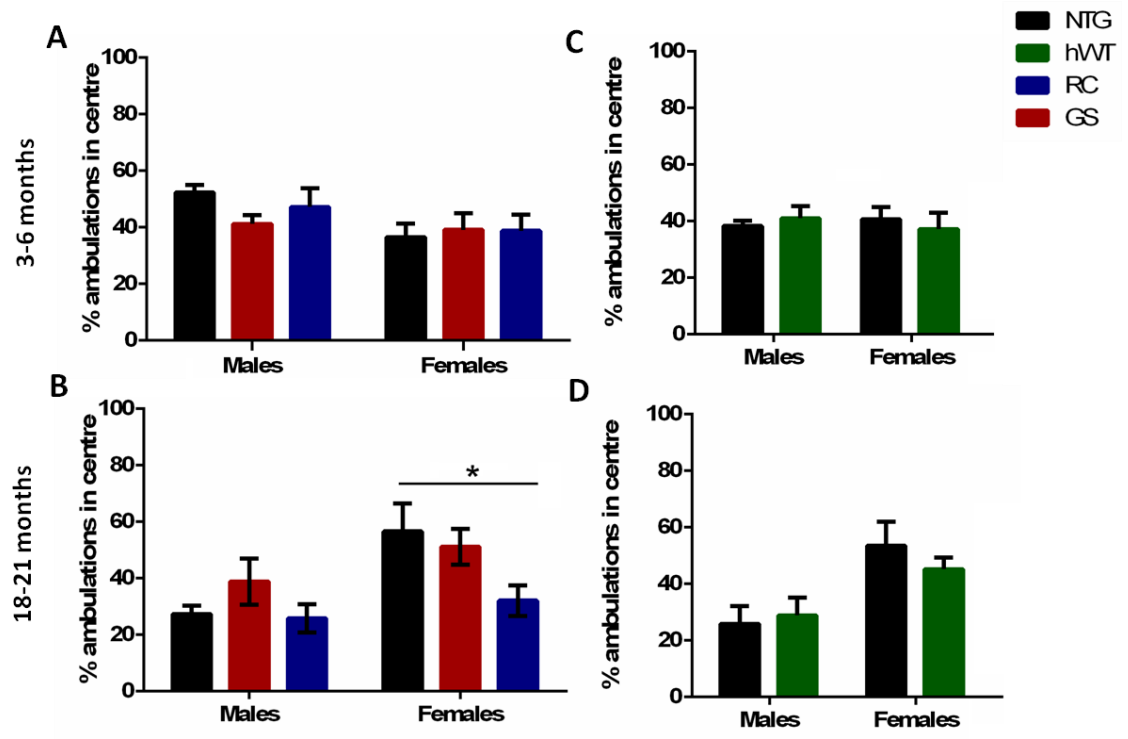

Figure 4.7. Aged R1441C females show increased wall-hugging behaviour. Ambulations in the centre versus the periphery of the cage over 4 hours were assessed. **(A)** Young G2019S and R1441C animals showed no differences in central ambulatory activity compared to age-matched non-transgenic rats (Two-way ANOVA: no main effect of gender: $p>0.05$, no main effect of genotype: $p>0.05$; n=16 per genotype). **(B)** Aged R1441C but not G2019S animals show reduced central ambulatory activity compared to age-matched non-transgenic rats (Two -way ANOVA: main effect of gender: $p<0.01$, main effect of genotype: $p<0.05$; n=9-14 per genotype). Neither young hWT **(C)** (Two-way ANOVA: no main effect of gender: $p>0.05$, no main effect of genotype: $p>0.05$; n=16 per genotype) nor aged hWT **(D)** (Two-way ANOVA: main effect of gender: $p<0.01$, no main effect of genotype: $p>0.05$; n=9-12 per genotype) animals show differences in central ambulatory activity compared to age-matched non-transgenic rats. Data are expressed as mean ± SEM. Dunnett post-hoc tests * $p<0.05$.

4.4 L-DOPA reverses impaired motor co-ordination in G2019S mutant rats

The diagnosis of PD is usually confirmed by responsiveness of motor dysfunction to L-DOPA treatment. A prior experiment demonstrated the effective rescue with L-DOPA of reduced rearing

within a cylinder of aged *LRRK2* transgenic mice (Li *et al.,* 2009). We subjected a large cohort of G2019S animals to the cylinder test (Fig. 4.8). As L-DOPA treatment required the dividing of our cohort in half (for L-DOPA and saline controls) we were unable to perform the test on R1441C animals due to insufficient numbers. In the cylinder, G2019S animals demonstrated 43% increased levels of rearing over the course of 5 minutes compared to non-transgenic controls. hWT animals showed no difference in rearing when compared to non-transgenic controls. Contrary to what was expected, therefore, we found that G2019S animals showed increased rearing activity, potentially reflecting hyperactivity.

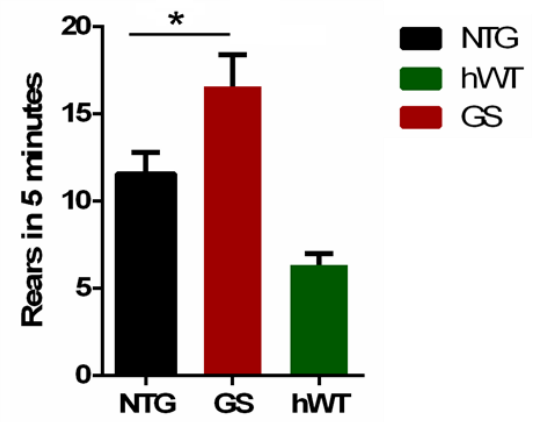

Figure 4.8. G2019S rats show increased cylinder rearing. 18-21 month old G2019S but not hWT rats showed significantly increased rearing in the cylinder over 5 minutes compared to non-transgenic rats (One Way ANOVA: main effect of genotype; $p<0.001$, n=6-12 per genotype). Data are expressed as mean ± SEM. Dunnett post-hoc tests * $p<0.05$.

Following pre-treatment with benzerazide (6.25mg/kg IP), L-DOPA (25 mg/kg IP) was administered to G2019S and non-transgenic rats in an attempt to rescue the behavioural phenotypes observed previously in the rotarod and cylinder test (Fig. 4.9). In the rotarod test, animals were pre-trained on the rotarod for 5 days in order to extinguish any learning effects. Animal performances were compared to pre-treatment performances from the prior day. G2019S animals treated with L-DOPA showed a 87% increase in latency to fall compared to saline treated animals which showed no

significant improvement. Conversely, non-transgenic animals treated with L-DOPA showed no improvement in latency to fall when compared to saline treated G2019S animals. In the cylinder test, G2019S animals showed little change in rearing following L-DOPA treatment, in line with saline-treated G2019S animals. A similar lack of change in rearing was seen in L-DOPA treated non-transgenic controls. It appeared, therefore, that L-DOPA treatment was able to effectively rescue the impaired motor co-ordination seen in G2019S but had no effect upon the cylinder rearing.

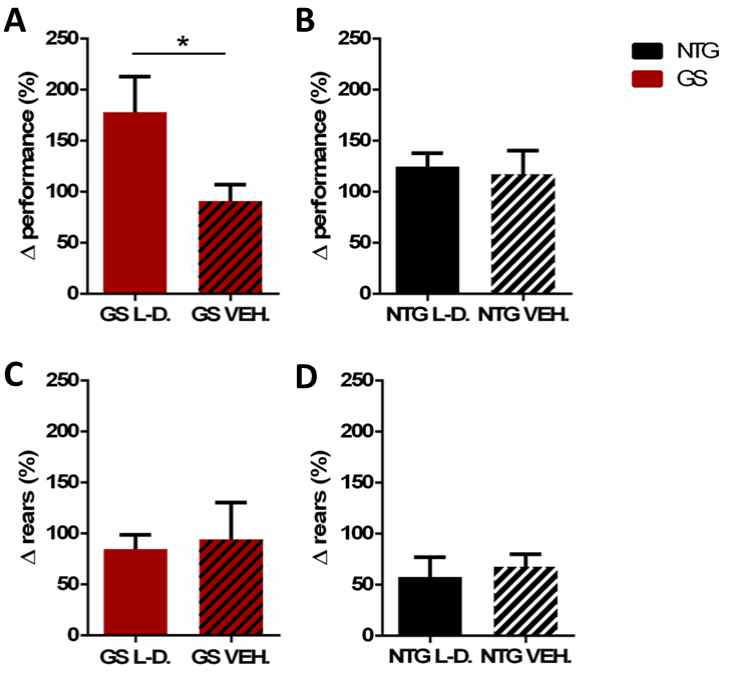

Figure 4.9. Rotarod but not rearing phenotype is L-DOPA responsive in aged G2019S rats. 18-21 month old G2019S and non-transgenic rats, previously trained on the rotarod to extinguish the effect of learning, were administered either benzerazide (6.25mg/kg IP) and L-DOPA (25 mg/kg IP) or saline. One hour later, animal performance was assessed on the rotarod and cylinder test. **(A)** A significant improvement in rotarod performance was seen in response to L-DOPA treatment specific to the G2019S transgenic rat line (Mann-Whitney test *$p<0.05$, $n=6$ per treatment condition). **(B)** No significant difference in rotarod performance was seen in non-transgenic rats in response to L-DOPA treatment (Mann-Whitney test $p>0.05$, $n=4$ per treatment condition). No significant difference in cylinder rearing was seen in response to L-DOPA treatment specific to the **(C)** G2019S (Mann-Whitney test $p>0.05$, $n=6$ per treatment condition) or **(D)** non-transgenic rat line (Mann-Whitney test $p>0.05$, $n=4$ per treatment condition). Abbreviations: L-D=L-DOPA, VEH=saline.

4.5 *LRRK2* transgenic rats demonstrate late-stage non-motor dysfunction

4.5.1 R1441C rats show progressively impaired cognitive function

Spontaneous alternation within a T-maze is a commonly used test for assessing memory function. Because of frequently reported cognitive dysfunction in PD patients (Park & Stacy, 2009) and due to the rats' high levels of hLRRK2 protein levels observed within the hippocampus, an area associated with working memory function (Olson *et al.,* 2006), this test was deemed relevant alongside more typical Parkinsonian tests.

Aged R1441C but not G2019S animals showed a 29% impaired performance compared to non-transgenic animals with R1441C animals' selections being close to chance (50%) (Fig. 4.10). This effect was specific to aged animals, with young R1441C and G2019S animals performing similarly to non-transgenic controls. Additionally, both young and aged hWT animals performed similarly to non-transgenic controls.

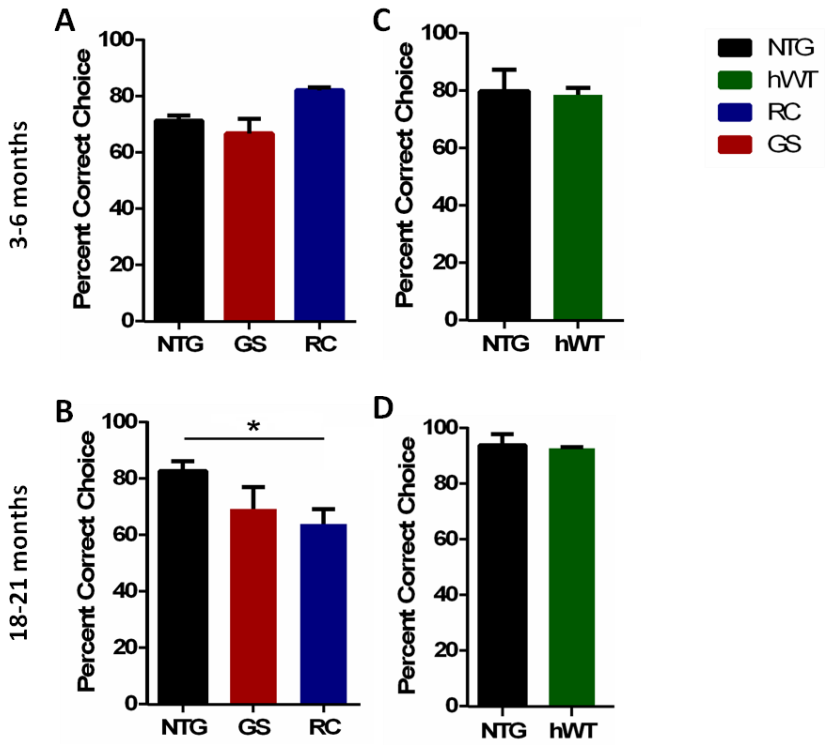

Figure 4.10. R1441C rats show progressive cognitive impairment. (A) Young G2019S and R1441C animals show no differences in alternation performance compared to age-matched non-transgenic rats (One-way ANOVA: no main effect of genotype: $p>0.05$; n=16 per genotype). **(B)** Aged R1441C but not G2019S animals show impaired alternation performance compared to age-matched non-transgenic rats (One-way ANOVA: main effect of genotype: $p<0.05$; n=9-14 per genotype). Neither young hWT **(C)** (Welch's t-test: $p>0.05$; n=16 per genotype) nor aged hWT **(D)** (Welch's t-test: $p>0.05$; n=10-11 per genotype) animals show differences in alternation performance compared to age-matched non-transgenic rats. Data are expressed as mean ± SEM. Dunnett post-hoc tests * $p<0.05$.

In order to investigate whether the deficit seen in aged R1441C animals was a result of altered decision times, we analysed the time taken to choose a T-maze arm in the spontaneous alternation test (Fig. 4.11). We found that there was no difference between aged R1441C, G2019S and non-transgenic controls in the time taken to select an arm. However, young R1441C animals showed, on average, a 55% reduction in decision times when compared to non-transgenic controls. Young G2019S animals did not differ significantly in speed from non-transgenic controls. hWT animals showed no differences in decision time compared to non-transgenic controls at either young or aged time points. These data suggest that the impaired performance of the aged R1441C animals in the spontaneous alternation task was not a consequence of their increased decision times.

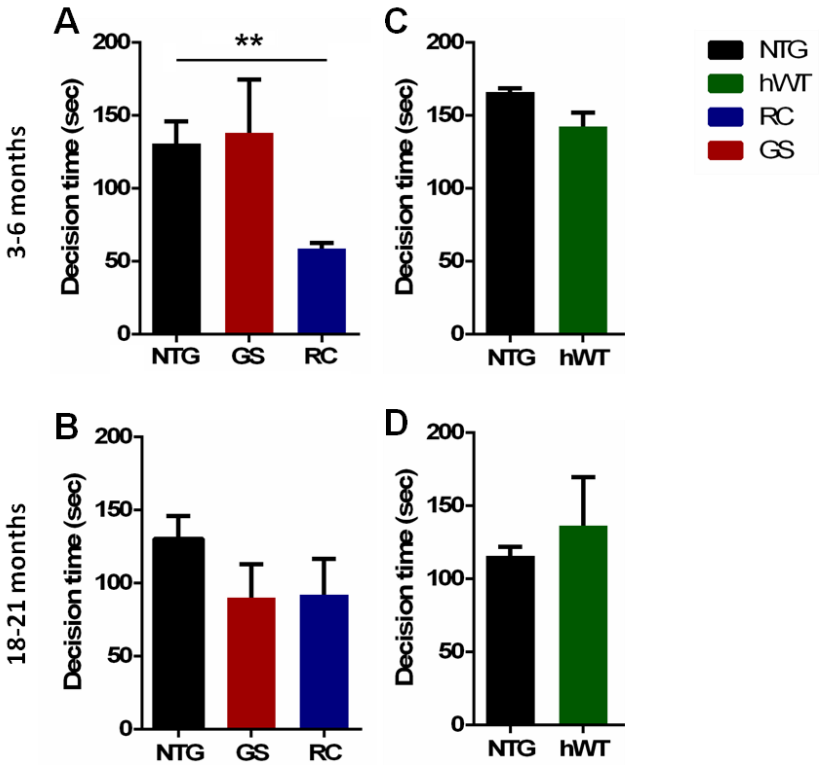

Figure 4.11. R1441C rats show increased decision speed in the spontaneous alternation test. (A) Young R1441C but not G2019S animals show increased decision speed compared to age-matched non-transgenic rats (One-way ANOVA: main effect of genotype: $p<0.01$; n=16 per genotype). **(B)** Aged G2019S and R1441C animals show no differences in decision speed compared to age-matched non-transgenic rats (One-way ANOVA: no main effect of genotype: $p>0.05$; n=9-14 per genotype). Neither young hWT **(C)** (Welch's t-test: $p>0.05$; n=16 per genotype) nor aged hWT **(D)** (Welch's t-test: $p>0.05$; n=10-11 per genotype) animals show differences in decision speed compared to age-matched non-transgenic rats. Data are expressed as mean ± SEM. Dunnett post-hoc tests ** $p<0.01$.

4.5.2 Mutant *LRRK2* rats show no alterations in gastrointestinal function

Gastrointestinal dysfunction, in particular, constipation, is a commonly reported non-motor feature of PD (Magerkurth *et al.,* 2005). To assess whether there were any alterations in gastrointestinal function, we collected stool over a 1 hour period to determine stool weight, frequency and percentage water content (Fig. 4.12). G2019S, R1441C and hWT animals showed similar stool pellet frequencies, stool weight and stool water content to non-transgenic controls in all tests, suggesting no effect of transgene expression on gastrointestinal function.

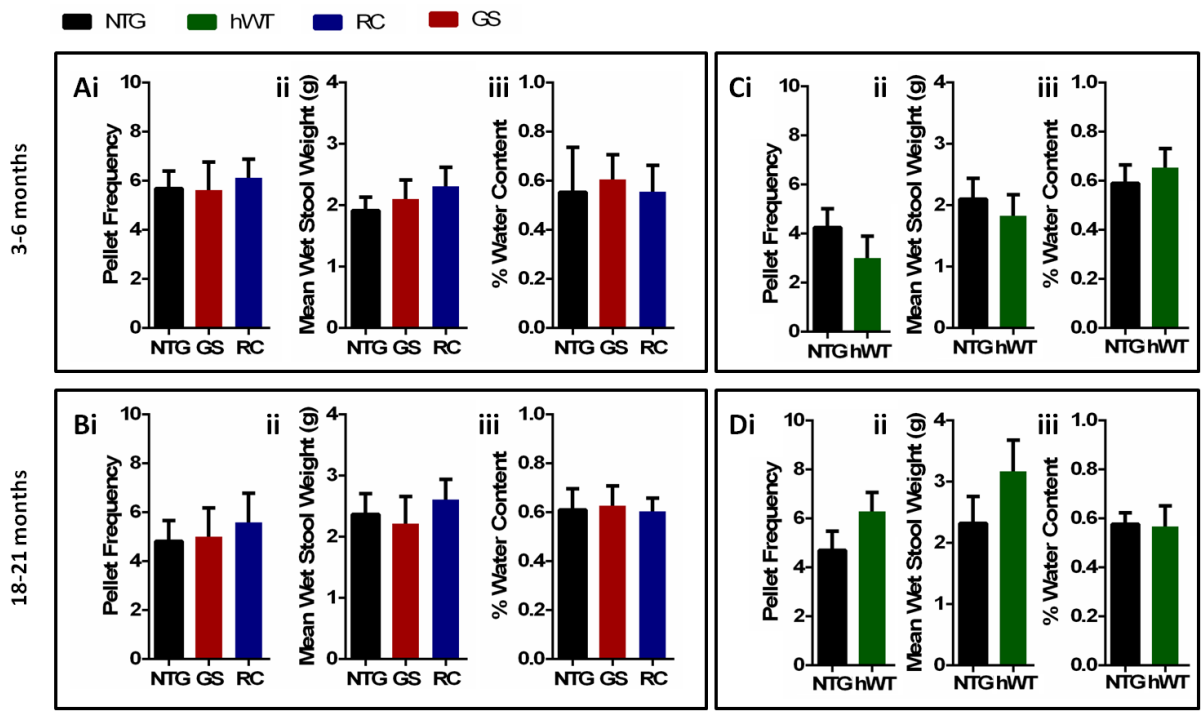

Figure 4.12. Mutant *LRRK2* rats show no change in gastrointestinal function. (A) Young G2019S and R1441C animals showed no change in **(i)** stool pellet frequency , **(ii)** wet stool weight or **(iii)** percentage water content compared to age-matched non-transgenic rats (One-way ANOVA: no main effect of genotype: $p>0.05$; n=16 per genotype). **(B)** Aged G2019S and R1441C animals showed no change in **(i)** stool pellet frequency, **(ii)** wet stool weight or **(iii)** percentage water content compared to age-matched non-transgenic rats (One-way ANOVA: no main effect of genotype: $p>0.05$; n=9-14 per genotype). Neither young hWT **(C)** (Welch's t-test: $p>0.05$; n=16 per genotype) nor aged hWT **(D)** (Welch's t-test: $p>0.05$; n=9-12 per genotype) animals showed any change in **(i)** stool pellet frequency, **(ii)** wet stool weight or **(iii)** percentage water content compared to age-matched non-transgenic rats**.** Data are expressed as mean ± SEM.

4.6 Chapter discussion

In this Chapter, we performed a broad-range behavioural analysis of the *LRRK2* transgenic rats which were generated in Chapter 3. In summary, our analysis revealed a progressive impairment in motor co-ordination which, while present in both the G2019S and R1441C genotypes, was more robust in the R1441C mutation. This impairment in motor co-ordination was partially rescuable, at least in the case of the G2019S mutation, by administration of L-DOPA. In contrast with other reports, however, these animals displayed hyperactivity rather than hypokinesia (Li *et al.,* 2009). Finally, our analysis revealed a late-age impairment in cognition, specific to the R1441C mutation.

4.6.1 *LRRK2* mutations lead to late-stage motor dysfunction

The impairment of the R1441C and G2019S but not hWT rats on both the rotarod and the static rod at a late age indicates PD-like symptoms, specific to mutant LRRK2. The lack of any evident muscle weakness reinforces the hypothesis that the impaired performance on these tests arises from impaired motor co-ordination and balance. While not seen in all *LRRK2* rodent models, impaired rotarod and static rod performance have been previously reported, although not always in an age-dependent fashion (Dranka *et al.,* 2013; Maekawa *et al.,* 2012; Walker *et al.,* 2014). Our gait analysis using the Noldus Catwalk revealed a number of disturbances in the gait of R1441C animals including impaired limb co-ordination and altered feet positioning, the latter of which may indicate compensatory posture resulting from impaired balance. The absence of gait disturbances in our G2019S animals may be due to the seemingly less severe impairment, as seen on the rotarod. Alternatively, the hyperactivity seen in this line, discussed later, may explain the differences seen, along with the increased stride length. A recent study utilised the Noldus Catwalk to assess gait in R1441C transgenic mice but found no gait disturbances (Tsika *et al.,* 2014). However, this study did not assess phase dispersion and these animals showed very little in the way of a general behavioural phenotype, showing no alterations in rotarod performance.

In line with a number of studies showing the successful reversal of hypokinesia in *LRRK2* transgenic animals with L-DOPA, we were able to successfully improve impaired rotarod performance in G2019S mutant animals by L-DOPA treatment (Li *et al.,* 2009; Chen *et al.,* 2012; Chou *et al.,* 2014). These data are particularly useful in the context of the use of a *LRRK2* endogenous promoter which results in transgene expression throughout the brain, including non-nigrostriatal regions associated with balance and motor co-ordination such as the cerebellum. Our findings were in contrast to a recent study which was unable to reverse a rotarod deficit in G2019S BAC transgenic rats (Walker *et al.,* 2014). It is not clear why our results differ, although the rotarod deficit observed by Walker and colleagues did not appear to be late-stage-progressive in the fashion we report, suggesting a

potentially different source of dysfunction. The collective data from these experiments suggests an impairment of nigro-striatal DAergic function specific to the G2019S and R1441C mutant *LRRK2* lines which develops over the course of the animals' lifetimes.

4.6.2 *LRRK2* mutations cause hyperactivity

The impairment in motor co-ordination in the *LRRK2* transgenic rats is not accompanied by hypokinesia as might be expected in a model of PD (Jankovic, 2008). Rather our G2019S and R1441C mutant animals display hyperactivity. The hyperactivity seen is specific to the mutant transgene and appears to reflect a phenotype seen consistently throughout the literature, although little attempt has been made to address its source (Lin *et al.,* 2009; Li *et al.,* 2010; Zhou *et al.,* 2011; Herzig *et al.,* 2012; Lee *et al.,* 2014; Longo *et al.,* 2014). Reports of hyperactivity do not seem specific to a particular genetic design, with the phenotype not being restricted to high expression levels, the use of specific promoters, use of BACs vs cDNA or model strain or species. It seems, therefore, that the hyperkinesia is a genuine effect of *LRRK2* mutation. Given that L-DOPA treatment did not have an effect upon the hyperactive phenotype, observed in the cylinder, it seems likely that the source of the behaviour does not arise from DAergic systems. Hyperactivity is not traditionally associated with PD. However, a study has suggested that sufferers of PD have increased early-life symptoms of hyperactivity (Walitza *et al.,* 2007). However, this study utilised retrospective reports of behaviour which may be unreliable. Nonetheless, the indication that hyperactivity may be indicative of increased risk for PD is a potentially valuable one.

In our mutant transgenic rats, this hyperactivity manifested at different age points depending upon the genotype. R1441C rats showed increased ambulatory activity, increased decision speed in the spontaneous alternation test and the appearance of alopecia, previously suggested to reflect increased grooming behaviour (Andres-Mateos *et al.,* 2009) at 3-6 months but not at 18-21 months. Conversely, G2019S rats showed little evidence of hyperactivity at 3-6 months but at 18-21 months, these animals showed increased stride length, increased ambulatory activity and increased rearing in

the cylinder test. It is also possible that the weight loss seen in the aged G2019S animals was a consequence of their increased activity, although studies of *Lrrk2* KO rodents have suggested that LRRK2 plays a role in metabolism (Ness *et al.,* 2013). It is not clear if the improved performance of the young G2019S animals on the rotarod reflects hyperactivity as the same improved performance is not observed in R1441C animals, which show an even greater degree of hyperactivity. This phenotype has been previously reported in G2019S lines but no theory was posited for its underlying mechanism (Lin *et al.,* 2009). Nonetheless, if this effect were preserved into older ages, it may explain the reduced impairment on the rotarod seen in aged G2019S lines. Interestingly, treatment with LRRK2 kinase inhibitors has been found to impair performance on the rotarod suggesting that the improved rotarod performance may be a reflection of increased LRRK2 kinase activity (Longo *et al.,* 2014).

The purportedly increased aggressiveness of the R1441C mutation compared to the G2019S mutation may explain the earlier onset of the hyperactive phenotype in the former (Kumari & Tan, 2009). Why R1441C animals only appear to show hyperactivity at young but not old time points is not entirely clear, though it is possible that the onset of PD-like symptoms, which appear to be more severe in R1441C animals, may offset the effects of hyperactivity which have been reported to be resistant to age (Longo *et al.,* 2014). Similarly biphasic behavioural effects have been reported in α-synuclein transgenic animal models, with hyperactivity occurring at a young age transitioning, with time, into more typical Parkinsonian behaviour (Lam *et al.,* 2011). In support of this, Longo and colleagues (2014) do appear to detect ameliorations of the hyperactive phenotype at late age points (~19 months).

It has been recently proposed that the hyperactive phenotype is a consequence of LRRK2 kinase hyperactivity (Longo *et al.,* 2014). This was assessed by the administration of LRRK2 kinase inhibitors, using phosphorylation of LRRK2 at ser935 as a read-out of LRRK2 kinase activity. Shortly (~30 minutes) following the administration of kinase inhibitors, this hyperactivity could be reversed in

G2019S mutants. Furthermore, kinase dead *LRRK2* transgenic mice did not appear to show this hyperactive phenotype (Longo *et al.,* 2014). However, our findings, that hyperactivity is also seen in R1441C mutants, a mutation which is not currently thought to cause elevated LRRK2 kinase activity, suggests that the hyperactivity has an alternate source. It is also interesting that no hyperactivity is seen in hWT overexpressers given their elevated abundance of hLRRK2 protein.

4.6.3 *LRRK2* mutations cause Parkinsonian non-motor symptoms

The observed presence of an impairment to cognition at an aged time point in the R1441C rats is the first time that a cognitive phenotype has been reported in a *LRRK2* rodent model. Impaired spatial cognition and short term memory, such as that assessed by the spontaneous alternation test, is indeed reportedly impaired in PD patients and cognitive defects have additionally been reported in α-synuclein animal models (Park & Stacy, 2009; Chesselet & Richter, 2011). Furthermore, *LRRK2* carriers have been reported to show decreased hippocampal volume (Reetz *et al.,* 2010). It is likely that such a cognitive defect may be brought about by altered hippocampal or, potentially, cortical function, both areas of high hLRRK2 protein expression in our models. Whether the cognitive dysfunction reflects degeneration within hippocampal areas or more subtle cellular alterations is unclear and requires further investigation. Earlier reports of altered hippocampal neurogenesis in G2019S transgenic rodents suggest a potentially more elaborate source of hippocampal dysfunction (Winner *et al.,* 2010). However, as this phenotype was shown only by a single test, further verification of a cognitive defect using, for example, the Morris water maze, should be used to solidify the findings.

Our observation of increased wall hugging behaviour, observed in aged female R1441C animals resembles that previously reported in G2019S transgenic mice (Melrose *et al.,* 2010). Though this phenotype may reflect elevated levels of anxiety, previous assessments in G2019S *LRRK2* rodents have seen no evidence of anxiety (Herzig *et al.,* 2012). It has been alternatively suggested that impaired spatial memory may also lead to increased wall hugging behaviour (Melrose *et al.,* 2010).

To more effectively assess the potential presence of anxiety in our rats, tests such as the elevated plus maze would provide valuable further information.

Finally, the absence of gastrointestinal dysfunction, as assessed by stool weight and water content, in our mutant rats was not in line with previous reports of such a defect in R1441G mice (Bichler *et al.,* 2013). However, the authors of this study do report that these gastrointestinal defects fluctuate between constipation and diarrhoea, in addition to the animals showing normal digestive function at 2, 9 and 12 months. This variability may make detection of a phenotype difficult without examining large cohorts of animals at numerous time points.

4.6.4 Chapter summary

In summary, our *LRRK2* rats developed late-stage motor and non-motor behavioural phenotypes, specific to the G2019S and R1441C mutations, reminiscent of PD. While these animals displayed the expected impairment to motor coordination seen in PD models which could be reversed with L-DOPA treatment, they also displayed hyperactivity at numerous ages which appeared to be L-DOPA unresponsive. In addition to motor phenotypes, R1441C animals also displayed impaired cognitive function and potential signs of anxiety which, to this date, have not been previously reported in a *LRRK2* rodent model.

CHAPTER 5 – MOLECULAR CHARACTERISATION

5.1 Chapter introduction: motivations and aims

In PD, it is thought that the cardinal motor symptoms arise as a consequence of impaired DAergic input to the dorsal striatum due to the degeneration of DAergic neurons of the SNpc (Ehringer & Hornykiewicz, 1960). Along with the loss of DAergic neurons, a large proportion of PD patients demonstrate LBs in surviving neurons of the SNpc which label positive for α-synuclein (Spillantini *et al.,* 1997). In addition to Lewy pathology, numerous reports of tau tangles, comprised of hyperphosphorylated tau, have been reported in PD patients, particularly in those possessing a *LRRK2* mutation, in addition to a number of rodent *LRRK2* transgenic models (Haugarvoll & Wszolek, 2009; Li *et al.,* 2010; Li *et al.,* 2009; Melrose *et al.,* 2010; Dusonchet *et al.,* 2011). Following the behavioural characterisation of our *LRRK2* transgenic rats, whose behavioural phenotype indicated the presence of a DAergic deficit, we set out to investigate whether these animals displayed any of the neuropathological symptoms associated with PD at a late-age and whether dysfunction within the DAergic system could be determined.

In addition to the previous Chapter's indication of PD-like motor dysfunction in mutant *LRRK2* transgenic rats, fast-scan cyclic voltammetry (FCV), performed by our colleagues, Dr Dawid Potgeiter and Dr Richard Exley, indicated impaired DA release within the striatum of aged G2019S, R1441C and, to a somewhat lesser extent, hWT *LRRK2* rats at a late age point (Fig. 5.1). In line with our behavioural data, R1441C rats seemed to show a more aggressive phenotype than G2019S rats with a slightly greater reduction in evoked DA (39% and 32% reduction, respectively). Additionally interesting was the finding that this DAergic deficit was also present, although to a somewhat lesser extent (27% reduction), in the hWT rats also. These data support the notion that *LRRK2* transgenic rats develop abnormalities in the nigro-striatal DAergic system.

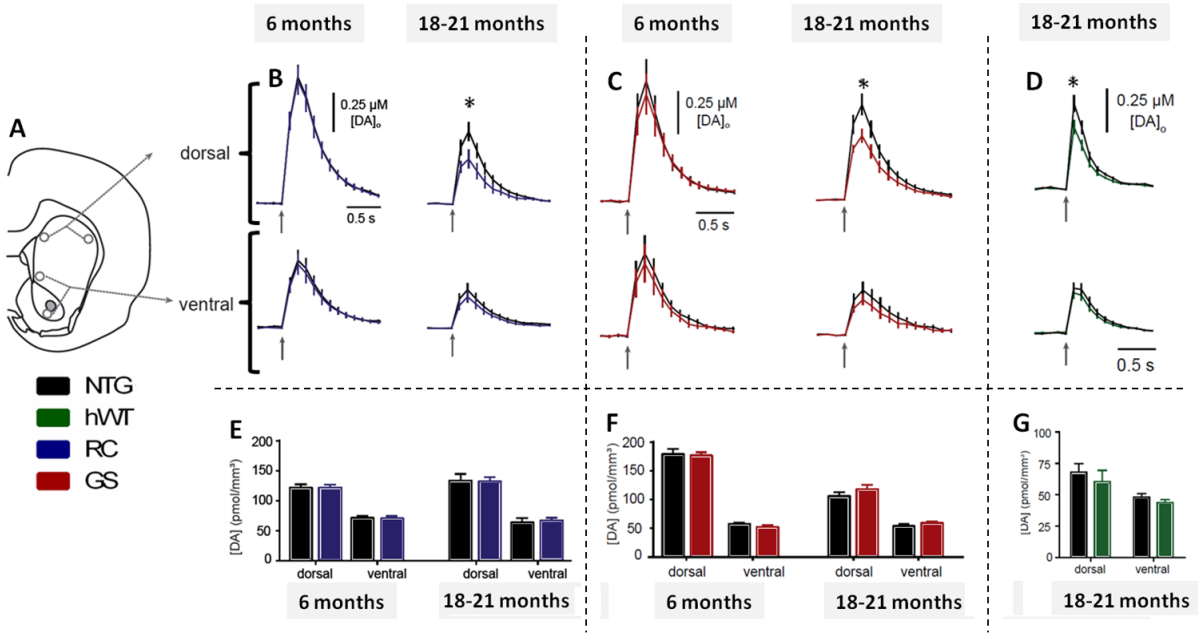

Figure 5.1. *LRRK2* transgenic rats develop late-stage DA transmission deficits in the dorsal striatum. (A) Recording site locations in striatal slices from R1441C, G2019S, hWT and non-transgenic rats. **(B-D)** Mean extracellular dopamine concentration ($[DA]_o$) profiles vs. time (mean ± SEM) following single pulse stimulation (↑200 µs, 600 µA) in dorsal or ventral striatum of **(B)** R1441C or **(C)** G2019S **(D)** hWT 6 and 18-21 month old rats. Mean peak evoked $[DA]_o$ was not significantly different between R1441C and non-transgenic littermates in either dorsal or ventral striatum at 6 and 12 months of age ($p>0.05$; Mann Whitney U; n = 15–29); however at 18-21 months mean peak 1p evoked $[DA]_o$ was significantly lower in R1441C (0.30 ± 0.06 µM) compared with non-transgenic littermates (0.49 ± 0.06 µM) in dorsal striatum (*$p< 0.05$; Mann Whitney U; n = 15) but not ventral striatum ($p>0.05$; Mann Whitney U test; n=12). Mean peak evoked $[DA]_o$ was not significantly different between G2019S and non-transgenic littermates in either dorsal or ventral striatum at 6 and 12 months of age ($p>0.05$; Mann Whitney U; n = 11–21); however at 18-21 months mean peak 1p evoked $[DA]_o$ was significantly lower in G2019S (0.40 ± 0.04 µM) compared with non-transgenic littermates (0.59 ± 0.07 µM) in dorsal striatum (*$p< 0.05$; Mann Whitney U test; n = 36) but not ventral striatum ($p>0.05$; Mann Whitney U; n=25). At 22 months, mean peak evoked $[DA]_o$ was significantly lower in *LRRK2* hWT rats (0.27 ± 0.03 µM) compared with non-transgenic littermates (0.37 ± 0.04 µM) in dorsal striatum (*$p< 0.05$; Mann Whitney U test; n = 30) but not ventral striatum ($p> 0.05$; Mann Whitney U test; n = 29-30). (Figures created in collaboration with Dr Sarah Threlfell, Dr Dawid Potgeiter and Dr Richard Exley).

In addition to investigating the potential emergence of late stage neuropathology, typically associated with PD, our *LRRK2* transgenic rats additionally gave us the opportunity to investigate molecular alterations previously reported in *LRRK2* rodent models. Specifically, we aimed to investigate reports of altered microtubule stability which has been reported to be enhanced by mutant or wild-type LRRK2 overexpression (Lin *et al.,* 2009; Maekawa *et al.,* 2012). Furthermore, while only a single study has reported autophagic changes in LRRK2 transgenic rodents (Ramonet *et*

al., 2011), *Lrrk2* KO rodents and numerous *in vitro* studies have indicated a central role for LRRK2 in autophagy (Alegre-Abarrategui *et al.,* 2009; Tong *et al.,* 2010; Herzig *et al.,* 2011; Tong *et al.,* 2012). Finally, a number of *in vitro* studies of LRRK2 have reported alterations in LRRK2 phosphorylation as a result of LRRK2 mutations which have been proposed to inhibit interaction with 14-3-3 proteins (Nichols *et al.,* 2010). We deemed it valuable to determine whether these findings translated to our *LRRK2* BAC transgenic rats.

5.1.1 Chapter aims

1) To determine whether expression of mutant hLRRK2 can lead to progressive DAergic neurodegeneration within the SNpc

2) To determine whether mechanisms responsible for DA release and recycling are dysfunctional in *LRRK2* transgenic rats

3) To determine whether aged rats display neuropathological accumulations of PD-associated proteins

4) To determine whether *LRRK2* transgenic rats display the molecular changes previously observed in other transgenic *LRRK2* rodents which may inform upon the function or dysfunction of the LRRK2 protein

5.2 *LRRK2* mutant rats do not display SNpc DA neuronal loss

The progressive degeneration of DAergic neurons is a defining feature of PD (Dickson *et al.,* 2009) and has been infrequently reported in transgenic *LRRK2* overexpressing mice (Ramonet *et al.,* 2011; Chen *et al.,* 2012). To determine whether overexpression of mutant LRRK2 leads to DAergic neurodegeneration at a late age, we conducted an unbiased stereological count of TH-positive neurons of the SNpc in 18-21 month old non-transgenic, G2019S and R1441C rats (Fig. 5.2). TH was used as a marker of DAergic neurons. Our analysis revealed no differences in TH-positive neuronal

populations in the SNpc between genotypes (Non-transgenic: 11453±811, G2019S: 12823±2044, R1441C: 13217±2471). Similarly, we found no differences in the populations of neuronal nuclei between genotypes (Non-transgenic: 25072±1979, G2019S: 24808±2698, R1441C: 25763±6049). Because PD patients tend to show sub-region specific loss of DAergic neurons in the SNpc (Dickson *et al.,* 2009), we additionally examined separately the lateral, medial and dorsal areas of the SNpc. However, no differences were seen between sub-regions of the SNpc. As almost every study of LRRK2 function has found mutant LRRK2 more likely to promote neurodegeneration over wild-type LRRK2 (Li *et al.,* 2009; Chen *et al.,* 2012; Lee *et al.,* 2014), we did not perform further stereology on aged hWT rats.

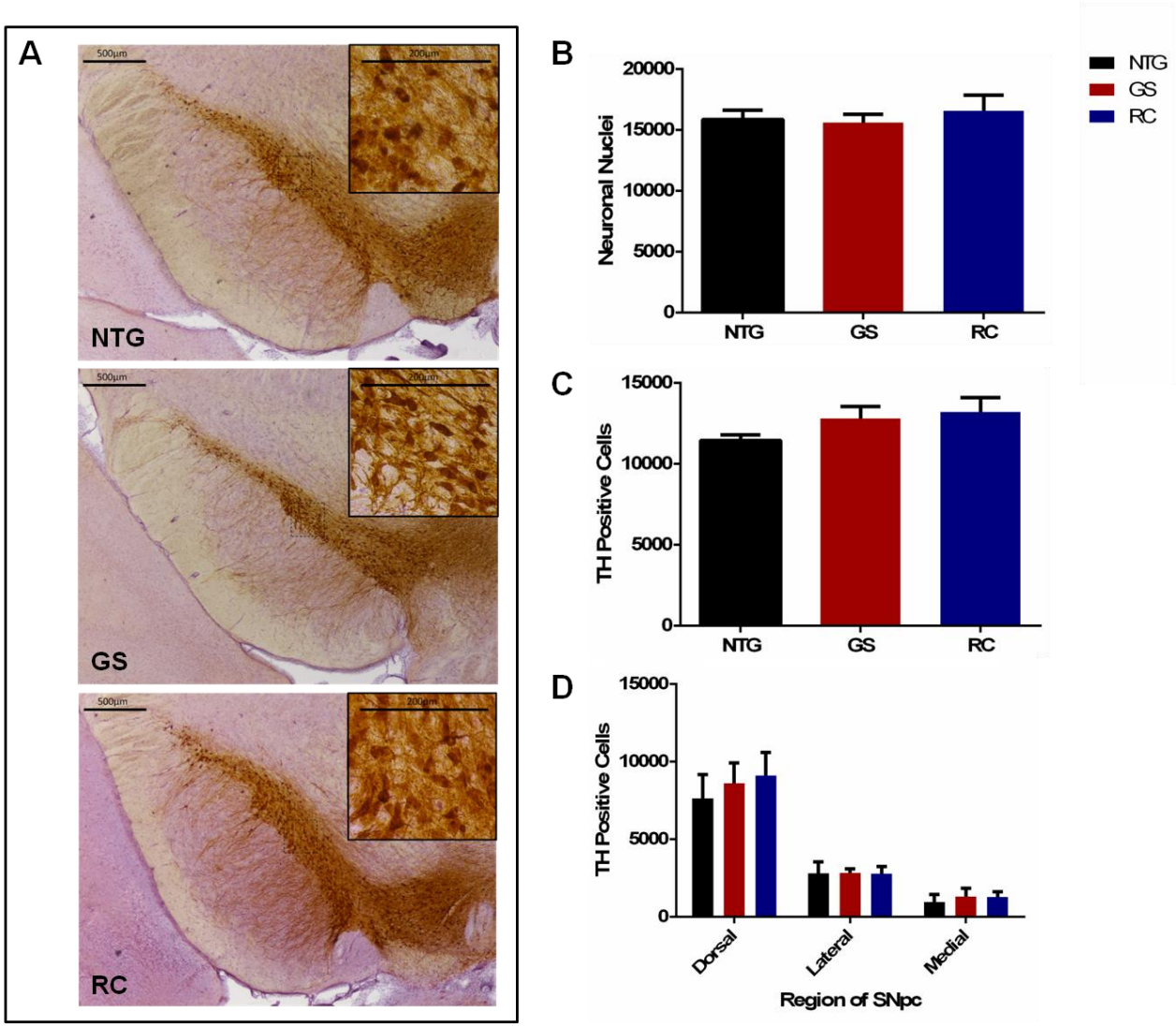

Figure 5.2. Stereological quantification revealed no differences in SNpc neuronal populations in 18-21 month old rats. (A) Representative immunohistochemistry for TH in the SNpc of non-transgenic, G2019S and R1441C 18-21 month old rats. **(B)** No differences in TH-positive neuronal populations were seen between genotypes (One-way ANOVA: no main effect of genotype: $p>0.05$, n=5-10 per genotype). **(C)** No differences in overall neuronal nuclei populations were seen between genotypes (One-way ANOVA: no main effect of genotype: $p>0.05$, n=5-10 per genotype). **(D)** Sub-divisions of the SNpc show no differences in TH-positive neuronal populations between genotypes (Two-way ANOVA: main effect of region $p<0.001$; no main effect of genotype: $p>0.05$, n=5-10 per genotype). Data are expressed as mean ± SEM.

5.3 *LRRK2* mutant rats show no evidence of dysfunctional striatal release mechanisms

5.3.1 No change in key DAergic markers in the striatum of aged *LRRK2* mutant rats

Although no detectable loss of DAergic cell bodies was found within the SNpc, it was theorised that nigrostriatal projections may have deteriorated, leading to reduced DAergic input to the striatum of aged hWT, G2019S and R1441C rats. We examined TH expression within the striatum using both immunohistochemistry and Western blotting techniques to determine distribution and relative expression levels, respectively (Fig. 5.3). No changes in striatal TH expression could be detected however, indicating normal DAergic terminal presence in the striatum and an intact nigro-striatal DAergic pathway. This evidence is supported by the work of our collaborators which found no changes in striatal DA content, determined by high-performance liquid chromatography (HPLC) (Potgieter, 2014), also indicating normal DAergic input to the striatum (Fig. 5.1).

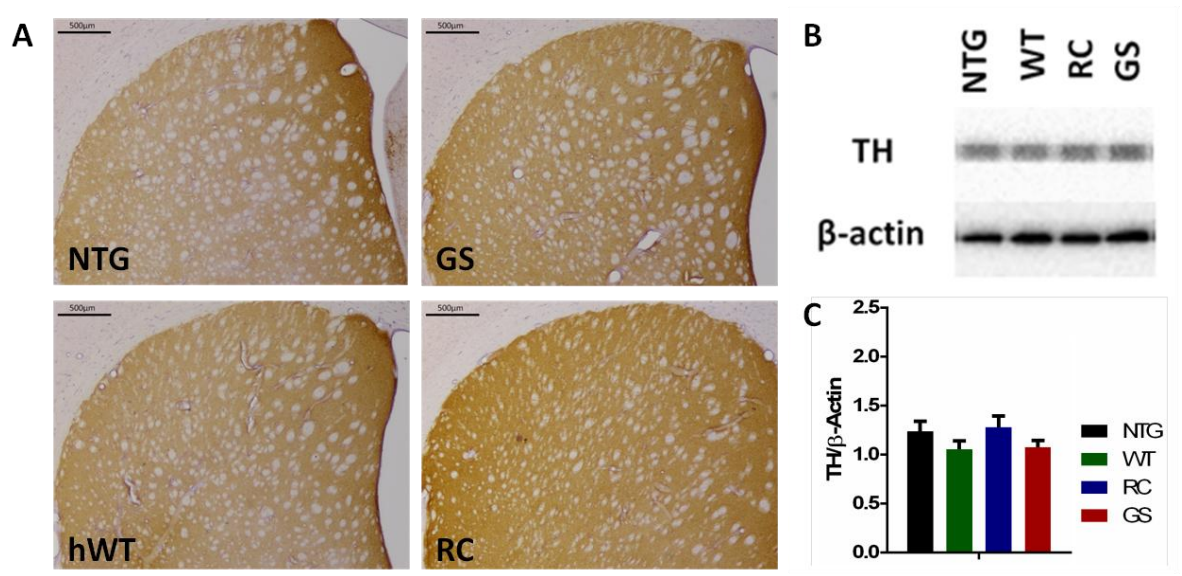

Figure 5.3. Expression of TH in the striatum of 18-21 month old *LRRK2* rats. (A) Representative immunohistochemistry for TH in the striatum of G2019S, R1441C and hWT 18-21 month old rats showing no overt differences in expression patterns when compared to non-transgenic controls. **(B)** Representative Western blots for TH in the striatum of non-transgenic, G2019S, R1441C and hWT 18-21 month old rats. **(C)** Quantification of TH Western blots showing no changes in striatal TH for G2019S, R1441C and hWT rats at 18-21 months when compared to non-transgenic controls (One-way ANOVA: no main effect of genotype: $p>0.05$, $n=3$ per genotype). Data are expressed as mean ± SEM.

As there was no detectable loss of DAergic SNpc neurons and no evidence of reduced DAergic input to the striatum, it was hypothesised that a dysregulation of proteins involved in the maintenance of DA release and reuptake within the striatum may underlie the altered DA release seen in aged transgenic animals. A key protein involved in DA homeostasis is[w1] VMAT2, which acts to package cytosolic monoamines, including DA, into synaptic vesicles. We utilised both immunohistochemistry and Western blotting to determine the distribution and relative levels of VMAT2 in the striatum of 18-21 month old non-transgenic, G2019S, R1441C and hWT rats (Fig. 5.4). No changes in striatal VMAT2 expression could be detected, however.

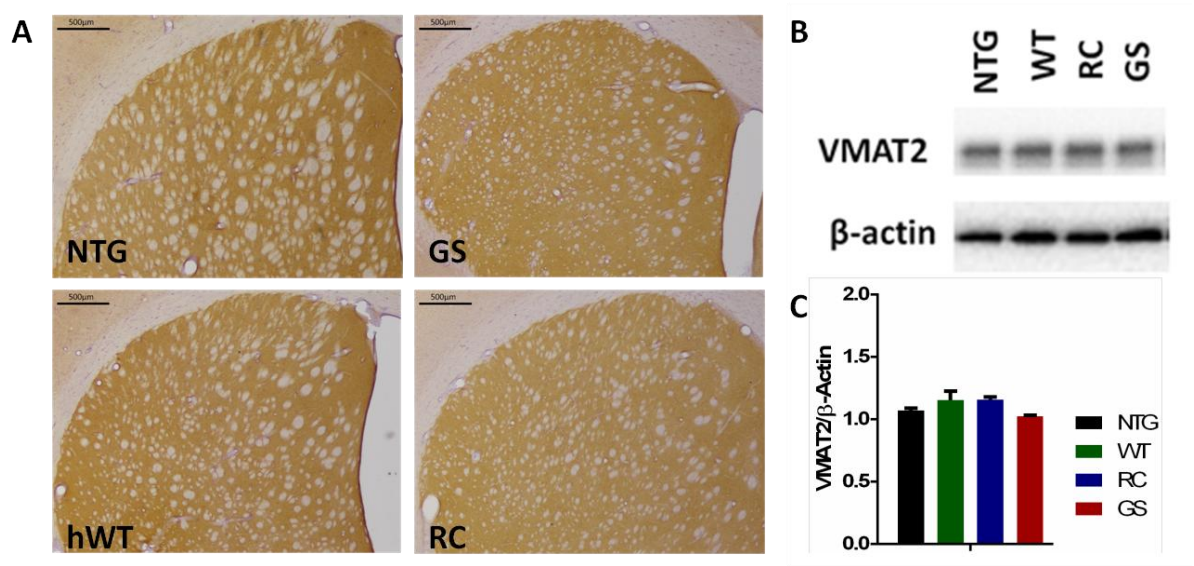

Figure 5.4. Expression of VMAT2 in the striatum of 18-21 month old *LRRK2* rats. (A) Representative immunohistochemistry for VMAT2 in the striatum of G2019S, R1441C and hWT 18-21 month old rats showing no overt differences in expression patterns when compared to non-transgenic controls. **(B)** Representative Western blots for VMAT2 in the striatum of non-transgenic, G2019S, R1441C and hWT 18-21 month old rats. **(C)** Quantification of VMAT2 Western blots showing no changes in striatal VMAT2 for G2019S, R1441C and hWT rats at 18-21 months when compared to non-transgenic controls (One-way ANOVA: no main effect of genotype: $p>0.05$, $n=3$ per genotype). Data are expressed as mean ± SEM.

We also examined the levels of DAT, which is responsible for DA clearance from the synaptic cleft back into the cytosol, as DAT dysfunction has been previously observed in LRRK2 transgenic rodents (Zhou *et al.,* 2011). Though immunohistochemistry was attempted with numerous antibodies, no consistent results could be determined. Hence, only Western blotting was used to assess striatal DAT content in non-transgenic, G2019S, R1441C and hWT 18-21 month old rats (Fig. 5.5). Western blotting for the glycosylated (mature) form of DAT revealed no changes in striatal DAT expression. These data imply unaltered functional DA clearance from the synapse in these rats. The absence of any changes in the levels of VMAT2 or DAT indicates functional DA recycling and repackaging of DA in the striatum of our *LRRK2* transgenic rats. Our findings of normal levels of striatal DAT are supported by our collaborators' findings of impaired DA release rather than reuptake (Potgieter *et al.,* 2014).

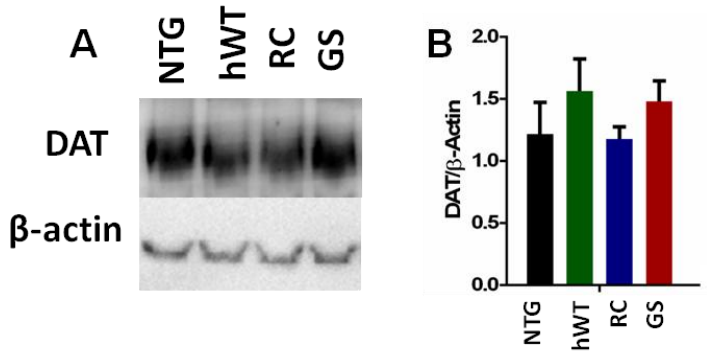

Figure 5.5. Expression of DAT in the striatum of 18-21 month old *LRRK2* rats. (A) Representative Western blots for DAT in the striatum of non-transgenic, G2019S, R1441C and hWT 18-21 month old rats. **(B)** Quantification of DAT Western blots showing no changes in striatal DAT for G2019S, R1441C and hWT rats at 18-21 months when compared to non-transgenic controls (One-way ANOVA: no main effect of genotype: $p>0.05$, n=3 per genotype). Data are expressed as mean ± SEM.

5.3.2 No changes in striatal pre-synaptic proteins in aged *LRRK2* mutant rats

While no gross changes could be detected in DAergic markers in the striatum, the evidence of impaired striatal DA release suggested a potential dysfunction of synaptic release mechanisms. Additionally, LRRK2 dysfunction has previously been implicated in altered synaptic release and LRRK2 has been suggested to perform a scaffolding function at the synapse (Tong *et al.,* 2009; Cirmaru *et al.,* 2014; Piccoli *et al.,* 2014); LRRK2 has, by immunoprecipitation, been proposed to interact with numerous presynaptic proteins (Piccoli *et al.,* 2011; Piccoli *et al.,* 2014). To attempt to further elucidate the dysfunction within the striatum, we investigated whether there were any detectable changes in a number of pre-synaptic proteins, all of which have previously been reported to interact with LRRK2. Synaptosome-associated protein 25 (SNAP-25) and vesicle-associated membrane protein 2 (vamp2) are both proteins involved in the formation of the soluble NSF attachment protein receptor (SNARE) complex which mediates the docking and fusion of synaptic vesicles with cell membranes in order to perform exocytosis. Synapsin and complexin proteins are both associated with synaptic vesicles and are thought to be involved in synaptic vesicle localisation and neurotransmitter release. We assessed changes in expression of these proteins by Western blot

in the striatum of 18-21 month old non-transgenic, G2019S, R1441C and hWT rats (Fig. 5.6). No changes in any of the assessed synaptic proteins were seen, however.

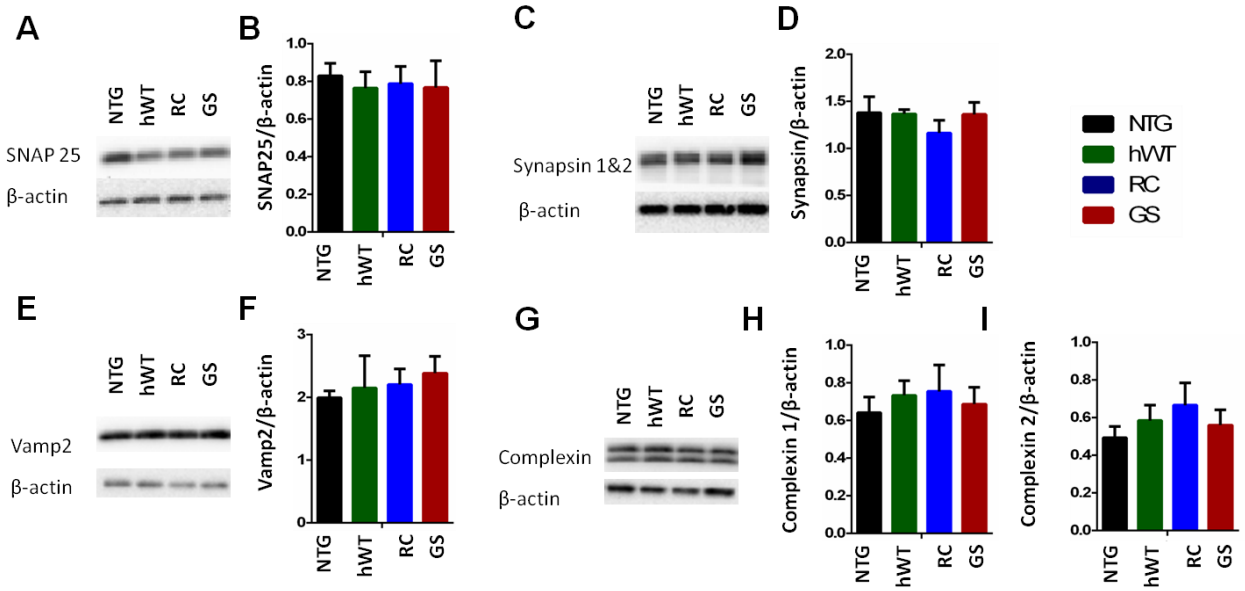

Figure 5.6. Expression of presynaptic proteins in the striatum of 18-21 month old *LRRK2* rats. (A, C, E, G) Representative Western blots for **(A)** SNAP-25**, (C)** synapsin 1 & 2, **(E)** vamp2, **(G)** complexin 1 & 2 in the striatum of non-transgenic, G2019S, R1441C and hWT 18-21 month old rats. **(B, D, F, H, I)** Quantification of Western blots showing no changes in striatal **(B)** SNAP-25 (One-way ANOVA: no main effect of genotype: $p>0.05$, $n=3$ per genotype), **(D)** synapsin 1 & 2 (One-way ANOVA: no main effect of genotype: $p>0.05$, $n=3$ per genotype), **(F)** vamp2 (One-way ANOVA: no main effect of genotype: $p>0.05$, $n=3$ per genotype), **(H, I)** complexin 1 (One-way ANOVA: no main effect of genotype: $p>0.05$, $n=3$ per genotype) & complexin 2 (One-way ANOVA: no main effect of genotype: $p>0.05$, $n=3$ per genotype) in any genotype at 18-21 months. Data are expressed as mean ± SEM.

5.4 No evidence of neuropathological markers of Parkinson's disease in aged *LRRK2* rats

In addition to DAergic dysfunction, PD patients commonly present with widespread neuropathological features such as LBs and tau tangles, the latter, particularly in the case of *LRRK2* mutations (Braak *et al.,* 2003; Haugarvoll & Wszolek, 2009). In general, very little evidence of α-synuclein pathology has been detected in *LRRK2* models of PD. Conversely, reports of tau, phosphorylated at a variety of residues, have been reported in *LRRK2* rodent models, usually

increasing with the progression of age (MacLeod *et al.,* 2006; Li *et al.,* 2010; Li *et al.,* 2009; Melrose *et al.,* 2010; Dusonchet *et al.,* 2011). We therefore examined aged animals for the accumulation of proteins associated with PD, including α-synuclein, hyperphosphorylated tau and ubiquitin.

5.4.1 No accumulation of PD-linked proteins in aged *LRRK2* mutant rats

A hallmark of PD is the accumulation of α-synuclein and development of Lewy pathology, revealed by α-synuclein staining. To investigate whether our rats developed α-synuclein accumulation we first assessed α-synuclein levels throughout the brains of 18-21 month non-transgenic, G2019S, R1441C and hWT rats (Fig. 5.7). No changes in α-synuclein levels could be detected in the striatum, cortex, hippocampus or midbrain. Attempts were also made to detect α-synuclein, phosphorylated at ser129, given that phosphorylation at this residue is frequently used to detect Lewy body pathology (Lin *et al.,* 2009). However, we were unable to effectively optimise the antibody (Santa Cruz) for Western blot.

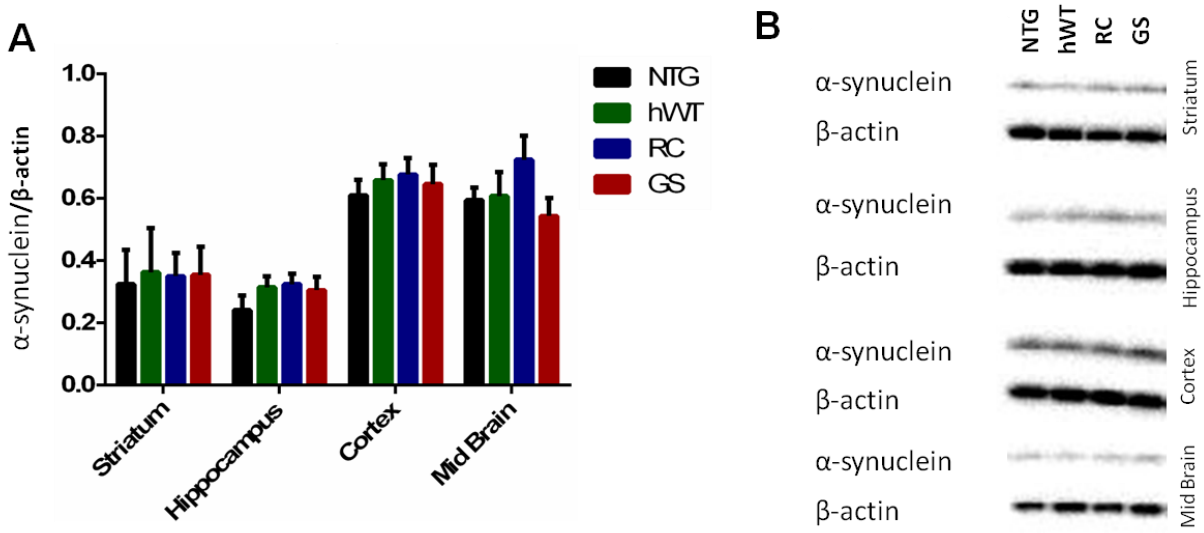

Figure 5.7. Analysis of α-synuclein levels in key brain regions of 18-21 month old *LRRK2* rats. (A) Quantification of α-synuclein levels in the striatum, hippocampus, cortex and midbrain of aged non-transgenic, G2019S, R1441C and hWT *LRRK2* transgenic rats showing no change in levels of α-synuclein (Two-way ANOVA: no main effect of genotype: $p>0.05$, n=3 per genotype). **(B)** Representative blots for α-synuclein of non-transgenic, G2019S, R1441C and hWT 18-21 month old rats in each brain region. Data are expressed as mean ± SEM.

While no overall change in α-synuclein levels was detected in any area of the brain regions assayed, it was hypothesised that Lewy pathology may occur in the absence of any overall changes in α-synuclein levels. Additionally, pathology may be restricted to specific brain regions and thus be difficult to detect in coarsely dissected tissue. Consequentially, aged rats were further assessed for PD pathology by immunohistochemistry. In addition to examining α-synuclein pathology, we assessed the potential accumulation of other proteins associated with *LRRK2* PD including hyperphosphorylated tau, specifically, that recognised by the AT8 antibody, and ubiquitin (Haugarvoll & Wszolek, 2006).

To ensure our ability to successfully detect Lewy pathology and hyperphosphorylated tau, we optimised staining protocols for the detection of Lewy bodies and tau tangles in human PD patient tissue, positive for these pathologies (Figure 5.8).

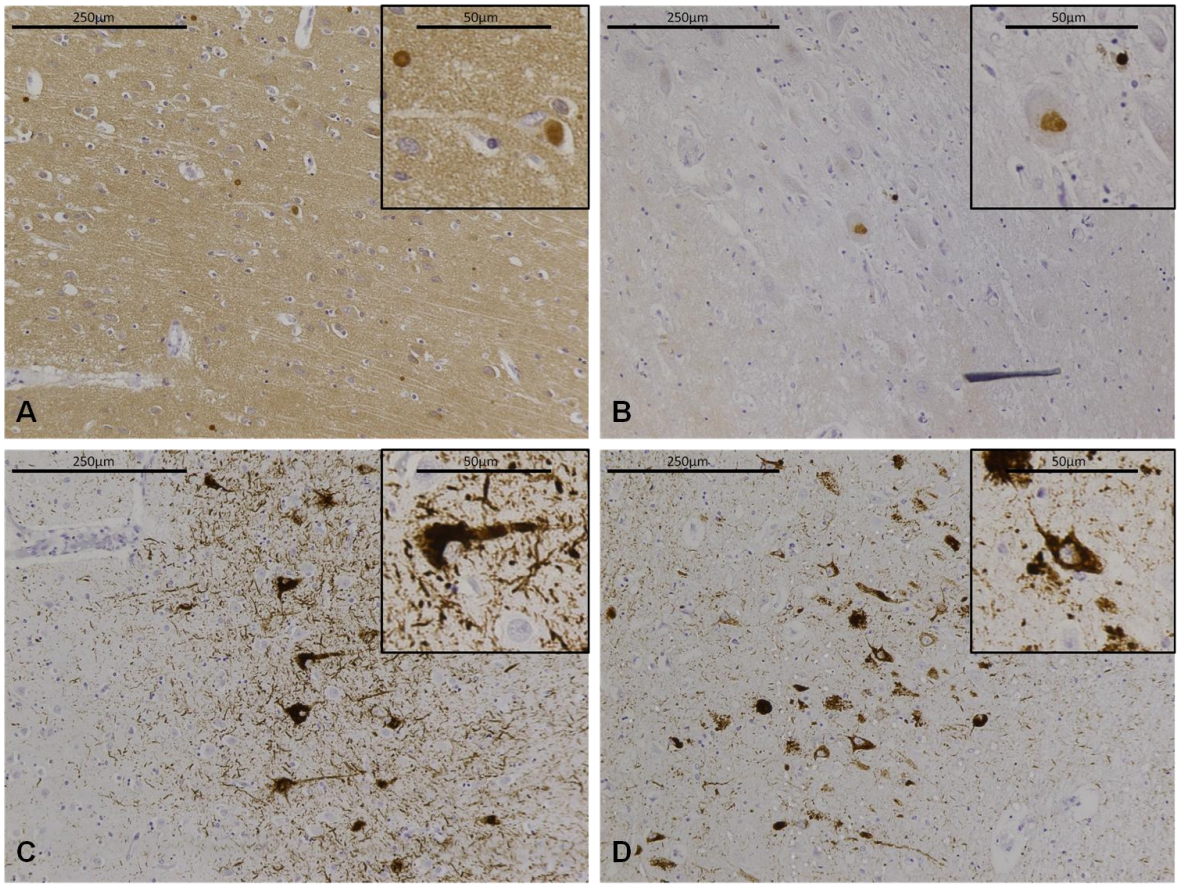

Figure 5.8. Positive controls for LB and tau tangle pathology in human brain tissue. (A-B) Human post-mortem tissue from PD patients, positive for Lewy pathology, was stained using an α-synuclein antibody which recognises both human and rat α-synuclein, revealing LBs in **(A)** the cingulate gyrus and **(B)** the SNpc. **(C-D)** Human post-mortem tissue from PD patients, positive for tau tangle pathology, was stained using the AT8 antibody which recognises both human and rat phosphorylated (ser202/thr205) tau, revealing neurofibrillary tangle pathology in **(C)** entorhinal cortex and **(D)** the hippocampus. Staining conditions used here were identical to those used in subsequent staining performed in aged rats.

In our analysis, we assessed cortical and SNpc areas, as the former showed high levels of hLRRK2 expression and prior studies of *LRRK2* transgenic rodents have shown tau pathology to be restricted to the SNpc (Chen *et al.,* 2012). Neuropathological assessment of aged (18-21 month) *LRRK2* transgenic rats revealed no noticeable changes in α-synuclein or ubiquitin staining in any of the genotypes (Figs. 5.9, 5.10). A degree of somatic α-synuclein staining was revealed in both cortical and SNpc regions which has previously been used as an indication of the early stages of α-synuclein pathology (Lin *et al.,* 2009). However, none of these observations was specific to the *LRRK2* transgenic lines**.** Similarly, very little detectable AT8 signal was present in any of the aged *LRRK2* lines, suggesting no hyperphosphorylated tau pathology (Fig. 5.11).

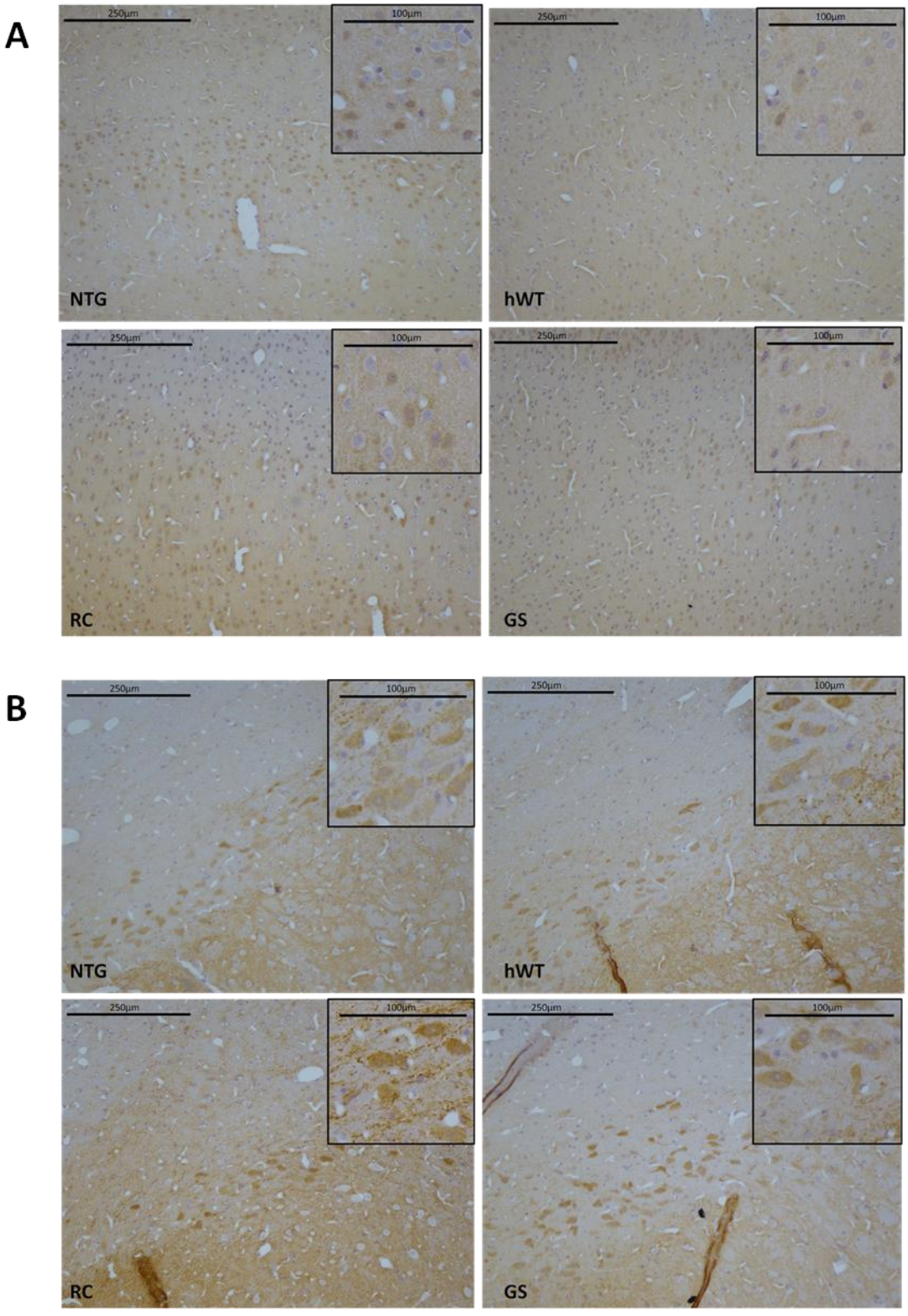

Figure 5.9. Immunohistochemistry for α-synuclein in 18-21 month old *LRRK2* rat cortex and SNpc.
Representative immunohistochemistry for α-synuclein in **(A)** the cortex and **(B)** the SNpc of non-transgenic, G2019S, R1441C and hWT 18-21 month old rats (n≥3 per genotype). Although a substantial amount of somatic α-synuclein staining was seen, no overt changes in expression patterns or accumulation relative to the non-transgenic control were seen.

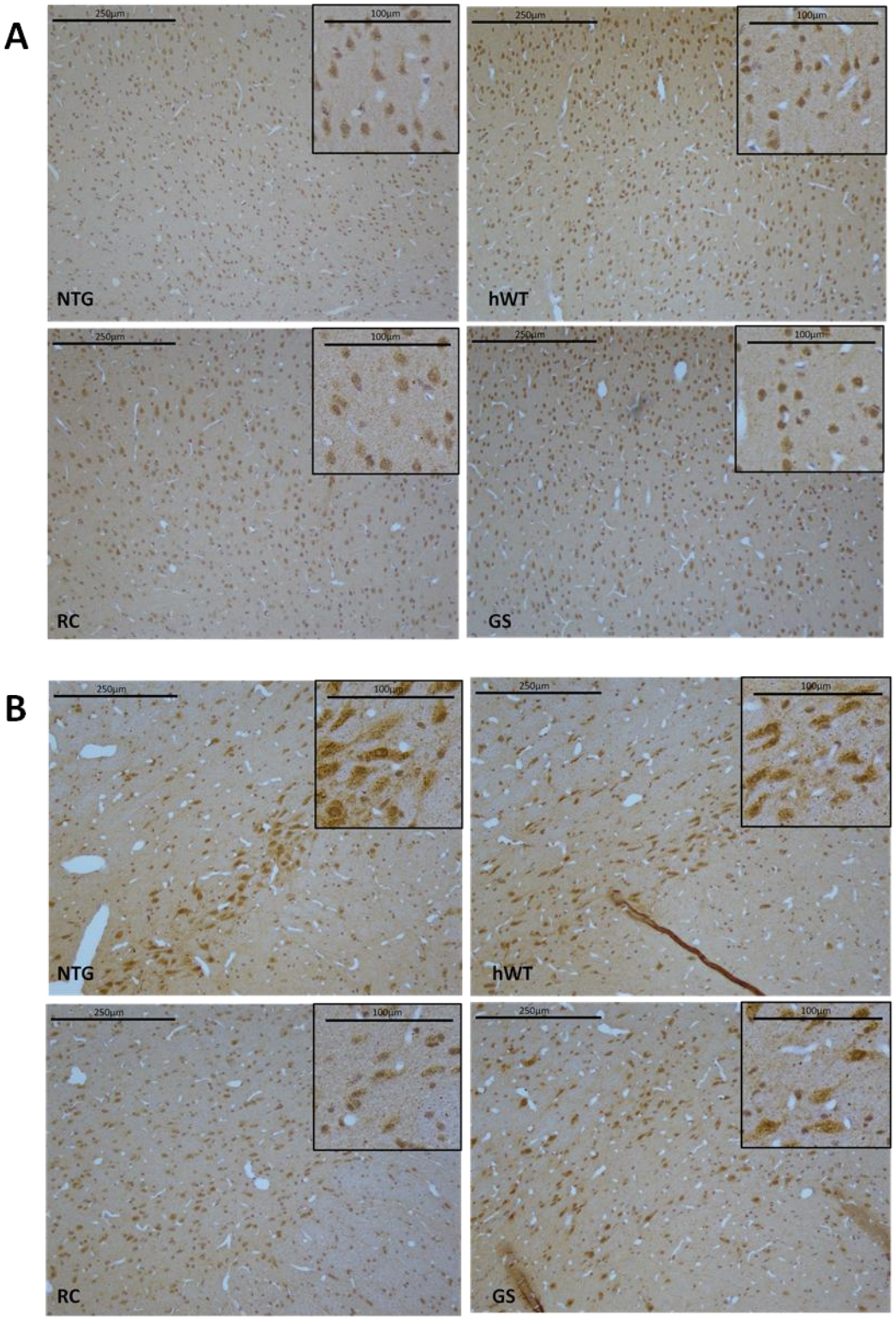

Figure 5.10. Immunohistochemistry for ubiquitin in 18-21 month old *LRRK2* rat cortex and SNpc. Representative immunohistochemistry for ubiquitin in **(A)** the cortex and **(B)** the SNpc of non-transgenic, G2019S, R1441C and hWT 18-21 month old rats (n≥3 per genotype). No overt changes in expression patterns or accumulation relative to the non-transgenic control were seen.

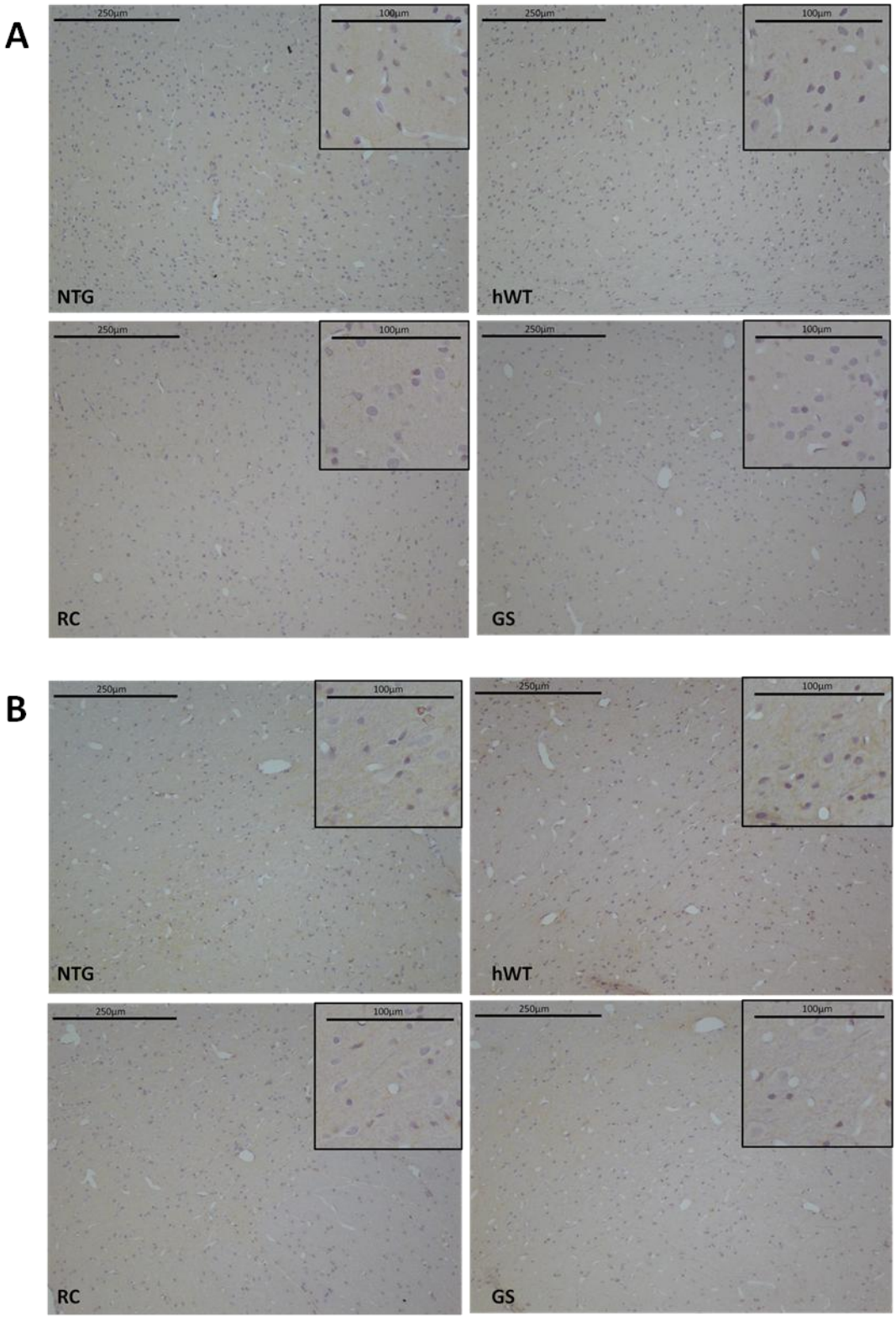

Figure 5.11. Immunohistochemistry for hyperphosphorylated tau in 18-21 month old *LRRK2* rat cortex and SNpc. Representative immunohistochemistry for AT8 (pser202/thr205) tau in **(A)** the cortex and **(B)** the SNpc of non-transgenic, G2019S, R1441C and hWT 18-21 month old rats (n≥3 per genotype). No overt changes in expression patterns or accumulation relative to the non-transgenic control were seen.

5.4.2 No evidence of elevated immune response in mutant *LRRK2* rats

Numerous links have been drawn between LRRK2 and the immune system. To date, a number of studies have reported changes in immune activity in the brains of *LRRK2* transgenic rats (Melrose *et al.,* 2010; Lee *et al.,* 2014). We therefore investigated the possibility of enhanced microglial activation, as assessed by Iba1 staining (Fig. 5.12). However, no evidence of elevated microglial activity was found compared to non-transgenic controls.

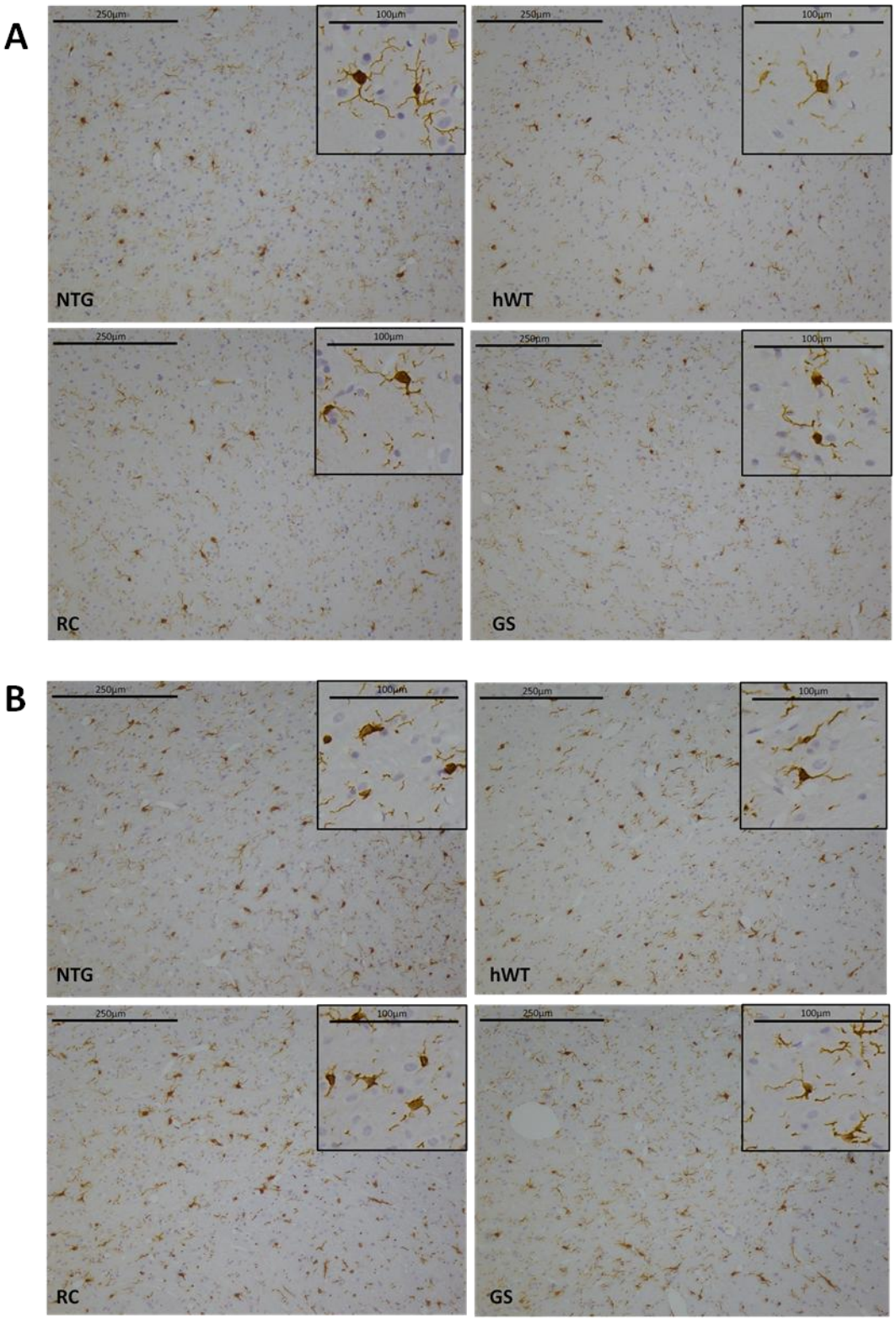

Figure 5.12. Immunohistochemistry for Iba1 in 18-21 month old *LRRK2* rat cortex and SNpc. Representative immunohistochemistry for Iba1 in **(A)** the cortex and **(B)** the SNpc of non-transgenic, G2019S, R1441C and hWT 18-21 month old rats (n≥3 per genotype). No overt changes in microglial activation relative to the non-transgenic control were seen.

5.5 No evidence of altered autophagic markers in aged *LRRK2* rats

A considerable amount of *in vitro* evidence points towards a role of LRRK2 in autophagic function. However, few papers have reported altered autophagic processes in the brains of *LRRK2* mutants. To assess whether any autophagic changes occurred in our models, we examined two key autophagic markers, LC3 and P62, in brain regions associated with high levels of hLRRK2 protein expression, the hippocampus and cortex, along with the striatum, due to its apparent dysfunction in our models. LC3-II and P62 are both markers of autophagy and have both been previously found to co-localise with LRRK2 and be upregulated as a result of mutant LRRK2 expression (Plowey *et al.,* 2008; Alegre-Abarrategui *et al.,* 2009). We did not examine midbrain autophagy due to the comparatively low levels of transgene expression, the lack of neurodegeneration in the SNpc and the highly heterogeneous structures within the midbrain.

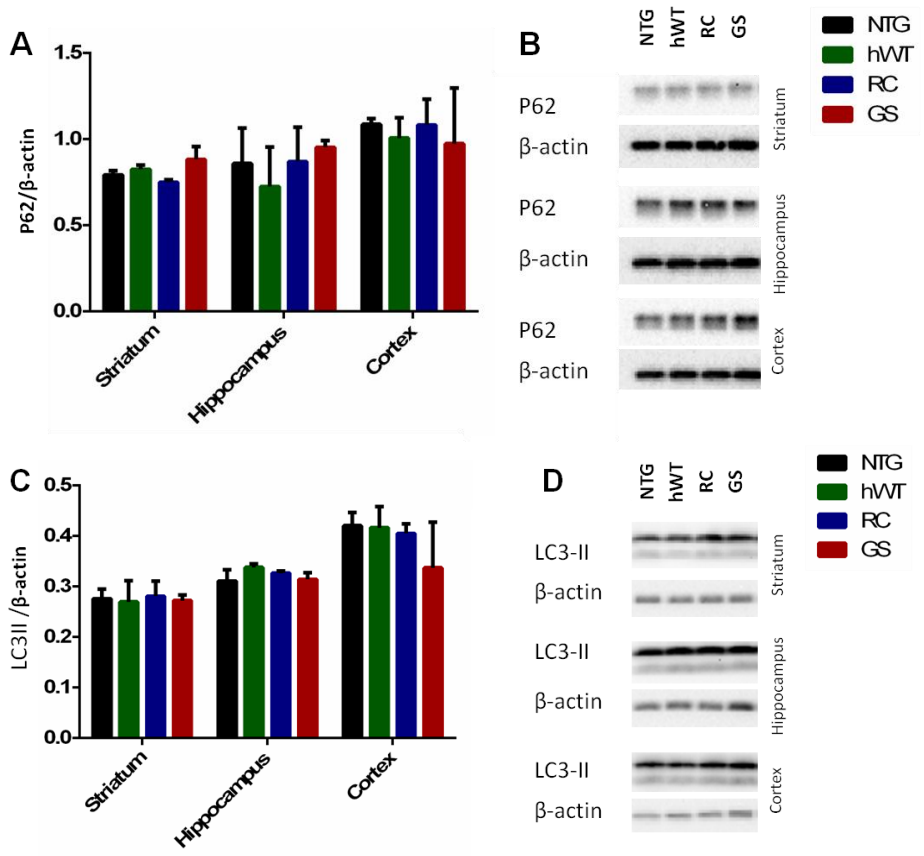

Figure 5.13. Expression of autophagic markers in key brain regions of 18-21 month old *LRRK2* rats. (A) Quantification of P62 Western blots showing no changes in striatum, hippocampus and cortex in any genotype at 18-21 months (Two-way ANOVA: no main effect of genotype: $p>0.05$, n=3 per genotype). **(B)** Representative Western blots for P62 in the striatum, hippocampus and cortex of non-transgenic, G2019S, R1441C and hWT 18-21 month old rats. **(C)** Quantification of LC3-II Western blots (lower band) showing no changes in striatum, hippocampus and cortex in any genotype at 18-21 months (Two-way ANOVA: no main effect of genotype: $p>0.05$, n=3 per genotype). **(D)** Representative Western blots for LC3-II in the striatum, hippocampus and cortex of non-transgenic, G2019S, R1441C and hWT 18-21 month old rats. Data are expressed as mean ± SEM.

5.6 No evidence of altered microtubule stability in either young or old *LRRK2* mutant rats

A number of papers have reported increased microtubule stability as a result of either wild-type or mutant LRRK2 overexpression (Lin *et al.,* 2009; Maekawa *et al.,* 2012). Assays for microtubule stability are often technically challenging but tubulin acetylation, a post-translational modification which stable microtubules accumulate, is often used as a measure of microtubule stability

(Takemura *et al.,* 1992). As altered microtubule stability has been reported in younger animals, we assessed the levels of acetylated α-tubulin in both 3-6 and 18-21 month old non-transgenic, wild-type, G2019S and R1441C rats. No changes in tubulin acetylation were seen in either young or old transgenic rats, suggesting no changes to microtubule stability (Fig. 5.14).

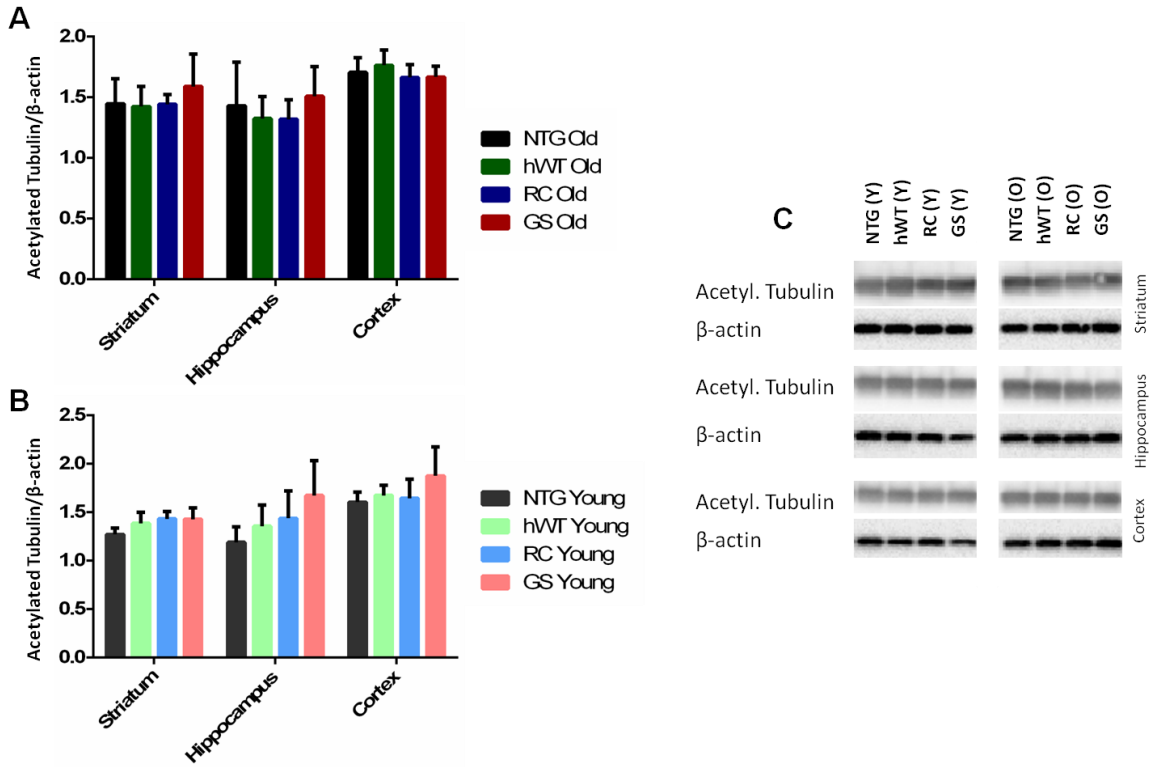

Figure 5.14. Analysis of acetylated tubulin levels in key brain regions of 3-6 and 18-21 month *LRRK2* rats. (A, B) Quantification of Western blot analysis in the striatum, hippocampus and cortex of **(A)** 3-6 and **(B)** 18-21 month non-transgenic, G2019S, R1441C and hWT *LRRK2* transgenic rats showing no change in levels of acetylated tubulin (Two-way ANOVA: $p>0.05$, n=3 per genotype). **(C)** Representative blots for acetylated tubulin of non-transgenic, G2019S, R1441C and hWT 3-6 (Y) and 18-21 (O) month old rats in each brain region. Data are expressed as mean ± SEM.

5.7 *LRRK2* mutations affect hLRRK2 phosphorylation

A number of *in vitro* reports have been made suggesting that LRRK2 phosphorylation is affected by the PD-promoting *LRRK2* mutations. To investigate changes in the phosphorylation of hLRRK2, we used two antibodies, UDD1 and UDD2, which recognise LRRK2 phosphorylated at ser910 and 935, respectively (Fig 5.15). These sites have been regularly used to determine kinase activity of the

LRRK2 protein, although they are not considered LRRK2 autophosphorylation sites (Nichols *et al.,* 2010; Longo *et al.,* 2014). We first assessed pLRRK2 levels in 3 month old rats. R1441C mutant hLRRK2 showed 82% and 85% reduced levels of phosphorylation at both ser910 and ser935, respectively, when compared to hWT controls. G2019S mutant hLRRK2 showed no change in ser910 phosphorylation and a 23% increase in ser935 phosphorylation. We then performed immunohistochemistry with the UDD2 antibody on tissue from both young and aged animals. This revealed similarly reduced staining for ser935 hLRRK2 in the R1441C mutant throughout the brain at both ages, indicating that this phosphorylation is consistently reduced throughout the lifetime of the animal. It appears, therefore that the R1441C and G2019S mutations have opposing effects upon LRRK2 phosphorylation *in vivo* and that these effects are maintained throughout the lifespan of the animal.

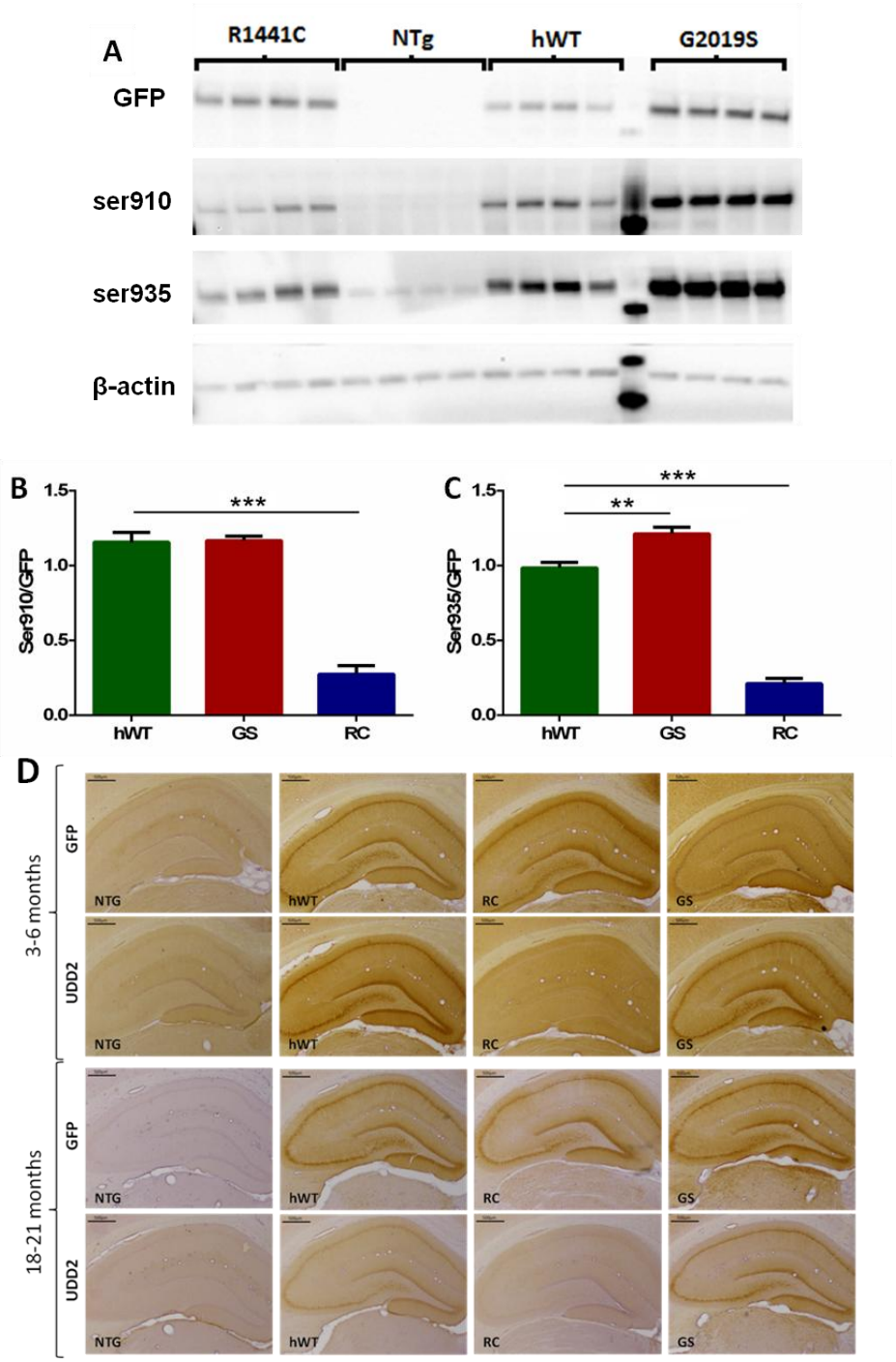

Figure 5.15. G2019S and R1441C rats show altered levels of hLRRK2 phosphorylation. (A-C) At 3 months of age, when normalised to hLRRK2 levels, ser910 phosphorylation of hLRRK2 in R1441C rats is greatly reduced (One-way ANOVA: main effect of genotype: $p<0.0001$, n=4 per genotype) and ser935 hLRRK2 phosphorylation is increased in G2019S rats and decreased in R1441C rats (One-way ANOVA: main effect of genotype: $p<0.0001$, n=4 per genotype) as determined by Western blot of whole brain homogenates. **(D)** DAB immunohistochemistry for ser935 (UDD2) hLRRK2 and GFP in the hippocampus shows greatly reduced hLRRK2 ser935 phosphorylation at both 3-6 months and 18-21 months in R1441C rats. Bonferroni post-hoc tests ** $p<0.01$, ***$p< 0.001$. Data are expressed as mean ± SEM.

5.8 Chapter discussion

Following the discovery of a late-stage Parkinsonian phenotype and, supported by information from our collaborators suggesting dysfunctional striatal DA release, we investigated the potential for DAergic dysfunction and neuropathology within our *LRRK2* transgenic rats at a late time point. However, our analysis revealed very little in the way of overt DAergic system pathology or PD-associated pathological markers. We additionally investigated a number of molecular markers associated with LRRK2 dysfunction and found that mutant hLRRK2 displays altered phosphorylation in an age independent fashion.

5.8.1 Aged mutant *LRRK2* rats show no SNpc neurodegeneration

The absence of any overt neuronal loss within the SNpc of 18-21 month old G2019S or R1441C rats implies that the motor phenotype observed in our hLRRK2 transgenic rats is not due to the degeneration of DAergic SNpc neurons. These findings are largely in line with the vast majority of *LRRK2* transgenic rodent literature. Besides viral vector and transgenic models utilising exogenous promoters, no neurodegeneration has been reported in rodent *LRRK2* transgenic models (Li *et al.,* 2009; Chen *et al.,* 2012; Lee *et al.,* 2014). Why these techniques appear to cause a more aggressive phenotype is unclear, though it is possible that they may cause very high levels of expression in a subset of cells or for a short period of time, resulting in heightened pathological processes. Additionally, stereotaxic injection may promote an immune response which could amplify the deleterious effects of transgene expression, especially given that LRRK2 has been associated with immune processes (Daher *et al.,* 2014). While SNpc neurodegeneration has never been reported in *LRRK2* BAC transgenic rodent models, several have detected subtle morphological changes in SNpc DA neurons. Li and colleagues (2009) found, in R1441G BAC transgenic mice, a reduction in cell body size along with an apparent reduction in TH-positive dendrites in the SNpr. Similarly, Lee and colleagues (2014) found, in G2019S BAC transgenic rats, a 'flattening' in SNpc neuronal morphology. Additionally, altered nuclear morphology has been reported in the SNpc neurons of R1441C *LRRK2*

mice (Tsika *et al.,* 2014). Whether the variation in observations reflects different phenotypes or differential methods of morphometric analysis is unclear. While we do not know what these changes in morphology indicate, it is tempting to suggest that they are indicative of early-stage neurodegeneration. Though we were unable perform any morphometric analysis, given the constraints of time, it would be a viable area for further investigation. It would, similarly, be valuable to determine whether these morphological changes are present in the surviving SNpc DA cells of post-mortem PD patients or in early stages of α-synuclein models which display progressive neurodegeneration (Janezic *et al.,* 2013).

5.8.2 Aged mutant *LRRK2* rats do not show altered DAergic or synaptic machinery

To develop upon our collaborators' work, which indicated a DA release deficit in the striatum of our aged *LRRK2* transgenic rats, we investigated the levels of markers central to DA recycling and vesicle release at a late age. As determined by Western blot and immunohistochemistry, we observed no gross changes in TH, VMAT and DAT levels within the striatum. Our findings are largely in line with other *LRRK2* rodent models which tend to not see any changes in these proteins (Li *et al.,* 2010; Walker *et al.,* 2014). Although DAT dysfunction has been previously noted following *LRRK2* conditional expression, this was inferred from an impaired response to amphetamine administration, suggesting that dysfunction may occur in the absence changes to overall DAT levels (Zhou *et al.,* 2011).

We further investigated the release deficit in the striatum by assessing a number of presynaptic striatal proteins involved in vesicle release which have been previously suggested to interact with LRRK2 (Piccoli *et al.,* 2011; Piccoli *et al.,* 2014). No changes were seen in any of these markers, though LRRK2 dysfunction may have a more sophisticated impact upon pre synaptic proteins which may not be identifiable by assessing overall levels of these proteins. For example, it has been hypothesised that LRRK2 acts as a scaffolding protein at the synapse, interacting with proteins such as SNAP-25, VAMP, synapsin and actin which, in turn, modulate synaptic vesicle mobility (Cinaru *et*

al., 2014). Disruption to the formation of such a complex may interfere with vesicle release. Furthermore, the functions of a number of pre synaptic proteins involved in vesicle release are additionally modulated by post-translation modifications, such as phosphorylation, which can affect the mobilisation of synaptic vesicles (Belluzzi *et al.,* 2012). Finally, LRRK2 has previously been reported to interact with synaptic vesicle protein 2A, which acts to modulate Ca^{2+}-induced exocytosis (Piccoli *et al.,* 2014). It is therefore possible that *LRRK2* mutation causes alterations to neurotransmitter release in the absence of changes to overall protein levels. A viable method to further probe the potentially altered vesicle dynamics would be to perform electron microscopy to determine whether there are alterations in the distribution of synaptic vesicles within the terminals of the striatum. Changes to the distributions of readily releasable vesicle pools have been previously reported in neurons following *Lrrk2* knock-down (Piccoli *et al.,* 2011).

An additional area for potential further investigation would be to determine whether levels of D2 receptor density are changed in our aged *LRRK2* transgenic rats. D2 receptors, which are expressed by SNpc DAergic neurons, act as autoreceptors to modulate the release of DA into the synaptic cleft (Wooten, 2001). Potentially, an upregulation of D2 receptors may cause impaired DA release. In line with this hypothesis, Melrose and colleagues (2010) previously reported trends towards increased levels of D2 receptor density within the striatum of G2019S mice. Determining the modulation of DA release within the striatum following the application of D2 receptor antagonists could be used to explore this possibility.

Finally, cholinergic neurons within the striatum have previously shown to be capable of modulating DA release (Calabresi *et al.,* 2000). It is possible that LRRK2 plays a role in modulating the function of these neurons which, in turn, may have lead to the impaired release of DA in our *LRRK2* transgenic rats. Interestingly, the high transgene expressing, sparsely distributed neurons in the *LRRK2* BAC rat striatum have previously been identified to be cholinergic in nature (West *et al.,* 2014).

5.8.3 Aged mutant *LRRK2* rats show no evidence of PD neuropathological features

In addition to an investigation of reported DAergic striatal dysfunction, we also examined aged rats for neuropathology characteristic of *LRRK2* PD, including the accumulation of α-synuclein, hyperphosphorylated tau and ubiquitin (Haugarvoll & Wszolek, 2006). We additionally assessed microglial activation by way of Iba1 staining to determine whether these animals displayed an elevated immune response. Our studies revealed no overt brain pathology at late ages, however.

Staining for α-synuclein often revealed an accumulation of somatic α-synuclein which has, before, been considered to represent pathological processes (Lin *et al.,* 2009) but these features were found in all lines, suggesting that they represented normal physiological function. To my knowledge, no reports exist of the development of α-synuclein neuropathology in *LRRK2* transgenic rodents, although a number of co-expression studies have suggested that expression of LRRK2 can exacerbate the pathology caused by mutant α-synuclein expression (Lin *et al.,* 2009; Daher *et al.,* 2012). It is possible, however, that, since both LRRK2 and α-synuclein are degraded by the same processes, overexpression of one protein may indirectly exacerbate the effects of the other by impairing its degradation (Webb *et al.,* 2003; Orenstein *et al.,* 2014).

Similar to the lack of α-synuclein pathology, ubiquitin pathology is rarely reported in *LRRK2* rodent models, with the exception of a single mouse model expressing high levels of LRRK2 protein (Lin *et al.,* 2009). Why *LRRK2* mutations do not cause α -synuclein or ubiquitin accumulation in rodent models is unclear. It is possible that the human form of α -synuclein is more prone to forming toxic aggregates than rodent α-synuclein. If this is indeed the case, it may explain why *LRRK2* rodents fail to develop α-synuclein pathology yet co-expression of LRRK2 in a model expressing human α-synuclein causes the exacerbation of pathology.

Similarly, no evidence of hyperphosphorylated tau was seen in our transgenic rats, despite a number of reports in the literature of AT8 neuropathology (Li *et al.,* 2009; Dusonchet *et al.,* 2011; Chen *et al.,*

2012). In line with our findings, other studies have probed for phosphorylated tau, including those utilizing the AT8 antibody, and found no differences in *LRRK2* transgenics, although these studies were performed in younger animals than those in our experiments (Maekawa *et al.,* 2012). It has been suggested by a number of studies that expression levels of LRRK2 play an important role in the development of tau pathology (Melrose *et al.,* 2010; Dusonchet *et al.,* 2011). However, our rats expressed hLRRK2 at a level similar to these studies. Furthermore, it has been shown that tau phosphorylation at the sites recognised by the AT8 antibody (ser202/thr205) is typical of more advanced tau pathology (extra neuronal tangles) and that pre-tangle pathology more typically shows tau phosphorylated at thr153, ser262 and thr231 (Augustinack *et al.,* 2002). Hence, while we demonstrated the ability to detect tangles, it may be the case that pre-tangle pathology was not sufficiently detectable by our methods. It would therefore be useful to examine further our rats for other forms of phosphorylated tau which have been reported in other papers (MacLeod *et al.,* 2006; Li *et al.,* 2009; Melrose *et al.,* 2010).

As LRRK2 is increasingly linked to immune function and PD patient post-mortem studies have reported elevated microglial activity (Croisier *et al.,* 2005), we also examined the recruitment of microglia by Iba1 staining. Our analysis revealed no obvious differences in Iba1 staining in key brain regions as a result of hLRRK2 overexpression. Though no changes were detected in microglial morphology or proliferation, this does not rule out the possibility of an immune response. For example, a recent BAC transgenic rat paper found changes in nitric oxide synthase, a common marker of neuroinflammation, in aged animals, despite seeing no changes in Iba1 staining (Lee *et al.,* 2014). It was noted that a single R1441C animal displayed dramatic Iba1 staining throughout the midbrain region (data not shown). However, these findings were not seen in other samples and may reflect the development of a pituitary tumour, a common feature of old SD rats.

5.8.4 The molecular effects of LRRK2 dysfunction

No evidence of altered autophagy in *LRRK2* rats

In vitro studies have consistently shown mutant LRRK2 to increase autophagic activity and upregulate the formation of AVs and MVBs (Plowey *et al.,* 2008; Alegre-Abarrategui *et al.,* 2009; Manzoni *et al.,* 2013; Yakhine-Diop *et al.,* 2014). Furthermore, *Lrrk2* KO animals display kidney pathology which includes dramatic alterations in P62 and LC3-II levels (Tong *et al.,* 2010; Herzig *et al.,* 2011; Tong *et al.,* 2012). In the brains of our *LRRK2* transgenic animals, however, we detected no differences in autophagic activity. This is largely in line with the vast majority of *LRRK2* transgenic rodent models which have reported very little in the way of autophagic brain pathology. A single study, performed by Ramonet and colleagues (2011) in G0219S transgenic mice, found, at late stages, enlarged AVs and aggregated mitochondria, determined by electron microscopy. It is possible, therefore, that our assays for P62 and LC3II were not sensitive enough to detect more subtle autophagic changes in our *LRRK2* transgenic rats.

It is not clear why *in vitro* studies appear to show significantly different results to those seen *in vivo*. It should be noted, however, that most autophagy studies are performed in non-neuronal cells such as HEK293, SH-SY5Y and fibroblast cells (Plowey *et al.,* 2008; Alegre-Abarrategui *et al.,* 2009; Manzoni *et al.,* 2013; Yakhine-Diop *et al.,* 2014). It is therefore possible that neurons are more resistant to the effects of *LRRK2* mutation or there are compensatory processes performed by the brain which render neurons more resistant to the autophagic changes induced by mutant LRRK2. It is, furthermore, unclear why autophagic changes observed in *Lrrk2* KO rodents are restricted to the kidneys, though it has been noted that LRRK2 expression is far higher in the kidneys than in the brain, suggesting that more dramatic effects may result from its KO (Tong *et al.,* 2010).

No evidence of altered microtubule stability in *LRRK2* rats

Our evaluation of microtubule stability by the quantification of acetylated tubulin revealed no changes in microtubule stability in either young or old rats. Previous studies have found kinase

domain mutations to lead to, in the case of Lin and colleagues' model, dramatically increased microtubule stability (Lin *et al.,* 2009; Maekawa 2012). Conversely, Gillardon (2009) found that the brains of *Lrrk2* KO mice showed increased tubulin solubility. It is possible that the changes in tubulin stability are transitory throughout the life of the animal. For example, Maekawa and colleagues (2012) reported microtubule stability changes in I2020T rats at 10 weeks which disappeared by 6 months. If this is indeed the case, detection of this phenotype may prove challenging.

While acetylated tubulin is often used *in vitro* as an assay of microtubule stability, *LRRK2* transgenic rodent papers have utilised microtubule polymerisation assays which may prove more effective at the detection of alterations in microtubule stability. Further attempts could be made to investigate microtubule stability by such assays, although I have found these to be extremely technically challenging to execute.

LRRK2 mutations result in altered hLRRK2 phosphorylation

Finally, we assessed the phosphorylation states of the hLRRK2 protein using pLRRK2 antibodies UDD1 and UDD2, which recognise LRRK2 phosphorylated at ser910 and ser935, respectively. We found R1441C hLRRK2 to show dramatically reduced phosphorylation at these two sites, while G2019S hLRRK2 showed increases in ser935 phosphorylation. These data are in line with the reduced phosphorylation at ser935 and ser910 which has previously been reported in R1441C knock-in mice (Nichols *et al.,* 2010). Our data also indicate that the phosphorylation state of LRRK2 is consistent throughout the lifespan of the animal, with animals at young and aged time points showing similar hLRRK2 phosphorylation.

The LRRK2 ser910 and ser935 sites lie prior to the leucine-rich repeats and are highly conserved sites in mammals (Nichols *et al.,* 2010). It is unlikely that these sites are autophosphorylation sites as isolated, dephosphorylated LRRK2 has been shown to be unable to rephosphorylate these sites (Dzamko *et al.,* 2010). Despite this, phosphorylation of LRRK2, particularly at ser935, has been

frequently used as a read out of LRRK2 kinase activity, largely due to the fact that a number of the recently developed LRRK2 kinase inhibitors reduce phosphorylation at these sites (Longo *et al.,* 2014; Cinaru *et al.,* 2014). Our data appear to dispute this hypothesis, however, given that R1441C LRRK2 mutations are not generally thought to affect the activity of the LRRK2 kinase domain, yet R1441C hLRRK2 protein shows dramatically reduced ser935/ser910 phosphorylation (Greggio & Cookson, 2009). Moreover, G2019S hLRRK2 only appeared to show marginal increases in phosphorylation at one of these sites despite the fact that the G2019S mutation is thought to increase LRRK2 kinase activity by around 3-fold (Greggio & Cookson, 2009). This theory has been further called into question by a study demonstrating that kinase-hyperactive mutant LRRK2 does not show elevated levels of phosphorylation at these sites compared to wild-type LRRK2 (Ito *et al.,* 2014). Similarly, kinase-dead LRRK2 mutants appear to show variable phosphorylation at these sites, suggesting other factors at play besides the activity of the LRRK2 kinase domain (Ito *et al.,* 2014).

It has been previously suggested that phosphorylation at ser910 or ser935 mediates LRRK2's interaction with 14-3-3 proteins (Nichols *et al.,* 2010; Piccoli *et al.,* 2014). The functional relevance of this to PD pathology remains unclear, however. Given that the R1441C, but not the G2019S, mutation appears to impair ser910 or ser935 phosphorylation, it seems unlikely that the ablation of interaction between these proteins by this process alone is the source of the pathological mechanisms underlying *LRRK2* PD. Nonetheless, given that R1441C mutations appear to cause similar effects to those of LRRK2 inhibitors, the validity of using the latter for potentially combating the onset of PD may be questionable. Regardless, our findings that *LRRK2* mutations significantly affect phosphorylation at these sites highlight the need for further investigation into the functional roles of these effects along with the mechanism of LRRK2 kinase inhibitors.

5.8.5 Chapter summary

In summary, this Chapter has detailed a molecular characterisation of the *LRRK2* transgenic rats which were generated in Chapter 3, primarily at a late time point of 18-21 months. This characterisation focused, in particular, upon looking for cell loss and molecular changes within the nigro-striatal pathway. In correspondence with the majority of *LRRK2* rodent models, no significant molecular alterations could be detected in the model, despite the evidence of DAergic dysfunction, as revealed by FCV, and behavioural dysfunction reported in Chapter 4. Numerous avenues of more in depth characterisation are available for future investigations and may reveal more subtle neurophysiological changes.

CHAPTER 6 – EXPLORING THE FUNCTION AND DYSFUNCTION OF LRRK2 IN VITRO

6.1 Chapter introduction: motivations, background and aims

In the previous chapter, we attempted to molecularly characterise our *LRRK2* transgenic rats with the aim of uncovering late-stage dysfunction which might indicate PD pathology. However, we found little evidence of either neuropathological features or altered molecular function in the cellular processes in which LRRK2 is involved. While these findings are typical of *LRRK2* transgenic rodents, they provide little insight into the pathological processes underlying LRRK2 dysfunction. *In vitro* studies have been somewhat more fruitful at providing glimpses into the function and dysfunction of LRRK2. An advantage of *in vitro* work is that it allows for the exposure of cultured cells to specific conditions such as altered nutrient contents or chemical agents which can be used to explore various molecular pathways and exacerbate subtle phenotypes. Additionally, *in vitro* work allows for certain types of analysis which are far more difficult to perform *in vivo.* Because we had already developed *LRRK2* BAC transgenic rat lines, we were in a good position to generate primary neuronal cultures to further explore the function of LRRK2 *in vitro.*

It is well reported that LRRK2 mutations lead to altered neurite branching *in vitro*, although the process by which this occurs is unclear (MacLeod *et al.,* 2006; Plowey *et al.,* 2008; Parasiadou *et al.,* 2009; Dächsel *et al.,* 2010; Lee *et al.,* 2010, Ramonet *et al.,* 2011; Tsika *et al.,* 2014). However, the presentation of this altered branching phenotype can be variable, with some studies reporting differential effects of *LRRK2* mutations and potentially different effects seen between transduction studies versus neurons cultured from transgenic animals (MacLeod *et al.,* 2006; Ramonet *et al.,* 2011; Tsika *et al.,* 201). The altered branching phenotype appears to be dependent upon LRRK2 kinase function given that expression of either kinase dead LRRK2 or LRRK2 kinase inhibition has been reported to rescue these effects (MacLeod *et al.,* 2006; Plowey *et al.,* 2008). The presence of such a morphological phenotype is potentially useful given that it may represent a read-out of the effectiveness of treatments used to reverse the effect of *LRRK2* mutations. It is not clear, however,

that the processes which cause impaired neurite outgrowth are the same as those underlying the pathology developed by mutant *LRRK2* carriers.

It has previously been suggested that the cause of the neuritic phenotype seen as a result of mutant LRRK2 expression is the upregulation of autophagy (Plowey *et al.,* 2008). Plowey and colleagues found that, along with causing shortened neurites, expression of G2019S LRRK2 in SH-SY5Y cells caused an elevation of LC3-positive puncta, indicative of increased numbers of AVs. Inhibition of autophagic processes was found to reverse the neuritic phenotype (Plowey *et al.,* 2008). Since this study, a number of reports have drawn links between LRRK2 and autophagy. LRRK2 has been found to localise to MVBs and AVs and specifically co-localise with the autophagy-associated proteins LC3 and P62 (Alegre-Abarrategui *et al.,* 2009). Overexpression of wild-type, in addition to mutant, LRRK2 has been found to increase LC3 puncta and P62 levels in cells along with an accumulation of MVBs and AVs (Alegre-Abarrategui *et al.,* 2009; Gomez-Suaga *et al.,* 2012). Similarly, it has been shown that the G2019S *LRRK2* mutation enhances basal levels of autophagy in various cell lines (Gomez-Suaga *et al.,* 2012; Yakhine-Diop *et al.,* 2014). Furthermore, knockdown of LRRK2 has been shown to impair the induction of autophagy, as determined by LC3-II levels (Alegre-Abarrategui *et al.,* 2009).

A principal method of determining autophagic activity is to assess LC3 processing by Western blot. During the induction of autophagy, LC3-I is conjugated with phosphatidylethanolamine to become LC3-II and moves from the cytosol to become associated with autophagosomes. This is reflected, in Western blots, by the increase in LC3-II levels which have been shown to correlate with the number of autophagosomes (Mizushima & Yoshimori, 2007). A second protein, used as a marker of autophagic activity, is P62. P62 is a protein which is effectively degraded by autophagy (though also by the ubiquitin proteasome system) (Zhang *et al.,* 2012). An accumulation of P62 is therefore indicative of impaired autophagic degradation and is often used in conjunction with LC3 assays to determine autophagic activity (Alegre-Abarrategui *et al.,* 2009).

6.1.1 Chapter aims

1) To investigate the effect of *LRRK2* mutations upon the neurite branching of cultured primary neurons

2) To determine the effects of mutant hLRRK2 expression upon autophagic activity *in vitro*

6.2 Development of cortical neuronal cultures

To more effectively explore the function of LRRK2, we generated cortical neuronal cultures from the *LRRK2* transgenic rats characterised in chapter 3. Our choice of working in cortical neurons, as opposed to midbrain cultures, was several-fold. Firstly, cortical transgene expression was far higher than in the SNpc. Secondly, the majority of studies of *in vitro* LRRK2 function have been performed in either cortical or hippocampal neurons (e.g. MacLeod *et al.,* 2006, Shin *et al.,* 2008). Thirdly, the technical challenges of generating DAergic midbrain cultures are significantly greater than that of generating cortical cultures.

In order to confirm that we could culture primary cortical neurons expressing the hLRRK2 protein, we performed immunocytochemistry on our cell cultures to first confirm the presence of NeuN and microtubule-associated protein 2 (MAP2), both neuronal markers (Fig. 6.1).

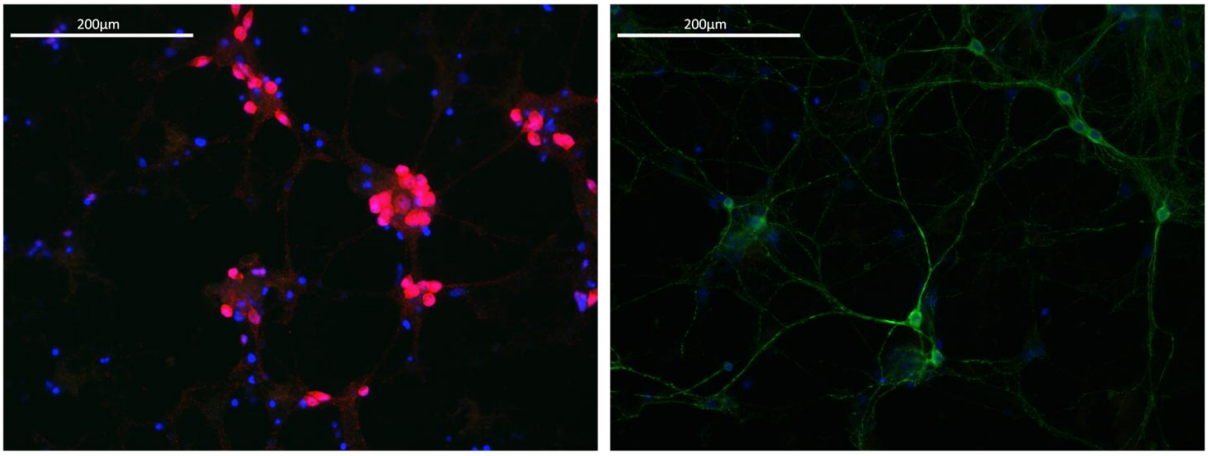

Figure 6.1. Markers of neurons in cortical cultures from P0-3 rats. At 2 weeks of culturing, primary cortical neuronal cultures label positive for **(A)** NeuN and **(B)** MAP2. Representative images are shown.

We then performed immunocytochemistry for the YPet tag to determine whether hLRRK2 protein was expressed and, if so, in which cell type (Fig. 6.1). This revealed transgene expression in the cultured neurons for all genotypes.

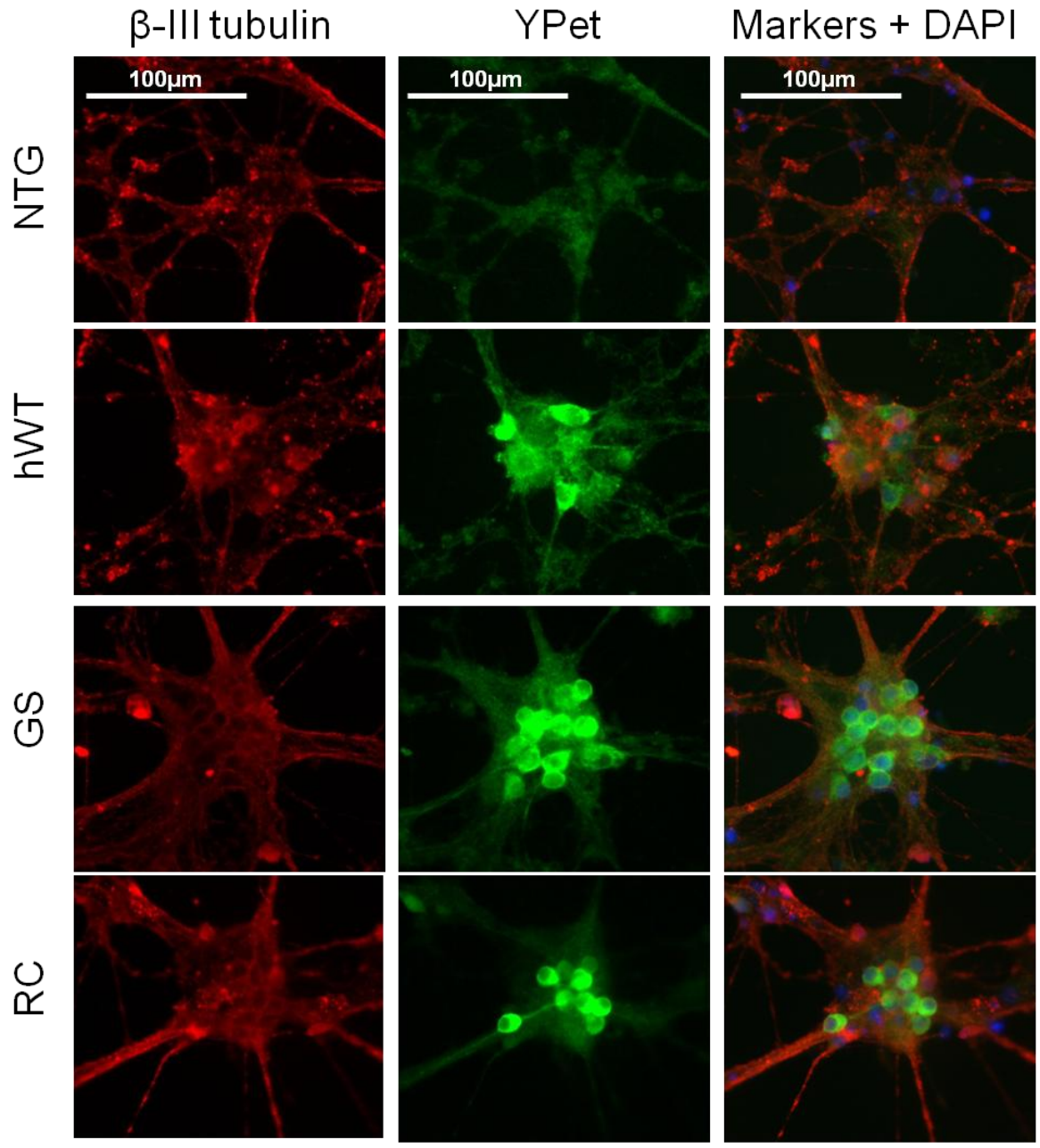

Figure 6.2. Presence of the hLRRK2 protein in the primary cortical neurons. At 2 weeks of culturing, cortical neurons, (labelled with neuronal marker, β-III tubulin) from hWT, G2019S and R1441C animals label positive for hLRRK2 protein. Representative images are shown.

6.3 *LRRK2* mutations do not affect neurite branching *in vitro*

A frequently reported neuronal phenotype in response to mutant LRRK2 overexpression is altered neurite branching, often taking the form of reduced total neurite length. To assess this in our neurons, we performed Sholl analysis on fixed, 3 day old cortical neurons from G2019S, R1441C and hWT rats and compared them to non-transgenic littermate control cultures (Fig. 6.3). To perform this analysis, we utilised the *fastSholl* semi-automated method devised by Gutierrez and Davies (2007) (see methods). We saw no difference in either neuronal branching or total neurite length for either hWT, G2019S or R1441C lines. Additionally, neurons from each genotype showed similar Sholl profiles to non-transgenic control neurons. These data suggest that the *LRRK2* mutations have no effect upon neurite branching.

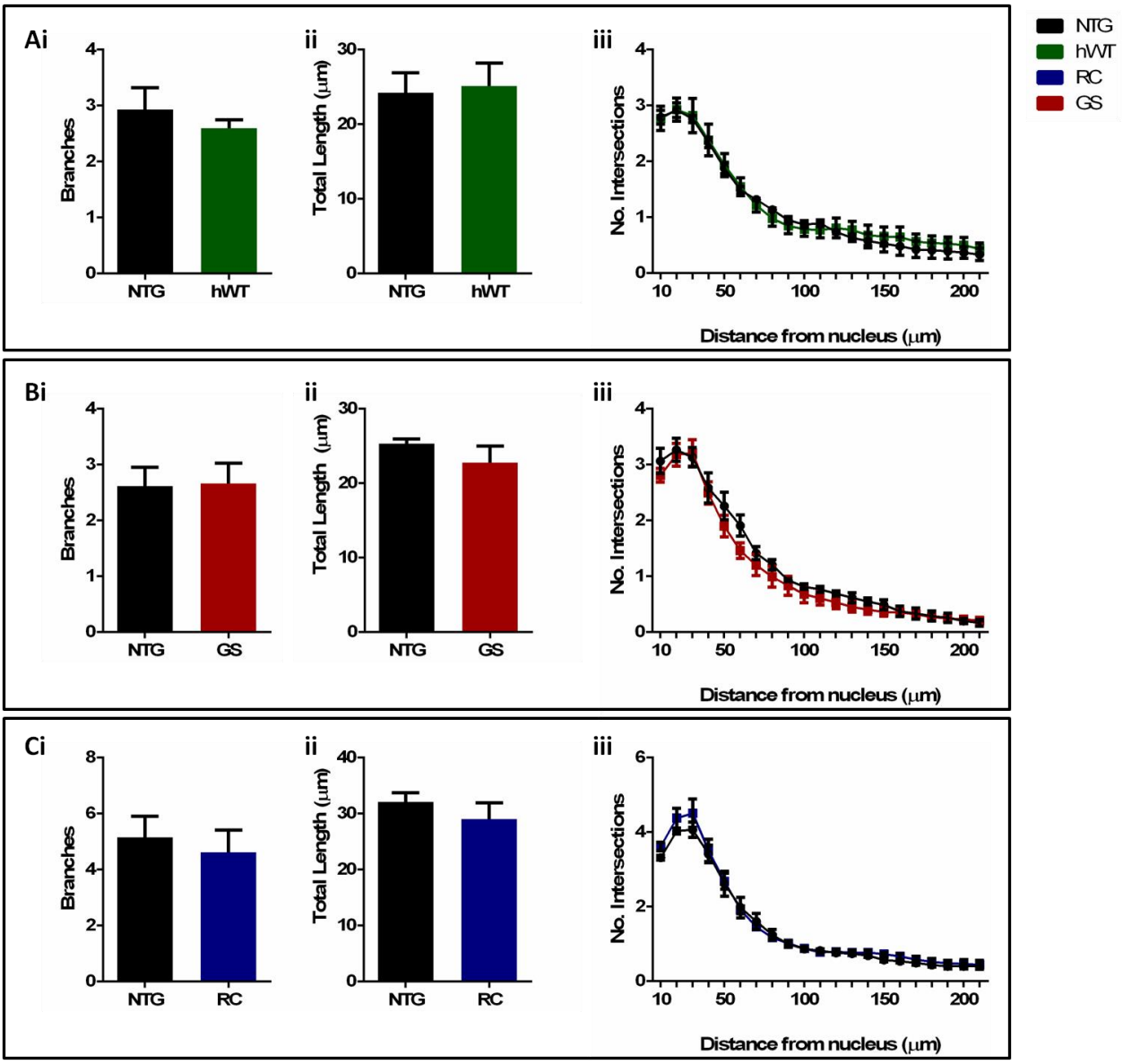

Figure 6.3. *LRRK2* mutations have no effect upon neurite outgrowth. Cortical neurons derived from transgenic **(A)** hWT, **(B)** G2019S and **(C)** R1441C *LRRK2* P0-3 pups, fixed 3 days after plating, and analysed (120 total neurons per genotype) for altered neurite outgrowth show no changes in either **(i)** the number of neurite branches for hWT (Welch's t-test: $p>0.05$, $n=4$ per genotype), G2019S (Welch's t-test: $p>0.05$, $n=4$ per genotype) or R1441C (Welch's t-test: $p>0.05$, $n=4$ per genotype) **(ii)** the total length of the neurite network for hWT (Welch's t-test: $p>0.05$, $n=4$ per genotype), G2019S (Welch's t-test: $p>0.05$, $n=4$ per genotype) or R1441C (Welch's t-test: $p>0.05$, $n=4$ per genotype) or **(iii)** the Sholl profiles of hWT (RM Two-way ANOVA: main effect of distance from nucleus: $p<0.0001$; no main effect of genotype: $p>0.05$, $n=4$ per genotype), G2019S (RM Two-way ANOVA: main effect of distance from nucleus: $p<0.0001$; no main effect of genotype: $p>0.05$, $n=4$ per genotype) or R1441C (RM Two-way ANOVA: main effect of distance from nucleus: $p<0.0001$; no main effect of genotype: $p>0.05$, $n=4$ per genotype) neurons when compared to non-transgenic control cultures from littermates. Data are expressed as mean ± SEM.

6.4 LRRK2 and autophagy

6.4.1 R1441C mutations cause elevated autophagic activity *in vitro*

In the previous chapter, no evidence of altered autophagic processes could be seen in the brains of aged transgenic animals. However, we wanted to determine whether altered autophagic capacity could be detected in neurons expressing mutant hLRRK2 in response to an increase in demand for autophagy (in starvation).

Assessment of the basal levels of autophagy in primary cortical neurons cultured from R1441C, G2019S and hWT rats revealed an increase in the amounts of LC3-II (127% increase) and P62 (135% increase) levels in R1441C but not G2019S or hWT neurons, when compared to non-transgenic controls. Levels of lamp1 in all three genotypes did not differ from non-transgenic controls (Fig. 6.4). This suggested increased levels of AVs present in the cells, indicative of their increased formation or impaired degradation.

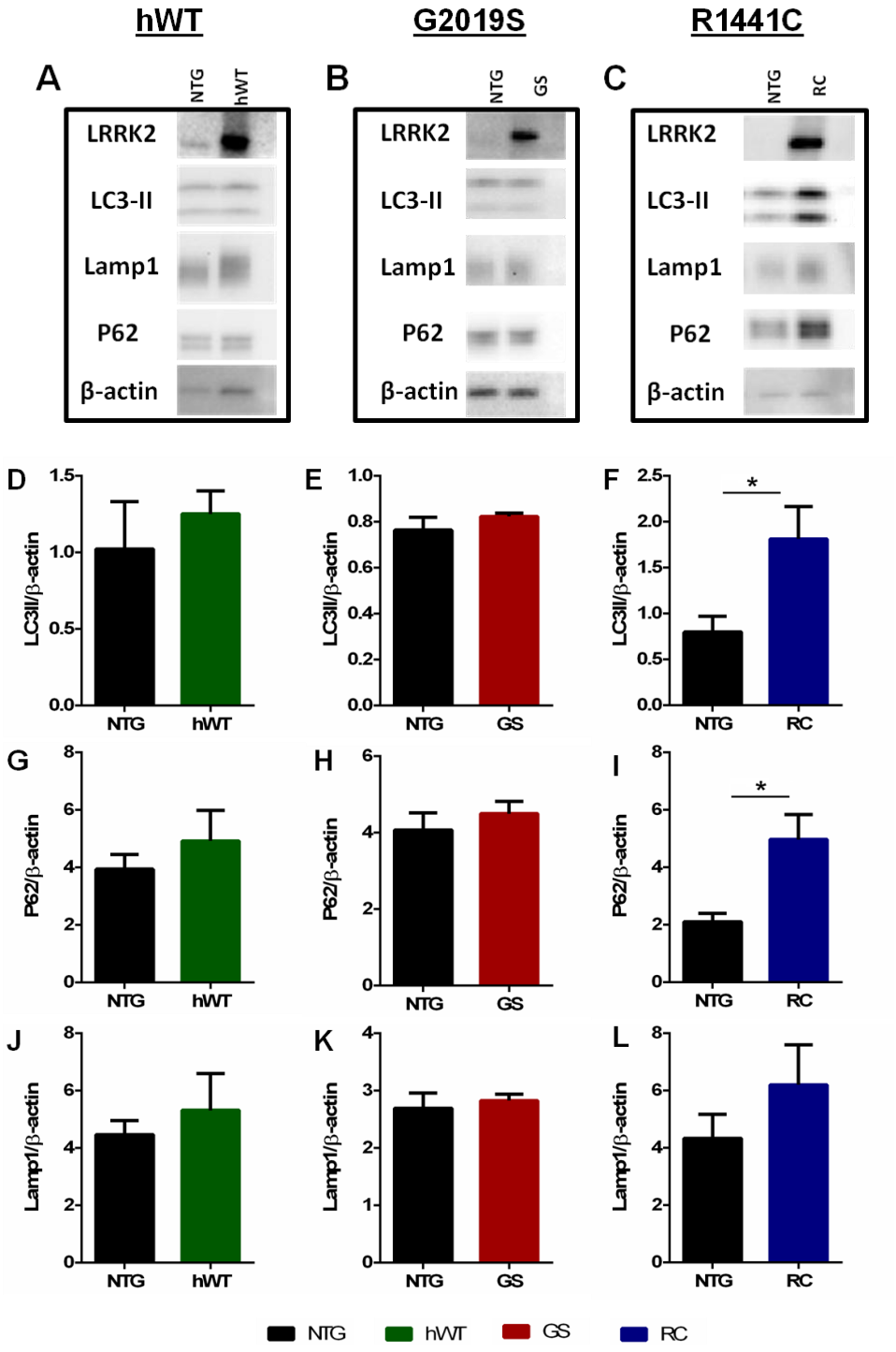

Figure 6.4. R1441C cortical neurons show elevated autophagic markers under nutrient-rich conditions. Cortical neurons cultured for 2 weeks. **(A-C)** Representative westerns for autophagic proteins in neuronal cultures under nutrient rich conditions from **(A)** hWT **(B)** G2019S and **(C)** R1441C *LRRK2* rats compared to non-transgenic controls. **(D-F)** Quantification of neuronal westerns for LC3-II show elevated levels for R1441C (Welch's t-test: *p<0.05, n=4 per genotype) but not G2019S (Welch's t-test: p>0.05, n=4 per genotype) or hWT (Welch's t-test: p>0.05, n=4 per genotype) animals compared to non-transgenic controls. **(G-I)** Quantification of neuronal westerns show elevated P62 levels for R1441C (Welch's t-test: *p<0.05, n=4 per genotype) but not

G2019S (Welch's t-test: p>0.05, n=4 per genotype) or hWT (Welch's t-test: p>0.05, n=4 per genotype) animals compared to non-transgenic controls. **(J-L)** Quantification of neuronal westerns show no change in lamp1 levels for R1441C (Welch's t-test: p>0.05, n=4 per genotype), G2019S (Welch's t-test: p>0.05, n=4 per genotype) or hWT (Welch's t-test: p>0.05, n=4 per genotype) animals compared to non-transgenic controls. Data are expressed as mean ± SEM.

6.4.2 Starvation exacerbates autophagic elevation caused by R1441C mutation

Previous *in vitro* investigations have found that cell starvation, which results in an upregulation of autophagic activity, can reveal alterations to the capacity for the induction of autophagy, as measured by LC3-II levels (Alegre-Abarrategui *et al.,* 2009). It is possible that the pathological processes which drive PD are driven by an initial insult which, due to the ineffective responsiveness of autophagic functioning, leads to the onset of pathology. In order to induce increased autophagic activity, we performed similar experiments (section 6.4.1) under starvation conditions. Similarly to that seen in basal conditions, starvation of R1441C neurons revealed a significant increase in the amounts P62 (413% increase) and a marginally significant increase in LC3-II (337% increase; significance p=0.052) when compared to non-transgenic controls. No differences were seen in autophagic markers for G2019S or hWT neurons. This effect was more pronounced than that seen in basal conditions although there was a high degree of inter-experiment variability.

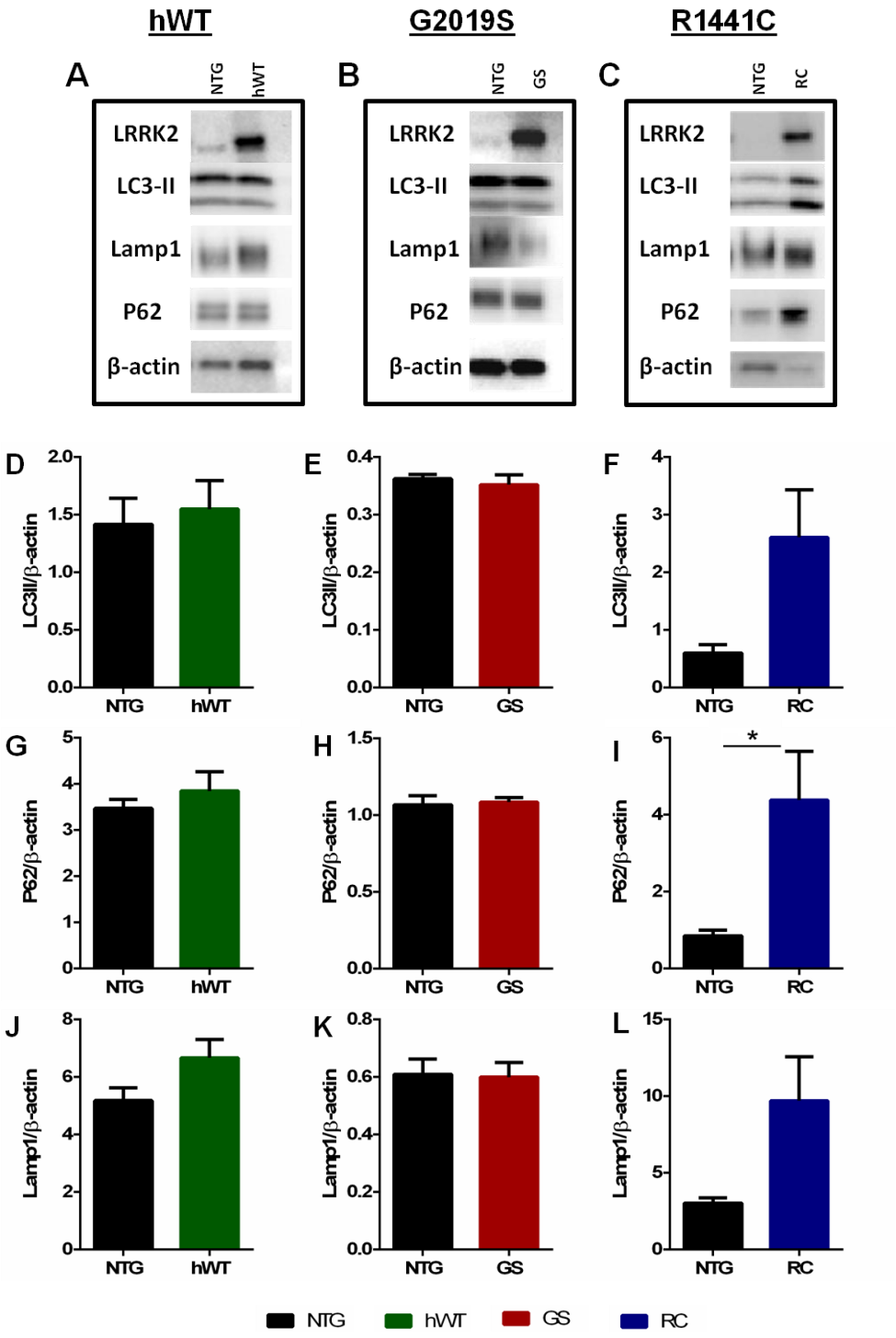

Figure 6.5. R1441C cortical neurons show elevated autophagic flux under starvation conditions. Cortical neurons cultured for 2 weeks and starved for 6 hours. **(A-C)** Representative westerns for autophagic proteins in neuronal cultures under starvation conditions from **(A)** hWT **(B)** G2019S and **(C)** R1441C *LRRK2* rats compared to non-transgenic controls. **(D-F)** Quantification of neuronal westerns for LC3-II show no change in levels for R1441C (Welch's t-test: $p>0.05$, n=4 per genotype), G2019S (Welch's t-test: $p>0.05$, n=4 per genotype) or hWT (Welch's t-test: $p>0.05$, n=4 per genotype) animals compared to non-transgenic controls. **(G-I)** Quantification of neuronal westerns show elevated P62 levels for R1441C (Welch's t-test: *$p<0.05$, n=4 per genotype) but not G2019S (Welch's t-test: $p>0.05$, n=4 per genotype) or hWT (Welch's t-test: $p>0.05$, n=4 per genotype) animals compared to non-transgenic controls. **(J-L)** Quantification of neuronal westerns show

no change in lamp1 levels for R1441C (Welch's t-test: p>0.05, n=4 per genotype), G2019S (Welch's t-test: p>0.05, n=4 per genotype) or hWT (Welch's t-test: p>0.05, n=4 per genotype) animals compared to non-transgenic controls. Data are expressed as mean ± SEM.

6.5 Chapter discussion

In this chapter, we investigated several of the purported effects of mutant hLRRK2 expression *in vitro.* While we did not detect the expected alterations to neurite branching, R1441C mutant hLRRK2 expression appeared to cause an upregulation in basal levels of autophagy as determined by quantification of autophagic markers.

6.5.1 *LRRK2* mutation causes no changes to neurite outgrowth

The lack of an effect of *LRRK2* mutation upon neurite branching and length was contrary to the majority of previous studies which show considerable reduction of neurite length following the expression of mutant LRRK2 (MacLeod *et al.,* 2006; Plowey *et al.,* 2008; Dachsel *et al.,* 2010) (although see Tsika *et al.,* 2014; Ramonet *et al.,* 2011), along with similar results *in vivo* (MacLeod *et al.,* 2006; Winner *et al.,* 2010). These effects are similar in both cells transfected with mutant LRRK2 or cultured from transgenic animals. However, there are a number of potential explanations for the lack of an observed phenotype.

It is possible that the lack of an observed phenotype was due to the assessment of neurite branching being performed too soon after neuronal plating. The neurons in our experiment were fixed 3 days following plating to allow for easy differentiation of neuronal neurite networks. However, the majority of studies reporting the effects of *LRRK2* mutation upon neurite branching have examined neurite density more than a week after neuronal plating (Macleod *et al.,* 2006; Dachsel *et al.,* 2010; Ramonet *et al.,* 2011; Sepulveda *et al.,* 2013). In particular, in the case of transfection experiments, neurite branching is usually assessed several weeks post-transfection (Macleod *et al.,* 2006; Dachsel *et al.,* 2010). While previous studies, including our own research, have indicated that LRRK2 protein

is expressed within 7 days post-natally, it has been suggested that *LRRK2* mRNA is not highly expressed at very early post-natal stages (Piccoli *et al.,* 2011; Westerlund *et al.,* 2008). It is therefore possible that the early timepoint used in our experiments did not allow for the maximal expression and subsequent deleterious effects of the hLRRK2 protein. This hypothesis is supported by several studies which examined the effects of the *LRRK2* mutations upon neurons assessed at 3 to 7 days post-plating and found far more profound effects of the mutations upon branching at 7 days than at 3 days (Ramonet *et al.,* 2011; Sepulveda *et al.,* 2013).

Importantly, however, the vast majority of studies investigating the effect of *LRRK2* mutations of neurite arborisation have been performed by transfection of *LRRK2*. Only a minority of studies utilise primary neurons cultured from transgenic animals. In these cases, results are more unclear. Ramonet and colleagues (2011) found that, G2019S transgenic neurites showed subtly increased Sholl profiles at 3 days which subsequently reverted to impaired outgrowth by day 7. Similarly, Tsika and colleagues (2014) found that cultured DAergic neurons from R1441C transgenic mice show increased neurite arborisation. Finally, neurons cultured from *Lrrk2* KO mice displayed reduced neurite length and arborisation, contrary to what the majority of knockdown and kinase inhibition studies have indicated (Gillardon *et al.,* 2009). Whether these differences in neurite branching patterns are driven principally by cell type, time of analysis or culturing conditions (e.g. the use of Geltrex vs poly-l-lysine) is unclear. Nonetheless, it is likely that the reproducibility of the neuritic phenotype may vary depending upon a number of factors.

Finally, a recent study has suggested that the principal effect which LRRK2 has upon neurite outgrowth is one of altering neurite motility rather than absolute length. These authors show that, by live imaging of neuritic processes, mutant LRRK2 had a far more dramatic effect upon the extension and retraction of processes rather than overall neurite length (Sepulveda *et al.,* 2013).

6.5.2 Preliminary evidence of elevated autophagy in mutant *LRRK2* neuronal culture

Our investigation of autophagic activity, as assessed by LC3-II quantification, indicated upregulated autophagy as a consequence of R1441C hLRRK2 expression in cortical neurons under nutrient rich conditions. This was corroborated by a similar upregulatation of P62, another marker of autophagy. In contrast, hWT and G2019S lines showed no detectable changes in autophagic activity. In an attempt to draw out dysfunction in these lines, we exposed the neuronal cultures to starvation conditions which have previously been shown to induce high levels of autophagy (Alegre-Abarrategui *et al.,* 2009). Our results were largely similar to those seen under basal conditions, however. While the effect of the R1441C mutation upon autophagy was seen to be preserved in P62 assays, we only observed a marginally significant effect of LC3-II induction. This may be due to the considerable amount of variability which existed from experiment to experiment, potentially obscuring transgene effects. Alternatively, starvation may have masked the differences between genotypes by dramatically upregulating autophagy in both mutant and non-transgenic cells, resulting in a ceiling effect for autophagy induction. Interestingly, we observed that the effect of elevated autophagic activity in R1441C lines appeared to correlate with the levels of mutant hLRRK2 expression between experiments, potentially explaining the high levels of variability (data not shown).

The results observed in our experiments are largely in line with those seen in the literature. Studies have consistently reported elevated autophagic activity as a consequence of mutant LRRK2 expression, with more dramatic effects reported under starvation conditions (Plowey *et al.,* 2008; Alegre-Abarrategui *et al.,* 2009; Xiong *et al.,* 2010; Gomez-Suaga *et al.,* 2012; Yakhine-Diop *et al.,* 2014). Similarly, while G2019S mutations have been reported to also result in upregulated autophagy, it appears that R1441C mutations induce a more aggressive phenotype (Alegre-Abarrategui *et al.,* 2009). It is unclear why we detected upregulated autophagic dysfunction under

basal conditions *in vitro* but not *in vivo*. Potentially, stressors brought about by the process of neuronal culture may have had the effect of inducing autophagy beyond those levels seen in the brain. Alternatively, the upregulated autophagy which we observed may be present in animals at a very young age – a time point which we did not assess *in vivo.*

A number of important considerations must be made when interpreting the data from these experiments, however. Firstly, is that it is not clear that the autophagic changes seen are driven by the neurons or other populations in the cell culture such as glia. Given that hLRRK2 appeared to be expressed predominantly within the neurons, this seems unlikely. However, further immunocytochemistry should be performed to confirm that the autophagic induction is neuron specific. A second important consideration, with regards to our observations, is that we are unable to discern whether the upregulated levels of AVs, as indicated by increased LC3-II and P62 levels, are indicative of an upregulation in AV formation or an impairment to AV degradation (Zhang *et al.,* 2012). The lack of change in lamp1 levels appears to indicate that lysosomal populations are normal. However, defective lysosomal function has previously been reported as a result of mutant LRRK2 expression which suggested that LRRK2 has the effect of deacidifying lysosomes (Gomez-Suaga *et al.,* 2012).

In order to further dissect dysfunction within the autophagic pathway, a number of chemical agents can be used to impair various pathways to elucidate the source of dysfunction. Bafilomycin A1 has been used in numerous experiments to block autophagic flux by the deacidification of lysosomes (Klionsky et al,2008; Alegre-Abarrategui *et al.,* 2009; Manzoni *et al.,* 2013; Yakhine-Diop *et al.,* 2014). This has the effect of eliminating the degradation of autophagosomes and their cargo, allowing for the experimental dissection of the molecular underpinnings of an accumulation of AVs. Subsequent experimentation should take advantage of these chemical agents to determine more precisely the effect which mutant LRRK2 has upon the autophagic pathway.

6.5.3 Chapter summary

In summary, we have been unable to observe a change in neurite branching, potentially due to the time after plating at which we conducted our assays. We have, however, seen preliminary indications of an abnormal regulation of autophagic processes by mutant LRRK2 *in vitro.* More investigation needs to be performed to dissect the nature and source of these autophagic changes in the future.

CHAPTER 7 – GENERAL DISCUSSION

7.0 General discussion

Transgenic rodent models offer us a unique opportunity to gain fundamental insights into the underlying pathogeneses of neurodegenerative disease. By exploiting the existence of monogenic forms of PD, we have generated *LRRK2* BAC transgenic rats with which to model PD. Our aim was to develop and characterise these rats in order explore the pathological processes underlying mutant *LRRK2* PD. Our findings, including those of our collaborators, provide a degree of further insight into the consequences of *LRRK2* mutation, in addition to serving to reinforce and expand upon those findings observed in transgenic *LRRK2* mouse models. Here, I shall attempt to synthesise the principal findings of the chapters, draw out some key questions and discuss the implications which our findings have for the broader field, along with proposing steps for what future work may be done.

7.1 The *LRRK2* BAC transgenic rat model: strengths and weaknesses

This thesis initially focussed upon the development, characterisation and eventual selection of three BAC transgenic *LRRK2* rat lines expressing the entire human *LRRK2* sequence of either hWT, G2019S or R1441C genotype. In line with our expectations, the use of the entire human *LRRK2* gene and regulatory elements, using a BAC transgenic approach, led to widespread transgene expression throughout the brain, with highly similar regional and cellular expression patterns from line to line. These expression patterns also closely resembled those seen in humans and rodents (Biskup *et al.,* 2006; Sharma *et al.,* 2011; West *et al.,* 2014). These data strongly suggest that, despite the random chromosomal integration sites of the BAC construct, similar expression patterns were achieved, implying that positional effects of insertion upon expression patterns were minimal. This consistency is of critical importance when it comes to comparing the phenotypes of different lines.

A drawback of our approach, however, is that we were unable to control the number of BAC transgene copies that were integrated. This meant that, while we attempted to select similarly-

expressing founders, our lines did not show identical transgene expression levels. However, our hWT and R1441C lines, the latter of which consistently developed the more aggressive phenotype of the two mutant lines, showed highly similar expression levels. Nonetheless, the elevated expression of the G2019S lines compared to the hWT controls illustrates a limitation within our models which should be kept in mind when interpreting the data. Despite this, our simultaneous characterisation of both an R1441C and G2019S *LRRK2* transgenic model was informative, given that these mutations are rarely compared within a single study (Saha *et al.,* 2009; Ramonet *et al.,* 2011), and have never been done so using a BAC transgenic approach. It was, therefore, encouraging that both mutations, with the exception of our findings of altered hLRRK2 phosphorylation, showed directionally similar effects throughout our subsequent assessments.

Our decision to select lines with higher expression levels than those of endogenous rat LRRK2 was based on the relative paucity of phenotypes seen in knock-in versus overexpressing models (Tong *et al.,* 2009; Longo *et al.,* 2014; Tsika *et al.,* 2014). When attempting to model a neurodegenerative disease such as PD, which typically only arises in individuals after more than half a century of life, in animals which live for only a few years, there exists a constant struggle to produce a form of the disease which typifies that arising from conditions seen in humans, yet one which, almost paradoxically, arises far more rapidly. Because of these two opposing goals, investigators often face a difficult decision when deciding upon expression levels of genes, especially those such as *LRRK2*, mutations in which are not fully penetrant. Models expressing more 'physiological' levels of protein often display very little in the way of phenotypes (e.g. Tsika *et al.,* 2014) and, thus, may not produce much information for the considerable financial and temporal investment required to perform assessments of large-scale ageing cohorts. Similarly, the expression of rarer, more atypical mutations such as the R1441C mutation, which is thought to cause a more aggressive phenotype, versus a potentially milder, more common form, such as the G2019S mutation, represents a compromise between representativeness and informational content (Healy *et al.,* 2008; Kumari & Tan, 2009). It is

likely, therefore, that, while often considered to be a weakness, the heterogeneity of approaches adopted in the animal modelling of neurodegenerative disease represents a core strength, with multiple investigations allowing for the triangulation of underlying pathological mechanisms.

Finally, our use of a YPet tag, fused to the *LRRK2* transgene, proved to be extremely useful for the purposes of protein localisation, both in tissue and *in vitro,* and allowed us to effectively discriminate between endogenous rat LRRK2 and the hLRRK2 protein. Unfortunately, because of the generally low expression levels of hLRRK2, visualisation by native fluorescence was not possible, despite the effective functionality of the YPet protein. Nonetheless, antibodies directed against the tag proved to be greatly useful and far more specific than commercially available LRRK2 antibodies. In future models, however, the use of a brighter fluorescent tag may save time and would allow for the localisation of the LRRK2 protein without the need for tissue fixation or homogenisation which would be highly useful for live-imaging experiments and, potentially, rapid genotyping.

7.2 *LRRK2* rat behaviour in the context of molecular characterisation

Our behavioural experiments, performed in young and aged rats, revealed a number of phenotypes, specific to the mutant transgene, which appeared to be strongly reminiscent of PD. These phenotypes included progressive impairments to motor co-ordination and cognition. The subsequent molecular characterisation of these animals, by both us and our collaborators, informs upon our interpretation of these behavioural data.

The FCV data generated by our collaborators appear to somewhat contradict our behavioural data in that, while our observations of impaired motor co-ordination were restricted to the mutant transgenic rats, the FCV work indicated a DA release deficit in the hWT as well as the G2019S and R1441C lines. Importantly, however, the severity of this deficit was lowest in the hWT line, followed by the G2019S mutation with the R1441C mutants developing the most severe pathology – data in line with our own reports of behavioural deficits. It is possible, therefore, that a minimum threshold

of DAergic impairment is required for the development of Parkinsonian symptoms, a hypothesis supported by the fact that PD symptoms usually do not arise in patients until a substantial number of DAergic neurons are lost (Fearnley & Lees, 1991). The notion that hWT LRRK2 expression may lead to the development of pathology within the DAergic system, albeit one less severe than that seen as a result of mutant LRRK2 expression, is one which has been reported previously (Melrose *et al.,* 2010) (although see Li *et al.,* 2010). In line with this, our collaborators have made *in vivo* electrophysiological recordings of DAergic SNpc neurons in R1441C and hWT rats (Kaufmann *et al.,* unpublished). These recordings have shown an age-dependent reduction in the burst firing of SNpc DA neurons in R1441C and, to a lesser extent, hWT animals.

Administration of L-DOPA to our G2019S animals rescued the observed impairments to motor co-ordination. Correspondingly, previous *LRRK2* transgenic rodent models which demonstrate hypokinesia appear to be treatable with L-DOPA (Li *et al.,* 2009; Chen *et al.,* 2012; Chou *et al.,* 2014). Our study represents the first example of a *LRRK2* mutant rescue on a measure of motor co-ordination. This is very much in line with mutant *LRRK2* PD patients who respond well to L-DOPA treatment, reinforcing the notion that the phenotypes developed by *LRRK2* transgenic rodents are Parkinsonian (Trinh & Farrer, 2013). The successful rescue-effect of L-DOPA administration in G2019S animals is interesting given the fact that HPLC data from our collaborators suggest that there is no DA content deficit within the striatum of G2019S or R1441C animals (Potgeiter et al., unpublished). As L-DOPA acts to increase the amount of DA produced by DA neurons, the reason why increased DA counteracts the motor deficit is unclear. It is possible, however, that elevated DA levels may compensate for other deficits developed by these animals, by elevating DA available for release. It would be valuable, in future, to confirm that administration of L-DOPA in this model does, indeed, rescue the release of DA in the striatum potentially by administering L-DOPA to animals prior to performing FCV.

Rather than hypokinesia, as would be predicted by some *LRRK2* rodent models (Li *et al.,* 2009; Chen *et al.,* 2012; Chou *et al.,* 2014) our animals displayed hyperactivity over the course of their lives. As with the other observed phenotypes, the hyperactivity appeared to be specific to the expression of mutant *LRRK2*. What underlying dysfunction the hyperactivity reflects and whether there are any symptomatic parallels in human patients is not clear. There is little mention of hyperactivity in early PD patients' lifetimes although a single study suggests that PD patients report increased hyperactivity and attentional deficiency in childhood (Walitza *et al.,* 2007). The lack of responsiveness of the hyperactivity phenotype to L-DOPA (observed in the cylinder test) suggests that it not a result of impaired DAergic release. This is supported by the FCV work done in parallel on these rats (Potgeiter et al., unpublished) which suggests normal DA release within the striatum at young time points where hyperactivity is observed. A potential explanation for the hyperactivity could be increased levels of post-synaptic D1 receptors which have been previously reported in *LRRK2* transgenic mice and *in vitro* (Melrose *et al.,* 2010; Migheli *et al.,* 2013). Alternatively, given the widespread expression of the transgene in areas such as the cortex and cerebellum, it is possible that the hyperactivity emerges from other areas. In support of this, Tsika and colleagues (2014) do not report any hyperactivity in an R1441C mouse model which restricted transgene expression to neurons expressing DAT, suggesting that the phenotype may emerge as a consequence of alterations to other systems. Importantly, however, Tsika and colleagues (2014) show very little in the way of a behavioural phenotype, suggesting that levels of mutant LRRK2 may simply be too low for the effective generation of motor dysfunction.

Finally, we have also reported, for the first time in a *LRRK2* transgenic rodent, impaired cognition, as determined by the spontaneous alternation test. The high levels of expression of the hLRRK2 protein in the hippocampus and cortex help reinforce the plausibility of these results, given the links between these areas and spatial navigation (Muller & Kubie, 1989). However, PD patient studies have found a high correlation between cognitive impairment and LB or tau tangle pathology (Hurtig

et al., 2000). It is surprising, therefore, that we see no pathological markers in the brains of our rats. Given that LRRK2 has been associated with altered hippocampal neurogenesis, however, it is possible that animals may develop neurological defects in the absence of neurodegeneration (Winner *et al.,* 2010). Alternatively, it is possible that the impaired performance on the spontaneous alternation task is reflective of a phenotype other than impaired cognition, *per se.* Our preliminary evidence of increased wall hugging behaviour, suggesting an anxious phenotype in the R1441C animals, may represent an alternative explanation, given that anxiety has well-known effects upon task performance in tests requiring working memory (Vytal *et al.,* 2013). Therefore, more studies need to be performed to validate the phenotype and to then determine underlying mechanisms.

7.3 Why don't *LRRK2* transgenic rodents develop neuropathology?

While our *LRRK2* transgenic rats developed what could be considered early Parkinsonian features, they displayed no SNpc neurodegeneration. Though this fact challenges, to an extent, the utility of our *LRRK2* transgenic rats as a model of late stage PD, it does provide some insight into the sequence of pathological events within the PD patient brain. Our data suggest that dysfunction within the nigro-striatal system begins with impaired striatal DA release, preceding any SNpc degeneration, and leads to the development of the impairments to motor co-ordination observed behaviourally. These findings are in line with not only the majority of *LRRK2* rodent models, but also with numerous reports which suggest that DAergic terminals within the striatum are lost prior to SNpc neuronal death (Burke & O'Malley, 2013). Additionally, more subtle changes to SNpc neurons may precede overt neurodegeneration and, as indicated by our collaborators' *in vivo* electrophysiology, may have a functional impact upon nigrostriatal DAergic function in the absence of neurodegeneration (Li *et al.,* 2009; Lin *et al.,* 2009; Lee *et al.,* 2014; Tsika *et al.,* 2014; Kaufmann *et al.,* unpublished). It is possible, therefore, that cell death within the SNpc represents later stages of a pathological process which causes earlier, more subtle alterations to neuronal cell bodies and terminal function.

In addition to the lack of neurodegeneration observed in the SNpc, no evidence was found of any overt neurodegeneration or Lewy/tau-tangle pathology. This lack of neuropathology is predominantly observed across the majority of rodent models of LRRK2 dysfunction (Li *et al.,* 2009; Lin *et al.,* 2009; Tong *et al.,* 2009; Li *et al.,* 2010; Maekawa *et al.,* 2012; Dranka *et al.,* 2013; Chou *et al.,* 2014). It is unclear why, despite frequently high levels of LRRK2 expression, *LRRK2* transgenic rodents do not generally develop particularly aggressive pathology. The most probable explanation is that insufficient time exists for the development of pathology over the course of a rodent's lifetime. Although α-synuclein transgenic models appear to develop more robust pathology, patients with pathological α-synuclein mutations also display an earlier disease onset than that seen in *LRRK2* mutation carriers (Chesselet & Richter, 2011; Klein & Westenberger, 2012). It is additionally likely that a degree of developmental compensation occurs which ameliorates the effects of mutant LRRK2 expression. Temporally expressing G2019S LRRK2 after early development appears to produce a more dramatic phenotype than that seen following constitutive expression (Zhou *et al.,* 2011). However, these models still show no signs of neurodegeneration or neuropathology (Zhou *et al.,* 2011; Tsika *et al.,* 2014). Furthermore, if compensatory processes exist which ameliorate mutant LRRK2-induced pathology in rodents, it is not clear why humans would not display these same processes.

It has also been suggested that wild-type LRRK2 may eliminate the deleterious effects that result from mutant LRRK2 overexpression, either by exerting a compensatory role or by interacting with the mutant LRRK2 protein. In a similar vein, previous studies have found that KO of endogenous mouse α-synuclein can exacerbate the effects of mutant α-synuclein expression (Cabin *et al.,* 2005). These hypotheses appear unlikely for a number of reasons, however. Firstly, as *LRRK2* mutations are autosomal dominant, mutant LRRK2 is able to cause pathology in the presence of wild-type LRRK2 protein. In line with this, LRRK2 G2019S homozygotes do not appear to develop PD more quickly than LRRK2 G2019S hemizygotes (who also possess wild-type *LRRK2*) (Ishihara *et al.,* 2007) – a

surprising fact given the seemingly increased effectiveness of LRRK2 overexpression in rodent models. Secondly, *LRRK2* homozygous KI rodent models do not appear to develop more aggressive phenotypes than other transgenic models, although this may be a consequence of the use of the mouse LRRK2 gene and low levels of expression (Tong *et al.,* 2009; Longo *et al.,* 2014).

Alternatively, while little evidence exists linking LRRK1 to PD, it has been proposed that an explanation for the lack of a phenotype seen in LRRK2 transgenic rodents is compensation by LRRK1 (Biskup *et al.,* 2007). In support of this, *Lrrk2* KO animals display pathology predominantly in the kidney, where expression of LRRK1 and LRRK2 overlap to a lesser extent than in the brain (Tong *et al.,* 2010; Westerlund *et al.,* 2008). The generation of *LRRK2* mutant transgenic rodent on a *Lrrk1* KO background may reveal more dramatic pathology.

A final possibility is that endogenous human α-synuclein co-expression may be required for the effective development of pathology. *LRRK2*/*SNCA* double-transgenic rodents do appear to develop a more pronounced pathology than α-synuclein transgenics alone (Lin *et al.,* 2009; Daher *et al.,* 2012). In line with this hypothesis, mouse α-synuclein appears to act protectively against mutant α-synuclein overexpression (Cabin *et al.,* 2005). However, it should be noted that expression of G2019S LRRK2 in *C. elegans* (animals which do not express endogenous α-synuclein) appears to cause neurodegeneration, suggesting that the lack of human α-synuclein may not be explanation for the lack of observed neurodegeneration (Saha *et al.,* 2009).

Overall, it is important to acknowledge that the lack of neurodegeneration observed in BAC transgenic *LRRK2* rodents may represent a fundamental limitation with the approach given the lifespan of the animals. Without further manipulations such as α-synuclein co-expression or the knockout of key homeostatic mechanisms such as autophagy, late-stage PD pathology may be difficult to achieve.

7.4 Future directions

As with any animal model, the potential avenues for further exploration are numerous. Drawing upon the data generated from the work covered in this thesis, there are a number of obvious areas for investigation in the *LRRK2* transgenic rats, some of which are currently being pursued by other members of the Oxford Parkinson's Disease Centre. These include:

- Performing electron microscopy to determine the distribution of synaptic vesicles within DAergic terminals of the striatum, in addition to examining the formation and potential accumulation of AVs and MVBs in regions of high expression

- Assessing the potential modulation of DA release within the striatum by cholinergic interneurons, which express high levels of hLRRK2

- Morphological analysis of SNpc neuronal cell bodies in addition to a more thorough quantification of TH-positive neurites within the striatum to probe for the presence of pre-degenerative features

- Assessment of *in vivo* DA receptor density and function by autoradiography assays to potentially elucidate the source of the LRRK2 mediated hyperactivity

- Investigation of neurotransmitter release and reuptake *in vitro,* using FM dyes in primary neuronal cultures in addition to further investigation into autophagic mechanisms, disrupted by *LRRK2* mutation

- An investigation of the immune response of the *LRRK2* transgenic rats to a proinflammatory insult (e.g. LPS treatment)

- Investigation into the potential presence of pre-tangle forms of abnormally phosphorylated tau

•Further behavioural characterisation to determine the veracity and source of the cognitive and anxious phenotype observed in aged R1441C animals

•Expression of mutant LRRK2 on a *Lrrk2* or *Lrrk1* KO background or co-expression of LRRK2 and α-synuclein in a rat BAC transgenic model

7.5 Conclusions

In conclusion, this thesis has described the development and characterisation of a novel *LRRK2* BAC transgenic rat model of PD. By generating rats which express either wild-type or mutant hLRRK2, we were able to demonstrate that mutations in *LRRK2* generate late-stage behavioural dysfunction resembling that seen in PD, as well as molecular alterations, which may provide clues as to the pathogenesis of *LRRK2* PD. Despite our and our collaborators demonstration of dysfunction within the DAergic system, we did not observe any signs of neuropathology in these animals. Though we have performed an extensive initial characterisation of these animals, there remains a great deal of further areas of investigation for which the rats are well suited. We, and our collaborators, therefore aim to continue to use these animals to better understand the functions of LRRK2 and its role in PD.

References

Aarsland D, Andersen K, Larsen JP, Lolk A, Nielsen H, Kragh-Sorensen P (2001) Risk of dementia in Parkinson's disease: a community-based, prospective study. Neurology 56:730-736.

Abbott RD, Petrovitch H, White LR, Masaki KH, Tanner CM, Curb JD, Grandinetti A, Blanchette PL, Popper JS, Ross GW (2001) Frequency of bowel movements and the future risk of Parkinson's disease. Neurology 57:456-462.

Albin RL, Young AB, Penney JB (1989) The functional anatomy of basal ganglia disorders. Trends Neurosci 12:366-375.

Alegre-Abarrategui J, Christian H, Lufino MM, Mutihac R, Venda LL, Ansorge O, Wade-Martins R (2009) LRRK2 regulates autophagic activity and localizes to specific membrane microdomains in a novel human genomic reporter cellular model. Hum Mol Genet 18:4022-4034.

Andres-Mateos E, Mejias R, Sasaki M, Li X, Lin BM, Biskup S, Zhang L, Banerjee R, Thomas B, Yang L, Liu G, Beal MF, Huso DL, Dawson TM, Dawson VL (2009) Unexpected lack of hypersensitivity in LRRK2 knock-out mice to MPTP (1-methyl-4-phenyl-1,2,3,6-tetrahydropyridine). J Neurosci 29:15846-15850.

Augustinack JC, Schneider A, Mandelkow EM, Hyman BT (2002) Specific tau phosphorylation sites correlate with severity of neuronal cytopathology in Alzheimer's disease. Acta Neuropathol 103:26-35.

Barrett JC, Hansoul S, Nicolae DL, Cho JH, Duerr RH, Rioux JD, Brant SR, Silverberg MS, Taylor KD, Barmada MM, Bitton A, Dassopoulos T, Datta LW, Green T, Griffiths AM, Kistner EO, Murtha MT, Regueiro MD, Rotter JI, Schumm LP, Steinhart AH, Targan SR, Xavier RJ, Consortium NIG, Libioulle C, Sandor C, Lathrop M, Belaiche J, Dewit O, Gut I, Heath S, Laukens D, Mni M, Rutgeerts P, Van Gossum A, Zelenika D, Franchimont D, Hugot JP, de Vos M, Vermeire S, Louis E, Belgian-French IBDC, Wellcome Trust Case Control C, Cardon LR, Anderson CA, Drummond H, Nimmo E, Ahmad T, Prescott NJ, Onnie CM, Fisher SA, Marchini J, Ghori J, Bumpstead S, Gwilliam R, Tremelling M, Deloukas P, Mansfield J, Jewell D, Satsangi J, Mathew CG, Parkes M, Georges M, Daly MJ (2008) Genome-wide association defines more than 30 distinct susceptibility loci for Crohn's disease. Nat Genet 40:955-962.

Beil J, Fairbairn L, Pelczar P, Buch T (2012) Is BAC transgenesis obsolete? State of the art in the era of designer nucleases. J Biomed Biotechnol 2012:308414.

Belluzzi E, Greggio E, Piccoli G (2012) Presynaptic dysfunction in Parkinson's disease: a focus on LRRK2. Biochem Soc Trans 40:1111-1116.

Bendor JT, Logan TP, Edwards RH (2013) The function of alpha-synuclein. Neuron 79:1044-1066.

Berger Z, Smith KA, Lavoie MJ (2010) Membrane localization of LRRK2 is associated with increased formation of the highly active LRRK2 dimer and changes in its phosphorylation. Biochemistry 49:5511-5523.

Betarbet R, Sherer TB, MacKenzie G, Garcia-Osuna M, Panov AV, Greenamyre JT (2000) Chronic systemic pesticide exposure reproduces features of Parkinson's disease. Nat Neurosci 3:1301-1306.

Bichler Z, Lim HC, Zeng L, Tan EK (2013) Non-motor and motor features in LRRK2 transgenic

mice. PLoS One 8:e70249.
Biskup S, Moore DJ, Rea A, Lorenz-Deperieux B, Coombes CE, Dawson VL, Dawson TM, West AB (2007) Dynamic and redundant regulation of LRRK2 and LRRK1 expression. BMC Neurosci 8:102.
Biskup S, Moore DJ, Celsi F, Higashi S, West AB, Andrabi SA, Kurkinen K, Yu SW, Savitt JM, Waldvogel HJ, Faull RL, Emson PC, Torp R, Ottersen OP, Dawson TM, Dawson VL (2006) Localization of LRRK2 to membranous and vesicular structures in mammalian brain. Ann Neurol 60:557-569.
Boeve BF, Silber MH, Parisi JE, Dickson DW, Ferman TJ, Benarroch EE, Schmeichel AM, Smith GE, Petersen RC, Ahlskog JE, Matsumoto JY, Knopman DS, Schenck CH, Mahowald MW (2003) Synucleinopathy pathology and REM sleep behavior disorder plus dementia or parkinsonism. Neurology 61:40-45.
Bolam JP, Pissadaki EK (2012) Living on the edge with too many mouths to feed: why dopamine neurons die. Mov Disord 27:1478-1483.
Bonifati V, Rizzu P, van Baren MJ, Schaap O, Breedveld GJ, Krieger E, Dekker MC, Squitieri F, Ibanez P, Joosse M, van Dongen JW, Vanacore N, van Swieten JC, Brice A, Meco G, van Duijn CM, Oostra BA, Heutink P (2003) Mutations in the DJ-1 gene associated with autosomal recessive early-onset parkinsonism. Science 299:256-259.
Bove J, Perier C (2012) Neurotoxin-based models of Parkinson's disease. Neuroscience 211:51-76.
Bower JH, Maraganore DM, McDonnell SK, Rocca WA (1999) Incidence and distribution of parkinsonism in Olmsted County, Minnesota, 1976-1990. Neurology 52:1214-1220.
Boyce S, Kelly E, Reavill C, Jenner P, Marsden CD (1984) Repeated administration of N-methyl-4-phenyl 1,2,5,6-tetrahydropyridine to rats is not toxic to striatal dopamine neurones. Biochem Pharmacol 33:1747-1752.
Braak H, Del Tredici K, Rub U, de Vos RA, Jansen Steur EN, Braak E (2003) Staging of brain pathology related to sporadic Parkinson's disease. Neurobiol Aging 24:197-211.
Brinster RL, Allen JM, Behringer RR, Gelinas RE, Palmiter RD (1988) Introns increase transcriptional efficiency in transgenic mice. Proc Natl Acad Sci USA 85:836-840.
Burchell VS, Nelson DE, Sanchez-Martinez A, Delgado-Camprubi M, Ivatt RM, Pogson JH, Randle SJ, Wray S, Lewis PA, Houlden H, Abramov AY, Hardy J, Wood NW, Whitworth AJ, Laman H, Plun-Favreau H (2013) The Parkinson's disease-linked proteins Fbxo7 and Parkin interact to mediate mitophagy. Nat Neurosci 16:1257-1265.
Burke RE, O'Malley K (2013) Axon degeneration in Parkinson's disease. Exp Neurol 246:72-83.
Burke RE, Dauer WT, Vonsattel JP (2008) A critical evaluation of the Braak staging scheme for Parkinson's disease. Ann Neurol 64:485-491.
Cabin DE, Gispert-Sanchez S, Murphy D, Auburger G, Myers RR, Nussbaum RL (2005) Exacerbated synucleinopathy in mice expressing A53T SNCA on a Snca null background. Neurobiol Aging 26:25-35.
Cachope R, Mateo Y, Mathur BN, Irving J, Wang HL, Morales M, Lovinger DM, Cheer JF (2012) Selective activation of cholinergic interneurons enhances accumbal phasic dopamine release: setting the tone for reward processing. Cell Rep 2:33-41.
Calabresi P, Centonze D, Gubellini P, Pisani A, Bernardi G (2000) Acetylcholine-mediated modulation of striatal function. Trends Neurosci 23:120-126.
Calabresi P, Di Filippo M, Ghiglieri V, Tambasco N, Picconi B (2010) Levodopa-induced

dyskinesias in patients with Parkinson's disease: filling the bench-to-bedside gap. Lancet Neurol 9:1106-1117.
Canet-Aviles RM, Wilson MA, Miller DW, Ahmad R, McLendon C, Bandyopadhyay S, Baptista MJ, Ringe D, Petsko GA, Cookson MR (2004) The Parkinson's disease protein DJ-1 is neuroprotective due to cysteine-sulfinic acid-driven mitochondrial localization. Proc Natl Acad Sci USA 101:9103-9108.
Cannon JR, Geghman KD, Tapias V, Sew T, Dail MK, Li C, Greenamyre JT (2013) Expression of human E46K-mutated alpha-synuclein in BAC-transgenic rats replicates early-stage Parkinson's disease features and enhances vulnerability to mitochondrial impairment. Exp Neurol 240:44-56.
Chaudhuri KR, Healy DG, Schapira AH, National Institute for Clinical E (2006) Non-motor symptoms of Parkinson's disease: diagnosis and management. Lancet Neurol 5:235-245.
Chen H, Jacobs E, Schwarzschild MA, McCullough ML, Calle EE, Thun MJ, Ascherio A (2005) Nonsteroidal antiinflammatory drug use and the risk for Parkinson's disease. Ann Neurol 58:963-967.
Chen CY, Weng YH, Chien KY, Lin KJ, Yeh TH, Cheng YP, Lu CS, Wang HL (2012) (G2019S) LRRK2 activates MKK4-JNK pathway and causes degeneration of SN dopaminergic neurons in a transgenic mouse model of PD. Cell Death Differ 19:1623-1633.
Chesselet MF, Richter F (2011) Modelling of Parkinson's disease in mice. Lancet Neurol 10:1108-1118.
Chou AP, Li S, Fitzmaurice AG, Bronstein JM (2010) Mechanisms of rotenone-induced proteasome inhibition. Neurotoxicology 31:367-372.
Chou JS, Chen CY, Chen YL, Weng YH, Yeh TH, Lu CS, Chang YM, Wang HL (2014) (G2019S) LRRK2 causes early-phase dysfunction of SNpc dopaminergic neurons and impairment of corticostriatal long-term depression in the PD transgenic mouse. Neurobiol Dis 68:190-199.
Chuang CS, Su HL, Cheng FC, Hsu SH, Chuang CF, Liu CS (2010) Quantitative evaluation of motor function before and after engraftment of dopaminergic neurons in a rat model of Parkinson's disease. J Biomed Sci 17:9.
Cirnaru MD, Marte A, Belluzzi E, Russo I, Gabrielli M, Longo F, Arcuri L, Murru L, Bubacco L, Matteoli M, Fedele E, Sala C, Passafaro M, Morari M, Greggio E, Onofri F, Piccoli G (2014) LRRK2 kinase activity regulates synaptic vesicle trafficking and neurotransmitter release through modulation of LRRK2 macro-molecular complex. Front Mol Neurosci 7:49.
Cohen G (1984) Oxy-radical toxicity in catecholamine neurons. Neurotoxicology 5:77-82.
Colotla VA, Flores E, Oscos A, Meneses A, Tapia R (1990) Effects of MPTP on locomotor activity in mice. Neurotoxicol Teratol 12:405-407.
Cookson MR (2010) The role of leucine-rich repeat kinase 2 (LRRK2) in Parkinson's disease. Nat Rev Neurosci 11:791-797.
Cotzias GC, Papavasiliou PS, Gellene R (1969) Modification of Parkinsonism-chronic treatment with L-dopa. N Engl J Med 280:337-345.
Croisier E, Moran LB, Dexter DT, Pearce RK, Graeber MB (2005) Microglial inflammation in the parkinsonian substantia nigra: relationship to alpha-synuclein deposition. J Neuroinflammation 2:14.
Cummings JL (1992) Depression and Parkinson's disease: a review. Am J Psychiatry 149:443-

454.
Dachsel JC, Behrouz B, Yue M, Beevers JE, Melrose HL, Farrer MJ (2010) A comparative study of Lrrk2 function in primary neuronal cultures. Parkinsonism Relat Disord 16:650-655.
Daher JP, Volpicelli-Daley LA, Blackburn JP, Moehle MS, West AB (2014) Abrogation of alpha-synuclein-mediated dopaminergic neurodegeneration in LRRK2-deficient rats. Proc Natl Acad Sci USA 111:9289-9294.
Daher JP, Pletnikova O, Biskup S, Musso A, Gellhaar S, Galter D, Troncoso JC, Lee MK, Dawson TM, Dawson VL, Moore DJ (2012) Neurodegenerative phenotypes in an A53T alpha-synuclein transgenic mouse model are independent of LRRK2. Hum Mol Genet 21:2420-2431.
Davies P, Hinkle KM, Sukar NN, Sepulveda B, Mesias R, Serrano G, Alessi DR, Beach TG, Benson DL, White CL, Cowell RM, Das SS, West AB, Melrose HL (2013) Comprehensive characterization and optimization of anti-LRRK2 (leucine-rich repeat kinase 2) monoclonal antibodies. Biochem J 453:101-113.
Deacon RM (2013) Measuring motor coordination in mice. J Vis Exp:e2609.
Deacon RM, Rawlins JN (2006) T-maze alternation in the rodent. Nat Protoc 1:7-12.
Dehay B, Ramirez A, Martinez-Vicente M, Perier C, Canron MH, Doudnikoff E, Vital A, Vila M, Klein C, Bezard E (2012) Loss of P-type ATPase ATP13A2/PARK9 function induces general lysosomal deficiency and leads to Parkinson disease neurodegeneration. Proc Natl Acad Sci USA 109:9611-9616.
Dickson DW, Braak H, Duda JE, Duyckaerts C, Gasser T, Halliday GM, Hardy J, Leverenz JB, Del Tredici K, Wszolek ZK, Litvan I (2009) Neuropathological assessment of Parkinson's disease: refining the diagnostic criteria. Lancet Neurol 8:1150-1157.
Do CB, Tung JY, Dorfman E, Kiefer AK, Drabant EM, Francke U, Mountain JL, Goldman SM, Tanner CM, Langston JW, Wojcicki A, Eriksson N (2011) Web-based genome-wide association study identifies two novel loci and a substantial genetic component for Parkinson's disease. PLoS Genet 7:e1002141.
Dranka BP, Gifford A, Ghosh A, Zielonka J, Joseph J, Kanthasamy AG, Kalyanaraman B (2013) Diapocynin prevents early Parkinson's disease symptoms in the leucine-rich repeat kinase 2 (LRRK2R1441G) transgenic mouse. Neurosci Lett 549:57-62.
Dusonchet J, Kochubey O, Stafa K, Young SM, Jr., Zufferey R, Moore DJ, Schneider BL, Aebischer P (2011) A rat model of progressive nigral neurodegeneration induced by the Parkinson's disease-associated G2019S mutation in LRRK2. J Neurosci 31:907-912.
Dzamko N, Deak M, Hentati F, Reith AD, Prescott AR, Alessi DR, Nichols RJ (2010) Inhibition of LRRK2 kinase activity leads to dephosphorylation of Ser(910)/Ser(935), disruption of 14-3-3 binding and altered cytoplasmic localization. Biochem J 430:405-413.
Ehringer H, Hornykiewicz O (1960) [Distribution of noradrenaline and dopamine (3-hydroxytyramine) in the human brain and their behavior in diseases of the extrapyramidal system]. Klin Wochenschr 38:1236-1239.
Elbaz A (2008) LRRK2: bridging the gap between sporadic and hereditary Parkinson's disease. Lancet Neurol 7:562-564.
Emmanouilidou E, Melachroinou K, Roumeliotis T, Garbis SD, Ntzouni M, Margaritis LH, Stefanis L, Vekrellis K (2010) Cell-produced alpha-synuclein is secreted in a calcium-dependent manner by exosomes and impacts neuronal survival. J Neurosci 30:6838-

6851.
Esteves AR, Swerdlow RH, Cardoso SM (2014) LRRK2, a puzzling protein: Insights into Parkinson's disease pathogenesis. Exp Neurol.
Feany MB, Bender WW (2000) A Drosophila model of Parkinson's disease. Nature 404:394-398.
Fearnley JM, Lees AJ (1991) Ageing and Parkinson's disease: substantia nigra regional selectivity. Brain 114 (Pt 5):2283-2301.
Ferree A, Guillily M, Li H, Smith K, Takashima A, Squillace R, Weigele M, Collins JJ, Wolozin B (2012) Regulation of physiologic actions of LRRK2: focus on autophagy. Neurodegener Dis 10:238-241.
Filloux F, Townsend JJ (1993) Pre- and postsynaptic neurotoxic effects of dopamine demonstrated by intrastriatal injection. Exp Neurol 119:79-88.
Forno LS (1987) The Lewy body in Parkinson's disease. Adv Neurol 45:35-43.
Fuchs J, Nilsson C, Kachergus J, Munz M, Larsson EM, Schule B, Langston JW, Middleton FA, Ross OA, Hulihan M, Gasser T, Farrer MJ (2007) Phenotypic variation in a large Swedish pedigree due to SNCA duplication and triplication. Neurology 68:916-922.
Funayama M, Hasegawa K, Kowa H, Saito M, Tsuji S, Obata F (2002) A new locus for Parkinson's disease (PARK8) maps to chromosome 12p11.2-q13.1. Ann Neurol 51:296-301.
Gardet A, Benita Y, Li C, Sands BE, Ballester I, Stevens C, Korzenik JR, Rioux JD, Daly MJ, Xavier RJ, Podolsky DK (2010) LRRK2 is involved in the IFN-gamma response and host response to pathogens. J Immunol 185:5577-5585.
German DC, Manaye KF, Sonsalla PK, Brooks BA (1992) Midbrain dopaminergic cell loss in Parkinson's disease and MPTP-induced parkinsonism: sparing of calbindin-D28k-containing cells. Ann N Y Acad Sci 648:42-62.
Gesi M, Soldani P, Giorgi FS, Santinami A, Bonaccorsi I, Fornai F (2000) The role of the locus coeruleus in the development of Parkinson's disease. Neurosci Biobehav Rev 24:655-668.
Giesert F, Hofmann A, Burger A, Zerle J, Kloos K, Hafen U, Ernst L, Zhang J, Vogt-Weisenhorn DM, Wurst W (2013) Expression analysis of Lrrk1, Lrrk2 and Lrrk2 splice variants in mice. PLoS One 8:e63778.
Gilks WP, Abou-Sleiman PM, Gandhi S, Jain S, Singleton A, Lees AJ, Shaw K, Bhatia KP, Bonifati V, Quinn NP, Lynch J, Healy DG, Holton JL, Revesz T, Wood NW (2005) A common LRRK2 mutation in idiopathic Parkinson's disease. Lancet 365:415-416.
Gillardon F (2009) Leucine-rich repeat kinase 2 phosphorylates brain tubulin-beta isoforms and modulates microtubule stability-a point of convergence in parkinsonian neurodegeneration? J Neurochem 110:1514-1522.
Gillardon F, Schmid R, Draheim H (2012) Parkinson's disease-linked leucine-rich repeat kinase 2(R1441G) mutation increases proinflammatory cytokine release from activated primary microglial cells and resultant neurotoxicity. Neuroscience 208:41-48.
Gilsbach BK, Kortholt A (2014) Structural biology of the LRRK2 GTPase and kinase domains: implications for regulation. Front Mol Neurosci 7:32.
Gilsbach BK, Ho FY, Vetter IR, van Haastert PJ, Wittinghofer A, Kortholt A (2012) Roco kinase structures give insights into the mechanism of Parkinson disease-related leucine-rich-repeat kinase 2 mutations. Proc Natl Acad Sci USA 109:10322-10327.

Goker-Alpan O, Schiffmann R, LaMarca ME, Nussbaum RL, McInerney-Leo A, Sidransky E (2004) Parkinsonism among Gaucher disease carriers. J Med Genet 41:937-940.
Goldman SM, Tanner CM, Oakes D, Bhudhikanok GS, Gupta A, Langston JW (2006) Head injury and Parkinson's disease risk in twins. Ann Neurol 60:65-72.
Gomez-Suaga P, Luzon-Toro B, Churamani D, Zhang L, Bloor-Young D, Patel S, Woodman PG, Churchill GC, Hilfiker S (2012) Leucine-rich repeat kinase 2 regulates autophagy through a calcium-dependent pathway involving NAADP. Hum Mol Genet 21:511-525.
Greggio E, Cookson MR (2009) Leucine-rich repeat kinase 2 mutations and Parkinson's disease: three questions. ASN Neuro 1.
Greggio E, Jain S, Kingsbury A, Bandopadhyay R, Lewis P, Kaganovich A, van der Brug MP, Beilina A, Blackinton J, Thomas KJ, Ahmad R, Miller DW, Kesavapany S, Singleton A, Lees A, Harvey RJ, Harvey K, Cookson MR (2006) Kinase activity is required for the toxic effects of mutant LRRK2/dardarin. Neurobiol Dis 23:329-341.
Gutierrez H, Davies AM (2007) A fast and accurate procedure for deriving the Sholl profile in quantitative studies of neuronal morphology. J Neurosci Methods 163:24-30.
Halliday G, Herrero MT, Murphy K, McCann H, Ros-Bernal F, Barcia C, Mori H, Blesa FJ, Obeso JA (2009) No Lewy pathology in monkeys with over 10 years of severe MPTP Parkinsonism. Mov Disord 24:1519-1523.
Halliday GM, Ophof A, Broe M, Jensen PH, Kettle E, Fedorow H, Cartwright MI, Griffiths FM, Shepherd CE, Double KL (2005) Alpha-synuclein redistributes to neuromelanin lipid in the substantia nigra early in Parkinson's disease. Brain 128:2654-2664.
Han BS, Iacovitti L, Katano T, Hattori N, Seol W, Kim KS (2008) Expression of the LRRK2 gene in the midbrain dopaminergic neurons of the substantia nigra. Neurosci Lett 442:190-194.
Haugarvoll K, Wszolek ZK (2006) PARK8 LRRK2 parkinsonism. Curr Neurol Neurosci Rep 6:287-294.
Haugarvoll K, Wszolek ZK (2009) Clinical features of LRRK2 parkinsonism. Parkinsonism Relat Disord 15 Suppl 3:S205-208.
Haugarvoll K, Rademakers R, Kachergus JM, Nuytemans K, Ross OA, Gibson JM, Tan EK, Gaig C, Tolosa E, Goldwurm S, Guidi M, Riboldazzi G, Brown L, Walter U, Benecke R, Berg D, Gasser T, Theuns J, Pals P, Cras P, De Deyn PP, Engelborghs S, Pickut B, Uitti RJ, Foroud T, Nichols WC, Hagenah J, Klein C, Samii A, Zabetian CP, Bonifati V, Van Broeckhoven C, Farrer MJ, Wszolek ZK (2008) Lrrk2 R1441C parkinsonism is clinically similar to sporadic Parkinson disease. Neurology 70:1456-1460.
Healy DG, Falchi M, O'Sullivan SS, Bonifati V, Durr A, Bressman S, Brice A, Aasly J, Zabetian CP, Goldwurm S, Ferreira JJ, Tolosa E, Kay DM, Klein C, Williams DR, Marras C, Lang AE, Wszolek ZK, Berciano J, Schapira AH, Lynch T, Bhatia KP, Gasser T, Lees AJ, Wood NW, International LC (2008) Phenotype, genotype, and worldwide genetic penetrance of LRRK2-associated Parkinson's disease: a case-control study. Lancet Neurol 7:583-590.
Heintz N (2001) BAC to the future: the use of bac transgenic mice for neuroscience research. Nat Rev Neurosci 2:861-870.
Hernan MA, Takkouche B, Caamano-Isorna F, Gestal-Otero JJ (2002) A meta-analysis of coffee drinking, cigarette smoking, and the risk of Parkinson's disease. Ann Neurol 52:276-284.

Herzig MC, Bidinosti M, Schweizer T, Hafner T, Stemmelen C, Weiss A, Danner S, Vidotto N, Stauffer D, Barske C, Mayer F, Schmid P, Rovelli G, van der Putten PH, Shimshek DR (2012) High LRRK2 levels fail to induce or exacerbate neuronal alpha-synucleinopathy in mouse brain. PLoS One 7:e36581.

Herzig MC, Kolly C, Persohn E, Theil D, Schweizer T, Hafner T, Stemmelen C, Troxler TJ, Schmid P, Danner S, Schnell CR, Mueller M, Kinzel B, Grevot A, Bolognani F, Stirn M, Kuhn RR, Kaupmann K, van der Putten PH, Rovelli G, Shimshek DR (2011) LRRK2 protein levels are determined by kinase function and are crucial for kidney and lung homeostasis in mice. Hum Mol Genet 20:4209-4223.

Hinkle KM, Yue M, Behrouz B, Dachsel JC, Lincoln SJ, Bowles EE, Beevers JE, Dugger B, Winner B, Prots I, Kent CB, Nishioka K, Lin WL, Dickson DW, Janus CJ, Farrer MJ, Melrose HL (2012) LRRK2 knockout mice have an intact dopaminergic system but display alterations in exploratory and motor co-ordination behaviors. Mol Neurodegener 7:25.

Hoglinger GU, Feger J, Prigent A, Michel PP, Parain K, Champy P, Ruberg M, Oertel WH, Hirsch EC (2003) Chronic systemic complex I inhibition induces a hypokinetic multisystem degeneration in rats. J Neurochem 84:491-502.

Hughes AJ, Daniel SE, Blankson S, Lees AJ (1993) A clinicopathologic study of 100 cases of Parkinson's disease. Arch Neurol 50:140-148.

Hurtig HI, Trojanowski JQ, Galvin J, Ewbank D, Schmidt ML, Lee VM, Clark CM, Glosser G, Stern MB, Gollomp SM, Arnold SE (2000) Alpha-synuclein cortical Lewy bodies correlate with dementia in Parkinson's disease. Neurology 54:1916-1921.

Ishihara L, Warren L, Gibson R, Amouri R, Lesage S, Durr A, Tazir M, Wszolek ZK, Uitti RJ, Nichols WC, Griffith A, Hattori N, Leppert D, Watts R, Zabetian CP, Foroud TM, Farrer MJ, Brice A, Middleton L, Hentati F (2006) Clinical features of Parkinson disease patients with homozygous leucine-rich repeat kinase 2 G2019S mutations. Arch Neurol 63:1250-1254.

Ishihara L, Gibson RA, Warren L, Amouri R, Lyons K, Wielinski C, Hunter C, Swartz JE, Elango R, Akkari PA, Leppert D, Surh L, Reeves KH, Thomas S, Ragone L, Hattori N, Pahwa R, Jankovic J, Nance M, Freeman A, Gouider-Khouja N, Kefi M, Zouari M, Ben Sassi S, Ben Yahmed S, El Euch-Fayeche G, Middleton L, Burn DJ, Watts RL, Hentati F (2007) Screening for Lrrk2 G2019S and clinical comparison of Tunisian and North American Caucasian Parkinson's disease families. Mov Disord 22:55-61.

Ito G, Fujimoto T, Kamikawaji S, Kuwahara T, Iwatsubo T (2014) Lack of correlation between the kinase activity of LRRK2 harboring kinase-modifying mutations and its phosphorylation at Ser910, 935, and Ser955. PLoS One 9:e97988.

Janezic S, Threlfell S, Dodson PD, Dowie MJ, Taylor TN, Potgieter D, Parkkinen L, Senior SL, Anwar S, Ryan B, Deltheil T, Kosillo P, Cioroch M, Wagner K, Ansorge O, Bannerman DM, Bolam JP, Magill PJ, Cragg SJ, Wade-Martins R (2013) Deficits in dopaminergic transmission precede neuron loss and dysfunction in a new Parkinson model. Proc Natl Acad Sci USA 110:E4016-4025.

Jankovic J (2008) Parkinson's disease: clinical features and diagnosis. J Neurol Neurosurg Psychiatry 79:368-376.

Jeon BS, Jackson-Lewis V, Burke RE (1995) 6-Hydroxydopamine lesion of the rat substantia nigra: time course and morphology of cell death. Neurodegeneration 4:131-137.

Jorgensen ND, Peng Y, Ho CC, Rideout HJ, Petrey D, Liu P, Dauer WT (2009) The WD40

domain is required for LRRK2 neurotoxicity. PLoS One 4:e8463.
Kalia LV, Kalia SK, McLean PJ, Lozano AM, Lang AE (2013) Alpha-synuclein oligomers and clinical implications for Parkinson disease. Ann Neurol 73:155-169.
Kawakami F, Yabata T, Ohta E, Maekawa T, Shimada N, Suzuki M, Maruyama H, Ichikawa T, Obata F (2012) LRRK2 phosphorylates tubulin-associated tau but not the free molecule: LRRK2-mediated regulation of the tau-tubulin association and neurite outgrowth. PLoS One 7:e30834.
Kett LR, Boassa D, Ho CC, Rideout HJ, Hu J, Terada M, Ellisman M, Dauer WT (2012) LRRK2 Parkinson disease mutations enhance its microtubule association. Hum Mol Genet 21:890-899.
Kieburtz K, Wunderle KB (2013) Parkinson's disease: evidence for environmental risk factors. Mov Disord 28:8-13.
Kitada T, Asakawa S, Hattori N, Matsumine H, Yamamura Y, Minoshima S, Yokochi M, Mizuno Y, Shimizu N (1998) Mutations in the parkin gene cause autosomal recessive juvenile parkinsonism. Nature 392:605-608.
Klein C, Westenberger A (2012) Genetics of Parkinson's disease. Cold Spring Harb Perspect Med 2:a008888.
Klionsky DJ, Elazar Z, Seglen PO, Rubinsztein DC (2008) Does bafilomycin A1 block the fusion of autophagosomes with lysosomes? Autophagy 4:849-850.
Kowal SL, Dall TM, Chakrabarti R, Storm MV, Jain A (2013) The current and projected economic burden of Parkinson's disease in the United States. Mov Disord 28:311-318.
Kruger R, Kuhn W, Muller T, Woitalla D, Graeber M, Kosel S, Przuntek H, Epplen JT, Schols L, Riess O (1998) Ala30Pro mutation in the gene encoding alpha-synuclein in Parkinson's disease. Nat Genet 18:106-108.
Kumari U, Tan EK (2009) LRRK2 in Parkinson's disease: genetic and clinical studies from patients. FEBS J 276:6455-6463.
Kuwahara T, Koyama A, Gengyo-Ando K, Masuda M, Kowa H, Tsunoda M, Mitani S, Iwatsubo T (2006) Familial Parkinson mutant alpha-synuclein causes dopamine neuron dysfunction in transgenic Caenorhabditis elegans. J Biol Chem 281:334-340.
Lakso M, Vartiainen S, Moilanen AM, Sirvio J, Thomas JH, Nass R, Blakely RD, Wong G (2003) Dopaminergic neuronal loss and motor deficits in Caenorhabditis elegans overexpressing human alpha-synuclein. J Neurochem 86:165-172.
Lam HA, Wu N, Cely I, Kelly RL, Hean S, Richter F, Magen I, Cepeda C, Ackerson LC, Walwyn W, Masliah E, Chesselet MF, Levine MS, Maidment NT (2011) Elevated tonic extracellular dopamine concentration and altered dopamine modulation of synaptic activity precede dopamine loss in the striatum of mice overexpressing human alpha-synuclein. J Neurosci Res 89:1091-1102.
Langston JW, Ballard P, Tetrud JW, Irwin I (1983) Chronic Parkinsonism in humans due to a product of meperidine-analog synthesis. Science 219:979-980.
Langston JW, Forno LS, Tetrud J, Reeves AG, Kaplan JA, Karluk D (1999) Evidence of active nerve cell degeneration in the substantia nigra of humans years after 1-methyl-4-phenyl-1,2,3,6-tetrahydropyridine exposure. Ann Neurol 46:598-605.
Lee CS, Sauer H, Bjorklund A (1996) Dopaminergic neuronal degeneration and motor impairments following axon terminal lesion by instrastriatal 6-hydroxydopamine in the rat. Neuroscience 72:641-653.

Lee JW, Tapias V, Di Maio R, Greenamyre JT, Cannon JR (2014) Behavioral, neurochemical, and pathologic alterations in bacterial artificial chromosome transgenic G2019S leucine-rich repeated kinase 2 rats. Neurobiol Aging.

Lee BD, Shin JH, VanKampen J, Petrucelli L, West AB, Ko HS, Lee YI, Maguire-Zeiss KA, Bowers WJ, Federoff HJ, Dawson VL, Dawson TM (2010) Inhibitors of leucine-rich repeat kinase-2 protect against models of Parkinson's disease. Nat Med 16:998-1000.

Leroy E, Boyer R, Auburger G, Leube B, Ulm G, Mezey E, Harta G, Brownstein MJ, Jonnalagada S, Chernova T, Dehejia A, Lavedan C, Gasser T, Steinbach PJ, Wilkinson KD, Polymeropoulos MH (1998) The ubiquitin pathway in Parkinson's disease. Nature 395:451-452.

Li X, Wang QJ, Pan N, Lee S, Zhao Y, Chait BT, Yue Z (2011) Phosphorylation-dependent 14-3-3 binding to LRRK2 is impaired by common mutations of familial Parkinson's disease. PLoS One 6:e17153.

Li X, Patel JC, Wang J, Avshalumov MV, Nicholson C, Buxbaum JD, Elder GA, Rice ME, Yue Z (2010) Enhanced striatal dopamine transmission and motor performance with LRRK2 overexpression in mice is eliminated by familial Parkinson's disease mutation G2019S. J Neurosci 30:1788-1797.

Li Y, Liu W, Oo TF, Wang L, Tang Y, Jackson-Lewis V, Zhou C, Geghman K, Bogdanov M, Przedborski S, Beal MF, Burke RE, Li C (2009) Mutant LRRK2(R1441G) BAC transgenic mice recapitulate cardinal features of Parkinson's disease. Nat Neurosci 12:826-828.

Lin X, Parisiadou L, Gu XL, Wang L, Shim H, Sun L, Xie C, Long CX, Yang WJ, Ding J, Chen ZZ, Gallant PE, Tao-Cheng JH, Rudow G, Troncoso JC, Liu Z, Li Z, Cai H (2009) Leucine-rich repeat kinase 2 regulates the progression of neuropathology induced by Parkinson's-disease-related mutant alpha-synuclein. Neuron 64:807-827.

Longo F, Russo I, Shimshek DR, Greggio E, Morari M (2014) Genetic and pharmacological evidence that G2019S LRRK2 confers a hyperkinetic phenotype, resistant to motor decline associated with aging. Neurobiol Dis.

MacLeod D, Dowman J, Hammond R, Leete T, Inoue K, Abeliovich A (2006) The familial Parkinsonism gene LRRK2 regulates neurite process morphology. Neuron 52:587-593.

Maekawa T, Kubo M, Yokoyama I, Ohta E, Obata F (2010) Age-dependent and cell-population-restricted LRRK2 expression in normal mouse spleen. Biochem Biophys Res Commun 392:431-435.

Maekawa T, Mori S, Sasaki Y, Miyajima T, Azuma S, Ohta E, Obata F (2012) The I2020T Leucine-rich repeat kinase 2 transgenic mouse exhibits impaired locomotive ability accompanied by dopaminergic neuron abnormalities. Mol Neurodegener 7:15.

Magerkurth C, Schnitzer R, Braune S (2005) Symptoms of autonomic failure in Parkinson's disease: prevalence and impact on daily life. Clin Auton Res 15:76-82.

Manzoni C, Mamais A, Dihanich S, Abeti R, Soutar MP, Plun-Favreau H, Giunti P, Tooze SA, Bandopadhyay R, Lewis PA (2013) Inhibition of LRRK2 kinase activity stimulates macroautophagy. Biochim Biophys Acta 1833:2900-2910.

Marras C, Goldman S, Smith A, Barney P, Aston D, Comyns K, Korell M, Langston JW, Ross GW, Tanner CM (2005) Smell identification ability in twin pairs discordant for Parkinson's disease. Mov Disord 20:687-693.

McLelland GL, Soubannier V, Chen CX, McBride HM, Fon EA (2014) Parkin and PINK1

function in a vesicular trafficking pathway regulating mitochondrial quality control. EMBO J 33:282-295.
Melrose HL, Dachsel JC, Behrouz B, Lincoln SJ, Yue M, Hinkle KM, Kent CB, Korvatska E, Taylor JP, Witten L, Liang YQ, Beevers JE, Boules M, Dugger BN, Serna VA, Gaukhman A, Yu X, Castanedes-Casey M, Braithwaite AT, Ogholikhan S, Yu N, Bass D, Tyndall G, Schellenberg GD, Dickson DW, Janus C, Farrer MJ (2010) Impaired dopaminergic neurotransmission and microtubule-associated protein tau alterations in human LRRK2 transgenic mice. Neurobiol Dis 40:503-517.
Migheli R, Del Giudice MG, Spissu Y, Sanna G, Xiong Y, Dawson TM, Dawson VL, Galioto M, Rocchitta G, Biosa A, Serra PA, Carri MT, Crosio C, Iaccarino C (2013) LRRK2 affects vesicle trafficking, neurotransmitter extracellular level and membrane receptor localization. PLoS One 8:e77198.
Miklossy J, Arai T, Guo JP, Klegeris A, Yu S, McGeer EG, McGeer PL (2006) LRRK2 expression in normal and pathologic human brain and in human cell lines. J Neuropathol Exp Neurol 65:953-963.
Mizushima N, Yoshimori T (2007) How to interpret LC3 immunoblotting. Autophagy 3:542-545.
Moehle MS, Webber PJ, Tse T, Sukar N, Standaert DG, DeSilva TM, Cowell RM, West AB (2012) LRRK2 inhibition attenuates microglial inflammatory responses. J Neurosci 32:1602-1611.
Montgomery EB, Jr., Baker KB, Lyons K, Koller WC (1999) Abnormal performance on the PD test battery by asymptomatic first-degree relatives. Neurology 52:757-762.
Morris HR, Wood NW, Lees AJ (1999) Progressive supranuclear palsy (Steele-Richardson-Olszewski disease). Postgrad Med J 75:579-584.
Muller RU, Kubie JL (1989) The firing of hippocampal place cells predicts the future position of freely moving rats. J Neurosci 9:4101-4110.
Muller B, Assmus J, Herlofson K, Larsen JP, Tysnes OB (2013) Importance of motor vs. non-motor symptoms for health-related quality of life in early Parkinson's disease. Parkinsonism Relat Disord 19:1027-1032.
Mutez E, Larvor L, Lepretre F, Mouroux V, Hamalek D, Kerckaert JP, Perez-Tur J, Waucquier N, Vanbesien-Mailliot C, Duflot A, Devos D, Defebvre L, Kreisler A, Frigard B, Destee A, Chartier-Harlin MC (2011) Transcriptional profile of Parkinson blood mononuclear cells with LRRK2 mutation. Neurobiol Aging 32:1839-1848.
Nalls MA, Pankratz N, Lill CM, Do CB, Hernandez DG, Saad M, DeStefano AL, Kara E, Bras J, Sharma M, Schulte C, Keller MF, Arepalli S, Letson C, Edsall C, Stefansson H, Liu X, Pliner H, Lee JH, Cheng R, International Parkinson's Disease Genomics C, Parkinson's Study Group Parkinson's Research: The Organized GI, andMe, GenePd, NeuroGenetics Research C, Hussman Institute of Human G, Ashkenazi Jewish Dataset I, Cohorts for H, Aging Research in Genetic E, North American Brain Expression C, United Kingdom Brain Expression C, Greek Parkinson's Disease C, Alzheimer Genetic Analysis G, Ikram MA, Ioannidis JP, Hadjigeorgiou GM, Bis JC, Martinez M, Perlmutter JS, Goate A, Marder K, Fiske B, Sutherland M, Xiromerisiou G, Myers RH, Clark LN, Stefansson K, Hardy JA, Heutink P, Chen H, Wood NW, Houlden H, Payami H, Brice A, Scott WK, Gasser T, Bertram L, Eriksson N, Foroud T, Singleton AB (2014) Large-scale meta-analysis of genome-wide association data identifies six new risk loci for Parkinson's disease. Nat Genet 46:989-993.

Ness D, Ren Z, Gardai S, Sharpnack D, Johnson VJ, Brennan RJ, Brigham EF, Olaharski AJ (2013) Leucine-rich repeat kinase 2 (LRRK2)-deficient rats exhibit renal tubule injury and perturbations in metabolic and immunological homeostasis. PLoS One 8:e66164.
Neumann J, Bras J, Deas E, O'Sullivan SS, Parkkinen L, Lachmann RH, Li A, Holton J, Guerreiro R, Paudel R, Segarane B, Singleton A, Lees A, Hardy J, Houlden H, Revesz T, Wood NW (2009) Glucocerebrosidase mutations in clinical and pathologically proven Parkinson's disease. Brain 132:1783-1794.
Nichols RJ, Dzamko N, Morrice NA, Campbell DG, Deak M, Ordureau A, Macartney T, Tong Y, Shen J, Prescott AR, Alessi DR (2010) 14-3-3 binding to LRRK2 is disrupted by multiple Parkinson's disease-associated mutations and regulates cytoplasmic localization. Biochem J 430:393-404.
Nichols WC, Pankratz N, Hernandez D, Paisan-Ruiz C, Jain S, Halter CA, Michaels VE, Reed T, Rudolph A, Shults CW, Singleton A, Foroud T, Parkinson Study Group Pi (2005) Genetic screening for a single common LRRK2 mutation in familial Parkinson's disease. Lancet 365:410-412.
Nicklas WJ, Vyas I, Heikkila RE (1985) Inhibition of NADH-linked oxidation in brain mitochondria by 1-methyl-4-phenyl-pyridine, a metabolite of the neurotoxin, 1-methyl-4-phenyl-1,2,5,6-tetrahydropyridine. Life Sci 36:2503-2508.
Nikonova EV, Xiong Y, Tanis KQ, Dawson VL, Vogel RL, Finney EM, Stone DJ, Reynolds IJ, Kern JT, Dawson TM (2012) Transcriptional responses to loss or gain of function of the leucine-rich repeat kinase 2 (LRRK2) gene uncover biological processes modulated by LRRK2 activity. Hum Mol Genet 21:163-174.
Olanow CW, Brundin P (2013) Parkinson's disease and alpha synuclein: is Parkinson's disease a prion-like disorder? Mov Disord 28:31-40.
Olson IR, Moore KS, Stark M, Chatterjee A (2006) Visual working memory is impaired when the medial temporal lobe is damaged. J Cogn Neurosci 18:1087-1097.
Orenstein SJ, Kuo SH, Tasset I, Arias E, Koga H, Fernandez-Carasa I, Cortes E, Honig LS, Dauer W, Consiglio A, Raya A, Sulzer D, Cuervo AM (2013) Interplay of LRRK2 with chaperone-mediated autophagy. Nat Neurosci 16:394-406.
Ozelius LJ, Senthil G, Saunders-Pullman R, Ohmann E, Deligtisch A, Tagliati M, Hunt AL, Klein C, Henick B, Hailpern SM, Lipton RB, Soto-Valencia J, Risch N, Bressman SB (2006) LRRK2 G2019S as a cause of Parkinson's disease in Ashkenazi Jews. N Engl J Med 354:424-425.
Paisan-Ruiz C, Bhatia KP, Li A, Hernandez D, Davis M, Wood NW, Hardy J, Houlden H, Singleton A, Schneider SA (2009) Characterization of PLA2G6 as a locus for dystonia-parkinsonism. Ann Neurol 65:19-23.
Parisiadou L, Xie C, Cho HJ, Lin X, Gu XL, Long CX, Lobbestael E, Baekelandt V, Taymans JM, Sun L, Cai H (2009) Phosphorylation of ezrin/radixin/moesin proteins by LRRK2 promotes the rearrangement of actin cytoskeleton in neuronal morphogenesis. J Neurosci 29:13971-13980.
Park A, Stacy M (2009) Non-motor symptoms in Parkinson's disease. J Neurol 256 Suppl 3:293-298.
Parkinson J (2002) An essay on the shaking palsy. 1817. J Neuropsychiatry Clin Neurosci 14:223-236.
Piccoli G, Condliffe SB, Bauer M, Giesert F, Boldt K, De Astis S, Meixner A, Sarioglu H, Vogt-Weisenhorn DM, Wurst W, Gloeckner CJ, Matteoli M, Sala C, Ueffing M (2011) LRRK2

controls synaptic vesicle storage and mobilization within the recycling pool. J Neurosci 31:2225-2237.
Piccoli G, Onofri F, Cirnaru MD, Kaiser CJ, Jagtap P, Kastenmuller A, Pischedda F, Marte A, von Zweydorf F, Vogt A, Giesert F, Pan L, Antonucci F, Kiel C, Zhang M, Weinkauf S, Sattler M, Sala C, Matteoli M, Ueffing M, Gloeckner CJ (2014) Leucine-Rich Repeat Kinase 2 Binds to Neuronal Vesicles through Protein Interactions Mediated by Its C-Terminal WD40 Domain. Mol Cell Biol 34:2147-2161.
Plowey ED, Cherra SJ, 3rd, Liu YJ, Chu CT (2008) Role of autophagy in G2019S-LRRK2-associated neurite shortening in differentiated SH-SY5Y cells. J Neurochem 105:1048-1056.
Polymeropoulos MH, Lavedan C, Leroy E, Ide SE, Dehejia A, Dutra A, Pike B, Root H, Rubenstein J, Boyer R, Stenroos ES, Chandrasekharappa S, Athanassiadou A, Papapetropoulos T, Johnson WG, Lazzarini AM, Duvoisin RC, Di Iorio G, Golbe LI, Nussbaum RL (1997) Mutation in the alpha-synuclein gene identified in families with Parkinson's disease. Science 276:2045-2047.
Potgieter D (2013) Using fast-scan cyclic voltammetry to investigate monoamine release in BAC transgenic rodent models of Parkinson’s Disease. DPhil Thesis: University of Oxford.
Prejean JD, Peckham JC, Casey AE, Griswold DP, Weisburger EK, Weisburger JH (1973) Spontaneous tumors in Sprague-Dawley rats and Swiss mice. Cancer Res 33:2768-2773.
Ramirez A, Heimbach A, Grundemann J, Stiller B, Hampshire D, Cid LP, Goebel I, Mubaidin AF, Wriekat AL, Roeper J, Al-Din A, Hillmer AM, Karsak M, Liss B, Woods CG, Behrens MI, Kubisch C (2006) Hereditary parkinsonism with dementia is caused by mutations in ATP13A2, encoding a lysosomal type 5 P-type ATPase. Nat Genet 38:1184-1191.
Ramonet D, Daher JP, Lin BM, Stafa K, Kim J, Banerjee R, Westerlund M, Pletnikova O, Glauser L, Yang L, Liu Y, Swing DA, Beal MF, Troncoso JC, McCaffery JM, Jenkins NA, Copeland NG, Galter D, Thomas B, Lee MK, Dawson TM, Dawson VL, Moore DJ (2011) Dopaminergic neuronal loss, reduced neurite complexity and autophagic abnormalities in transgenic mice expressing G2019S mutant LRRK2. PLoS One 6:e18568.
Reetz K, Tadic V, Kasten M, Bruggemann N, Schmidt A, Hagenah J, Pramstaller PP, Ramirez A, Behrens MI, Siebner HR, Klein C, Binkofski F (2010) Structural imaging in the presymptomatic stage of genetically determined parkinsonism. Neurobiol Dis 39:402-408.
Rice ME, Cragg SJ (2004) Nicotine amplifies reward-related dopamine signals in striatum. Nat Neurosci 7:583-584.
Ristevski S (2005) Making better transgenic models: conditional, temporal, and spatial approaches. Mol Biotechnol 29:153-163.
Ross OA, Wu YR, Lee MC, Funayama M, Chen ML, Soto AI, Mata IF, Lee-Chen GJ, Chen CM, Tang M, Zhao Y, Hattori N, Farrer MJ, Tan EK, Wu RM (2008) Analysis of Lrrk2 R1628P as a risk factor for Parkinson's disease. Ann Neurol 64:88-92.
Rudenko IN, Cookson MR (2010) 14-3-3 proteins are promising LRRK2 interactors. Biochem J 430:e5-6.
Saha S, Guillily MD, Ferree A, Lanceta J, Chan D, Ghosh J, Hsu CH, Segal L, Raghavan K, Matsumoto K, Hisamoto N, Kuwahara T, Iwatsubo T, Moore L, Goldstein L, Cookson

M, Wolozin B (2009) LRRK2 modulates vulnerability to mitochondrial dysfunction in Caenorhabditis elegans. J Neurosci 29:9210-9218.
Samii A, Nutt JG, Ransom BR (2004) Parkinson's disease. Lancet 363:1783-1793.
Sanchez G, Varaschin RK, Bueler H, Marcogliese PC, Park DS, Trudeau LE (2014) Unaltered striatal dopamine release levels in young Parkin knockout, Pink1 knockout, DJ-1 knockout and LRRK2 R1441G transgenic mice. PLoS One 9:e94826.
Scaglione C, Vignatelli L, Plazzi G, Marchese R, Negrotti A, Rizzo G, Lopane G, Bassein L, Maestri M, Bernardini S, Martinelli P, Abbruzzese G, Calzetti S, Bonuccelli U, Provini F, Coccagna G, Bologna GP (2005) REM sleep behaviour disorder in Parkinson's disease: a questionnaire-based study. Neurol Sci 25:316-321.
Schuurman AG, van den Akker M, Ensinck KT, Metsemakers JF, Knottnerus JA, Leentjens AF, Buntinx F (2002) Increased risk of Parkinson's disease after depression: a retrospective cohort study. Neurology 58:1501-1504.
Sepulveda B, Mesias R, Li X, Yue Z, Benson DL (2013) Short- and long-term effects of LRRK2 on axon and dendrite growth. PLoS One 8:e61986.
Sharma S, Bandopadhyay R, Lashley T, Renton AE, Kingsbury AE, Kumaran R, Kallis C, Vilarino-Guell C, O'Sullivan SS, Lees AJ, Revesz T, Wood NW, Holton JL (2011) LRRK2 expression in idiopathic and G2019S positive Parkinson's disease subjects: a morphological and quantitative study. Neuropathol Appl Neurobiol 37:777-790.
Sheng Z, Zhang S, Bustos D, Kleinheinz T, Le Pichon CE, Dominguez SL, Solanoy HO, Drummond J, Zhang X, Ding X, Cai F, Song Q, Li X, Yue Z, van der Brug MP, Burdick DJ, Gunzner-Toste J, Chen H, Liu X, Estrada AA, Sweeney ZK, Scearce-Levie K, Moffat JG, Kirkpatrick DS, Zhu H (2012) Ser1292 autophosphorylation is an indicator of LRRK2 kinase activity and contributes to the cellular effects of PD mutations. Sci Transl Med 4:164-161.
Shin N, Jeong H, Kwon J, Heo HY, Kwon JJ, Yun HJ, Kim CH, Han BS, Tong Y, Shen J, Hatano T, Hattori N, Kim KS, Chang S, Seol W (2008) LRRK2 regulates synaptic vesicle endocytosis. Exp Cell Res 314:2055-2065.
Shojaee S, Sina F, Banihosseini SS, Kazemi MH, Kalhor R, Shahidi GA, Fakhrai-Rad H, Ronaghi M, Elahi E (2008) Genome-wide linkage analysis of a Parkinsonian-pyramidal syndrome pedigree by 500 K SNP arrays. Am J Hum Genet 82:1375-1384.
Simon-Sanchez J, Schulte C, Bras JM, Sharma M, Gibbs JR, Berg D, Paisan-Ruiz C, Lichtner P, Scholz SW, Hernandez DG, Kruger R, Federoff M, Klein C, Goate A, Perlmutter J, Bonin M, Nalls MA, Illig T, Gieger C, Houlden H, Steffens M, Okun MS, Racette BA, Cookson MR, Foote KD, Fernandez HH, Traynor BJ, Schreiber S, Arepalli S, Zonozi R, Gwinn K, van der Brug M, Lopez G, Chanock SJ, Schatzkin A, Park Y, Hollenbeck A, Gao J, Huang X, Wood NW, Lorenz D, Deuschl G, Chen H, Riess O, Hardy JA, Singleton AB, Gasser T (2009) Genome-wide association study reveals genetic risk underlying Parkinson's disease. Nat Genet 41:1308-1312.
Singleton AB, Farrer M, Johnson J, Singleton A, Hague S, Kachergus J, Hulihan M, Peuralinna T, Dutra A, Nussbaum R, Lincoln S, Crawley A, Hanson M, Maraganore D, Adler C, Cookson MR, Muenter M, Baptista M, Miller D, Blancato J, Hardy J, Gwinn-Hardy K (2003) Alpha-synuclein locus triplication causes Parkinson's disease. Science 302:841.
Spillantini MG, Schmidt ML, Lee VM, Trojanowski JQ, Jakes R, Goedert M (1997) Alpha-synuclein in Lewy bodies. Nature 388:839-840.
Sulzer D, Surmeier DJ (2013) Neuronal vulnerability, pathogenesis, and Parkinson's disease.

Mov Disord 28:715-724.
Surmeier DJ, Guzman JN, Sanchez-Padilla J (2010) Calcium, cellular aging, and selective neuronal vulnerability in Parkinson's disease. Cell Calcium 47:175-182.
Szabadkai G, Rizzuto R (2004) Participation of endoplasmic reticulum and mitochondrial calcium handling in apoptosis: more than just neighborhood? FEBS Lett 567:111-115.
Takemura R, Okabe S, Umeyama T, Kanai Y, Cowan NJ, Hirokawa N (1992) Increased microtubule stability and alpha tubulin acetylation in cells transfected with microtubule-associated proteins MAP1B, MAP2 or tau. J Cell Sci 103 (Pt 4):953-964.
Tan EK, Zhao Y, Skipper L, Tan MG, Di Fonzo A, Sun L, Fook-Chong S, Tang S, Chua E, Yuen Y, Tan L, Pavanni R, Wong MC, Kolatkar P, Lu CS, Bonifati V, Liu JJ (2007) The LRRK2 Gly2385Arg variant is associated with Parkinson's disease: genetic and functional evidence. Hum Genet 120:857-863.
Tandberg E, Larsen JP, Karlsen K (1998) A community-based study of sleep disorders in patients with Parkinson's disease. Mov Disord 13:895-899.
Tanner CM, Kamel F, Ross GW, Hoppin JA, Goldman SM, Korell M, Marras C, Bhudhikanok GS, Kasten M, Chade AR, Comyns K, Richards MB, Meng C, Priestley B, Fernandez HH, Cambi F, Umbach DM, Blair A, Sandler DP, Langston JW (2011) Rotenone, paraquat, and Parkinson's disease. Environ Health Perspect 119:866-872.
Taylor KS, Cook JA, Counsell CE (2007) Heterogeneity in male to female risk for Parkinson's disease. J Neurol Neurosurg Psychiatry 78:905-906.
Taymans JM (2012) The GTPase function of LRRK2. Biochem Soc Trans 40:1063-1069.
Taymans JM, Van den Haute C, Baekelandt V (2006) Distribution of PINK1 and LRRK2 in rat and mouse brain. J Neurochem 98:951-961.
Tong Y, Pisani A, Martella G, Karouani M, Yamaguchi H, Pothos EN, Shen J (2009) R1441C mutation in LRRK2 impairs dopaminergic neurotransmission in mice. Proc Natl Acad Sci USA 106:14622-14627.
Tong Y, Yamaguchi H, Giaime E, Boyle S, Kopan R, Kelleher RJ, 3rd, Shen J (2010) Loss of leucine-rich repeat kinase 2 causes impairment of protein degradation pathways, accumulation of alpha-synuclein, and apoptotic cell death in aged mice. Proc Natl Acad Sci USA 107:9879-9884.
Tong Y, Giaime E, Yamaguchi H, Ichimura T, Liu Y, Si H, Cai H, Bonventre JV, Shen J (2012) Loss of leucine-rich repeat kinase 2 causes age-dependent bi-phasic alterations of the autophagy pathway. Mol Neurodegener 7:2.
Trabzuni D, Ryten M, Emmett W, Ramasamy A, Lackner KJ, Zeller T, Walker R, Smith C, Lewis PA, Mamais A, de Silva R, Vandrovcova J, International Parkinson Disease Genomics C, Hernandez D, Nalls MA, Sharma M, Garnier S, Lesage S, Simon-Sanchez J, Gasser T, Heutink P, Brice A, Singleton A, Cai H, Schadt E, Wood NW, Bandopadhyay R, Weale ME, Hardy J, Plagnol V (2013) Fine-mapping, gene expression and splicing analysis of the disease associated LRRK2 locus. PLoS One 8:e70724.
Trinh J, Farrer M (2013) Advances in the genetics of Parkinson disease. Nat Rev Neurol 9:445-454.
Tsika E, Kannan M, Foo CS, Dikeman D, Glauser L, Gellhaar S, Galter D, Knott GW, Dawson TM, Dawson VL, Moore DJ (2014) Conditional Expression of Parkinson's Disease-Related R1441C LRRK2 in Midbrain Dopaminergic Neurons of Mice Causes Nuclear Abnormalities without Neurodegeneration. Neurobiol Dis.
Valente EM, Abou-Sleiman PM, Caputo V, Muqit MM, Harvey K, Gispert S, Ali Z, Del Turco D,

Bentivoglio AR, Healy DG, Albanese A, Nussbaum R, Gonzalez-Maldonado R, Deller T, Salvi S, Cortelli P, Gilks WP, Latchman DS, Harvey RJ, Dallapiccola B, Auburger G, Wood NW (2004) Hereditary early-onset Parkinson's disease caused by mutations in PINK1. Science 304:1158-1160.

von Campenhausen S, Bornschein B, Wick R, Botzel K, Sampaio C, Poewe W, Oertel W, Siebert U, Berger K, Dodel R (2005) Prevalence and incidence of Parkinson's disease in Europe. Eur Neuropsychopharmacol 15:473-490.

Vytal KE, Cornwell BR, Letkiewicz AM, Arkin NE, Grillon C (2013) The complex interaction between anxiety and cognition: insight from spatial and verbal working memory. Front Hum Neurosci 7:93.

Walitza S, Melfsen S, Herhaus G, Scheuerpflug P, Warnke A, Muller T, Lange KW, Gerlach M (2007) Association of Parkinson's disease with symptoms of attention deficit hyperactivity disorder in childhood. J Neural Transm Suppl:311-315.

Walker MD, Volta M, Cataldi S, Dinelle K, Beccano-Kelly D, Munsie L, Kornelsen R, Mah C, Chou P, Co K, Khinda J, Mroczek M, Bergeron S, Yu K, Cao LP, Funk N, Ott T, Galter D, Riess O, Biskup S, Milnerwood AJ, Stoessl AJ, Farrer MJ, Sossi V (2014) Behavioral Deficits and Striatal DA Signaling in LRRK2 p.G2019S Transgenic Rats: A Multimodal Investigation Including PET Neuroimaging. J Parkinsons Dis.

Webb JL, Ravikumar B, Atkins J, Skepper JN, Rubinsztein DC (2003) Alpha-synuclein is degraded by both autophagy and the proteasome. J Biol Chem 278:25009-25013.

West AB, Moore DJ, Biskup S, Bugayenko A, Smith WW, Ross CA, Dawson VL, Dawson TM (2005) Parkinson's disease-associated mutations in leucine-rich repeat kinase 2 augment kinase activity. Proc Natl Acad Sci USA 102:16842-16847.

West AB, Cowell RM, Daher JP, Moehle MS, Hinkle KM, Melrose HL, Standaert DG, Volpicelli-Daley LA (2014) Differential LRRK2 expression in the cortex, striatum, and substantia nigra in transgenic and nontransgenic rodents. J Comp Neurol 522:2465-2480.

Westerlund M, Belin AC, Anvret A, Bickford P, Olson L, Galter D (2008) Developmental regulation of leucine-rich repeat kinase 1 and 2 expression in the brain and other rodent and human organs: Implications for Parkinson's disease. Neuroscience 152:429-436.

Winner B, Melrose HL, Zhao C, Hinkle KM, Yue M, Kent C, Braithwaite AT, Ogholikhan S, Aigner R, Winkler J, Farrer MJ, Gage FH (2011) Adult neurogenesis and neurite outgrowth are impaired in LRRK2 G2019S mice. Neurobiol Dis 41:706-716.

Wirdefeldt K, Gatz M, Reynolds CA, Prescott CA, Pedersen NL (2011) Heritability of Parkinson disease in Swedish twins: a longitudinal study. Neurobiol Aging 32:1923 e1921-1928.

Wooten GF (2001) Anatomy and function of dopamine receptors: understanding the pathophysiology of fluctuations in Parkinson's disease. Parkinsonism Relat Disord 8:79-83.

Xiong Y, Dawson VL, Dawson TM (2012) LRRK2 GTPase dysfunction in the pathogenesis of Parkinson's disease. Biochem Soc Trans 40:1074-1079.

Xiong Y, Yuan C, Chen R, Dawson TM, Dawson VL (2012) ArfGAP1 is a GTPase activating protein for LRRK2: reciprocal regulation of ArfGAP1 by LRRK2. J Neurosci 32:3877-3886.

Xiong Y, Coombes CE, Kilaru A, Li X, Gitler AD, Bowers WJ, Dawson VL, Dawson TM, Moore DJ (2010) GTPase activity plays a key role in the pathobiology of LRRK2. PLoS Genet

6:e1000902.
Yakhine-Diop SM, Bravo-San Pedro JM, Gomez-Sanchez R, Pizarro-Estrella E, Rodriguez-Arribas M, Climent V, Aiastui A, de Munain AL, Fuentes JM, Gonzalez-Polo RA (2014) G2019S LRRK2 mutant fibroblasts from Parkinson's disease patients show increased sensitivity to neurotoxin 1-methyl-4-phenylpyridinium dependent of autophagy. Toxicology.
Yuan HH, Chen RJ, Zhu YH, Peng CL, Zhu XR (2013) The neuroprotective effect of overexpression of calbindin-D(28k) in an animal model of Parkinson's disease. Mol Neurobiol 47:117-122.
Zhang XJ, Chen S, Huang KX, Le WD (2013) Why should autophagic flux be assessed? Acta Pharmacol Sin 34:595-599.
Zheng S, Geghman K, Shenoy S, Li C (2012) Retake the center stage--new development of rat genetics. J Genet Genomics 39:261-268.
Zhou H, Huang C, Tong J, Hong WC, Liu YJ, Xia XG (2011) Temporal expression of mutant LRRK2 in adult rats impairs dopamine reuptake. Int J Biol Sci 7:753-761.
Zhu X, Siedlak SL, Smith MA, Perry G, Chen SG (2006) LRRK2 protein is a component of Lewy bodies. Ann Neurol 60:617-618; author reply 618-619.
Zimprich A, Biskup S, Leitner P, Lichtner P, Farrer M, Lincoln S, Kachergus J, Hulihan M, Uitti RJ, Calne DB, Stoessl AJ, Pfeiffer RF, Patenge N, Carbajal IC, Vieregge P, Asmus F, Muller-Myhsok B, Dickson DW, Meitinger T, Strom TM, Wszolek ZK, Gasser T (2004) Mutations in LRRK2 cause autosomal-dominant parkinsonism with pleomorphic pathology. Neuron 44:601-607.